Intranasal Targeting of Neuropeptides to the Central Nervous System: Evaluation of Pharmacokinetics, Pharmacodynamics, and a Novel Vasoconstrictor Formulation

A DISSERTATION
SUBMITTED TO THE FACULTY OF THE GRADUATE SCHOOL
OF THE UNIVERSITY OF MINNESOTA
BY

Shyeilla V. Dhuria

IN PARTIAL FULFILLMENT OF THE REQUIREMENTS
FOR THE DEGREE OF
DOCTOR OF PHILOSOPHY

William H. Frey II, Advisor

February 2009

ACKNOWLEDGMENTS

A number of individuals contributed to the completion of this dissertation. I would like to gratefully acknowledge my advisor, Dr. William H. Frey II, for his guidance and support during my academic research experiences. I am most thankful to Bill for his scientific vision and capacity to see the big picture, for his ability to always find a silver-lining in all that we do, and for his encouragement in exploring new ideas and approaches.

It is equally important to recognize the contributions of Dr. Leah R. Hanson. Though the official paperwork does not acknowledge her contributions, she has acted as an advisor to me during every stage of my academic career. From Leah, I learned the art of writing and presenting scientific research, designing and executing experiments, setting goals, and balancing work and play. Leah has been a mentor and a friend to me and has positively influenced the way in which I will lead and manage people going forward. Without her scientific input, constant support, and clear direction, this journey would have been far more difficult to complete.

I would like to acknowledge my colleagues at the Alzheimer's Research Center, including those who no longer work there. Those who contributed to various aspects of my experiments are specifically recognized in the acknowledgments sections in Chapter 2 and in Chapter 4. A special thanks to Dianne Marti who assisted with a significant number of experiments by weighing tubes and dissecting tissues. There are also those who provided non-scientific support throughout my time in the lab, including Michelle Brady and Judy Johnson. I am also thankful to Paula Martinez, Elizabeth Bordayo,

Reshma Rao, Jean Crow and Susann Remington, who provided much needed perspective and three o'clock espresso breaks to discuss both scientific and non-scientific topics. I feel fortunate to have had the opportunity to work among such a fun, dynamic, and team-oriented group of people.

I am thankful for the opportunity to conduct the behavioral studies presented in Chapter 3 in collaboration with Dr. Deborah Bingham and Dr. Scott S. Panter at the San Francisco VA Medical Center. A special thanks to the individuals who conducted the experiments related to the behavioral studies, including Aleta Svitak and Rachel Matthews, who carried out the biodistribution study, and Amanda Baillargeon, who developed the immunoblot methods and conducted the cell signaling studies. The hard work of these individuals is sincerely appreciated.

I am grateful to my parents for their sacrifices to provide me with the opportunity to pursue a liberal arts education, which ultimately led me to find myself and realize my dreams. My parents have encouraged me and supported me throughout my life to allow me to achieve what they could not do themselves and I am forever grateful for this. Thanks also to the rest of the family (Shalini, Pim, Atul, Rahul) for their encouragement and support over the years.

Finally, I am eternally grateful to my partner, Belle Vengco, who has been a source of unfaltering support and happiness for the past ten years. Seven years ago, she took a leap and traveled with me to a place called Minnesota. Since then she has endured: the late nights of studying and finishing experiments, the countless practice seminars, the seemingly never ending process of writing, shoveling, mowing, cleaning the house, doing the laundry, the frigid cold, the moments of frustration, and the

moments of success. Belle has provided me with incredible perspective and insight into my research and into my life. No words can fully capture her contribution to the completion of this dissertation. All I know is that without her, I could not have done this.

TABLE OF CONTENTS

ACKNOWLEDGMENTS ..... **i**

LIST OF TABLES ..... **ix**

LIST OF FIGURES ..... **xi**

PROLOGUE **1**

INTRANASAL DELIVERY TO THE CENTRAL NERVOUS SYSTEM: MECHANISMS AND EXPERIMENTAL CONSIDERATIONS **11**

1.1 Introduction and Background 11

1.2 Pathways and Mechanisms 17

1.2.1 Olfactory Nerve Pathways 17

1.2.2 Trigeminal Nerve Pathways 21

1.2.3 Vascular Pathways 23

1.2.4 Pathways Involving the Cerebrospinal Fluid and Lymphatics 25

1.3 Experimental Considerations 26

1.3.1 Head Position 27

1.3.2 Administration Technique 28

1.3.3 Volume 30

1.3.4 Assessment of CNS Distribution 32

1.4 Formulation Considerations 33

1.4.1 Formulation Strategies to Improve Drug Solubility 34

1.4.2 Formulations Affecting Membrane Permeability 36

1.4.3 Strategies to Reduce Clearance and Increase Residence Time 38

1.5 The Future of Intranasal Delivery to the CNS 42

INTRANASAL DRUG TARGETING OF HYPOCRETIN-1 (OREXIN-A) TO THE CENTRAL NERVOUS SYSTEM 46

2.1 Introduction 46

2.2 Materials and Methods 49

2.2.1 Experimental Design 49

2.2.2 Drugs and Reagents 49

2.2.3 Animals 50

2.2.4 Preparation of Dose Solutions 50

2.2.5 Animal Surgeries and Drug Administration 50

2.2.6 Blood Sampling 51

2.2.7 Brain and Peripheral Tissue Dissection 52

2.2.8 Sample Analysis 53

2.2.9 Cerebrospinal Fluid Sampling 53

2.2.10 Autoradiography 54

2.2.11 Stability Assessment using HPLC 54

2.2.12 Data Analysis 55

2.3 Results 57

2.3.1 Pharmacokinetics in Blood and Tissues after Intranasal and Intravenous Delivery 57

2.3.2 Drug Targeting to CNS Tissues and Lymphatics after Intranasal and Intravenous Delivery 60

2.3.3 Qualitative Autoradiography after Intranasal and Intravenous Delivery 61

2.3.4 Qualitative Assessment of Stability after Intranasal and Intravenous Delivery 62

2.4 Discussion 63

2.5 Conclusions 70

2.6 Acknowledgments 71

2.7 Supplementary Material 84

2.7.1 Qualitative Assessment of Intact Hypocretin-1 in the Brain and Blood Using Reverse-Phase High Performance Liquid Chromatography 84

BEHAVIORAL ASSESSMENTS AFTER INTRANASAL ADMINISTRATION OF HYPOCRETIN-1 (OREXIN-A) IN RATS: EFFECTS ON APPETITE AND LOCOMOTOR ACTIVITY 113

3.1 Introduction 113

3.2 Material and Methods 115

3.2.1 Animals and Housing 115

3.2.2 Drugs and Reagents 116

3.2.3 Dose Solutions 116

3.2.4 Intranasal Administration 117

3.2.5 Behavioral Study 118

3.2.6 Biodistribution Study 118

3.2.7 Cell Signaling Study 120

3.2.8 Data and Statistical Analysis 122

3.3 Results 123

3.3.1 Behavioral Effects of Intranasal HC (100 nmol) 123

3.3.2 Biodistribution following Intranasal HC (100 nmol and 10 nmol) 123

3.3.3 Cell Signaling Effects of Intranasal HC (100 nmol) 125

3.4 Discussion 125

NOVEL VASOCONSTRICTOR FORMULATION TO ENHANCE INTRANASAL TARGETING OF NEUROPEPTIDES TO THE CENTRAL NERVOUS SYSTEM 143

4.1 Introduction 143

4.2 Methods 146

4.2.1 Experimental Design 146

4.2.2 Materials 148

4.2.3 Animals 148

4.2.4 Animal Surgeries 148

4.2.5 Preparation of Formulations 149

4.2.6 Drug Administration 149

4.2.7 Tissue and Fluid Sampling 150

4.2.8 Sample and Data Analysis 151

4.3 Results 153

4.3.1 HC Biodistribution With and Without 1% PHE 153

4.3.2 HC Drug Targeting to the CNS and Lymphatics With and Without 1% PHE 155

4.3.3 D-KTP Biodistribution Following Intranasal and Intravenous Delivery ... 155

4.3.4 D-KTP Biodistribution With and Without PHE 157

4.3.5 D-KTP Drug Targeting to the CNS and Lymphatics With and Without PHE 159

4.4 Discussion 160

4.5 Acknowledgments 165

4.6 Supplementary Material 177

4.6.1 Pilot Study to Evaluate Different Vasoactive Agents 177

4.6.2 Effect of Cerebrospinal Fluid Sampling on Drug Distribution after Intranasal and Intravenous Delivery of Neuropeptides 196

CONCLUSIONS 221

REFERENCES 231

LIST OF TABLES

CHAPTER 2: INTRANASAL DRUG TARGETING OF HYPOCRETIN-1 (OREXIN-A) TO THE CENTRAL NERVOUS SYSTEM

Table 1: Pharmacokinetic Parameters in Blood Following Intranasal and Intravenous Delivery……73

Table 2: CNS and Lymphatic Tissue Concentrations of HC Following Intranasal and Intravenous Delivery……..74

Table 3: Intranasal Drug Targeting Index and Direct Transport Percentage to CNS Tissues……...75

Supplementary Material (2.7.1) Table 1: Summary of HPLC Analysis of Brain and Blood Following Intranasal and Intravenous Administration…….. 96

CHAPTER 3: BEHAVIORAL ASSESSMENTS AFTER INTRANASAL ADMINISTRATION OF HYPOCRETIN-1 (OREXIN-A) IN RATS: EFFECTS ON APPETITE AND LOCOMOTOR ACTIVITY

Table 1: Time Course of Effect of Intranasal HC (100 nmol) on Wheel Running Activity……...130

Table 2: Biodistribution in CNS and CNS-Related Tissues Following Intranasal Administration……...131

Table 3: Biodistribution in Blood, Peripheral Tissues, and Lymph Nodes Following Intranasal Administration……. 132

NOVEL VASOCONSTRICTOR FORMULATION TO ENHANCE INTRANASAL TARGETING OF NEUROPEPTIDES TO THE CENTRAL NERVOUS SYSTEM

Table 1: Concentrations Following Intranasal Administration of HC (10 nmol) With and Without 1% PHE……167

Table 2: Concentrations Following Intravenous Administration and Intranasal Administration of D-KTP (10 nmol) With and Without PHE……168

Supplementary Material (4.6.1) Table 1: Intranasal Co-Administration of Hypocretin-1 and Vasoactive Compounds……188

Supplementary Material (4.6.1) Table 2: Intranasal Pretreatment with Vasoconstrictors, Followed by Intranasal Co-Administration of Hypocretin-1 and Vasoconstrictor Compounds……. 189

Supplementary Material (4.6.1) Table 3: Hypocretin-1 Concentrations in CNS and Peripheral Tissues at 30 Minutes with Different Pretreatment Time Intervals in the Absence of Phenylephrine……. 190

Supplementary Material (4.6.1) Table 4: Hypocretin-1 Concentrations in CNS and Peripheral Tissues at 30 Minutes with Different Pretreatment Time Intervals in the Presence of 1% Phenylephrine……..191

LIST OF FIGURES

CHAPTER 1: INTRANASAL DELIVERY TO THE CENTRAL NERVOUS SYSTEM: MECHANISMS AND EXPERIMENTAL CONSIDERATIONS

Figure 1: Pathways of Drug Distribution in the Nasal Cavity and Central Nervous System……44

CHAPTER 2: INTRANASAL DRUG TARGETING OF HYPOCRETIN-1 (OREXIN-A) TO THE CENTRAL NERVOUS SYSTEM

Figure 1: Blood Concentration-Time Profiles of HC Following Intranasal and Intravenous Delivery to Anesthetized Rats……76

Figure 2: Concentration-Time Profiles of HC in Kidney, Liver, and Muscle Following Intranasal and Intravenous Delivery to Anesthetized Rats……78

Figure 3: CNS Tissue-to-Blood Concentration Ratios Following Intranasal and Intravenous Delivery to Anesthetized Rats……80

Figure 4: Qualitative Autoradiography of ^{125}I-HC at 30 Minutes Following Intranasal and Intravenous Delivery to Anesthetized Rats……...82

Supplementary Material (2.7.1) Figure 1: Peptide Extraction Scheme……97

Supplementary Material (2.7.1) Figure 2: Brain Supernatant Following Intranasal Administration to Rat #1 and Extraction in 1000 mM Tris Buffer……100

Supplementary Material (2.7.1) Figure 3: Brain Supernatant Following Intravenous Administration to Rat #1 and Extraction in 1000 mM Tris Buffer…101

Supplementary Material (2.7.1) Figure 4: Blood Following Intranasal and Intravenous Administration and Extraction in 1000 mM Tris Buffer……... 102

Supplementary Material (2.7.1) Figure 5: HPLC Analysis of Brain Processing Control……...103

Supplementary Material (2.7.1) Figure 6: HPLC Analysis of Blood Processing Control……...104

Supplementary Material (2.7.1) Figure 7: Brain Supernatant Following Intranasal Administration to Rat #2……... 105

Supplementary Material (2.7.1) Figure 8: Brain Supernatant Following Intranasal Administration to Rat #3..... 106

Supplementary Material (2.7.1) Figure 9: Brain Supernatant Following Intranasal Administration to Rat #4..... 107

Supplementary Material (2.7.1) Figure 10: Brain Supernatant Following Intravenous Administration to Rat #2..... 108

Supplementary Material (2.7.1) Figure 11: Brain Supernatant Following Intravenous Administration to Rat #3..... 109

Supplementary Material (2.7.1) Figure 12: Blood Following Intranasal Administration to Rat #2 and Rat #3.....110

Supplementary Material (2.7.1) Figure 13: Blood Following Intranasal Administration to Rat #4..... 111

Supplementary Material (2.7.1) Figure 14: Blood Following Intravenous Administration to Rat #2 and Rat #3.....112

CHAPTER 3: BEHAVIORAL ASSESSMENTS AFTER INTRANASAL ADMINISTRATION OF HYPOCRETIN-1 (OREXIN-A) IN RATS: EFFECTS ON APPETITE AND LOCOMOTOR ACTIVITY

Figure 1: Changes in Food Consumption Following Intranasal HC (100 nmol).....133

Figure 2: Effect on Water Intake Following Intranasal HC (100 nmol)..... 135

Figure 3: Wheel Running Activity Following Intranasal HC (100 nmol).....137

Figure 4: Phosphorylated MAPK in Brain at 30 Minutes Following Intranasal HC (100 nmol)..... 139

Figure 5: PDK-1 in Brain at 30 Minutes Following Intranasal HC (100 nmol).....141

CHAPTER 4: NOVEL VASOCONSTRICTOR FORMULATION TO ENHANCE INTRANASAL TARGETING OF NEUROPEPTIDES TO THE CENTRAL NERVOUS SYSTEM

Figure 1: Blood Concentration-Time Profiles of HC Following Intranasal Administration with and without 1% PHE..... 169

Figure 2: CNS Tissue-to-Blood Concentration Ratios of HC at 30 Minutes Following Intranasal Administration with and without 1% PHE……171

Figure 3: Blood Concentration-Time Profiles of D-KTP Following Intravenous Administration, Intranasal Administration without PHE, and Intranasal Administration with 1% PHE or 5% PHE…… 173

Figure 4: CNS Tissue-to-Blood Concentration Ratios of D-KTP at 30 Minutes Following Intravenous Administration, Intranasal Administration without PHE, and Intranasal Administration with 1% PHE or 5% PHE……175

Supplementary Material (4.6.1) Figure 1: Structures of Vasoactive Agents…… 192

Supplementary Material (4.6.1) Figure 2: Effect of Pretreatment Time Interval on Blood Absorption of Hypocretin-1 Following Intranasal Administration in the Presence and Absence of 1% Phenylephrine…… 194

Supplementary Material (4.6.2) Figure 1: Hypocretin-1 Blood Concentrations with and without Cerebrospinal Fluid Sampling……..205

Supplementary Material (4.6.2) Figure 2: L-Tyr-D-Arg Blood Concentrations with and without Cerebrospinal Fluid Sampling……..207

Supplementary Material (4.6.2) Figure 3: Effect of Cerebrospinal Fluid Sampling on L-Tyr-D-Arg Concentrations in the Brain after Intravenous Administration……...209

Supplementary Material (4.6.2) Figure 4: Effect of Cerebrospinal Fluid Sampling on L-Tyr-D-Arg Concentrations in Other Tissues after Intravenous Administration……...211

Supplementary Material (4.6.2) Figure 5: Effect of Cerebrospinal Fluid Sampling on L-Tyr-D-Arg Concentrations in the Brain after Intranasal Administration… 213

Supplementary Material (4.6.2) Figure 6: Effect of Cerebrospinal Fluid Sampling on L-Tyr-D-Arg Concentrations in Other Tissues after Intranasal Administration…… 215

Supplementary Material (4.6.2) Figure 7: Effect of Cerebrospinal Fluid Sampling on L-Tyr-D-Arg Concentrations in the Brain after Intranasal Administration with 1% PHE……217

Supplementary Material (4.6.2) Figure 8: Effect of Cerebrospinal Fluid Sampling on L-Tyr-D-Arg Concentrations in Other Tissues after Intranasal Administration with 1% PHE……219

PROLOGUE

The blood-brain barrier (BBB) limits the distribution of systemically administered therapeutics to the central nervous system (CNS), posing a significant challenge to drug development efforts to treat neurological and psychiatric diseases and disorders. Direct delivery of therapeutics to the brain and spinal cord can be achieved by intracerebroventricular (ICV) or intraparenchymal administration; however these methods are invasive, costly, and impractical, especially when considering the need for frequent dosing regimens. Intranasal delivery is a non-invasive and convenient method that rapidly targets therapeutics to the CNS along olfactory and trigeminal nerve pathways, bypassing the BBB, minimizing systemic exposure, and potentially reducing side effects. Traditionally, the intranasal route of administration has been used to deliver drugs to the systemic circulation via absorption into the nasal vasculature. A growing body of evidence demonstrates that intranasal administration of a broad spectrum of therapeutics results in significant delivery to the cerebrospinal fluid (CSF), brain, and spinal cord in animals and in humans (Chen et al., 1998; Chow et al., 1999; Dahlin et al., 2001; Born et al., 2002; Frey, 2002; Banks et al., 2004; Ross et al., 2004; Thorne et al., 2004; Fliedner et al., 2006; Han et al., 2007; Wang et al., 2007; Hashizume et al., 2008; Nonaka et al., 2008; Thorne et al., 2008). Moreover, studies demonstrate CNS-mediated effects following intranasal administration (Liu et al., 2004; De Rosa et al., 2005; Kosfeld et al., 2005; Shimizu et al., 2005; Benedict et al., 2007; Gozes and Divinski, 2007; Yamada et al., 2007; Buddenberg et al., 2008; Hashizume et al., 2008; Reger et al., 2008b).

While the exact mechanisms underlying intranasal delivery to the CNS are not understood, olfactory and trigeminal nerves, which connect the nasal cavity and the CNS, clearly play an important role in direct delivery to the CNS. Vascular pathways, involving the absorption of therapeutics into blood vessels lining the nasal mucosa, followed by distribution from the systemic blood to different brain regions, also have a role in intranasal delivery to the CNS, particularly for small, lipophilic molecules as well as for some peptides and proteins (Chow et al., 1999; Banks, 2008). In addition, pathways involving transport within perivascular spaces surrounding blood vessels (Thorne et al., 2004) and pathways involving connections between the nasal lymphatics and the CSF compartment in the CNS are implicated in intranasal delivery to the CNS (Bradbury and Westrop, 1983; Thorne et al., 2004). A combination of these pathways into the CNS is likely followed after intranasal administration and may be heavily dependent on the specific properties of the therapeutic as well as the composition of the nasal formulation.

While the intranasal route of drug administration for CNS delivery is a promising alternative to more invasive routes, one limitation is the low efficiency of delivery into the brain, with typically less than 1% of the administered dose reaching the brain. The low efficiency of delivery is due to the presence of multiple types of barriers present in the nasal mucosa, including mucociliary clearance mechanisms, drug metabolizing enzymes, efflux transporters, and nasal congestion. In the last decade, research efforts have focused on improving delivery efficiency and drug targeting to the CNS with the intranasal method by using a variety of formulations strategies.

The overall goal of this research was to investigate intranasal targeting of neuropeptides to the CNS by evaluating pharmacokinetics, pharmacodynamics, and a novel nasal formulation for CNS therapeutics containing a vasoconstrictor. It was hypothesized that intranasal administration would target neuropeptides to the CNS of rats as compared to intravenous administration and result in sufficient brain concentrations to activate cell signaling pathways and produce CNS effects. It was further hypothesized that inclusion of a vasoconstrictor in nasal formulations containing CNS therapeutics would enhance intranasal targeting of neuropeptides to the CNS by reducing absorption into the blood and increasing deposition in the nasal epithelium. This could increase the amount of drug available for transport into the brain along direct pathways, including the olfactory and trigeminal neural pathways, perivascular pathways, and/or pathways involving the CSF or lymphatic system.

The specific aims of this research were:

(1) To assess intranasal targeting to the CNS by comparing the pharmacokinetics and drug targeting following intranasal and intravenous administration.

(2) To evaluate effects on CNS-mediated behaviors following intranasal administration.

(3) To determine if a vasoconstrictor formulation enhances intranasal targeting to the CNS by comparing drug targeting after intranasal administration with and without a vasoconstrictor.

Overview of Dissertation

The dissertation is presented in six sections, including a prologue, four chapters, and a conclusion. References for all sections are presented at the end of the dissertation. The prologue to the dissertation provides an overview of the research undertaken and highlights significant findings.

Chapter 1 is entitled "Intranasal delivery to the central nervous system: mechanisms and experimental considerations" and will be submitted as a review article for publication in a pharmaceutics scientific journal. This chapter provides an introduction to the field of intranasal administration for CNS drug targeting and includes a literature review of the current understanding of intranasal delivery mechanisms, experimental and formulation considerations for intranasal studies, and future directions. The purpose of the review is to focus on the current understanding of the mechanisms underlying intranasal delivery to the CNS, including pathways involving the olfactory and trigeminal nerves, the vasculature, the CSF, and the lymphatic system. Understanding the pathways important for intranasal delivery is critical for the development of intranasal treatments for CNS diseases. The underlying theme of the review is that in addition to the properties of the therapeutic, the deposition of the drug formulation within the nasal epithelium and the composition of the formulation can influence the pathway a therapeutic follows from the nasal cavity to the CNS. Experimental factors, such as head position, volume, and method of administration, can significantly influence deposition of the formulation within the nasal passages. Formulation parameters, such as pH and osmolarity, or inclusion of additives, such as permeation enhancers, mucoadhesives, or protein inhibitors, can also

affect the pathways followed into the CNS, as well as the deposition in the nasal cavity. The review also highlights the diversity of therapeutics administered by the intranasal route, the details of which are left to several comprehensive reviews that have recently been published on the subject. While intranasal administration holds great promise for improving the treatment of CNS diseases and disorders, significant research will be required to develop and improve current intranasal treatments, and careful consideration should be given to the factors discussed in the review.

Chapter 2 is entitled, "Intranasal drug targeting of hypocretin-1 (orexin-A) to the central nervous system" and has been published in the Journal of Pharmaceutical Sciences (Dhuria SV, Hanson LR, Frey WH II (2008) DOI:10.1002/jps.21604). This chapter is presented in the format originally submitted to the scientific journal, with minor changes to the format of the references. Minor editorial modifications were made by the journal editors in the published version of this manuscript. This chapter assesses intranasal targeting to the CNS by comparing the pharmacokinetics and drug targeting of a neuropeptide (hypocretin-1, HC) following intranasal and intravenous administration (10 nmol) over a two hour period in anesthetized rats. Hypocretin-1 (also known as orexin-A) is an important endogenous peptide involved in the regulation of appetite, sleep, and other physiological functions, with potential in the treatment of the sleep disorder, narcolepsy. In these biodistribution studies, concentrations in CNS tissues, peripheral tissues, and blood were determined based on measurements of ^{125}I-labeled HC. Results indicated that despite a 10-fold lower blood concentration of HC with intranasal administration, both routes of drug administration resulted in similar brain concentrations over two hours, suggesting that direct pathways are involved in

intranasal delivery of HC to the CNS. In fact, approximately 80% of the area under the brain concentration-time curve after intranasal administration was found to be due to direct transport pathways from the nasal cavity to the CNS. Tissue-to-blood concentration ratios after intranasal administration were significantly greater in all brain regions over two hours compared to intravenous administration, with the greatest ratios observed in the trigeminal nerve (14-fold) and olfactory bulbs (9-fold). Intranasal administration increased drug targeting to the brain and spinal cord 5- to 8-fold compared to the intravenous route of administration. In the supplementary material for Chapter 2, results are presented from experiments using high performance liquid chromatography (HPLC) to assess the stability of ^{125}I-HC in the brain and blood following intranasal and intravenous administration. HPLC results indicated that a portion of the administered peptide reached the brain intact, while in the blood little to no ^{125}I-HC was present. Taken together, results from these biodistribution and HPLC studies provide support that intranasal administration rapidly targets intact HC to the CNS, resulting in significantly greater drug targeting compared to intravenous administration.

Chapter 3 is entitled, "Behavioral assessments after intranasal administration of hypocretin-1 (orexin-A) in rats: effects on appetite and locomotor activity" and will be submitted for publication in a neuroscience scientific journal. This chapter evaluates the effects of intranasal HC (100 nmol) on behaviors including food consumption, water intake, and wheel running activity in rats. Results from these experiments indicated that intranasal administration of HC significantly increased food consumption in rats in the first four hours after dosing, but had no effect on water intake compared to control rats

receiving intranasal phosphate-buffered saline (PBS). Intranasal dosing was conducted during the early light phase of the light-dark cycle, during a time when animals are normally inactive and satiated from eating during the dark phase, indicating that the HC reaching the brain was sufficient to overcome satiety signals. In addition, HC increased wheel running activity during the first four hours after intranasal dosing, with the most significant difference observed between 1-2 hours after dosing. The effects of intranasal HC on appetite and locomotion are consistent with the rapid entry of biologically active HC to the CNS. The underlying mechanisms of the observed behavioral effects of a 100 nmol intranasal dose of HC were investigated by evaluating biodistribution and activation of signaling pathways using radiotracer methods and Western blot. In cell culture, HC has been shown to activate downstream targets of the mitogen-activated protein kinase (MAPK) signaling pathway and the phosphatidyl-inositol 3-kinase (PI3K) signaling pathway at nanomolar concentrations (Ammoun et al., 2006b; Ammoun et al., 2006a; Goncz et al., 2008). Concentrations achieved in the brain (4-14 nM) within 30 minutes of intranasal administration of ^{125}I-HC were within the range of the affinity of HC for hypocretin receptors (Sakurai et al., 1998). The greatest concentrations were observed in the olfactory bulbs (14 nM) and hypothalamus (13 nM). Intranasal HC (100 nmol) reduced levels of phosphorylated MAPK in the olfactory bulbs (66% reduction), but had no effect on phosphorylated MAPK in the diencephalon (contains hypothalamus and thalamus) or brainstem at 30 minutes compared to vehicle (PBS) treated controls. Evaluation of a different downstream signaling protein of HC, phosphoinositide-dependent kinase-1 (PDK-1), showed that intranasal HC significantly increased phosphorylation of PDK-1 in the diencephalon

(26% increase) and in the brainstem (21% increase), which are brain areas that play an important role in the regulation of appetite and locomotion, respectively. Additional cell signaling studies are necessary to further understand the molecular mechanisms underlying the behavioral effects of intranasal HC. Results from these behavior studies are the first evidence of CNS-mediated effects of HC in rodents following intranasal administration, indicating that HC reaches the CNS in its biologically active form to bind to receptors and activate signaling pathways.

Chapter 4 is entitled, "Novel vasoconstrictor formulation to enhance intranasal targeting of neuropeptides to the central nervous system" and has been published in the Journal of Pharmacology and Experimental Therapeutics (Dhuria SV, Hanson LR, Frey WH II, JPET, 328:312-20, 2009). This chapter is presented in the format originally submitted to the scientific journal, with minor changes to the format of the references. Minor editorial modifications were made by the journal editors in the published version of this manuscript. This chapter assesses the effect of vasoconstrictors on intranasal delivery to the CNS by comparing CNS targeting of neuropeptides (^{125}I-HC and the dipeptide, L-Tyr-D-Arg, ^{125}I-D-KTP) at 30 minutes after intranasal administration with and without a vasoconstrictor (phenylephrine, PHE). D-KTP is a considerably smaller neuropeptide compared to HC (MW 337 and MW 3562, respectively), is an enzymatically stable structural analog of the endogenous dipeptide, kyotorphin (L-Tyr-L-Arg, KTP), and is involved in antinociception. Compared to intranasal controls, inclusion of 1% PHE in nasal formulations reduced absorption into the blood for HC (65% reduction) and for D-KTP (56% reduction), while significantly increasing deposition in the olfactory epithelium by ~3-fold for both. Olfactory bulb

concentrations were significantly increased with PHE for HC (2.1-fold) and for D-KTP (3.0-fold), indicating that the vasoconstrictor enhanced intranasal delivery to the CNS along olfactory nerve pathways. PHE reduced concentrations in the trigeminal nerve for HC (65% reduction) and for D-KTP (39% reduction) and reduced concentrations in most remaining brain regions (~50% reduction for both), suggesting that delivery along trigeminal nerve pathways to the CNS was diminished with the vasoconstrictor. Intranasal administration with 1% PHE increased brain concentrations relative to concentrations in a non-target tissue such as the blood for HC (1.6- to 6.8-fold), while for D-KTP this was only observed in the olfactory bulbs (5.3-fold). Increasing the vasoconstrictor concentration to 5% resulted in increased tissue-to-blood ratios for D-KTP in additional CNS areas (1.5- to 16-fold). Results from these studies suggest that use of vasoconstrictors in nasal formulations could be beneficial for reducing systemic exposure of CNS therapeutics with adverse effects and for enhancing delivery to rostral brain regions. In the supplementary material for Chapter 4, results are presented from pilot studies that evaluated different vasoactive compounds (vasoconstrictors: tetrahydrozoline, endothelin-1, and phenylephrine; vasodilator: histamine) and the effect of pretreatment of the nasal cavity with a vasoconstrictor solution. Results from these studies formed the basis of the rationale to co-administer phenylephrine with neuropeptides in intranasal studies. In addition, the supplementary material for Chapter 4 presents results from a study evaluating the effect of CSF sampling on CNS drug distribution. These results indicated that CSF sampling significantly altered drug distribution following intranasal, but not intravenous administration, suggesting the

need for a separate group of animals for intranasal experiments where CSF concentrations will be assessed.

The final section of the dissertation is the conclusions section, which highlights key findings from this research and the broader implications of the findings. The conclusions section also discusses recommendations for future work in light of the challenges faced in the present work. The key findings of this research are that intranasal administration targets neuropeptides to the CNS compared to intravenous administration. The concentrations of HC achieved in the brain are sufficient to affect CNS-mediated behaviors and HC signaling pathways, indicating the presence of biologically active HC in the CNS following intranasal administration. Intranasal administration of HC has potential for treating CNS diseases involving the hypocretinergic system, including narcolepsy, Alzheimer's disease, and appetite disorders. In addition, use of a vasoconstrictor nasal formulation could improve intranasal treatments by reducing systemic exposure and enhancing delivery to rostral brain areas, which could be important for CNS therapeutics having adverse systemic effects.

CHAPTER 1

INTRANASAL DELIVERY TO THE CENTRAL NERVOUS SYSTEM: MECHANISMS AND EXPERIMENTAL CONSIDERATIONS

1.1 Introduction and Background

Despite the immense network of the cerebral vasculature, systemic delivery of therapeutics to the central nervous system (CNS) is not effective for greater than 98% of small molecules and for nearly 100% of large molecules (Pardridge, 2005). The lack of effectiveness is due to the presence of the blood-brain barrier (BBB), which prevents foreign substances, even beneficial therapeutics, from entering the brain from the circulating blood. While certain small molecule, peptide, and protein therapeutics given systemically reach the brain parenchyma by crossing the BBB (Banks, 2008), generally high systemic doses are needed to achieve therapeutic levels which can result in adverse effects in the body. Therapeutics can be introduced directly into the CNS by intracerebroventricular or intraparenchymal injections; however, for multiple dosing regimens both delivery methods are invasive, risky, and expensive techniques requiring surgical expertise. An additional limitation to the utility of these methods is inadequate CNS exposure due to slow diffusion from the injection site and rapid turnover of the cerebrospinal fluid (CSF). Intranasal delivery has come to the forefront as an alternative to invasive delivery methods to bypass the BBB and rapidly target therapeutics directly to the CNS utilizing pathways along olfactory and trigeminal

nerves innervating the nasal passages (Frey, 2002; Thorne et al., 2004; Dhanda et al., 2005).

The primary goal of this review is to discuss the present understanding of the pathways and mechanisms underlying intranasal drug delivery to the CNS. With this background in mind, experimental considerations and formulation strategies for enhancing intranasal drug delivery and targeting to the CNS will be discussed. This review will also briefly highlight the diversity of therapeutic drugs that have been shown to be delivered intranasally, the details of which have been recently published in several comprehensive reviews (Thorne and Frey, 2001; Frey, 2002; Illum, 2003, 2004; Dhanda et al., 2005; Costantino et al., 2007).

The intranasal route of administration is not a novel approach for drug delivery to the systemic circulation. The novelty lies in using this noninvasive method to rapidly deliver drugs directly from the nasal mucosa to the brain and spinal cord with the aim of treating CNS disorders while minimizing systemic exposure. Early research demonstrated that tracers, such as wheat-germ agglutinin conjugated to horseradish peroxidase (WGA-HRP), were transported within olfactory nerve axons to reach the olfactory bulbs in the CNS (Balin et al., 1986). These findings were subsequently confirmed in a quantitative study comparing intranasal and intravenous administration of WGA-HRP (Thorne et al., 1995). Direct intranasal delivery of therapeutics to the brain was first proposed in 1989 and patented by William H. Frey II of the Alzheimer's Research Center (Frey, 1991, 1997). Subsequently, numerous reports have shown that therapeutics given by the intranasal route are delivered to the CNS and have the

potential to treat neurological diseases and disorders (Frey, 2002; Dhanda et al., 2005; Costantino et al., 2007).

Intranasal administration of insulin, which is currently under investigation for the treatment of Alzheimer's disease, was initially developed as a noninvasive alternative to subcutaneous insulin injections used by diabetic patients. Insulin, like many therapeutic peptides and proteins, is not effective when given orally because of the rapid degradation that occurs in the gastrointestinal tract and the poor pharmacokinetic profile. Inhalable insulin (Exubera®) was a promising alternative to injectable insulin, but unexpectedly failed due to concerns of lung toxicity and the development of lung cancer (Mitri and Pittas, 2009). In order to enter the systemic circulation, intranasal formulations of insulin required the use of enzyme inhibitors, mucoadhesives, and absorption enhancers to overcome barriers present in the nasal passages that limit systemic bioavailability. Nasal irritation from these additives, in addition to high and frequent dosing regimens, resulted in limited clinical success with intranasal insulin for diabetes management (Owens et al., 2003).

Several decades after initial investigations of intranasal insulin, use of the intranasal method was proposed for direct delivery of insulin to the brain along olfactory pathways for the treatment of Alzheimer's disease and other brain disorders (Frey, 2001). Using this method, researchers discovered profound improvements in memory and mood in normal individuals following intranasal administration of insulin (Benedict et al., 2004) and an insulin analog (Benedict et al., 2007). Intranasal insulin did not alter blood insulin or glucose levels to cause these effects, consistent with observations noted in earlier investigations. Instead, the protein rapidly gains direct

access to the CSF following intranasal administration (Born et al., 2002) and, similar to insulin-like growth factor-I (IGF-I), also likely gains direct access to the brain itself from the nasal mucosa (Thorne et al., 2004). Intranasal insulin is now being considered as a treatment for Alzheimer's disease, considered by some as "diabetes of the brain" or "type 3 diabetes" (Steen et al., 2005), and clinical investigations are underway in patients with the disease. Intranasal insulin dose-dependently improves memory after acute treatment (Reger et al., 2006; Reger et al., 2008a), and improves attention, memory, and cognitive function after 21 days of intranasal treatment (Reger et al., 2008b).

In addition to insulin, other peptides and proteins administered by the intranasal route are proving to have beneficial effects in humans. For example, an eight amino acid peptide fragment of activity-dependent neuroprotective protein (ADNP) is in Phase II clinical trials for the treatment of mild cognitive impairment and schizophrenia and is also in development for treating Alzheimer's disease (Gozes and Divinski, 2007). The weight regulatory peptide, melanocortin, reaches the CSF in humans within minutes of intranasal administration, without affecting blood concentrations (Born et al., 2002) and decreases body weight in normal volunteers after chronic intranasal administration for 6 weeks (Fehm et al., 2001). The peptide hormone, oxytocin, has been intranasally delivered to humans, resulting in significant changes in centrally-mediated behaviors, such as increased trust (Kosfeld et al., 2005; Baumgartner et al., 2008), decreased fear and anxiety (Kirsch et al., 2005; Parker et al., 2005), and improved social behavior (Domes et al., 2007b; Domes et al., 2007a; Guastella et al., 2008) and social memory (Rimmele et al., 2009).

In animals, detailed pharmacokinetic and pharmacodynamic studies have shown that a broad spectrum of therapeutics not only reach specific areas of the brain, but also have effects on CNS-mediated behaviors within a short time frame, making the case for a rapid, extracellular pathway into the brain following intranasal administration. Small, lipophilic molecules, such as cocaine (Chow et al., 1999), morphine (Westin et al., 2005; Westin et al., 2006), raltitrexed (Wang et al., 2006a), and testosterone (Banks et al., 2008; de Souza Silva et al., 2009), are able to reach the brain after intranasal administration in rodents. Intranasal studies with these drugs demonstrate that in addition to a portion of the drug being absorbed into the blood from the nasal mucosa, the drug gains access to the brain via direct pathways from the nasal cavity. Cocaine effects are observable within minutes of nasal administration, even before being detectable in the blood, indicating that an alternative pathway into the brain exists (Chow et al., 1999). Benzoylecgonine, the polar metabolite of cocaine, also reached the brain after intranasal administration via direct pathways, to a greater extent than cocaine (Chow et al., 2001). Intranasal administration of larger therapeutics, such as the protein hormone, leptin, results in direct delivery to the CNS (Fliedner et al., 2006) with significant reductions in food intake in rats (Schulz et al., 2004; Shimizu et al., 2005). Recently, intranasal leptin was shown to have anti-convulsant effects in rodent models of epilepsy (Diano and Horvath, 2008; Xu et al., 2008). The largest therapeutic agent reported to be delivered to the brain after intranasal administration in animals is nerve growth factor (NGF, 27.5 kDa), which reached multiple brain regions in rats, with the greatest concentrations in the olfactory bulbs (Frey et al., 1997; Chen et al., 1998). Further, intranasal administration of NGF demonstrated neuroprotective effects in

cerebral ischemic rats (Zhao et al., 2004) and reduced tau hyperphosphorylation and Aβ accumulation in mouse model of Alzheimer's disease (Capsoni et al., 2002; De Rosa et al., 2005). Recently, it was shown that intranasal administration of an oligonucleotide inhibited brain tumor growth and increased survival in rats (Hashizume et al., 2008). Further, different sizes of plasmid DNA, ranging from 3.5 kb to 14.2 kb, were successfully delivered to the brain intact after intranasal administration in rats (Han et al., 2007).

While there are numerous examples of the success and potential of intranasal delivery to rapidly target a great diversity of CNS therapeutics to the brain and spinal cord, direct transport following intranasal administration is not always evident. Researchers from Leiden University maintain that for several different therapeutics evaluated in their lab, including hydroxycobalamin (vitamin B12), melatonin, and estradiol, no evidence has been found for direct transport into the CSF following intranasal compared to intravenous administration (Van den Berg et al., 2003, 2004b; van den Berg et al., 2004a). Using microdialysis, other researchers have observed limited distribution of lidocaine (Bagger and Bechgaard, 2004a), fluorescein labeled dextran (Bagger and Bechgaard, 2004b), and stavudine (Yang et al., 2005) following intranasal compared to intravenous administration. Interestingly, while van den Berg et al. (2004) concluded that intranasal estradiol held no advantage in drug targeting to the CSF over intravenous administration (van den Berg et al., 2004a), other groups have shown that intranasal estradiol, as well as an estradiol prodrug, significantly target the brain relative to the intravenous route (Al-Ghananeem et al., 2002; Wang et al., 2006b). Born et al. (2002) have shown that melatonin and vitamin B12 reach the CSF in humans

within minutes of nasal administration without changing blood concentration (Born et al., 2002). These contrasting conclusions for similar drugs may be due to differences in methodologies employed in studies and raise important issues relating to experimental and formulation factors that can significantly influence the outcome of studies. Understanding the pathways and mechanisms underlying intranasal delivery to the CNS is critical to advance the development of intranasal treatments for neurological diseases and disorders.

1.2 Pathways and Mechanisms

While the exact mechanisms underlying intranasal drug delivery to the CNS are not entirely understood, an accumulating body of evidence demonstrates that pathways involving nerves connecting the nasal passages to the brain and spinal cord are important (Thorne et al., 1995; Ross et al., 2004; Thorne et al., 2004; Ross et al., 2008; Thorne et al., 2008). In addition, pathways involving the vasculature, cerebrospinal fluid, and lymphatic system have also been implicated in the transport of molecules from the nasal cavity to the CNS. It is likely that a combination of these pathways is responsible for the transport of molecules from the nasal mucosa to the brain, although one pathway may predominate, depending on the properties of the therapeutic and characteristics of the formulation.

1.2.1 Olfactory Nerve Pathways

Therapeutics can rapidly gain access to the CNS following intranasal administration along olfactory nerve pathways leading from the nasal cavity directly to

the CNS. Olfactory nerve pathways are a major component of intranasal delivery, evidenced by the fact that fluorescent tracers are associated with olfactory nerves as they traverse the cribriform plate (Jansson and Bjork, 2002), drug concentrations in the olfactory bulbs are generally among the highest CNS concentrations observed (Banks et al., 2004; Ross et al., 2004; Thorne et al., 2004; Graff et al., 2005; Nonaka et al., 2008; Ross et al., 2008; Thorne et al., 2008), and a strong, positive correlation exists between concentrations in the olfactory epithelium and olfactory bulbs (Dhuria et al., 2009).

Olfactory pathways arise in the upper portion of the nasal passages, in the olfactory region, where olfactory receptor neurons (ORNs) are interspersed among supporting cells (sustentacular cells), microvillar cells, and basal cells (Figure 1, Box A). ORNs mediate the sense of smell by conveying sensory information from the peripheral environment to the CNS (Clerico et al., 2003). Beneath the epithelium, the lamina propria contains mucous secreting Bowman's glands, axons, blood vessels, lymphatic vessels, and connective tissue. The dendrites of ORNs extend into the mucus layer of the olfactory epithelium, while axons of these bipolar neurons extend centrally through the lamina propria and through perforations in the cribriform plate of the ethmoid bone, which separates the nasal and cranial cavities (Figure 1, Box B). The axons of ORNs pass through the subarachnoid space containing CSF and terminate on mitral cells in the olfactory bulbs. From there, neural projections extend to multiple brain regions including the olfactory tract, anterior olfactory nucleus, piriform cortex, amygdala, and hypothalamus (Buck, 2000).

The unique characteristics of the ORNs contribute to a dynamic cellular environment critical for intranasal delivery to the CNS. Due to the direct contact with

toxins in the external environment, ORNs regenerate every 3 to 4 weeks from basal cells residing in the olfactory epithelium (Mackay-Sim, 2003). As a result, proteins characteristic of the BBB (i.e. proteolytic enzymes, tight junction proteins, efflux transporters), which are present in the nasal passages (Miragall et al., 1994; Hussar et al., 2002; Graff and Pollack, 2003; Kandimalla and Donovan, 2005a; Takano et al., 2005), may not be fully functional during the maturation of ORNs. The nasal barrier to the CNS could be considered "leaky" (Balin et al., 1986) from the constant turnover of the ORNs. Special Schwann cell-like cells called olfactory ensheathing cells (OECs) envelope the axons of ORNs and have an important role in axonal regeneration, regrowth, and remyelination (Field et al., 2003; Li et al., 2005b; Li et al., 2005a). The OECs create continuous, fluid-filled perineurial channels that, interestingly, remain open, despite the degeneration and regeneration of ORNs (Williams et al., 2004).

Given the unique environment of the olfactory epithelium, it is possible for intranasally administered therapeutics to reach the CNS via extracellular or intracellular mechanisms of transport along olfactory nerves. Extracellular transport mechanisms involve the rapid movement of molecules between cells in the nasal epithelium, requiring only several minutes to 30 minutes for a drug to reach the olfactory bulbs and other areas of the CNS after intranasal administration (Balin et al., 1986; Frey, 2002). Transport likely involves bulk flow mechanisms (Thorne and Frey, 2001; Thorne et al., 2004) within the channels created by the OECs (Figure 1, Box B). Drugs may also be propelled within these channels by the structural changes that occur during depolarization and axonal propagation of the action potential in adjacent axons (Luzzati et al., 2004). Intracellular transport mechanisms involve the uptake of molecules into

ORNs by passive diffusion, receptor-mediated endocytosis or adsorptive endocytosis, followed by slower axonal transport, taking several hours to days for a drug to appear in the olfactory bulbs and other brain areas (Kristensson and Olsson, 1971; Broadwell and Balin, 1985; Baker and Spencer, 1986). Intracellular transport in ORNs has been demonstrated for small, lipophilic molecules such as gold particles (de Lorenzo, 1970; Gopinath et al., 1978), aluminum salts (Perl and Good, 1987), and for substances with receptors on ORNs such as wheat-germ agglutinin conjugated to horseradish peroxidase (Shipley, 1985; Baker and Spencer, 1986; Itaya et al., 1986; Thorne et al., 1995).

Intracellular mechanisms, while important for certain therapeutics, are not likely to be the predominant mode of transport into the CNS. The vast majority of published intranasal studies demonstrate rapid delivery, with high CNS concentrations and effects observed almost immediately after or within an hour of intranasal administration, consistent with extracellular mechanisms of transport (Banks et al., 2004; Hanson et al., 2004; Ross et al., 2004; Thorne et al., 2004; Charlton et al., 2008; Hashizume et al., 2008; Nonaka et al., 2008). Further, receptor-mediated transport mechanisms involve specific interactions and cannot account for the broad spectrum of therapeutics shown to be delivered to the CNS following intranasal administration. It has been shown, at least for large molecules such as NGF and insulin-like growth factor-I (IGF-I), that intranasal delivery into the brain is non-saturable and not receptor mediated (Chen et al., 1998; Thorne et al., 2004; Zhao et al., 2004), suggesting that extracellular processes predominate.

1.2.2 Trigeminal Nerve Pathways

An often overlooked but important pathway connecting the nasal passages to the CNS involves the trigeminal nerve, which arises in the lamina propria of the respiratory region of the nasal passages and enters the CNS in the pons (Gray, 1978; Clerico et al., 2003). The cellular composition of the respiratory region is different from that of the olfactory region, with ciliated epithelial cells distributed among mucous secreting goblet cells (Figure 1, Box A). These cells contribute to mucociliary clearance mechanisms that remove mucous along with foreign substances from the nasal cavity to the nasopharynx. The trigeminal nerve conveys sensory information from the nasal cavity, the oral cavity, the eyelids, and the cornea, to the CNS via the ophthalmic division (V1), the maxillary division (V2), or the mandibular division (V3) of the trigeminal nerve (Gray, 1978; Clerico et al., 2003). Branches from the ophthalmic division of the trigeminal nerve provide innervation to the dorsal nasal mucosa and the anterior portion of the nose, while branches of the maxillary division provide innervation to the lateral walls of the nasal mucosa. The mandibular division of the trigeminal nerve extends to the lower jaw and teeth, with no direct neural inputs to the nasal cavity. The three branches of the trigeminal nerve come together at the trigeminal ganglion and extend centrally to enter the brain at the level of the pons, terminating in the spinal trigeminal nuclei in the brainstem. Interestingly, a small portion of the trigeminal nerve also terminates in the olfactory bulbs (Schaefer et al., 2002). As a result, a unique feature of the trigeminal nerve is that it enters the brain from the respiratory epithelium of the nasal passages at two sites: (1) through the anterior lacerated foramen near the pons and (2) through the cribriform plate near the olfactory

bulbs, creating entry points into both caudal and rostral brain areas following intranasal administration. While there are no published reports of ensheathing cells and channels associated with the trigeminal nerve comparable to those observed with the olfactory nerves, these anatomical features may be present along the trigeminal nerve.

Intranasal drug delivery along trigeminal pathways was first clearly demonstrated for ^{125}I-IGF-I, where high levels of radioactivity were observed in the trigeminal nerve branches, trigeminal ganglion, pons, and olfactory bulbs, consistent with delivery along both trigeminal and olfactory nerves (Thorne et al., 2004). Because one portion of the trigeminal neural pathway enters the brain through the cribriform plate alongside the olfactory pathway, it is difficult to distinguish whether intranasally administered drugs reach the olfactory bulb and other rostral brain areas via the olfactory or trigeminal pathways or if both are involved. Intranasal studies with other proteins and peptides, including interferon-β1b (IFN-β1b) (Ross et al., 2004; Thorne et al., 2008), hypocretin-1(orexin-A) (Hanson et al., 2004; Dhuria et al., 2009), and peptoids (Ross et al., 2008), found similar results of high levels of radioactivity in the trigeminal nerve. It is important to note that these results came from one lab and that drug concentrations in the trigeminal nerve are not commonly measured in intranasal delivery studies. Other researchers have found significant drug distribution to caudal brain areas such as the brainstem and cerebellum after intranasal delivery, suggesting the involvement of the trigeminal nerves, though researchers were likely unaware of this pathway (Dufes et al., 2003; Banks et al., 2004; Charlton et al., 2008).

1.2.3 Vascular Pathways

Traditionally, the intranasal route of administration has been utilized to deliver drugs to the systemic circulation via absorption into the capillary blood vessels underlying the nasal mucosa. The nasal mucosa is highly vascular, receiving its blood supply from branches of the maxillary, ophthalmic and facial arteries, which arise from the carotid artery (Cauna, 1982; Clerico et al., 2003). The olfactory mucosa receives blood from small branches of the ophthalmic artery, whereas the respiratory mucosa receives blood from a large caliber arterial branch of the maxillary artery (DeSesso, 1993). The relative density of blood vessels is greater in the respiratory mucosa compared to the olfactory mucosa (Figure 1, Box A), making the former region an ideal site for absorption into the blood (DeSesso, 1993). The vasculature in the respiratory region contains a mix of continuous and fenestrated endothelia (Van Diest and Kanan, 1979; Grevers and Herrmann, 1987), allowing both small and large molecules to enter the systemic circulation following nasal administration.

Delivery to the CNS following absorption into the systemic circulation and subsequent transport across the BBB is possible, especially for small, lipophilic drugs, which more easily enter the blood stream and cross the BBB compared to large, hydrophilic therapeutics such as peptides and proteins. It is also possible that rather than being distributed throughout the systemic circulation, drugs can enter the venous blood supply in the nasal passages where they are rapidly transferred to the carotid arterial blood supply feeding the brain and spinal cord, a process known as counter-current transfer (Einer-Jensen and Larsen, 2000b, a; Stefanczyk-Krzymowska et al., 2000; Skipor et al., 2003; Einer-Jensen and Hunter, 2005). However, delivery through

the systemic circulation results in problems related to drug elimination via hepatic and renal mechanisms, and is limited by other factors including: the BBB, drug binding to plasma proteins, degradation by plasma proteases, and potential peripheral side effects.

Increasing evidence is emerging suggesting that mechanisms involving channels associated with blood vessels, or perivascular channels, are involved in intranasal drug delivery to the CNS (Figure 1, Box A and Box C). Perivascular spaces are bound by the outermost layer of blood vessels and the basement membrane of the surrounding tissue (Pollock et al., 1997). These perivascular spaces act as a lymphatic system for the brain, where neuron-derived substances are cleared from brain interstitial fluid by entering perivascular channels associated with cerebral blood vessels (Figure 1, Box C). For example, radiolabeled tracers, India ink, and amyloid beta, have been shown to be cleared from the brain via perivascular spaces (Bradbury et al., 1981; Yamada et al., 1991; Zhang et al., 1992; Weller and Nicoll, 2003; Li et al., 2005c; Carare et al., 2008). Perivascular transport is due to bulk flow mechanisms, as opposed to diffusion alone (Cserr et al., 1981; Groothuis et al., 2007), and arterial pulsations are also a driving force for perivascular transport (Rennels et al., 1985; Rennels et al., 1990). The resulting "perivascular pump" can account for the rapid distribution of therapeutics throughout the brain (Hadaczek et al., 2006; Schley et al., 2006). Intranasally applied drugs can move into perivascular spaces in the nasal passages or after reaching the brain and the widespread distribution observed within the CNS could be due to perivascular transport mechanisms (Thorne et al., 2004). Several intranasal studies show high levels of drug present in the walls of cerebral blood vessels and carotid arteries, even after

removal of blood by saline perfusion (Thorne et al., 2004; Thorne et al., 2008; Dhuria et al., 2009), suggesting that drugs can gain access to perivascular spaces.

1.2.4 Pathways Involving the Cerebrospinal Fluid and Lymphatics

Pathways connecting the subarachnoid space containing CSF, perineurial spaces encompassing olfactory nerves, and the nasal lymphatics are important for CSF drainage and these same pathways provide access for intranasally applied therapeutics to the CSF and other areas of the CNS. Several studies document that tracers injected into the CSF in the cerebral ventricles or subarachnoid space drain to the underside of the olfactory bulbs into channels associated with olfactory nerves traversing the cribriform plate and reach the nasal lymphatic system and cervical lymph nodes (Bradbury and Westrop, 1983; Kida et al., 1993; Johnston et al., 2004; Hatterer et al., 2006; Walter et al., 2006b; Walter et al., 2006a). Drugs can access the CNS via these same pathways after intranasal administration, moving from the nasal passages to the CSF to the brain interstitial spaces and perivascular spaces for distribution throughout the brain (Figure 1, Box C). These drainage pathways are significant in a number of animal species (sheep, rabbits, and rats) accounting for approximately 50% of CSF clearance (Bradbury et al., 1981; Cserr et al., 1992; Boulton et al., 1996; Boulton et al., 1999). However, in humans, solutes are primarily cleared into the blood due to pressure differences at arachnoid granulations present on blood vessels in the subarachnoid space. Pathways between the nasal passages and the CSF are still important and functional in humans, evidenced by the fact that therapeutics are directly delivered to

the CSF following intranasal delivery, without entering the blood to an appreciable extent (Born et al., 2002).

A number of intranasal studies demonstrate that drugs gain direct access to the CSF from the nasal cavity, followed by subsequent distribution to the brain and spinal cord. Many intranasally applied molecules rapidly enter the CSF, and this transport is dependent on the lipophilicity, molecular weight, and degree of ionization of the molecules (Kumar et al., 1974; Sakane et al., 1994; Sakane et al., 1995; Born et al., 2002; Dhanda et al., 2005; Wang et al., 2007). Assessing distribution into the CSF can provide information on the mechanism of intranasal delivery. For example, observing a decreasing concentration gradient from the CSF to brain tissues or observing drug distribution to brain areas distant from the olfactory bulbs are consistent with distribution via the CSF (Banks et al., 2004). However, trigeminal-mediated transport also plays a role in distribution of intranasally administered drugs to brain areas distant from the olfactory bulbs (Ross et al., 2004; Thorne et al., 2004). It is difficult to experimentally separate contributions of different pathways into the CNS after intranasal administration. As will be discussed in the subsequent sections, transport pathways into the CNS can be influenced by experimental factors and formulation characteristics.

1.3 Experimental Considerations

It is important to consider the different methodologies used in intranasal studies, since factors such as head position, method of delivery, including surgical interventions

(for animal studies), and delivery volume, can all influence drug deposition in the nasal cavity and the pathway a drug follows to the CNS after intranasal administration.

1.3.1 Head Position

The majority of preclinical work has been carried out in anesthetized mice and rats, with animals positioned in the supine position. In experiments evaluating dye deposition in the nasal passages, Thorne and Frey (1995) found that nose drops administered to animals lying on their backs resulted in consistent deposition in the olfactory epithelium (Thorne et al., 1995). Optimal delivery to the CNS along neural pathways required targeting of the drug to the upper-third of the nasal cavity (Frey, 1997). Van den Berg (2002) found that different head positions can alter absorption into the blood and CSF following nasal administration to rats when a tube inserted into the nostrils was used to deliver the drug solution (van den Berg et al., 2002). A supine position with the head angle at 70° or 90° was found to be most suitable for efficient delivery to the CSF using this method of intranasal administration. This head position would also likely favor drainage into the esophagus and trachea, which is why most researchers position animals with the head at 0° (horizontal). For chronic dosing regimens, Hanson et al. (2004) developed an intranasal method for delivery in unanesthetized mice (Hanson et al., 2004). The efficiency of delivery to brain tissues is approximately 5-fold less with awake intranasal administration because of the reduced time that mice are held in position on their backs (Hanson et al., 2004). Rats generally do not tolerate intranasal delivery in the unanesthetized state; however there are some reports of effective, minimal stress, intranasal delivery techniques in freely moving rats

(Danhof et al., 2008). Repeated use of isoflurane or ketamine anesthesia can be effective for chronic dosing in rats.

In nonhuman primate and clinical studies, different head positions can also influence the deposition of nasal drops in the nasal cavity (Raghavan and Logan, 2000; Thorne, 2002). When the head is tilted back, a liquid latex dye was shown to deposit primarily on the floor of the nasal cavity (Raghavan and Logan, 2000). When the head is extended off the side of a bed to tilt the head back further (Mygind's position) or when the head is positioned on the side and down (Ragan position), the dye reached the respiratory region of nasal cavity (Raghavan and Logan, 2000). The most promising position for targeting the olfactory region is with the "praying to Mecca" position, with the head-down-and-forward, however this position can be uncomfortable for patients, which could result in compliance issues.

1.3.2 Administration Technique

Differences in administration techniques employed by researchers can affect deposition within the nasal epithelium and delivery along pathways to the CNS. For intranasal drug administration in anesthetized mice and rats, several researchers, administer nose drops over a period of 10-20 minutes using a pipettor for delivering drops to alternating nostrils every 1-2 minutes to allow the solution to be absorbed into the nasal epithelium (Capsoni et al., 2002; Ross et al., 2004; Thorne et al., 2004; Dhuria et al., 2008; Francis et al., 2008; Martinez et al., 2008; Ross et al., 2008; Dhuria et al., 2009). This noninvasive method does not involve inserting the pipet tip into the nostril. Instead, drops are placed at the opening of the nostril, allowing the animal to sniff the

drop into the nasal cavity. For rats, which are obligatory nose breathers, the opposite nostril is occluded while introducing the nose drop to allow the drop to be "sniffed" forcefully to deliver the formulation to the respiratory and olfactory epithelia (Thorne et al., 1995). Other administration methods in anesthetized rats involve sealing the esophagus and inserting a breathing tube into the trachea to prevent the nasal formulation from being swallowed and to eliminate issues related to respiratory distress (Chow et al., 1999; Chow et al., 2001; Dahlin et al., 2001; Fliedner et al., 2006). Flexible tubing can be inserted into the nostrils for localized delivery of a small volume of the drug solution to the respiratory or olfactory epithelia, depending on the length of the tubing (Chow et al., 1999; van den Berg et al., 2002; Van den Berg et al., 2003; Banks et al., 2004; van den Berg et al., 2004b; Vyas et al., 2006b; Charlton et al., 2007b; Gao et al., 2007). When using tubing for intranasal administration, care must be taken to avoid damaging the nasal mucosa and to avoid delivery through the nasopharynx into the mouth and throat. It is also important to note that the length of the tubing can affect deposition in the respiratory and olfactory epithelia and delivery to the CNS and blood (Charlton et al., 2007b).

In clinical studies, nasal delivery devices, such as sprays, nose droppers or needle-less syringes, can target the drug to different regions of the nasal cavity. OptiMist^{TM} is a breath actuated device that targets liquid or powder nasal formulations to the nasal cavity, including the olfactory region, without deposition in the lungs or esophagus (Djupesland et al., 2006). This device is promising for targeting therapeutics to the olfactory epithelium for direct transport into the CNS along olfactory nerves; however studies so far have only evaluated deposition patterns and clearance rates in

the nasal cavity. The ViaNase™ device can also be used to target a nasal spray to the olfactory and respiratory epithelia of the nasal cavity. Nasal drops tend to deposit on the nasal floor and are subjected to rapid mucociliary clearance, while nasal sprays are distributed to the middle meatus of the nasal mucosa (Scheibe et al., 2008). For intranasal insulin, use of a needle-less syringe (Reger et al., 2006) or the ViaNase™ electronic atomizer (Reger et al., 2008a) have been shown to be effective to improve memory in patients with Alzheimer's disease. Efficient delivery to the CNS can be achieved in humans by selecting the right combination of head position and delivery device to target the therapeutics to specific regions of the nasal cavity.

1.3.3 Volume

While differences in delivery volumes can affect the deposition within the nasal cavity and distribution to the CNS, no systematic studies have been published that evaluate the effect of solution volume on the efficiency of intranasal delivery to the CNS. Delivery volume is important in terms of covering the surface area of the nasal passages in order for the drug to reach the respiratory and olfactory epithelia for transport to the CNS along trigeminal and olfactory neural pathways. The olfactory system in rodents is far more extensive as compared to humans, with the olfactory region in rats occupying approximately 50% of the surface area of the nasal cavity (Gross et al., 1982) and with a nasal cavity volume of 0.26 cm^3 (DeSesso, 1993; Gao et al., 2007). In the majority of intranasal studies, rats receive a total volume of 40-100 μL given as 6-10 μL nose drops using a pipettor or given all at once using flexible tubing. The volume of the nose drop can also affect deposition in the nasal passages, where a

small volume drop (i.e. 2 μL) will likely result in deposition primarily in the respiratory epithelium and a large volume drop (i.e. 20 μL) will result in deposition in the nasopharynx and could lead to respiratory distress. If tubing is used for drug administration, lower volumes of 20-40 μL are used for intranasal delivery because there is less surface area to cover (van den Berg et al., 2002; Van den Berg et al., 2003; van den Berg et al., 2004a; Charlton et al., 2007a; Gao et al., 2007). In mice, a total volume of 24 μL is administered in 3-4 μL nose drops. This total volume is less than the volume of the nasal cavity in mice (0.032 cm^3) (Gross et al., 1982). In humans, the nasal cavity has a volume of 25 cm^3 and the olfactory region occupies 8% of the nasal cavity surface area (DeSesso, 1993). Delivery volumes of 0.4 mL administered in 100 μL aliquots are sufficient to have CNS effects in humans (Reger et al., 2006; Benedict et al., 2007; Hallschmid et al., 2008; Reger et al., 2008a; Reger et al., 2008b).

Despite anatomical differences between rodents and humans, similar pathways are involved in intranasal delivery to the CNS, at least for IFNβ-1b in rats and primates (Thorne et al., 2008) and for melatonin and rats and humans (van den Berg et al., 2004b). Translation into the clinic is currently underway, with clinical trials of intranasal treatments for Alzheimer's disease demonstrating success (Born et al., 2002; Benedict et al., 2007; Gozes and Divinski, 2007; Reger et al., 2008a; Reger et al., 2008b). This is a testament to the fact that the same direct pathways into the CNS utilized in animals are also important and functional in humans.

1.3.4 Assessment of CNS Distribution

Assessing concentrations and distribution to different brain areas provides insight into pathways followed to the CNS after intranasal administration. For example, greater distribution in the olfactory bulbs and frontal cortex compared to the cerebellum and brainstem would be consistent with pathways involving the olfactory nerves following intranasal administration. Whole brain measurements of drug concentration generally underestimate the extent of distribution because of dilution effects and do not provide any information about pathways and mechanisms underlying delivery to the CNS after nasal administration. In many studies, drug concentrations in the CSF act as a surrogate for brain exposure, particularly in studies conducted in humans, even though concentrations in brain and CSF compartments are not necessarily the same.

Perhaps of greater importance is the evaluation of drug targeting, which evaluates the relative distribution of the drug to therapeutic target sites (i.e. brain or specific brain area) compared to exposure to non-target sites (i.e. blood, spleen or other peripheral tissues). Intravenous delivery is used as a control for evaluating blood-mediated delivery to the CNS. Since concentrations observed in the CNS after intranasal administration could be due to absorption into the nasal vasculature followed by distribution from the systemic circulation, intravenous delivery controls for distribution into the CNS from the blood. Comparing ratios of brain concentrations to blood concentrations after intranasal and intravenous administration provides an assessment of direct transport to the brain (Chow et al., 1999; Dhuria et al., 2008, 2009). Brain-to-blood ratios that are greater with intranasal compared to intravenous administration indicate that direct pathways other than the vasculature are important for

transport from the nasal cavity to the CNS. An alternative to determining brain-to-blood concentration ratios includes designing experiments such that blood exposure after intranasal and intravenous administration are similar (i.e. similar AUC) (Ross et al., 2004; Thorne et al., 2004), which allows for direct comparisons of concentrations between different routes of administration. Drug targeting efficiency (DTE) or the drug targeting index (DTI) compares the ratio of the brain AUC/blood AUC after intranasal administration to that after intravenous administration (Zhang et al., 2004b; Dhuria et al., 2008). Direct transport percentage (DTP), which can be derived from the DTE, determines the fraction of the brain AUC observed after intranasal administration involving pathways other than the vasculature (Zhang et al., 2004b; Dhuria et al., 2008). Intranasal compared to intravenous administration generally results in greater brain-to-blood ratios and drug targeting efficiency. These measures are helpful in comparing findings across different studies conducted in different labs and are useful for assessing the effects of formulations on enhancing intranasal delivery to the CNS.

1.4 Formulation Considerations

Protective barriers in the nasal mucosa contribute to the low efficiency of delivery observed following intranasal administration, with typically less than 1% of the administered dose reaching the brain (Thorne and Frey, 2001; Illum, 2004). Research efforts have focused on the development of formulation strategies to overcome the barriers present in the nasal mucosa to improve intranasal delivery efficiency and targeting to the CNS. Nasal mucociliary clearance mechanisms are in place to remove foreign substances towards the nasopharynx, which is accomplished by dissolution of

substances in the mucus layer and transport by ciliated cells in the nasal epithelium. Efflux transport proteins, such as p-glycoprotein (P-gp) and multidrug resistance-associated protein (MRP1), are expressed in the nasal mucosa (Wioland et al., 2000; Graff and Pollack, 2005; Kandimalla and Donovan, 2005b), and can significantly limit the uptake of substrates into the brain (Graff and Pollack, 2003; Graff et al., 2005; Kandimalla and Donovan, 2005). In addition, there is evidence of drug metabolizing enzymes (Sarkar, 1992; Minn et al., 2002) and tight junction proteins (Miragall et al., 1994) in the nasal epithelium, which can limit the efficiency of intranasal delivery to the CNS. The nasal vasculature can also be a limiting factor as it clears inhaled toxins and intranasally applied therapeutics into the systemic circulation for detoxification and elimination. Common themes in formulation approaches to overcome these barriers involve improving drug solubility, increasing permeability across the nasal epithelium, reducing clearance from the nasal passages, or a combination approach. While recently published reviews discuss formulation considerations for intranasal delivery (Vyas et al., 2006a; Costantino et al., 2007), here we focus on how changes in formulation parameters can affect CNS distribution and drug targeting after intranasal administration.

1.4.1 Formulation Strategies to Improve Drug Solubility

In order for a therapeutic to have adequate absorption and bioavailability in the CNS after intranasal administration, it should have sufficient solubility at the site of delivery in the nasal epithelium. Drugs can be encapsulated in carriers, such as cyclodextrins, microemulsions, and nanoparticles, to overcome these issues for

intranasal delivery to the CNS. Cyclodextrin inclusion complexes containing a hydrophobic cavity and a hydrophilic shell improve the solubility of poorly water-soluble drugs, enhancing brain uptake after intranasal administration. Alpha-cyclodextrin loaded with galanin-like peptide (GALP) enhanced delivery to all brain regions by 2- to 3-fold, with the greatest uptake in the olfactory bulbs and hypothalamus, while beta-cyclodextrin enhanced uptake of GALP specifically to the olfactory bulbs compared to an intranasal solution (Nonaka et al., 2008). Since alpha-cyclodextrin resulted in increased concentrations throughout the brain, this formulation likely affects blood-mediated pathways into the CNS. Beta-cyclodextrin appears to specifically enhance intranasal delivery to the CNS along olfactory pathways.

Microemulsion and nanoemulsion formulations can improve drug solubility and opportunities for direct transport into the CNS. These oil-in-water dispersions demonstrate increased brain uptake for small molecule therapeutics such as clonazepam (Vyas et al., 2006b), sumatriptan (Vyas et al., 2006c), risperidone (Kumar et al., 2008), zolmitriptan (Vyas et al., 2005b), and nimodipine (Zhang et al., 2004a; Zhang et al., 2004b). However, for clonazepam, sumatriptan succinate, and risperidone, the increased brain uptake was accompanied by increased uptake into the blood, resulting in drug targeting efficiencies that were comparable to simple intranasal solutions. Increased systemic exposure can lead to adverse side effects, which could be problematic for certain therapeutics. Studies with nimodipine showed the greatest increase in targeting in the olfactory bulbs (4.5-fold); suggesting that delivery along olfactory pathways was enhanced with this microemulsion formulation approach. An emulsion-like formulation was recently patented for use with water-insoluble peptides

and proteins (Hanson et al., 2008), though no data evaluating CNS distribution has been published using this intranasal formulation.

Polymeric nanoparticles, comprised of a hydrophobic core of polylactic acid (PLA) and a hydrophilic shell of methoxy-poly(ethylene glycol) (MPEG), have been evaluated for improving solubility and intranasal drug targeting to the CNS. Unlike the microemulsion formulation of nimodipine, nimodipine loaded into MPEG-PLA nanoparticles resulted in the greatest targeting increase to the CSF (14-fold) compared to a simple nimodipine solution, indicating that pathways involving the CSF were affected with this nanoparticle formulation (Zhang et al., 2006). The regional differences in targeting between the microemulsion and nanoparticle nimodipine formulations could be due to differences in particle size. Dramatic increases in CSF targeting using nanoparticles are not always observed. For example, chitosan nanoparticles loaded with estradiol modestly improved targeting to the CSF by 1.3-fold compared to an intranasal solution (Wang et al., 2006b; Wang et al., 2008). Taken together, these formulation approaches to improve solubility show promise for enhancing intranasal delivery efficiency to the CNS.

1.4.2 Formulations Affecting Membrane Permeability

In addition to solubility, efficient delivery to the CNS following intranasal administration is dependent on membrane permeability. For peptides and proteins or for hydrophilic compounds, where paracellular transport is hindered due to size and polarity, improving membrane permeability could enhance extracellular mechanisms of transport to the CNS via olfactory and trigeminal nerves. One approach to modifying

membrane permeability within the nasal epithelium is by using permeation enhancers, such as surfactants, bile salts, lipids, cyclodextrins, polymers, and tight junction modifiers. These compounds are often accompanied by nasal toxicity and increased permeation into the nasal vasculature, which could be problematic for therapeutics with systemic side effects. While there has been considerable research studying the effect of permeation enhancers on systemic absorption after intranasal delivery (Davis and Illum, 2003; Chen et al., 2006), there have been few reports evaluating effects on CNS distribution. However, *in situ* nasal perfusion studies evaluating brain uptake of VIP showed that the permeation enhancer, lauroylcarnitine (LC), improved brain uptake compared to a formulation without the permeation enhancer (Dufes et al., 2003). Effects of LC on VIP blood absorption were not reported in this study, so it is possible that the increased delivery to the brain could have been due to increased delivery to the blood.

Effects of changes in formulation parameters, such as osmolarity, on brain uptake of intranasal VIP were also evaluated (Dufes et al., 2003). Changes in osmolarity of a formulation can cause cells to expand or shrink, enhancing intracellular or extracellular transport mechanisms along olfactory and trigeminal nerves to the CNS. A hypertonic nasal solution was found to reduce VIP brain uptake after intranasal administration compared to an isotonic solution (Dufes et al., 2003). In addition to cell shrinking, it is possible that the hypertonic solution caused additional changes, such as increased mucus secretion, that hindered transport into the brain. No other studies have reported effects of osmolarity on CNS distribution of intranasally applied therapeutics.

The pH of the nasal formulation and ionization state of the drug can affect intranasal delivery efficiency to the CNS. Sakane (1994) showed that delivery of sulphisomidine to the CSF following intranasal administration increased as the fraction of unionized drug increased (Sakane et al., 1994). Similarly, brain uptake of VIP was greater when the peptide was in the unionized form at pH 9 compared to the positively charged peptide at pH 4 (Dufes et al., 2003). Green fluorescent protein conjugated to a cationization agent had limited uptake into the brain following intranasal administration, however when the pH was lowered to reduce the ionic interaction with the nasal epithelial cells, greater brain penetration was observed (Loftus et al., 2006). Positively charged drugs may form electrostatic interactions with the negatively charged nasal epithelial cells, effectively hindering transport beyond the nasal mucosa and into the brain. These findings may be drug-dependent since in a different study, negatively charged drugs were shown to have greater CNS bioavailability after intranasal administration compared to a neutral drug of similar size and lipophilicity (Charlton et al., 2008). There have not been many systematic studies that evaluate the effect of osmolarity and pH of nasal formulations on extracellular or intracellular mechanisms of delivery to the CNS.

1.4.3 Strategies to Reduce Clearance and Increase Residence Time

Mucociliary clearance mechanisms rapidly remove drugs from the delivery site, reducing contact with the nasal epithelium and delivery into the CNS after intranasal administration. Several approaches, including use of mucoadhesive agents, surface-engineered nanoparticles, efflux transporter inhibitors, and vasoconstrictors, have been

utilized to reduce clearance, to prolong the residence time of the formulation at the delivery site, and to increase transport along direct pathways to the CNS. Increasing the residence time at the delivery site potentially enhances delivery into the CNS along olfactory and trigeminal nerves, the vasculature, or CSF and lymphatic channels. When mucoadhesives, which adhere to the mucous membranes lining the nasal mucosa, were added to microemulsion formulations discussed in the previous section, drug targeting to the CNS was significantly increased (Vyas et al., 2005b; Vyas et al., 2006b, c; Jogani et al., 2008; Kumar et al., 2008). Addition of a mucoadhesive (sodium hyaluronate) and an emulsifying agent (castor oil, Cremophor RH40) to a nasal formulation of fluorescein isothiocyanate (MW 4400) increased uptake into different brain areas without affecting plasma levels (Horvat et al., 2008). Certain mucoadhesives, such as acrylic acid derivatives, lectin, and low methylated pectin, form a viscous gel upon contact with the nasal epithelium, resulting in reduced clearance from the administration site (Barakat et al., 2006; Charlton et al., 2007; Zhao et al., 2007; Cai et al., 2008). Chitosan, a cationic mucoadhesive, forms electrostatic interactions with the negatively charged surface of epithelial cells to reduce clearance from the nasal epithelium. Chitosan has the additional effect of reversibly opening tight junctions, with potential to increase extracellular transport along olfactory and trigeminal nerve pathways into the CNS. However, *in vivo* studies showed that compared to a simple intranasal solution, nasal formulations of a zwitterionic drug containing low methylated pectins or chitosan reduced uptake into the olfactory bulbs, while increasing uptake into the plasma, effectively reducing targeting to the olfactory bulbs (Charlton et al., 2007b). These additives affect delivery into the blood rather than increasing transport into the brain via

direct pathways. Mucoadhesives used in combination with microemulsion formulations show the greatest potential in terms of enhancing brain uptake and drug targeting to the CNS.

Surface engineering of nanoparticles with ligands that bind to specific cell surfaces is a promising approach to reduce clearance and enhance targeted delivery to the CNS. For example, the lectin, ulex europeus agglutinin I (UEA I), binds to receptors located predominantly in the olfactory epithelium, while wheat germ agglutinin (WGA) recognizes sugar molecules and binds to receptors expressed throughout the olfactory and respiratory epithelia. UEA I nanoparticles could enhance delivery to the CNS along olfactory pathways, whereas WGA nanoparticles could enhance delivery to the CNS along multiple pathways, including neural and vascular pathways. Intranasal studies using UEA I or WGA conjugated PEG-PLA nanoparticles loaded with a fluorescent marker resulted in increased delivery to different brain areas, including the olfactory bulbs, olfactory tract, cerebrum, and cerebellum, compared to a unmodified nanoparticles (Gao et al., 2006; Gao et al., 2007a). WGA nanoparticles, but not UEA I nanoparticles, also increased delivery into the blood. This finding is likely due to the nonspecific binding of WGA throughout the nasal epithelium compared to UEA I nanoparticles, which bypass the highly vascular respiratory epithelium. As a result, drug targeting to the CNS was greatest for the UEA I conjugated nanoparticle formulation. However, no regional differences in CNS distribution were observed with these formulation approaches. WGA conjugated nanoparticles carrying the therapeutic peptide, VIP, were shown to enhance brain uptake, with the greatest exposure observed in the cerebellum, without dramatically increasing blood absorption, and to improve

spatial memory in an Alzheimer's mouse model compared to unmodified particles (Gao et al., 2007), indicating that surface engineered nanoparticles have therapeutic potential following intranasal administration.

Reducing clearance from the nasal cavity due to efflux from transport proteins or due to absorption into the nasal vasculature are additional strategies that have been explored to increase the residence time at the delivery site and to enhance intranasal delivery efficiency to the CNS. Intranasal pretreatment with an inhibitor (rifampin) of the P-gp efflux transport protein prior to intranasal administration of a P-gp substrate (verapamil) resulted in significantly greater brain uptake as a result of reduced clearance from P-gp-mediated efflux (Graff and Pollack, 2003). Reducing clearance into the blood from the site of delivery by using a vasoconstrictor could allow more of the drug to be available for direct transport into the CNS. Intranasal administration of hypocretin-1 with the vasoconstrictor, phenylephrine, resulted in reduced absorption of hypocretin-1 into the blood (Dhuria et al., 2009). The reduced clearance from the nasal epithelium into the blood led to increased deposition in the olfactory epithelium and increased delivery along olfactory nerve pathways to the olfactory bulbs. However, concentrations in the trigeminal nerve and in remaining brain areas were reduced with the vasoconstrictor nasal formulation. These findings are in contrast to a study evaluating a different vasoconstrictor (ephedrine), where drug concentrations in the blood and brain were increased (Charlton et al., 2007b), suggesting the need for additional studies to understand the effect of vasoconstrictors on mechanisms underlying intranasal delivery to the CNS.

1.5 The Future of Intranasal Delivery to the CNS

This review has discussed the pathways and mechanisms involved in intranasal delivery to the CNS. In addition to olfactory pathways and vascular pathways into the CNS following intranasal administration, there is clear evidence that pathways involving trigeminal nerves, perivascular channels, the CSF, and lymphatic channels are also significant for transport from the nasal mucosa to the CNS. Drug transport within or along these pathways is governed by diffusion, bulk flow, perivascular pumping, and other mechanisms. This review has also highlighted how experimental factors including head position, delivery techniques, and volume can affect the deposition of the drug formulation within the nasal passages and the pathway a drug follows into the CNS following intranasal administration. Moreover, the characteristics of the drug formulation, such as the osmolarity, pH, or addition of enhancers, can influence deposition in the nasal cavity and transport pathways to the CNS. Emulsion-like formulations used in combination with mucoadhesive agents demonstrate great potential for enhancing targeted delivery to the CNS following intranasal administration.

Despite enormous progress that has been made over the last several decades since the introduction of the intranasal method to directly deliver therapeutics to the brain, considerable research remains in the area of intranasal delivery. Since neurological disease does not generally affect the brain in a global manner, additional formulation strategies will be required to improve the delivery efficiency and to target therapeutics to specific brain areas requiring treatment. For example, development of formulations that specifically target the trigeminal nerve could be used to specifically

deliver therapeutics to the brainstem and cerebellum for treating Parkinson's disease. Similarly, formulations designed to target the olfactory nerves could be used to deliver therapeutics to the olfactory bulbs and frontal cortex for treating Alzheimer's disease, dementia, and personality disorders. The future of this field lies in designing studies to elucidate the underlying mechanisms of intranasal drug delivery to the CNS and using this knowledge to develop formulation strategies and delivery devices to improve the treatment of neurological and psychiatric diseases.

Figure 1: Pathways of Drug Distribution in the Nasal Cavity and Central Nervous System. Following intranasal administration, drugs (blue circles) come into contact with the nasal mucosa, which is innervated by olfactory and trigeminal nerves. The nasal mucosa is comprised of the nasal epithelium, which contains different cell types, and the underlying lamina propria, which contains blood vessels, axons, glands, and connective tissue. (A) In the respiratory region, ciliated epithelial cells and goblet cells in the respiratory epithelium form the basis of mucociliary clearance mechanisms, which remove foreign substances towards the nasopharynx for elimination. In the olfactory region, olfactory receptor neurons are interspersed among supporting cells and basal cells to form the olfactory epithelium. The blood supply to the respiratory epithelium is relatively greater compared to the olfactory epithelium, making it an ideal site for systemic absorption. Drugs can be transported through the nasal mucosa to the CNS by entering perivascular channels (dashed lines surrounding blood vessels) in the lamina propria or via extracellular or intracellular mechanisms (dashed arrows). (B) After reaching the lamina propria, drugs can enter channels created by olfactory ensheathing cells surrounding the olfactory nerves, where they can access the cerebrospinal fluid (CSF) and olfactory bulbs (dashed arrows). (C) From the CSF, drugs can be distributed via bulk flow mechanisms and mix with brain interstitial fluid throughout the brain (dashed arrows). Drugs can also enter perivascular spaces after reaching the brain to be rapidly distributed throughout the CNS. These same pathways in the reverse direction are involved in the clearance of solutes from the CNS to the periphery.

Figure 1:

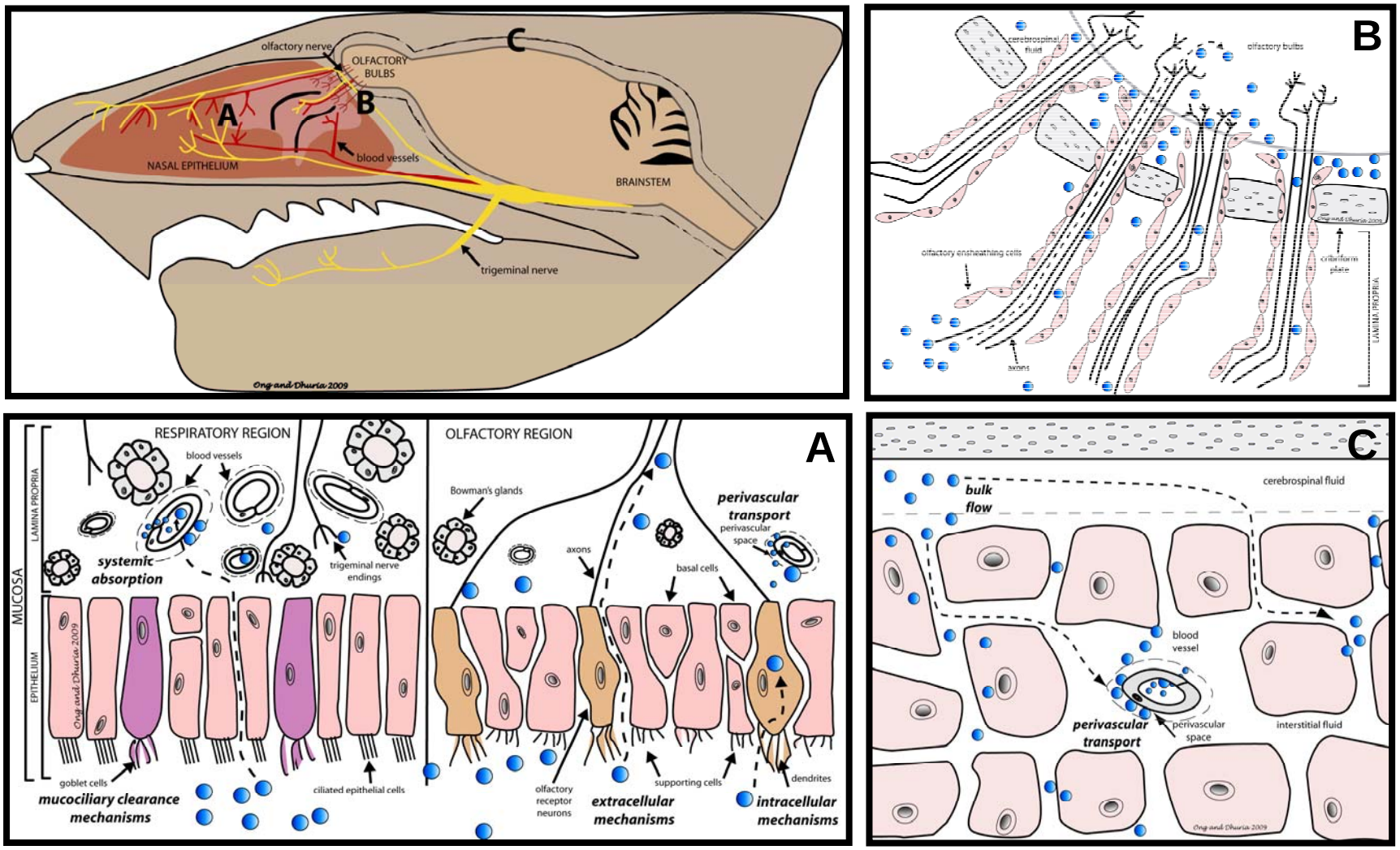
olfactory nerve
OLFACTORY BULBS
A
B
C
NASAL EPITHELIUM
blood vessels
BRAINSTEM
trigeminal nerve
Ong and Dhuria 2009
B
cerebrospinal fluid
olfactory bulbs
olfactory ensheathing cells
axons
LAMINA PROPRIA
RESPIRATORY REGION
OLFACTORY REGION
blood vessels
Bowman's glands
axons
basal cells
perivascular transport
perivascular space
systemic absorption
trigeminal nerve endings
MUCOSA
LAMINA PROPRIA
EPITHELIUM
goblet cells
ciliated epithelial cells
olfactory receptor neurons
supporting cells
dendrites
mucociliary clearance mechanisms
extracellular mechanisms
intracellular mechanisms
A
C
cerebrospinal fluid
bulk flow
blood vessel
perivascular transport
perivascular space
interstitial fluid

CHAPTER 2

INTRANASAL DRUG TARGETING OF HYPOCRETIN-1 (OREXIN-A) TO THE CENTRAL NERVOUS SYSTEM[1]

2.1 Introduction

Hypocretin-1 (HC, also known as orexin-A) is a neuropeptide synthesized in neurons of the hypothalamus of the central nervous system (CNS) that is involved in the regulation of appetite and the sleep-wake cycle, among other important physiological functions (Sakurai, 2002). Central administration of HC, either by direct microinjection into hypothalamic nuclei (Sweet et al., 1999) or by intracerebroventricular (ICV) administration (Sakurai et al., 1998), stimulates feeding in rats. Animal and human studies also clearly demonstrate an important role of HC in the regulation of sleep. In mice that lack the precursor protein to HC (Chemelli et al., 1999) and in mice that are genetically engineered to progressively lose hypocretin neurons (Hara et al., 2001), fragmented sleep patterns characteristic of the sleep disorder narcolepsy are apparent. Replacement of HC by ICV injection in these animals reduces episodes of cataplexy and restores fragmented sleep patterns to normal levels (Mieda et al., 2004). In humans, postmortem analysis of narcoleptic brain tissue shows significantly lower HC concentrations (Peyron et al., 2000) and loss of neurons synthesizing HC (Thannickal et al., 2000) compared to control brain tissue.

[1] Reprinted with permission from Wiley-Liss, Inc., a subsidiary of John Wiley & Sons, Inc.
Dhuria SV, Hanson LR, Frey WHF II. Intranasal drug targeting of hypocretin-1 (orexin-A) to the central nervous system. Journal of Pharmaceutical Sciences (2008) DOI:10.1002/jps.21604.

Delivery of HC or HC antagonists to the CNS may have therapeutic potential in the treatment of narcolepsy and obesity. However, an obstacle to the development of HC and other peptides and proteins as CNS therapeutic agents is their limited ability to cross the blood-brain barrier (BBB) to reach CNS drug targets at pharmacological levels following systemic administration. In addition within the systemic circulation, therapeutic peptides and proteins typically have short half-lives with distribution limited to the blood volume due to their large molecular weight, charge, and hydrophilic nature. Therapeutic CNS levels of HC, which has a molecular weight of 3,562 daltons, have been achieved in dogs following intravenous administration, however this route required large doses to improve cataplexy in HC deficient dogs (Fujiki et al., 2003). High systemic doses of HC are also accompanied by widespread distribution to peripheral tissues expressing HC receptors (Johren et al., 2001; Barreiro et al., 2005; Ehrstrom et al., 2005), which could lead to adverse effects. ICV injection into the lateral ventricles or injection into the brain parenchyma result in direct delivery to the brain and minimal systemic exposure, however, these techniques are invasive, costly, and impractical for translation into humans.

An alternative to systemic and invasive methods of delivery is the intranasal route of drug administration, which is rapidly emerging as a non-invasive method of bypassing the BBB to target therapeutic peptides and proteins to the CNS (Thorne et al., 2004; Dhanda et al., 2005; Vyas et al., 2005a). Studies evaluating the feasibility of intranasal administration of HC to target the CNS are limited. In mice it was shown that with intranasal administration significantly greater concentrations of HC were achieved in multiple brain regions, with significantly less delivery to blood and

peripheral tissues, compared to an equivalent intravenous dose (Hanson et al., 2004). However, in that study, there were not sufficient pharmacokinetic data available to draw conclusions about overall brain tissue exposure since a single time point was evaluated following drug administration. Recently, intranasal administration of HC was shown to significantly improve performance following sleep deprivation in non-human primates (Deadwyler et al., 2007) and to improve olfactory function in narcolepsy patients with cataplexy (Baier et al., 2008), who have low or undetectable CSF levels of HC (Nishino et al., 2001). Numerous studies evaluating other therapeutics have been published that demonstrate delivery and/or pharmacological effects of small molecules, peptides and proteins following nasal administration in animals and in humans (Born et al., 2002; Banks et al., 2004; Hanson et al., 2004; Liu et al., 2004; Ross et al., 2004; Thorne et al., 2004; De Rosa et al., 2005; Matsuoka et al., 2007; Benedict et al., 2008; Reger et al., 2008b). While the exact mechanisms of intranasal drug delivery are not completely understood, multiple pathways involving the olfactory and trigeminal nerves, the nasal vasculature, and the nasal lymphatic vessels have been suggested to play a role in transport from the nasal cavity to the CNS.

In the present work, we evaluated intranasal drug targeting of HC to the CNS relative to an intravenous infusion over the course of two hours in an anesthetized rat model. Pharmacokinetics were assessed in blood, CNS tissues, and peripheral tissues following intranasal and intravenous administration using concentrations calculated from radioactivity measured at 30, 60 and 120 minutes after the onset of drug delivery. Results from these experiments provide additional insight into the mechanisms involved in intranasal drug delivery to the CNS.

2.2 Materials and Methods

2.2.1 Experimental Design

This study was conducted in four sets of experiments. In the first set of experiments, CNS distribution of HC following intranasal or intravenous delivery was compared. A total of six groups of animals (n = 5 to 8) were evaluated at three different time points (30, 60, 120 min) after intranasal or intravenous administration of a mixture of unlabeled HC and ^{125}I- labeled HC. Concentrations in blood, CNS tissues, and peripheral tissues were determined based on radioactivity measured in tissues by gamma counting techniques. In the second set of experiments, cerebrospinal fluid (CSF) was sampled from two groups of animals (n = 6 or 7) at 30 minutes following intranasal or intravenous administration, and CSF concentrations were determined by gamma counting. In the third set of experiments, the qualitative distribution of ^{125}I-HC in the brain was assessed in two groups of animals (n = 5 to 8) at 30 minutes after intranasal or intravenous delivery using autoradiography techniques. The final set of experiments qualitatively assessed the stability of ^{125}I-HC in the brain and blood in two groups of animals (n = 3) after intranasal or intravenous delivery using HPLC.

2.2.2 Drugs and Reagents

Hypocretin-1 (HC, Cat # 46-2-70B, American Peptide Company, Sunnyvale, CA) was custom ^{125}I-labeled with a lactoperoxidase method (GE Healthcare, Woburn, MA). Solutions contained less than 1% unbound ^{125}I as determined by thin layer chromatography and less than 15% acetonitrile. The radiolabeled HC had an average

specific activity of 7.4 x 10^4 GBq/mmol at the reference date. Phosphate buffered saline (PBS, 10X concentrate) was purchased from Sigma-Aldrich (St. Louis, MO).

2.2.3 Animals

Adult male Sprague-Dawley rats (200-300 g; Harlan, Indianapolis, IN) were housed under a 12-h light/dark cycle with food and water provided *ad libitum*. Animals were cared for in accordance with institutional guidelines, and all experiments were approved by Regions Hospital, HealthPartners Research Foundation Animal Care and Use Committee.

2.2.4 Preparation of Dose Solutions

Intranasal and intravenous dose solutions consisted of a mixture of unlabeled HC and ^{125}I-labeled HC (10 – 11 nmol, 40 – 55 μCi) dissolved in PBS (10 mM sodium phosphate, 154 mM sodium chloride, pH 7.4) to a final volume of 48 μL and 500 μL, respectively. Dose solution aliquots for each experiment were stored at – 20 °C until the day of the experiment.

2.2.5 Animal Surgeries and Drug Administration

Animals were anesthetized with sodium pentobarbital (Nembutal, 50 mg/kg intraperitoneal, Abbott Laboratories, North Chicago, IL). Body temperature was maintained at 37 °C by insertion of a rectal probe connected to a temperature controller and heating pad (Fine Science Tools, Inc., Foster City, CA). For intranasal and intravenous experiments, the descending aorta was cannulated with a 20G, 1 ¼ inch

catheter (Jelco, Johnson and Johnson Medical Inc., Arlington, TX) connected to a 3-way stopcock (B. Braun Medical Inc., Bethlehem, PA) for blood sampling and perfusion. In addition, for intravenous experiments, the femoral vein was cannulated with a 25G, ¾ inch catheter (Becton Dickinson, Franklin Lakes, NJ) connected to tubing and a 3-way stopcock (B. Braun Medical Inc., Bethlehem, PA) for drug administration.

Intranasal administration was performed with animals lying on their backs and rolled gauze (½ inch diameter) placed under the neck to maintain rat head position which prevented drainage of the dose solution into the trachea and esophagus. A pipette (P20) was used to intranasally administer 48 μL of dose solution over 14 minutes. Eight-6 μL nose drops were given to alternating nares every two minutes while occluding the opposite naris. This method of administration was non-invasive as the pipette tip was not inserted into the naris, but rather, the drop was placed at the opening allowing the animal to snort the drop into the nasal cavity. Intravenous administration through the femoral vein was performed with animals lying on their backs, and an infusion pump (Harvard Apparatus, Inc., Holliston, MA) was used to administer 500 μL of a solution containing an equivalent dose over 14 minutes.

2.2.6 Blood Sampling

At 5, 10, 15, 20 and 30 minutes after the onset of drug delivery, blood samples (0.1 mL) were obtained via the descending aorta cannula from animals with sacrifice time at 30 minutes. For experiments with sacrifice times at 60 or 120 minutes after the onset of drug delivery, 5 to 9 blood samples were spaced out over the duration of the

experiment, not to exceed removal of more than 1% of the body weight of the animal in blood. After every other blood draw, 0.9% sodium chloride (0.35 mL) was replaced to maintain blood volume during the experiment.

2.2.7 Brain and Peripheral Tissue Dissection

At 30, 60, or 120 minutes after the onset of drug delivery, animals were sacrificed under anesthesia by perfusion and fixation through the descending aorta cannula with 60 mL of 0.9% sodium chloride, followed by 360 mL of 4% paraformaldehyde in 0.1 M Sorenson's phosphate buffer using an infusion pump (15 mL/min; Harvard Apparatus, Inc., Holliston, MA). A gross dissection of major peripheral organs was performed, as well as dissection of the superficial cervical lymph nodes, deep cervical lymph nodes, and the axillary lymph nodes. Olfactory bulbs were dissected away from the brain. Serial (2 mm) coronal sections of the brain were made using a coronal rat brain matrix (Braintree Scientific, Braintree, MA). Microdissection of specific brain regions was performed on coronal sections using the Rat Brain Atlas as a reference (Paxinos and Watson, 1997). A posterior portion of the trigeminal nerve was dissected from the base of the cranial cavity from the anterior lacerated foramen to the point at which the nerve enters the pons. This tissue sample contained the trigeminal ganglion and portions of the ophthalmic (V1) and maxillary (V2) branches of the trigeminal nerve. An anterior portion of trigeminal nerve was also dissected after hemisection of the nasal cavity and contained the anterior portion of the maxillary (V2) branch of the trigeminal nerve. Dura from the spinal cord was removed and sampled prior to dissecting the spinal cord into cervical, thoracic, and lumbar sections. The left

and right common carotid arteries were dissected from surrounding tissues in some animals with the aid of a dissection microscope. Each tissue sample was placed into a pre-weighed 5 mL tube, and the wet tissue weight was determined using a microbalance (Sartorius MC210S, Goettingen, Germany).

2.2.8 Sample Analysis

Radioactivity in each tissue sample was determined by gamma counting in a Packard Cobra II Auto Gamma counter (Packard Instrument Company, Meriden, CT). Concentrations were calculated, under the assumption of minimal degradation of ^{125}I-HC, using the specific activity of ^{125}I-HC determined from standards sampled from the dose solution, counts per minute in the tissue following subtraction of background radioactivity, and tissue weight in grams.

2.2.9 Cerebrospinal Fluid Sampling

In a separate group of animals, at approximately 30 minutes after the onset of drug delivery, CSF was sampled via cisternal puncture. Briefly, animals were placed on their ventral side over a rolled up towel to position the head at a 45 degree angle. A 20G needle attached to 30 cm long polyethylene tubing (PE90) was inserted into the cisterna magna. CSF was collected (~ 50 μL) into the tubing until flow stopped or until blood was observed. The tubing was immediately clamped if blood was observed to avoid contamination due to blood-derived radioactivity. Only CSF samples containing clear fluid were counted and included in the analysis. Brain tissues were sampled as

described above but were not included in the analysis due to significant differences in brain concentrations with and without CSF sampling.

2.2.10 Autoradiography

In a separate group of animals, at 30 minutes after the onset of drug delivery, animals were sacrificed as described above. Serial (1 mm) coronal sections of the whole brain were made using a coronal rat brain matrix and transferred to glass microscope slides. Sections were exposed to ^{125}I sensitive phosphor screens (Super Sensitive, ST, size: 12.5 x 25.2 cm) for approximately 28 days in an autoradiography cassette, digitized with a Cyclone Scanner and analyzed using OptiQuant software (Packard Instrument Company, Meriden, CT).

2.2.11 Stability Assessment using HPLC

In a separate group of animals, in order to assess the stability of ^{125}I-HC in the brain and blood following intranasal and intravenous administration, dose solutions containing a high level of radioactivity were administered to animals (100 – 250 μCi). Approximately 30 – 60 minutes after the onset of intranasal or intravenous administration, animals were perfused with 100 mL of 0.9% sodium chloride containing Complete protease inhibitor cocktail (Roche Diagnostics, Indianapolis, IN). For each animal, a blood sample (1 mL) and the brain were homogenized on ice according to a previously published protocol (Dufes et al., 2003), with some modifications. 10 mM Tris buffer (pH 8.0) containing Complete protease inhibitor cocktail was added to the brain and blood samples at a 1:3 dilution. The samples were manually homogenized

using a glass tissue homogenizer and centrifuged at 1,000 x g for 10 minutes at 4 ºC. The supernatant for each sample was collected and stored on ice. The pellets were subjected to an additional wash with two volumes of homogenization buffer, homogenization, and centrifugation as described above. The two supernatants for each sample were combined and subjected to ultracentrifugation at 100,000 x g for 30 minutes at 4 ºC to remove cellular debris. The supernatants were frozen in liquid nitrogen and subsequently dried by lyophilization (FreeZone 4.5, Labconco, Kansas City, MO). Lyophilized samples were stored at -80 ºC until HPLC analysis.

Lyophilized samples were reconstituted with 1 mL of mobile phase, vortexed for 1 minute, and centrifuged at 20,000 x g for 20 minutes at 4 ºC. 100 µL of the resulting brain and blood supernatant were separately injected onto a Supelcosil C18 column (5 µ, 100 Å, 4.6 x 250 mm) prefitted with a guard column (Sigma Aldrich, St. Louis, MO) using a mobile phase of water containing 0.1% trifluoracetic acid and 0.1% acetonitrile (eluent A), and acetonitrile containing 0.1% trifluoracetic acid (eluent B). A linear gradient of 35% - 55% eluent B was used over a period of 40 minutes with a flow rate of 1 mL/min. Fractions were collected every minute and counted using a Packard Cobra II Auto Gamma counter.

2.2.12 Data Analysis

Dose-normalized concentrations in blood, CNS tissues, and peripheral tissues from intranasal and intravenous experiments at 30, 60, and 120 minutes were calculated and expressed in nmol/L (assuming a density of 1 g/mL) as mean ± SE. Unpaired two-sample t-tests were performed on concentrations in blood, CNS tissues, and peripheral

tissues to compare intranasal and intravenous groups at each time point using GraphPad Prism software (version 3.03, GraphPad Software Inc., San Diego, CA). Differences were significant if $p < 0.05$.

The area under the tissue concentration-time curve was generated from mean concentration-time profiles from 0 to 120 minutes ($AUC_{0\text{-}120min}$) for blood, CNS tissues, and peripheral tissues using the trapezoidal method without extrapolation to infinity. Variance of the AUC was estimated using a method that takes into consideration destructive sampling techniques (Bailer, 1988). The terminal half-life in blood following intravenous administration was determined by linear regression of the terminal phase of the semilogarithmic concentration-time curve. Pharmacokinetic parameters were estimated using WinNonlin non-compartmental analysis.

Intranasal drug targeting of HC to the CNS was assessed by three approaches: (1) by normalizing CNS tissue concentrations to blood concentrations (Chow et al., 1999); (2) by determining the drug targeting index (DTI) (Hunt et al., 1986), a measure of the difference in targeting between intranasal and intravenous delivery; and (3) by calculating the direct transport percentage (DTP%) (Zhang et al., 2004a), which can be derived from the DTI and is a measure of direct transport from the nose to the brain. Tissue-to-blood concentration ratios were generated for CNS tissues at each time point. Unpaired two-sample t-tests were performed on CNS tissue-to-blood concentration ratios to compare intranasal and intravenous groups at each time point, and differences were significant if $p < 0.05$. The DTI was calculated as the ratio of brain AUC/blood AUC after intranasal administration to that after intravenous administration, after being corrected for dose. The DTP% subtracts the fraction of the brain AUC after intranasal

delivery arising from nose-to-blood-to-brain transport (B_x), leaving the fraction of the brain AUC due to direct transport from the nose to the brain via olfactory pathways, trigeminal pathways or other pathways. The DTP% was calculated as follows (Zhang et al., 2004a):

$$\frac{(AUC_{brain})_{iv}}{(AUC_{blood})_{iv}} = \frac{B_x}{(AUC_{blood})_{in}}$$

$$DTP\% = \frac{(AUC_{brain})_{in} - B_x}{(AUC_{brain})_{in}} \times 100\%$$

2.3 Results

2.3.1 Pharmacokinetics in Blood and Tissues after Intranasal and Intravenous Delivery

Blood

Intranasal delivery resulted in a significantly lower concentration of HC in the blood at all time points measured when compared to an equivalent intravenous dose (Figure 1). Intranasal administration of HC over a period of 14 minutes resulted in a gradual increase in blood concentration, reaching a peak concentration (C_{max}) of 6.5 nM and a time to peak concentration (T_{max}) at 105 minutes, while intravenous infusion of HC resulted in a maximum concentration of 48 nM at 10 min, with a slow decline to 27 nM at 120 minutes (Figure 1 and Table 1). The fraction of the dose absorbed into the

blood (F) over the two hours following intranasal administration was 0.14 (Table 1). Elimination of HC from the blood following intravenous delivery was very slow, with an elimination half-life ($t_{1/2}$) of 135 minutes and an elimination rate constant (k) of 0.005 min^{-1}. Non-compartmental analysis using WinNonlin calculated the $AUC_{0\text{-}120min}$ to be 3725 nmol*min/L, and after extrapolating to infinity, the $AUC_{0\text{-}\infty}$ was estimated to be 8990 nmol*min/L. Due to limitations in sampling, greater than 50% of the AUC was extrapolated, and as a result, considerable error may be associated with estimates of total body clearance (CL) and volume of distribution (V) (Table 1). Blood pharmacokinetic parameters after intranasal delivery could not be estimated due to the sampling scheme which resulted in insufficient data to fully characterize the terminal elimination phase.

Peripheral Tissues

Peripheral tissue concentration-time profiles demonstrated significantly less exposure of HC to the liver, kidneys, and muscle with intranasal administration compared to intravenous administration at all time points (Figure 2). The greatest concentrations of HC in the peripheral tissues were observed in the kidneys, regardless of the route of drug delivery.

CNS Tissues

The greatest concentrations in CNS tissues after both routes of administration were found in both segments of the trigeminal nerve, although the concentrations in the anterior trigeminal nerve after intranasal administration were approximately 25 times

higher than after intravenous administration (Table 2). With intranasal delivery, a decreasing concentration gradient was observed along the anterior to posterior segment of the trigeminal nerve at all time points. The concentration of the posterior trigeminal nerve decreased from 6.2 nM at 30 minutes to 2.1 nM at 120 minutes following intranasal administration, while there was little change in posterior trigeminal nerve concentration after intravenous delivery over the two hour experiment. Cerebrospinal fluid, sampled in a separate group of animals, contained low levels of HC at 30 minutes following drug delivery, with an average concentration of 0.2 nM with intranasal delivery and 1.3 nM after intravenous delivery, and this difference was found to be significant (Table 2).

Despite a 10-fold lower blood concentration with intranasal administration at 30 minutes (31 nM vs. 3.5 nM), both routes of administration resulted in similar concentrations of HC in multiple brain regions, including the olfactory bulbs, anterior olfactory nucleus, hippocampus, hypothalamus, pons, medulla, and cerebellum (Table 2). HC brain concentrations at 30 minutes ranged from 1.0 nM to 2.2 nM with intranasal delivery and from 1.4 nM to 2.4 nM with intravenous delivery. Significantly higher concentrations of HC were observed with intravenous administration, particularly at 60 minutes, in the anterior olfactory nucleus, frontal cortex, hippocampus, and cerebellum (Table 2). Concentrations of HC in the CNS did not change dramatically over two hours after intranasal and intravenous infusion of HC, demonstrating slow clearance of HC from the brain. In the spinal cord, a decreasing concentration gradient was observed in the rostral to caudal direction after intranasal

delivery, whereas intravenous delivery resulted in relatively uniform distribution across all segments of the spinal cord (Table 2).

Overall exposure of HC to brain and spinal cord tissues over two hours, as assessed by the $AUC_{0\text{-}120min}$ generated from mean concentration data, was greater following intravenous delivery compared to intranasal delivery (Table 2) . However, the greater exposure to CNS tissues with intravenous delivery was accompanied by significantly higher blood and peripheral tissue exposure.

Lymphatics

In the lymphatic system, high concentrations of HC were observed within the deep cervical lymph nodes after intranasal administration, reaching a maximum concentration of 16.5 nM at 120 min (Table 2). These concentrations were significantly greater at all time points compared to those observed after intravenous administration. Significantly less HC was delivered to the superficial cervical lymph nodes and the axillary lymph nodes with intranasal compared to intravenous administration at all times. As a result, the $AUC_{0\text{-}120min}$ following intranasal administration was significantly greater in the deep cervical nodes, and significantly less in the superficial cervical nodes and axillary nodes compared to intravenous administration (Table 2).

2.3.2 Drug Targeting to CNS Tissues and Lymphatics after Intranasal and Intravenous Delivery

Compared to the intravenous route, tissue-to-blood concentration ratios revealed significantly greater intranasal drug targeting at all times to all CNS tissues sampled.

The greatest differences between intranasal and intravenous administration were found within 30 minutes of drug delivery. The intranasal route of delivery resulted in significantly greater tissue-to-blood concentration ratios for the posterior trigeminal nerve (TN, 14-fold), olfactory bulbs (OB, 9-fold), hypothalamus (HT, 9-fold), pons (10-fold, data not shown), medulla (13-fold, data not shown), and cerebellum (CB, 7-fold) compared to intravenous administration (Figure 3). In addition, intranasal delivery resulted in significantly greater tissue-to-blood ratios in the deep cervical lymph nodes, demonstrating an 18-fold difference at 30 minutes compared to intravenous infusion (data not shown). Within the CNS tissues, drug targeting was greatest to the trigeminal nerve for both intranasal and intravenous routes of administration over the entire two hour period (Figure 3).

Intranasal delivery resulted in a 5- to 8-fold increase in overall drug targeting to the brain compared to intravenous delivery as determined by the drug targeting index (DTI, Table 3). In addition, a 2- to 6-fold difference in drug targeting was observed in the spinal cord compared to intravenous administration (DTI, Table 3). Approximately 80% of the brain AUC was generated from direct nose-to-brain transport, while only around 20% of the brain AUC was due to delivery from the nasal passages via systemic pathways (DTP, Table 3).

2.3.3 Qualitative Autoradiography after Intranasal and Intravenous Delivery

Qualitative autoradiography demonstrated that 30 minutes after intranasal administration signal intensity was high (red) in specific regions of tissue sections, while after intravenous administration the distribution pattern of ^{125}I-HC was relatively

uniform throughout the tissue sections (Figure 4). Following intranasal delivery, the highest signal intensity was observed in the frontal cortex and anterior olfactory nucleus (Figure 4a), which is directly adjacent to the olfactory bulbs where we found high concentrations of HC by gamma counting. Intranasal delivery also resulted in higher signal intensity in the hypothalamus compared to the frontal cortex, which is consistent with the gamma counting data presented above (Figure 4b). Following intranasal and intravenous delivery, the lowest signal intensity (blue) was observed in the tissue surrounding the cerebral aqueduct and lateral ventricles (Figure 4b-c).

2.3.4 Qualitative Assessment of Stability after Intranasal and Intravenous Delivery

HPLC analysis of brain samples following intranasal and intravenous administration resulted in a radioactive peak which eluted in the same position as ^{125}I-HC standards (consisting of ^{125}I-HC in brain or blood from untreated animals), indicating that a portion of the administered HC reached the brain intact and with the radiolabel attached (data not shown). Intact radiolabeled peptide was also detected in blood samples following both routes of drug administration, but to a lesser extent. In addition, brain and blood samples contained a peak corresponding to free iodine resulting from degradation *in vivo* and/or during the peptide extraction process. Blood samples from intravenously treated animals contained more free iodine compared to blood samples obtained following intranasal administration.

2.4 Discussion

Intranasal administration of HC (10 nmol) demonstrated a considerable advantage over intravenous administration by resulting in significantly less delivery to the blood and to peripheral tissues over the course of two hours, while achieving comparable or lower brain concentrations in the nanomolar range. Tissue-to-blood concentration ratios after intranasal delivery were significantly greater in all CNS tissues compared to intravenous delivery, with the greatest targeting to the trigeminal nerve, olfactory bulbs, and the deep cervical lymph nodes, indicating that pathways involving nerves and the lymphatic system play a key role in intranasal delivery. Brain AUC-to-blood AUC ratios in various brain regions demonstrated a 5- to 8-fold difference in drug targeting between intranasal and intravenous administration. These findings show that intranasal administration results in rapid delivery and targeting of intact HC to the CNS, making it a potential strategy not only for the treatment of CNS disorders affecting sleep and appetite regulation, but also for the treatment of disorders related to the trigeminal nerve, olfactory bulbs or lymphatic system. Further, these findings shed some light onto the mechanisms of intranasal drug delivery, demonstrating that pathways involving the blood and/or cerebrospinal fluid are not the sole, or even principle, routes of entry into the CNS after nasal administration.

In this study, the direct transport percentage (DTP, Table 3) demonstrated that approximately 20% of the brain AUC observed after intranasal administration was due to absorption of HC into the nasal vasculature, followed by distribution from the blood into the brain. Since brain and blood concentrations were only assessed for 120 minutes, it is important to note that the DTP does not take into account the full exposure

of the drug that would be observed over a longer period of time. Drug absorption into the nasal vasculature and subsequent diffusion or receptor-mediated transport across the BBB can play an important role in drug transport from the nasal cavity to the CNS, particularly for drugs with properties that allow for permeation through the nasal blood vessels and the BBB (i.e. small, lipophilic molecules which are not rapidly degraded in the blood) (Chow et al., 1999; van den Berg et al., 2004a). HC is a 33 amino acid peptide with a molecular weight of 3,562 daltons and an octanol-water partition coefficient of 0.232 (Kastin and Akerstrom, 1999). Although HC could enter the fenestrated capillary endothelium of the nasal mucosa, it was not expected to cross the tight junctions of the cerebral vasculature to enter the brain to a significant extent. It is generally thought that drugs with a molecular weight greater than 500 daltons are not able to diffuse across the BBB (Pardridge, 2005). However, Kastin and Akerstrom (1999) demonstrated that HC was rapidly transported from the blood to the brain in mice by mechanisms consistent with simple diffusion and this was due largely to the lipophilic properties of HC (Kastin and Akerstrom, 1999). Although HC entered the nasal vasculature following intranasal administration, the blood concentration at 30 minutes was 10-fold lower than that after intravenous administration of an equivalent dose. Despite this large difference, both intranasal and intravenous administration of HC yielded similar brain concentrations within 30 minutes of delivery. If the only pathway into the brain after intranasal delivery were via absorption into the systemic circulation, followed by transport across the BBB, a 10-fold difference in blood concentration should have generated a similar difference in brain concentration. The DTP demonstrated that for HC approximately 80% of the brain AUC was due to direct

transport along pathways other than the vasculature, such as along the olfactory nerves, trigeminal nerves, or along other pathways.

The high olfactory bulb concentrations and the distribution pattern of ^{125}I-HC in rostral tissue sections after intranasal delivery demonstrate that pathways along the olfactory nerves play a major role in transporting HC from the nasal cavity to the brain. Considerable research has suggested that intranasal delivery to the CNS occurs primarily by extracellular transport mechanisms (requiring only minutes) along olfactory nerves in the olfactory epithelium (Chen et al., 1998; Thorne et al., 2004; Westin et al., 2005), which send axonal projections through the cribriform plate and into the olfactory bulbs. One of the highest CNS tissue concentrations of HC after intranasal delivery was found in the olfactory bulbs, which was observed within 30 minutes of intranasal delivery (2.2 nM). This finding is consistent with extracellular mechanisms of transport accounting for this rapid delivery to the brain. In addition, following intranasal administration of HC, high intensity signals were observed in the anterior olfactory nucleus (Figure 4a), consistent with olfactory pathways of delivery. The driving force for delivery to the olfactory bulbs is likely the large depot of drug present in the olfactory epithelium.

Based on the high concentrations observed in the trigeminal nerve, these results suggest that the trigeminal nerve also has an important role in intranasal delivery of HC to the CNS. In addition to olfactory nerve pathways, Thorne et al. (2004) proposed an extracellular pathway along trigeminal nerves for the transport of molecules from the nasal cavity to the brainstem and spinal cord (Thorne et al., 2004). This was based on findings showing that after intranasal administration to rats, high concentrations of ^{125}I-

insulin-like growth factor-I (IGF-I) were observed in both rostral and caudal brain regions, consistent with entry points for the olfactory and trigeminal nerves, respectively. In the current work, the highest CNS tissue concentrations of HC following both intranasal and intravenous administration were observed in the anterior trigeminal nerve (the maxillary branch (V2) of the trigeminal nerve), and in the posterior segment of the trigeminal nerve (residing in base of the cranial cavity). In addition, a decreasing concentration gradient was observed from the anterior to posterior segments of the trigeminal nerve after intranasal administration, suggesting that a portion of the HC is transported within or along this nerve. Relatively higher concentrations in regions near the entry point of the trigeminal nerve were observed, for example in the hypothalamus and in the medulla. Similar trends for high trigeminal nerve concentrations have been observed following intranasal delivery for interferon-β (Ross et al., 2004).

The limited distribution of HC into the CSF compared to the rest of the brain after intranasal delivery indicates that the mechanism of intranasal delivery of HC to the CNS is not likely to be mediated by the CSF. Several studies have suggested that the mechanism of intranasal delivery to the CNS is due to diffusion from the nasal cavity into the subarachnoid space containing CSF, followed by distribution to the rest of the brain and spinal cord (Sakane et al., 1991; Born et al., 2002). Direct connections between the nasal cavity and the subarachnoid space containing CSF have been well documented (Bradbury and Westrop, 1983; Kida et al., 1993; Johnston et al., 2004; Nagra et al., 2006; Walter et al., 2006a). It is also possible that drugs given intranasally enter the bloodstream, diffuse across the blood-CSF-barrier to enter the choroid plexus

of the lateral, third and fourth ventricles, and enter the brain tissue. In the present experiments, concentrations of CSF sampled from the cisterna magna were much lower compared to brain concentrations at 30 minutes following intranasal and intravenous delivery (0.2 nM and 1.3 nM, respectively). Higher CSF concentrations may have been present at an earlier time point, consistent with observations from Sakane et al. (1991) where CSF concentrations of cephalexin were two-fold higher at 15 minutes than at 30 minutes (Sakane et al., 1991). However, due to difficulties associated with CSF sampling, only one time point could be evaluated in the current study. Qualitative autoradiography results also indicate that distribution into the CNS after intranasal delivery is not likely to be via the CSF. Low intensity signals were observed in the tissues surrounding the lateral ventricles and cerebral aqueduct, suggesting that HC did not enter the brain tissue following distribution from ventricular CSF.

The high concentrations of HC in the deep cervical lymph nodes provide evidence for transport of HC within lymphatic channels after intranasal administration. Numerous studies document drainage pathways for solutes from the CNS to the periphery: from the subarachnoid space containing CSF, to the nasal cavity containing networks of lymphatic vessels and finally to the cervical lymph nodes of the neck (Bradbury and Westrop, 1983; Cserr et al., 1992; Kida et al., 1993; Walter et al., 2006a). Drugs administered intranasally can enter the lymphatic vessels in the nasal cavity and possibly be transported into the CNS in the reverse pathway. In these experiments, we find that intranasally administered HC enters the nasal lymphatic system because of high concentrations observed in the deep cervical lymph nodes over the two hour period. The high concentrations in the cervical lymph nodes may explain

why the blood concentrations following intranasal administration slowly continue to rise over time. Drug entering the lymphatic capillaries in the nasal mucosa can drain into lymphatic vessels before entering the deep cervical lymph nodes. From the lymph nodes, drug can travel through larger lymph vessels before finally retuning to the venous circulation. Perhaps the reason we do not see a drop in blood concentrations after intranasal delivery is because of this lymphatic recycling that continuously transfers drug from the lymphatic system to the venous system. It is important to note, however, that the high concentrations of HC in the lymph nodes following intranasal administration has the potential to activate immunogenic responses to the drug therapy, which could lead to potential adverse effects. It is also possible that the nasal epithelium acts a depot to continuously release drug into the vasculature.

The high levels of HC found in walls of the blood vessels that were sampled suggest that HC is transported within spaces surrounding blood vessels following intranasal administration and may be rapidly distributed throughout the brain via transport mechanisms involving these perivascular spaces (Hadaczek et al., 2006). Thorne et al. (2004) also suggested the involvement of perivascular compartments in the rapid distribution of drugs throughout the CNS following intranasal delivery (Thorne et al., 2004). In the group of animals in which CSF had been sampled, the walls of the carotid arteries were also sampled after removal of blood with saline perfusion and found to contain high concentrations of HC after intranasal administration (83 nM), which were much higher than HC concentrations observed in the brain or blood (data not shown). The observation of high concentrations of intranasally administered drugs in blood vessel walls have also been noted in intranasal studies of

IGF-I in rats (Thorne et al., 2004) and of interferon-β in primates (Thorne et al., 2008), suggesting that mechanisms involving perivascular spaces are important for intranasal delivery to the CNS.

A shortcoming of using a ^{125}I-radiolabeled peptide in these studies is the possibility that peptide structure and properties may be affected by the presence of the radiolabel, thereby altering biological transport. Of greater importance is the possibility of detachment of the radiolabel from the peptide or of peptide degradation by enzymes present in the nasal mucosa, in the brain or in the blood. Since measurements are based on total radioactivity, it is possible that the concentrations reflect ^{125}I or ^{125}I-labeled peptide fragments. Several lines of evidence suggest that the radioactivity measured in the sampled tissues reflect, at least in part, intact peptide. Detachment of the radiolabel from the peptide or auto-degradation of the peptide are unlikely since a mild lactoperoxidase radiolabeling procedure was used resulting in a stable product (Wajchenberg et al., 1978; Redman and Tustanoff, 1984; Baumann and Amburn, 1986). HPLC analysis of brain and blood samples revealed that intact ^{125}I-HC was present following intranasal and intravenous administration. Other researchers have demonstrated with HPLC analysis that ^{125}I-HC given intravenously reaches the brain intact (Kastin and Akerstrom, 1999) and that an iodinated peptide with similar properties to HC reached CNS tissues intact after intranasal administration (Dufes et al., 2003). Further, intranasally administered peptides and proteins have been shown to reach CNS targets intact by the demonstration of pharmacological effects in both animals and in humans (Gozes et al., 2000; Alcalay et al., 2004; Ross et al., 2004; Matsuoka et al., 2007; Benedict et al., 2008; Reger et al., 2008b). Finally, in recent

studies with intranasal administration of HC in non-human primates (Deadwyler et al., 2007) and in humans (Baier et al., 2008), pronounced pharmacological effects were observed, suggesting that a significant portion of the intranasally administered HC reached the brain intact to produce these effects.

2.5 Conclusions

Intranasal administration of HC to anesthetized rats resulted in rapid and sustained delivery to the brain and spinal cord over two hours, with significantly less exposure to blood and peripheral tissues compared to intravenous administration. Intranasal drug targeting of HC to multiple brain regions was 5-fold to 8-fold greater than with intravenous drug administration. These results demonstrate that intranasal delivery is a promising alternative to more invasive methods of drug delivery to rapidly target HC to the CNS for the treatment of narcolepsy or other disorders involving the hypocretinergic system in the CNS, including Alzheimer's disease (Friedman et al., 2007), Parkinson's disease (Thannickal et al., 2007) or depression (Allard et al., 2004). While we recognize the limitations associated with using rodent models for translation to humans, it is encouraging to note recent reports demonstrating similar nose-to-brain transport pathways in rats and monkeys (Thorne et al., 2008) and that intranasal administration of HC and other neuropeptides in non-human primates and in humans can significantly effect CNS functions (Deadwyler et al., 2007; Yamada et al., 2007; Baier et al., 2008; Hallschmid and Born, 2008; Reger et al., 2008a) (Gozes and Divinski, 2007).

These findings also suggest that intranasal administration could be used for targeted delivery of other therapeutics. Intranasal targeting of immunotherapeutics to the lymphatic system may be a strategy for the treatment of immune disorders, while therapeutics targeting the trigeminal nerve may have potential in the treatment of facial pain or trigeminal neuralgia. This delivery method may be particularly suited for potent therapeutics with adverse effects in the blood or in peripheral tissues, for therapeutics that are extensively bound to plasma proteins or degraded in the blood, or for drugs that are subject to high first-pass metabolism in the gastrointestinal tract. Additional research is necessary to translate from animal models to clinical applications, and to improve the efficiency of intranasal delivery, which will likely come about in the future with novel formulations and delivery devices.

2.6 Acknowledgments

The authors thank the various staff from the Alzheimer's Research Center for assistance with animal care and anesthesia (Kate Faltesek and Jodi Henthorn), for training on surgical procedures (Dr. Paula Martinez and Reshma Rao), for assistance with tissue dissection and tube weighing (Jacob Cooner, Dianne Marti, Rachel Matthews, Thuhien Nguyen, Dan Renner, and Aleta Svitak) and for preparation of fixative solutions (Yevgenia Fridman). The authors also wish to thank individuals from the Department of Pharmaceutics at the University of Minnesota (Dr. William Elmquist, Dr. Cheryl Zimmerman, Dr. Belinda Cheung, Dr. Jayanth Panyam, Laura Maertens) and from the Department of Ophthalmology, HealthPartners Medical Group and Clinics (Dr. Susann Remington) for use of HPLC and lyophilization equipment and for

assistance with data interpretation. The authors are also grateful to Dr. Jared Fine (Alzheimer's Research Center at Regions Hospital, HealthPartners Research Foundation, St. Paul, MN), Dr. Robert Thorne (New York University School of Medicine, Department of Physiology and Neuroscience, New York, NY), and Dr. Paula Martinez (University of Minnesota School of Medicine, Department of Neurology, Minneapolis, MN) for reviewing the manuscript prior to submission.

Table 1: Pharmacokinetic Parameters in Blood Following Intranasal and Intravenous Delivery

Parameter[a]	Intranasal	Intravenous
F	0.14	1.0
C_{max} (nmol/L)	6.5	48
T_{max} (min)	105	10
$t_{1/2}$ (min)	—	135
k (min^{-1})	—	0.005
AUC_{0-120} (nmol × min/L)	454	3725
$AUC_{0-\infty}$ (nmol × min/L)	—	8990
CL (mL/min)	—	1.2
V (mL)	—	238

[a]Estimated using WinNonlin noncompartmental analysis of all blood concentration data (i.e., not only 30, 60, and 120 min concentrations).

Table 2: CNS and Lymphatic Tissue Concentrations of HC Following Intranasal and Intravenous Delivery

Concentration (nM)	Intranasal				Intravenous			
	30 min, Mean ± SE ($n = 8$)	60 min, Mean ± SE ($n = 6$)	120 min, Mean ± SE ($n = 7$)	AUC ± SE[a]	30 min, Mean ± SE ($n = 6$)	60 min, Mean ± SE ($n = 6$)	120 min, Mean ± SE ($n = 5$)	AUC ± SE[a]
Central nervous system								
Anterior trigeminal nerve	819 ± 176*	164 ± 106	418 ± 172	44492 ± 8794*	5.8 ± 0.4	6.5 ± 0.6	6.8 ± 0.8	673 ± 38
Posterior trigeminal nerve	6.2 ± 1.3	4.0 ± 0.9	2.1 ± 0.4	428 ± 58	3.9 ± 0.3	4.3 ± 0.2	4.5 ± 0.5*	442 ± 19
Cerebrospinal fluid	0.2 ± 0.0	—	—	—	1.3 ± 0.1*	—	—	—
Olfactory bulbs	2.2 ± 0.6	1.9 ± 0.7	1.5 ± 0.4	199 ± 36	2.4 ± 0.2	2.9 ± 0.3	2.6 ± 0.4	278 ± 19
Anterior olfactory nucleus	1.4 ± 0.4	0.9 ± 0.2	1.1 ± 0.2	113 ± 16	1.6 ± 0.1	1.5 ± 0.1*	1.3 ± 0.2	157 ± 7*
Frontal cortex	1.0 ± 0.2	0.7 ± 0.1	1.1 ± 0.2	95 ± 11	1.7 ± 0.1*	1.8 ± 0.2*	1.5 ± 0.2	176 ± 11*
Hippocampus	1.1 ± 0.3	0.6 ± 0.1	1.0 ± 0.2	93 ± 13	1.5 ± 0.1	1.6 ± 0.1*	1.2 ± 0.2	152 ± 7*
Hypothalamus	1.8 ± 0.6	1.3 ± 0.4	1.3 ± 0.3	149 ± 26	1.8 ± 0.1	1.8 ± 0.1	1.3 ± 0.2	174 ± 8
Pons	1.4 ± 0.4	0.9 ± 0.2	1.1 ± 0.2	118 ± 18	1.4 ± 0.1	1.4 ± 0.1	1.1 ± 0.1	135 ± 6
Medulla	2.0 ± 0.7	1.2 ± 0.4	1.0 ± 0.2	142 ± 27	1.4 ± 0.1	1.4 ± 0.1	1.1 ± 0.2	141 ± 8
Cerebellum	1.2 ± 0.3	0.7 ± 0.1	1.2 ± 0.3	102 ± 14	1.5 ± 0.1	1.5 ± 0.1*	1.1 ± 0.1	146 ± 7*
Cervical spinal cord	0.8 ± 0.2	1.1 ± 0.2	1.2 ± 0.2	109 ± 13	1.6 ± 0.1*	1.5 ± 0.2	1.5 ± 0.1	160 ± 9*
Thoracic spinal cord	0.4 ± 0.0	0.4 ± 0.1	0.8 ± 0.2	54 ± 7	1.4 ± 0.1*	1.4 ± 0.1*	1.2 ± 0.1	143 ± 7*
Lumbar spinal cord	0.4 ± 0.0	0.4 ± 0.0	0.8 ± 0.2	52 ± 6	1.9 ± 0.2*	1.8 ± 0.2*	1.9 ± 0.1*	196 ± 9*
Lymph system								
Superficial lymph nodes	2.8 ± 0.3	2.6 ± 0.2	2.2 ± 0.2	267 ± 16	5.9 ± 0.3*	6.8 ± 0.6*	6.8 ± 0.8*	689 ± 39*
Deep cervical lymph nodes	10.9 ± 2.0*	11.9 ± 2.6*	16.5 ± 4.5	1360 ± 188*	5.7 ± 0.4	5.2 ± 0.3	5.6 ± 0.4	570 ± 22
Axillary lymph nodes	0.9 ± 0.1	0.8 ± 0.1	1.7 ± 0.4	117 ± 13	10.1 ± 0.2*	10.6 ± 1.8*	9.6 ± 0.8*	1068 ± 85*

[a]Area under concentration-time curve from 0 to 120 min without extrapolation to infinity using linear trapezoid method ± SE (nmol × min/L), with SE calculated according to method of Bailer.[30]

*Significantly greater ($p < 0.05$, unpaired t-test comparing intranasal result with intravenous result at respective time point).

Table 3: Intranasal Drug Targeting Index and Direct Transport Percentage to CNS Tissues

Tissue	DTI[a]	DTP[b]
Posterior trigeminal nerve	7.9	87.4
Olfactory bulbs	5.9	83.0
Anterior olfactory nucleus	5.9	83.0
Frontal cortex	4.5	77.5
Hippocampus	5.0	80.0
Hypothalamus	7.0	85.8
Pons	7.1	86.0
Medulla	8.2	87.8
Cerebellum	5.7	82.4
Cervical spinal cord	5.6	82.1
Thoracic spinal cord	3.1	68.0
Lumbar spinal cord	2.2	54.0

[a]Drug targeting index $= [\mathrm{AUC}_{\mathrm{brain}}/\mathrm{AUC}_{\mathrm{blood}}]_{\mathrm{intranasal}}/[\mathrm{AUC}_{\mathrm{brain}}/\mathrm{AUC}_{\mathrm{blood}}]_{\mathrm{intravenous}}$.

[b]Direct transport percentage $= ([\mathrm{AUC}_{\mathrm{brain}}]_{\mathrm{intranasal}} - B_{\mathrm{x}})/[\mathrm{AUC}_{\mathrm{brain}}]_{\mathrm{intranasal}} \times 100\%$, where $B_{\mathrm{x}} = [\mathrm{AUC}_{\mathrm{brain}}/\mathrm{AUC}_{\mathrm{blood}}]_{\mathrm{intravenous}} \times [\mathrm{AUC}_{\mathrm{blood}}]_{\mathrm{intranasal}}$.

Figure 1: Blood Concentration-Time Profiles of HC Following Intranasal and Intravenous Delivery to Anesthetized Rats (mean concentration ± SE, n = 5 to 8 for most time points). At 75 and 105 min, only one determination was made. Intranasal administration resulted in significantly less delivery to the blood when compared to an equivalent intravenous dose over two hours (*$p < 0.05$, unpaired t-test comparing intranasal result with intravenous result at respective time point).

Figure 1:

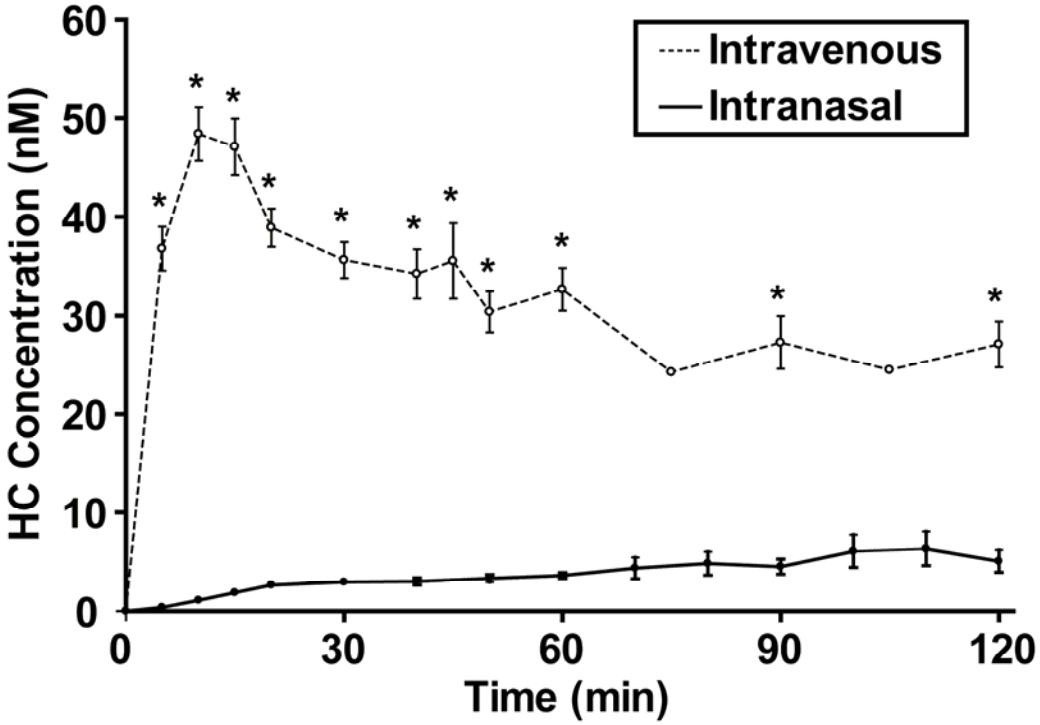
Intravenous
Intranasal
HC Concentration (nM)
Time (min)
0
10
20
30
40
50
60
0
30
60
90
120

Figure 2: Concentration-Time Profiles of HC in Kidney, Liver, and Muscle Following Intranasal and Intravenous Delivery to Anesthetized Rats (mean concentration ± SE, n = 5 to 8 for each time point). Intranasal administration compared to intravenous administration resulted in significantly less exposure to peripheral tissues at all time points (*$p < 0.05$, unpaired t-test comparing intranasal result with intravenous result at respective time point).

Figure 2:

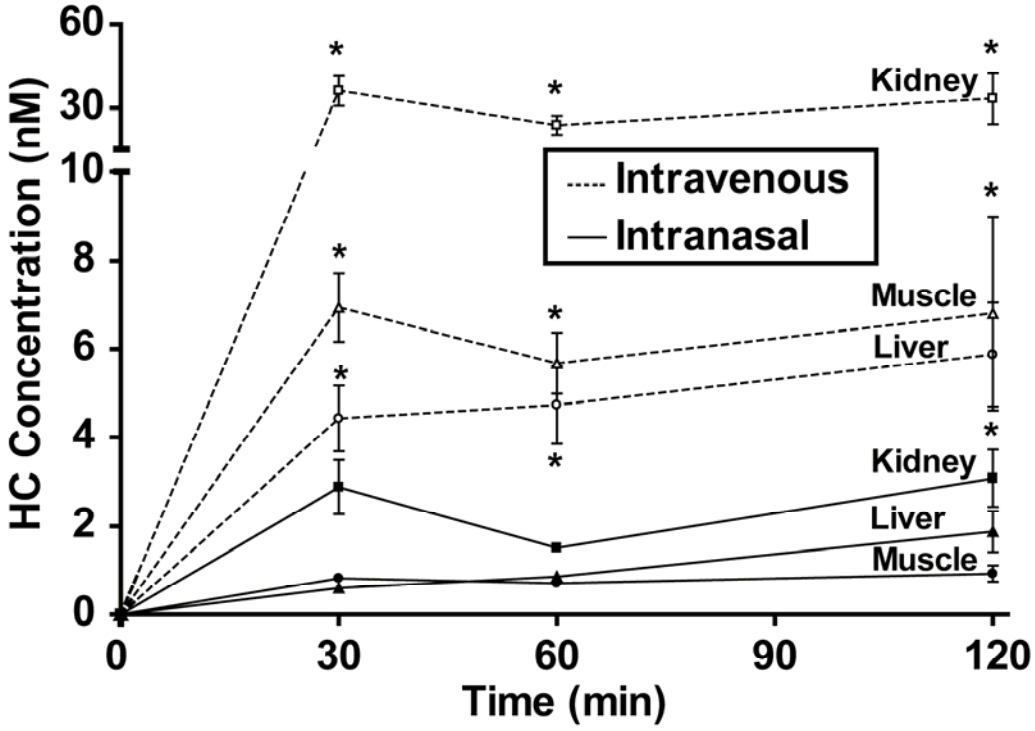
HC Concentration (nM)
60
30
10
8
6
4
2
0
0
30
60
90
120
Time (min)
Intravenous
Intranasal
Kidney
Muscle
Liver
Kidney
Liver
Muscle
*

Figure 3: CNS Tissue-to-Blood Concentration Ratios Following Intranasal and Intravenous Delivery to Anesthetized Rats (mean ratio ± SE, n = 5 to 8 for each time point). Tissues represent regions from the anterior to posterior portions of the brain: posterior trigeminal nerve (TN), olfactory bulbs (OB), hypothalamus (HT), and cerebellum (CB). Ratios were significantly greater in all CNS tissues sampled (including CNS tissues listed in Table 2) following intranasal compared to intravenous delivery at all time points (*$p < 0.05$, unpaired t-test comparing intranasal result with intravenous result at respective time point).

Figure 3:

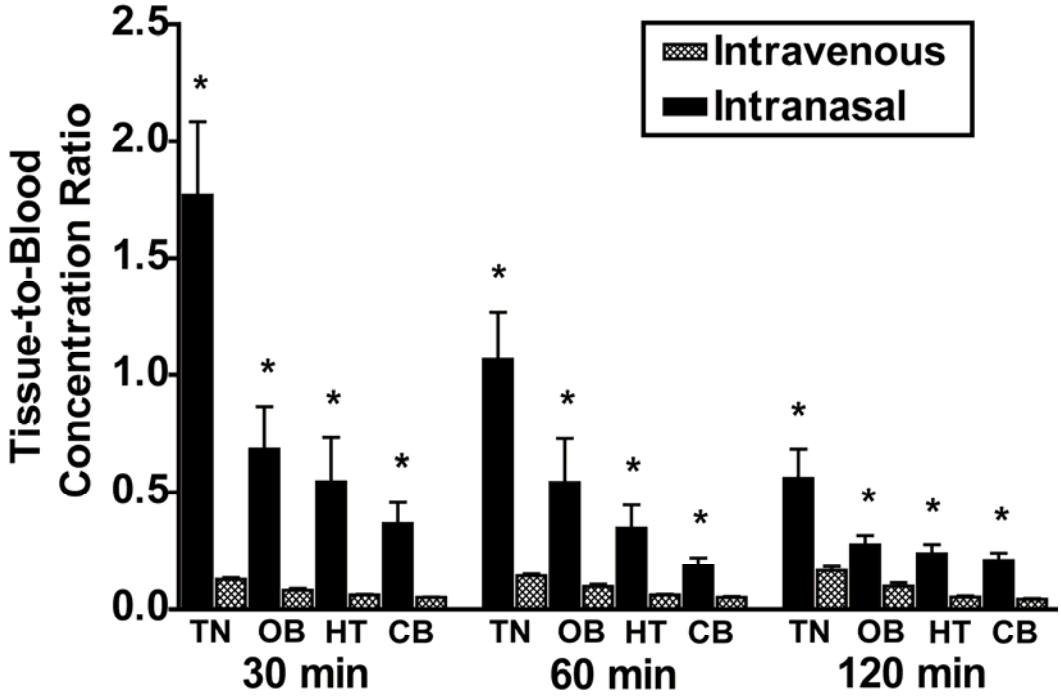
Intravenous
Intranasal
Tissue-to-Blood Concentration Ratio
2.5
2.0
1.5
1.0
0.5
0.0
TN OB HT CB
30 min
TN OB HT CB
60 min
TN OB HT CB
120 min

Figure 4: Qualitative Autoradiography of ^{125}I-HC at 30 Minutes Following Intranasal and Intravenous Delivery to Anesthetized Rats (intensity range: 456 to 10265). Coronal section at ~ bregma + 5.0 mm showing frontal cortex and anterior olfactory nucleus (a), coronal section at ~ bregma – 0.3 mm showing septal nucleus, lateral ventricles and hypothalamus (b), and coronal section at ~ bregma – 7.0 mm showing the cerebral aqueduct and pons (c). Intranasal administration resulted in high signal intensities (red) in specific regions in tissue sections, while intravenous administration resulted in a more diffuse pattern of distribution throughout tissue sections. Signal intensity was highest towards the interior of tissue sections after both routes of drug administration and lowest in tissue surrounding the ventricles containing cerebrospinal fluid.

Figure 4:

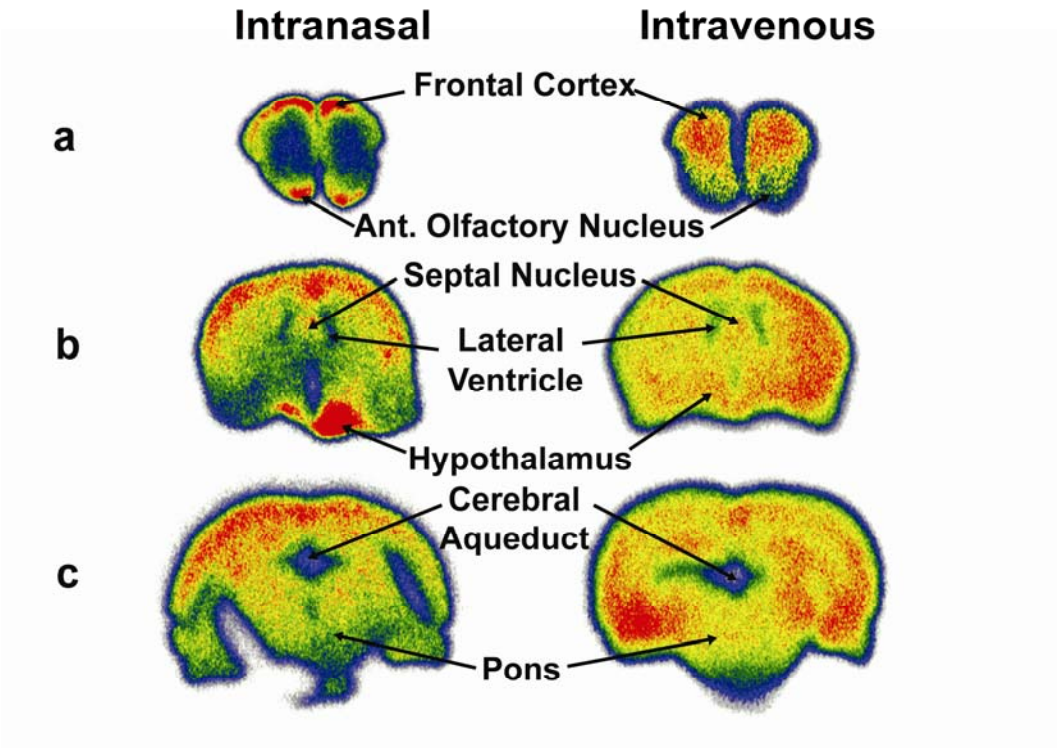
Intranasal
Intravenous
a
Frontal Cortex
Ant. Olfactory Nucleus
b
Septal Nucleus
Lateral
Ventricle
Hypothalamus
c
Cerebral
Aqueduct
Pons

2.7 Supplementary Material

2.7.1 Qualitative Assessment of Intact Hypocretin-1 in the Brain and Blood Using Reverse-Phase High Performance Liquid Chromatography

Introduction

Hypocretin-1 (HC, MW 3562) is a natural neuropeptide containing 33 amino acids with two disulfide bridges. Following binding to its receptor in the brain, which leads to its pharmacologic effect, it is expected that HC, like other neuropeptides, undergoes proteolysis and degradation. In the research presented in this dissertation, ^{125}I-HC was administered via intranasal and intravenous delivery over a period of 14-18 minutes but delivery was not assessed until after 30 minutes or longer. Consequently, some degradation was expected to occur during this time.

An important question that arises when working with radiolabeled peptides and proteins is whether concentrations, which are based on measurements of radioactivity, reflect concentrations of free radiolabel, radiolabel attached to a fragment of the peptide or the radiolabel attached to intact peptide. Ideally, measurements based on free drug concentrations would be most appropriate for assessing pharmacokinetics in the brain and the blood. However, due to the low quantities of drug present in the samples in the studies undertaken with this research, radiotracer methodologies were required.

Trichloroacetic acid (TCA) precipitation of intact proteins, including intact radiolabeled proteins, in brain and serum can provide an estimate of the percent of intact radiolabeled material present in samples (Banks et al., 2002; Nonaka et al., 2008).

TCA will lower the pH of the solution causing proteins to denature and precipitate out of solution. Intact radiolabeled proteins would also be expected to precipitate from solution, while free iodine would be left in solution. After centrifugation, radioactivity in the pellet (precipitate) and in the supernatant (solution) can be measured to obtain information about the relative amounts of intact radiolabeled protein and free iodine present. While the acid precipitation method is useful for proteins, it is not clear how effective this approach is for precipitating peptides, which generally lack tertiary structure and would not likely denature and precipitate in solution.

The question of intactness of peptides and proteins can also be addressed indirectly by using cell signaling assays and behavioral studies where presumably the peptide or protein must be intact to activate signaling pathways (Ross et al., 2004; Thorne et al., 2004) and to affect CNS behaviors (Liu et al., 2001; De Rosa et al., 2005; Gozes and Divinski, 2007; Hashizume et al., 2008; Reger et al., 2008a). A limitation of this approach is that it is not possible to discern if it is the intact material or a biologically active fragment that binds to receptors to produce the observed effects. ELISA can provide indirect information about intactness since an antibody must recognize the peptide or protein to obtain a measurable response. The more the peptide is degraded, the less likely it is that the antibody will detect it. Intranasally administered nerve growth factor (NGF) was shown to reach the brain to a similar extent whether it was detected by radiotracer methods (^{125}I-NGF) (Frey et al., 1997) or by ELISA (unlabeled NGF) (Chen et al., 1998), indicating that at least a portion of the neurotrophic factor reached tissues intact.

The problem with the methods described above is that they are not stability-indicating and provide no information about degradation products that may have formed. Stability-indicating high performance liquid chromatography (HPLC) assay can provide information about degradation processes that may be occurring. For these experiments, stability-indicating reverse-phase HPLC assay was used to qualitatively assess the stability of ^{125}I-HC in the brain and blood following intranasal and intravenous administration to anesthetized rats.

Methods

Detailed methods are presented in the *Methods* section of Chapter 2. Briefly, male, Sprague-Dawley rats were anesthetized, the descending aorta was cannulated for blood sampling and perfusion, and the trachea was cannulated to facilitate breathing if respiratory distress was observed. Approximately 30-60 minutes following the onset of intranasal (n = 4) or intravenous administration (n = 3) of dose solutions containing a mixture of unlabeled HC and ^{125}I-HC (100-250 μCi, 95-220 μL), animals were perfused with 100 mL of 0.9% sodium chloride containing Complete protease inhibitor cocktail (Roche Diagnostics, Indianapolis, IN).

For each animal, a blood sample (1 mL) and the brain were processed on ice according to the peptide extraction scheme outlined in Figure 1, which was modified from a previously published protocol (Dufes et al., 2003). 10 mM Tris buffer (pH 8.0) containing protease inhibitor cocktail was added to the brain and blood samples at a 1:3 dilution. Samples were manually homogenized using a Teflon pestle/glass tissue homogenizer (Thomas, Philadelphia, PA), centrifuged at 1,000 x g for 10 minutes at 4

ºC, and the supernatant for each sample was collected and stored on ice. This process was repeated on the pellet and the combined supernatants for each sample were ultracentrifuged at 100,000 x g for 30 minutes at 4 ºC to remove cellular debris. The supernatants were frozen in liquid nitrogen and subsequently dried by lyophilization and stored -80 ºC until HPLC analysis.

Lyophilized samples were reconstituted with 1 mL of mobile phase, vortexed for 1 minute, and centrifuged at 20,000 x g for 20 minutes at 4 ºC. 100 µL of brain and blood supernatant were separately injected onto a Supelcosil C18 column (5 µ 100 Å, 4.6 x 250 mm) prefitted with a guard column using a mobile phase of water containing 0.1% trifluoracetic acid and 0.1% acetonitrile (eluent A), and acetonitrile containing 0.1% trifluoracetic acid (eluent B). A linear gradient of 35% - 55% eluent B was used over a period of 40 minutes with a flow rate of 1.0 mL/min. Fractions were collected every minute and radioactivity (CPM) in each fraction was counted using a Packard Cobra II Auto Gamma counter.

Mobile phase standards were prepared by diluting ^{125}I-HC stock in mobile phase. Supernatant standards were prepared by subjecting brain and blood samples from untreated animals to the peptide extraction scheme outlined in Figure 1 and by diluting ^{125}I-HC stock in the resulting brain or blood supernatant immediately prior to HPLC injection (# in Figure 1). Processing controls were prepared by adding ^{125}I-HC to a brain or blood sample obtained from an untreated animal and subjecting the spiked samples to the peptide extraction scheme outline in Figure 1 (* in Figure 1).

Results

In the first set of experiments involving intranasal (IN) Rat #1 and intravenous (IV) Rat #1, 1000 mM Tris buffer was inadvertently used in the peptide extraction process and sample preparation, rather than 10 mM Tris buffer. The high salt concentration in the buffer led to high column pressure and blocked the column. In addition, mobile phase standards were analyzed for comparison with the samples, rather than using standards prepared in the same matrix as the sample, making it difficult to interpret the results due to the possibility of matrix effects on peak retention time. Mobile phase standards contained a peak that eluted between 17-22 minutes (Figure 2a and Figure 3a), corresponding to intact ^{125}I-HC. In the intranasal brain extract, a peak eluted between 3-5 minutes corresponding to free ^{125}I and a second peak eluted between 10-15 minutes (Figure 2b). In the intravenous brain extract, a similar profile was observed, with a peak that eluted between 3-5 minutes and a second peak that eluted between 12-17 minutes (Figure 3b). Blood standards of ^{125}I-HC contained a peak that eluted between 15-20 minutes (Figure 4a). In both the intranasal and intravenous blood extracts, a large peak eluted between 3-5 minutes corresponding to free ^{125}I (Figure 4b and Figure 4c). The percent of the radioactivity corresponding to free ^{125}I was greater for the intravenous compared to the intranasal blood extract (83% vs. 42%). No other major peaks were observed in the intranasal and intravenous blood extracts.

In the remaining experiments, 10 mM Tris buffer was used in the peptide extraction and sample preparation, and standards of ^{125}I-HC were prepared in brain or blood supernatant from untreated animals as described in the methods section. The effect of subjecting ^{125}I-HC in brain and blood samples to the peptide extraction process

was assessed by analyzing processing controls for the brain (n = 1) and blood (n = 1) by HPLC. The mobile phase standard contained a peak eluting between 18-23 minutes, corresponding to intact ^{125}I-HC (Figure 5a). When ^{125}I-HC was added to brain supernatant obtained from an untreated rat, a shift in retention time was noted such that the peak eluted slightly earlier between 14-19 minutes (Figure 5b). This peak likely corresponds to intact ^{125}I-HC since the relative percent of radioactivity corresponding to free ^{125}I (8%) did not change appreciably compared to the mobile phase standard (6%). When ^{125}I-HC was added to a brain from an untreated rat and was subjected to the peptide extraction process, the retention time was shifted to an earlier time again, with the peak eluting between 12-16 minutes (Figure 5c). This peak most likely represents a degradation product (i.e. fragment of ^{125}I-HC due to cleavage of one or two amino acids) that resulted from homogenization, centrifugation, and lyophilization of the sample. These data do not conclusively identify the nature of this peak since degradation products of HC were not available for analysis. When ^{125}I-HC was added to blood sample obtained from an untreated rat, a slight shift in retention time was observed compared to the mobile phase standard, with the peak eluting between 14-18 minutes (Figure 6b). When ^{125}I-HC was added to a blood sample from an untreated animal and subjected to the peptide extraction process, the retention time was between 16-20 minutes (Figure 6c). In addition, in both the processed brain and blood samples, a peak eluted between 3-5 minutes, corresponding to free ^{125}I. The key finding from this work is that the peptide extraction process can result in degradation of ^{125}I-HC present in brain and blood samples.

Figures 7-9 depict HPLC profiles of brain extracts following intranasal administration (n = 3), while Figure 10-11 show profiles of brain extracts after intravenous administration (n = 2), and these results are summarized in Table 1. Supernatant standards of ^{125}I-HC were analyzed on the same day as the sample for comparison. The retention time of the brain supernatant standards varied slightly from day to day, but on average eluted between 17-22 minutes as indicated in Table 1.

In 2 out of 3 of the intranasal brain extracts, peaks eluted between 3-5 minutes, 10-14 minutes, and 15-20 minutes (Figure 7b and Figure 8b). The first peak corresponds to free ^{125}I, while the second peak likely represents a degradation product of ^{125}I-HC resulting from either *in vivo* degradation of the peptide or from degradation of the peptide during the extraction process. The third peak represents intact ^{125}I-HC for IN Rat #2, where the supernatant standard and the brain extract elute in nearly the same position (Figure 7a and Figure 7b). For IN Rat #3, the brain extract elutes slightly earlier than the supernatant standard (Figures 8a and Figure 8b). For IN Rat #4, a broad peak eluted from 10-14 minutes and no significant peak corresponding to intact ^{125}I-HC was observed (Figure 9b). Intravenous brain extracts exhibited HPLC profiles that were similar to IN Rat #2 and #3, although the peaks were not as prominent (Figure 10b and Figure 11b).

Figures 12-13 and Figure 14 show HPLC profiles of blood extracts following intranasal administration (n = 3) and intravenous administration (n = 2), respectively, and these results are summarized in Table 1. Similar to what was observed using the 1000 mM Tris buffer, the blood standard contained a peak that generally eluted between

16-21 minutes corresponding to intact ^{125}I-HC (Figures 12a, Figure 13a, and Figure 14a) as indicated in the Table 1.

In both the intranasal and intravenous blood extracts, the major peak observed eluted between 3-5 minutes, representing free ^{125}I, with slightly greater levels of radioactivity in the free ^{125}I peak in the intravenous compared to the intranasal blood samples (Figure 12b, Figure 12c, Figure 13b, Figure 14b, and Figure 14c). The blood extract from IN Rat #2 and IV Rat #2 contained an additional broad peak eluting between 12-18 minutes (Figure 12b) and 10-17 minutes (Figure 14b), which may correspond to intact ^{125}I-HC or a peptide fragment. Additional sharp peaks were observed in the blood extract from IN Rat #3 (Figure 12c) and IN Rat #4 (Figure 13b). No other major peaks were detectable in the intravenous blood extracts (Figure 14b and Figure 14c).

Discussion

Results from these experiments show that following intranasal and intravenous administration of ^{125}I-HC the concentrations calculated in the studies presented in this dissertation do not simply reflect free ^{125}I that had detached from the radiolabeled peptide. In addition to the free ^{125}I peak that eluted between 3-5 minutes, additional peaks were observed in brain and blood samples. HPLC results indicate that a portion of the ^{125}I-HC administered to animals reflects intact peptide in the brain. In 4 of the 7 brain extracts (IN Rat #2, IN Rat #3, IV Rat #2, and IV Rat #3), a broad peak eluted close to the supernatant standard peak, which most likely corresponds to intact ^{125}I-HC. Of course, it is possible that the peptide lost an amino acid and may not be entirely

intact, which could explain the slightly earlier retention time. However, we are not able to conclusively confirm this with these data.

These HPLC results also provide evidence of peptide degradation due to the extraction process in brain samples. In 2 of the 7 brain extracts (IN Rat #1 and IV Rat #1), peaks eluted between 13-14 minutes, slightly earlier than the retention time of the supernatant standard peak. It is possible that the retention time shift observed in these two samples was due to the 100-fold higher Tris concentration that was inadvertently used, which could have altered the chromatography. It is also possible that the retention time shift is due to changes in the peptide that occurred during the peptide extraction process. In the experiment where ^{125}I-HC was added to a brain from an untreated animal and was subjected to the same extraction process as the samples, a peak eluted slightly earlier than the supernatant standard peak, suggesting that the extraction process alters the peptide resulting in an earlier retention time. Interestingly, in the 4 brain samples that contained intact ^{125}I-HC, a shoulder was also observed between 10-14 minutes in those samples, suggesting that a portion of the peptide was altered due to the extraction process.

In the blood, the HPLC results indicate that the major component present was free ^{125}I. The intravenous blood extracts contained greater levels of radioactivity of free ^{125}I compared to the intranasal samples. In 2 of the 7 blood extracts (IN Rat #2 and IV Rat #2), a broad peak eluted just before the blood standard, which is consistent with peptide alteration observed in brain samples due to the extraction process.

The development of an extraction method and HPLC method to assess the intactness of ^{125}I-HC in brain and blood samples has proven to be a challenging task.

Endogenous peptides, such as HC, are naturally degraded over time *in vivo*. In these experiments, brain and blood samples were obtained after *in vivo* exposure for 30-60 minutes, during which time peptide metabolism would have occurred. Our findings showing that a portion of the ^{125}I-HC was intact and that a portion had been degraded does not indicate that the peptide did not reach the brain intact. The peptide can reach the brain intact and bind to its receptor resulting in cell signaling and a pharmacological effect, followed by degradation and clearance from brain intersitial fluid. Further, we expect that peptide would be degraded to a greater extent in the blood in the presence of plasma proteases compared to in the brain. Therefore, it is possible that radiolabel measurements may reflect intact ^{125}I-HC reaching the brain followed by subsequent degradation of this natural peptide as would be expected to occur over time.

In addition to complications due to *in vivo* exposure, these data indicate that the peptide extraction process, which involves homogenization, centrifugation, and lyophilization, can have detrimental effects on the peptide. Although precautions were taken to minimize degradation due to the release of proteolytic enzymes from cells during homogenization by including protease inhibitors in the homogenization buffer and working at low temperatures, the peptide could still be degraded during the extraction process. In fact, significant degradation occurred during this peptide extraction process, resulting in a loss of approximately 42% of the intact peptide during extraction from brain and approximately 61% of the intact peptide during extraction from blood [estimated based on data in Figures 5b and 5c for brain and in Figures 6b and 6c for blood: (% intact before - % intact after) / % intact before X 100%]. The resulting supernatant was lyophilized and frozen until HPLC analysis. Lyophilization

can affect peptide and protein stability (Bhatnagar et al., 2007). After subjecting the peptide to all of these different conditions, it is actually remarkable that we generally observed a single peak that eluted very close to the standard peaks.

The larger issue at hand is the fact that concentrations at different time points following drug administration presented in Chapters 2-4 are based on measurements of radioactivity, which includes a mixture of free ^{125}I, intact ^{125}I-HC, and degraded ^{125}I-HC. Since pharmacokinetic parameters, such as clearance and volume of distribution, for the mixture of radiolabeled species will be different, it is difficult to draw reliable conclusions regarding *in vivo* peptide disposition. The stability of ^{125}I-HC in brain and blood samples could have been assessed using TCA precipitation, following which a correction factor could be applied to concentrations determined by radiotracer methods to account for degradation. Problems with this approach are that the TCA precipitation method provides a crude estimate of intact proteins and is not able to distinguish between free ^{125}I and ^{125}I-labeled low molecular weight peptides (Palmerini et al., 1985; Murao et al., 2007). In addition, the quantity of peptide reaching the brain is so low (< 1%) that it is not likely that it would be precipitable under those conditions. Alternative approaches could have been used, including the use of microdialysis methods to measure free drug concentrations in the brain interstitial fluid or the use of a synthetic peptide comprised of D-amino acids which would not be subject to degradation by proteases.

In conclusion, these results indicate that a portion of the ^{125}I-HC administered intranasally or intravenously is intact in the brain after 30 to 60 minutes following peptide administration. In HPLC studies by other researchers, intact ^{125}I-HC was

observed in the brain following intravenous administration in mice (Kastin and Akerstrom, 1999). In addition, a peptide with properties similar to HC was found intact in the brain using HPLC after intranasal administration, with no intact peptide observed after intravenous administration or in the blood after either route of administration (Dufes et al., 2003). Recent reports indicate that intranasal administration of HC in sleep-deprived monkeys showed improvements in cognition and cerebral glucose metabolism which were more effective than intravenous administration (Deadwyler et al., 2007). In narcoleptic patients, olfactory function was improved with intranasal HC (Baier et al., 2008). Results from behavioral studies, presented in Chapter 3, indicate that intranasal administration of HC significantly increases food consumption, increases wheel running activity, and activates HC signaling pathways in rats over a 4 hour period following dosing, providing indirect evidence that a significant portion of the intranasally administered reaches the brain intact to produce the observed CNS effects.

Supplementary Material (2.7.1) Table 1: Summary of HPLC Analysis of Brain and Blood Following Intranasal and Intravenous Administration

HPLC Analysis of Brain Supernatant Standards	Free ^{125}I		^{125}I-HC	
	RT	%	RT	%
Sup Std for IN Rat #2 (Figure 7a)	3-5	19	16-21	59
Sup Std for IN Rat #3 (Figure 8a)	3-5	28	19-24	45
Sup Std for IN Rat #4 (Figure 9a)	3-5	34	17-22	39
Sup Std for IV Rat #2 (Figure 10a)	3-5	25	17-22	54
Sup Std for IV Rat #3 (Figure 11a)	3-5	24	16-20	53

Brain Extracts	Free ^{125}I		^{125}I-Fragment		^{125}I-HC	
	RT	%	RT	%	RT	%
IN Rat #1	3-5	23	10-15	29	---	---
IN Rat #2	3-5	14	10-14	17	15-20	27
IN Rat #3	3-5	18	10-14	15	15-20	36
IN Rat #4	3-5	21	10-14	18	---	---
IN MEAN	**19%**		**20%**		**32%**	
IV Rat #1	3-5	17	12-17	32	---	---
IV Rat #2	3-5	35	10-14	16	15-20	28
IV Rat #3	3-5	49	10-14	11	15-20	21
IV MEAN	**34%**		**20%**		**25%**	

HPLC Analysis of Blood Standards	Free ^{125}I		^{125}I-HC	
	RT	%	RT	%
Blood Std for IN Rat #2 & #3 (Figure 12a)	3-5	34	16-21	32
Blood Std for IN Rat #4 (Figure 13a)	3-5	42	15-20	35
Blood Std for IV Rat #2 & #3 (Figure 14a)	3-5	21	16-21	56

Blood Extracts	Free ^{125}I		^{125}I-Fragment		^{125}I-HC	
	RT	%	RT	%	RT	%
IN Rat #1	3-5	42	---	---	---	---
IN Rat #2	3-5	91	12-18	3	---	---
IN Rat #3	3-5	95	---	---	18	1
IN Rat #4	3-5	74	10	2	---	---
IN MEAN	**76%**		**3%**		**1%**	
IV Rat #1	3-5	83	---	---	---	---
IV Rat #2	3-5	87	10-17	5	---	---
IV Rat #3	3-5	91	---	---	---	---
IV MEAN	**87%**		**5%**		**---**	

Supplementary Material (2.7.1) Figure 1: Peptide Extraction Scheme. Samples were manually homogenized in aqueous buffer containing protease inhibitor cocktail and centrifuged. The resulting supernatant was collected and stored on ice while the pellet was subjected to additional homogenization and centrifugation. The combined supernatants were subjected to ultracentrifugation to remove cellular debris. The resulting supernatant was frozen in liquid nitrogen and subsequently dried by lyophilization. Prior to HPLC analysis, lyophilized samples were reconstituted with mobile phase, vortexed, and centrifuged. For processing controls, ^{125}I-HC was added to brain or blood samples from an untreated animal and subjected to the peptide extraction (*). For supernatant standards, ^{125}I-HC was diluted in brain or blood supernatants from an untreated animal immediately prior to HPLC injection (#).

Supplementary Material (2.7.1) Figure 1:

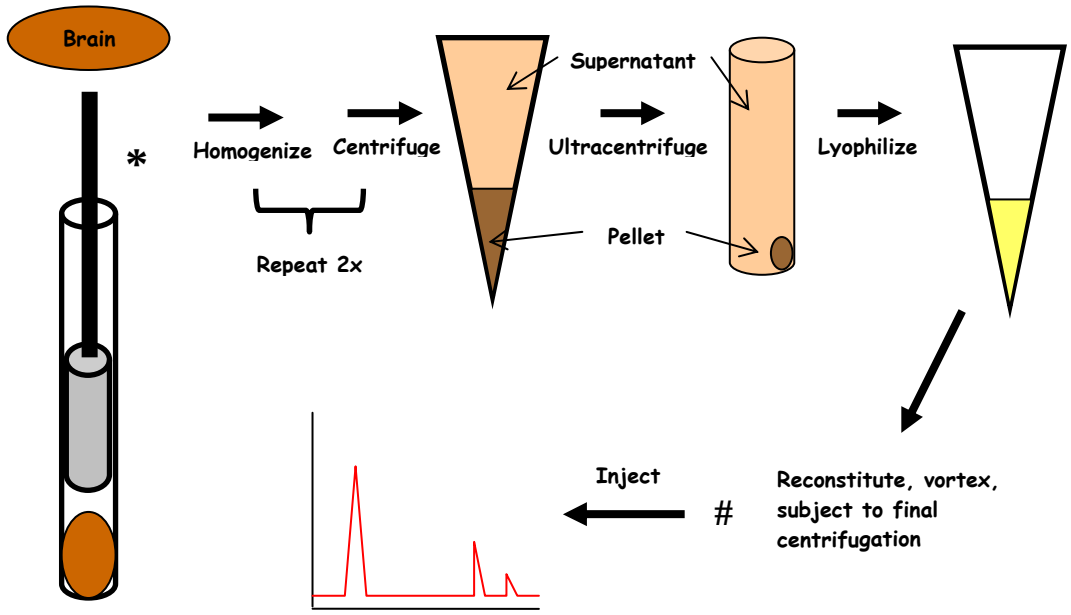

Supplementary Material (2.7.1) Figures 2-14: HPLC Profiles of Brain and Blood Extracts Following Intranasal and Intravenous Administration to Rats. HPLC profiles show elution of radioactivity recovered from brain and blood samples approximately 30-60 minutes following drug administration and peptide extraction. Radioactivity peaks are indicated with a horizontal bar spanning the retention time range of the peak. The percentage of total radioactivity present in each peak is shown in the figures and in Table 1. Abbreviations: RT = retention time, MP = mobile phase, Std = standard, Sup = supernatant IN = intranasal, IV = intravenous, CPM = counts per minute.

Supplementary Material (2.7.1) Figure 2: <u>Brain</u> Supernatant Following <u>Intranasal</u> Administration to Rat #1 and Extraction in 1000 mM Tris Buffer

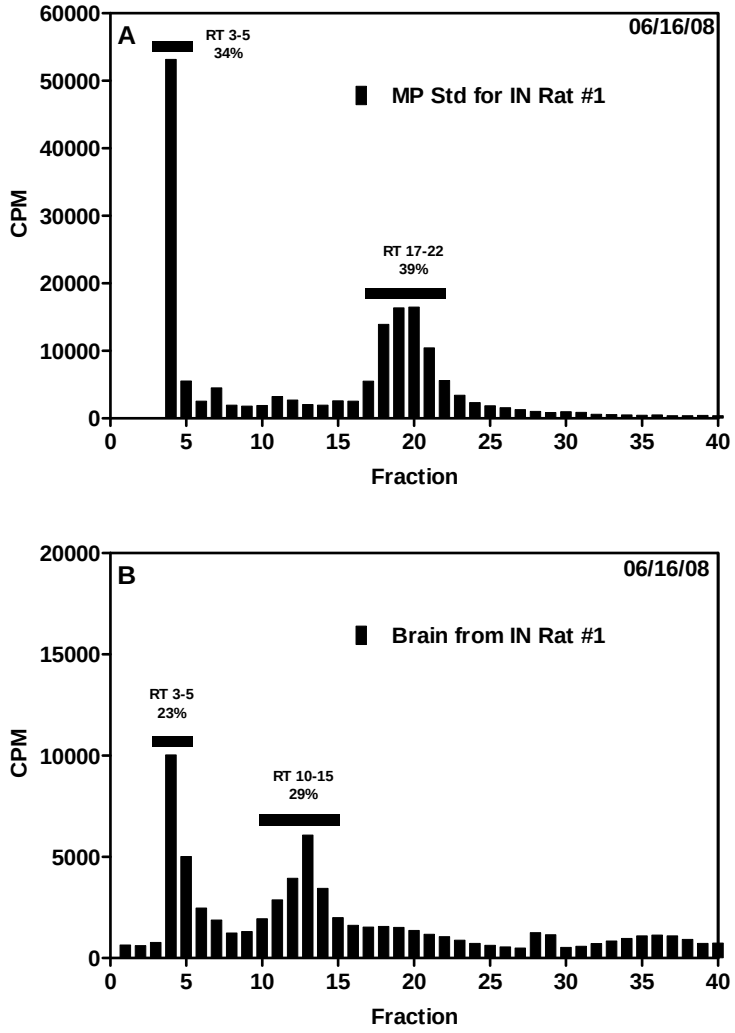

Supplementary Material (2.7.1) Figure 3: Brain Supernatant Following Intravenous Administration to Rat #1 and Extraction in 1000 mM Tris Buffer

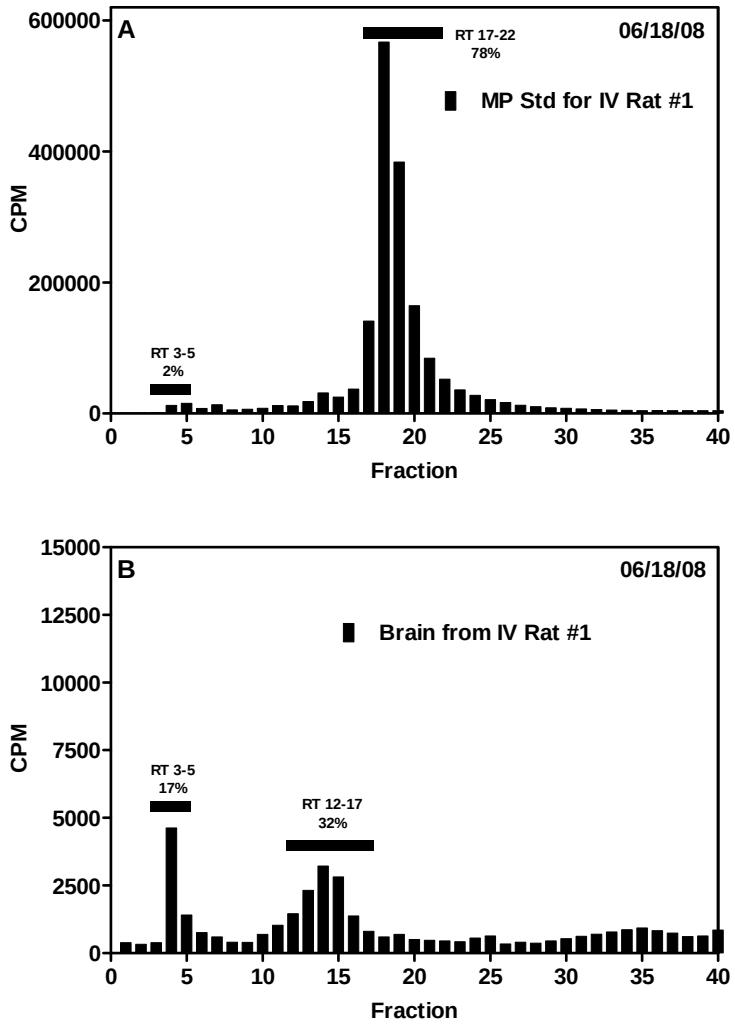

Supplementary Material (2.7.1) Figure 4: <u>Blood</u> Following <u>Intranasal</u> and <u>Intravenous</u> Administration and Extraction in 1000 mM Tris Buffer

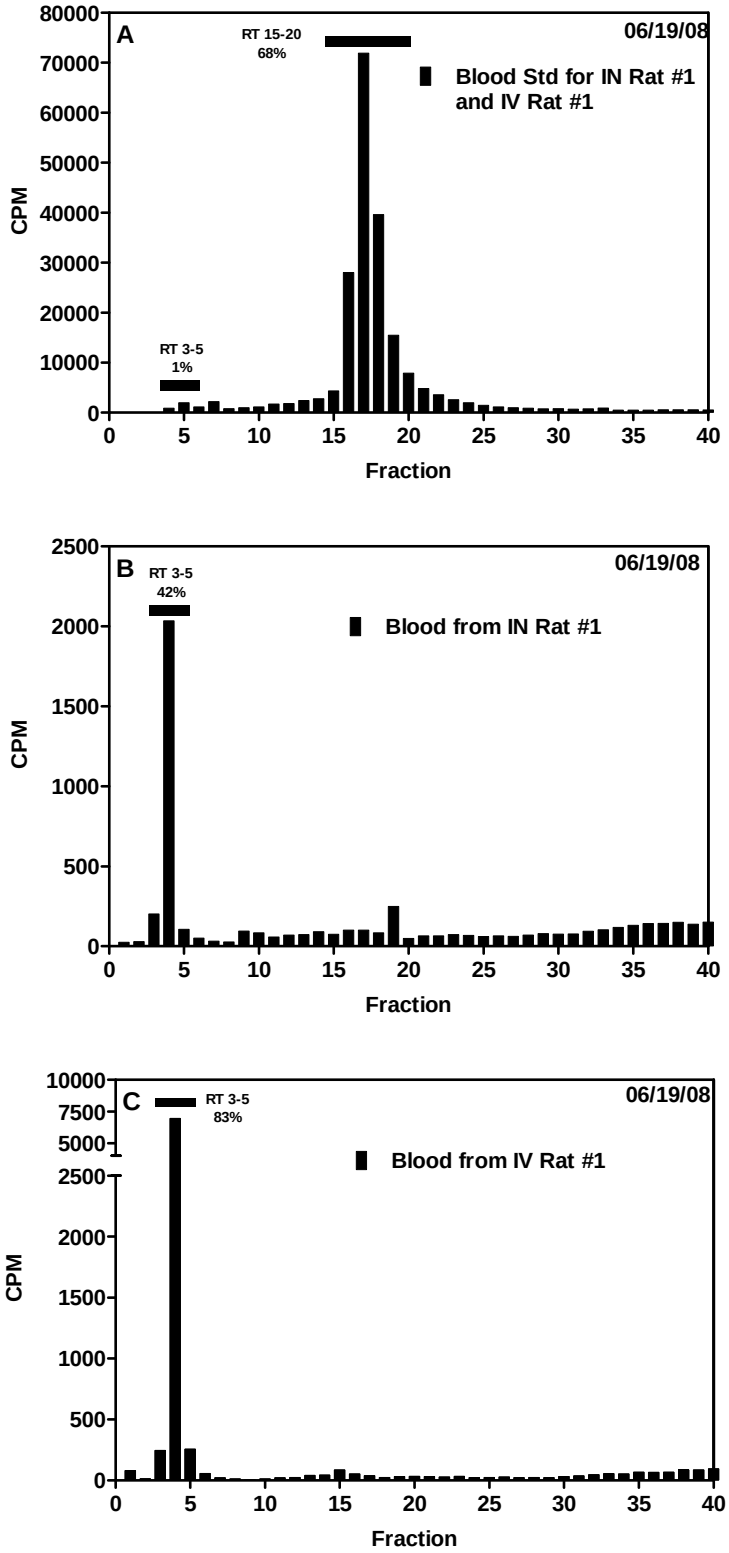

Supplementary Material (2.7.1) Figure 5: HPLC Analysis of Brain Processing Control

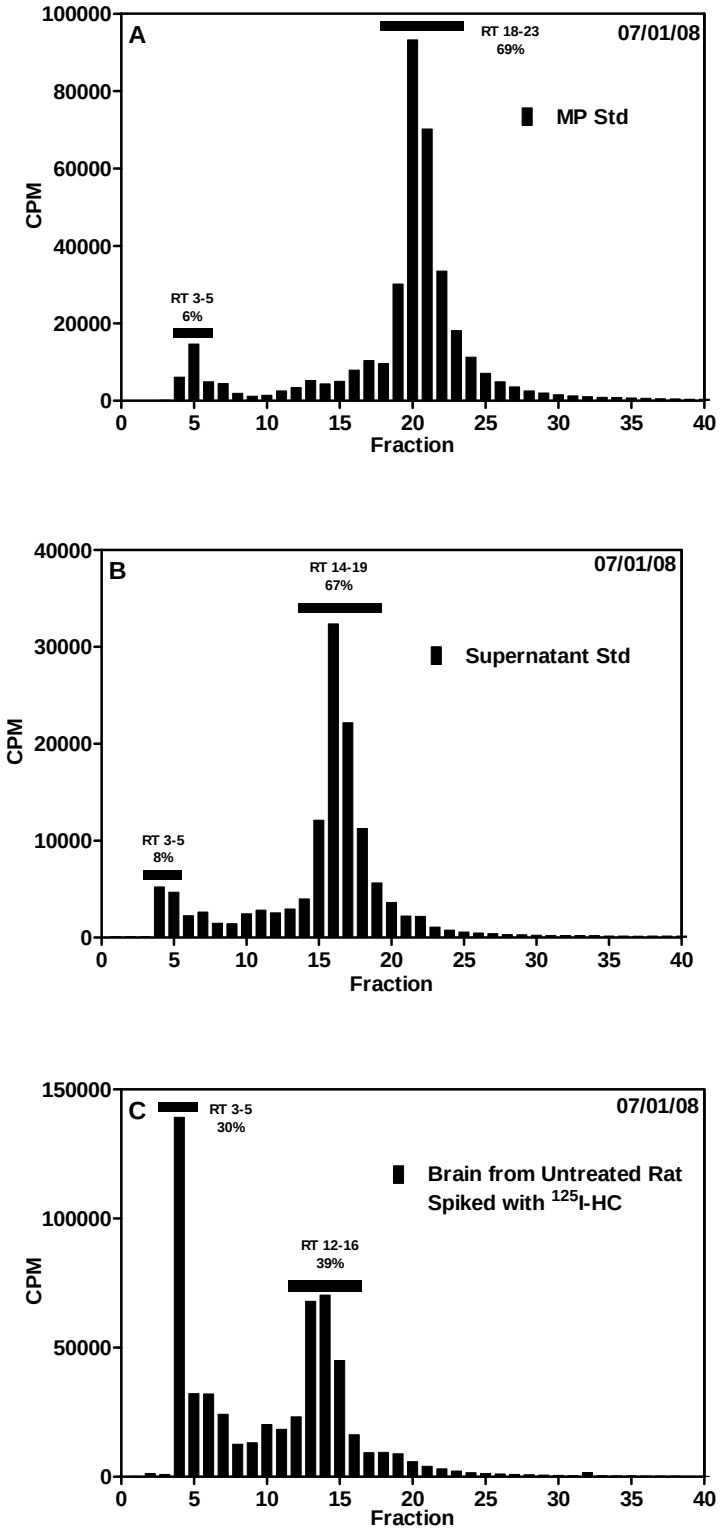

Supplementary Material (2.7.1) Figure 6: HPLC Analysis of Blood Processing Control

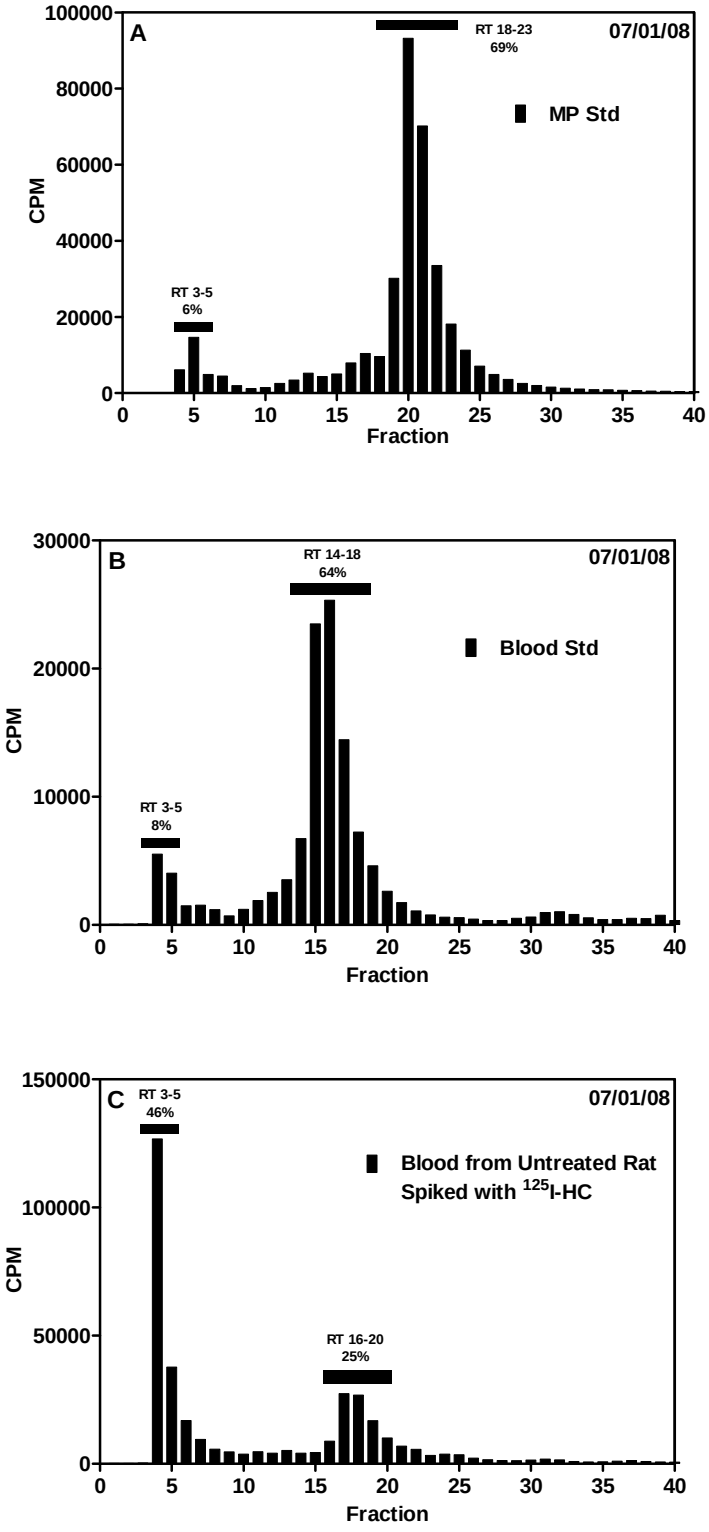

Supplementary Material (2.7.1) Figure 7: <u>Brain</u> Supernatant Following <u>Intranasal</u> Administration to Rat #2

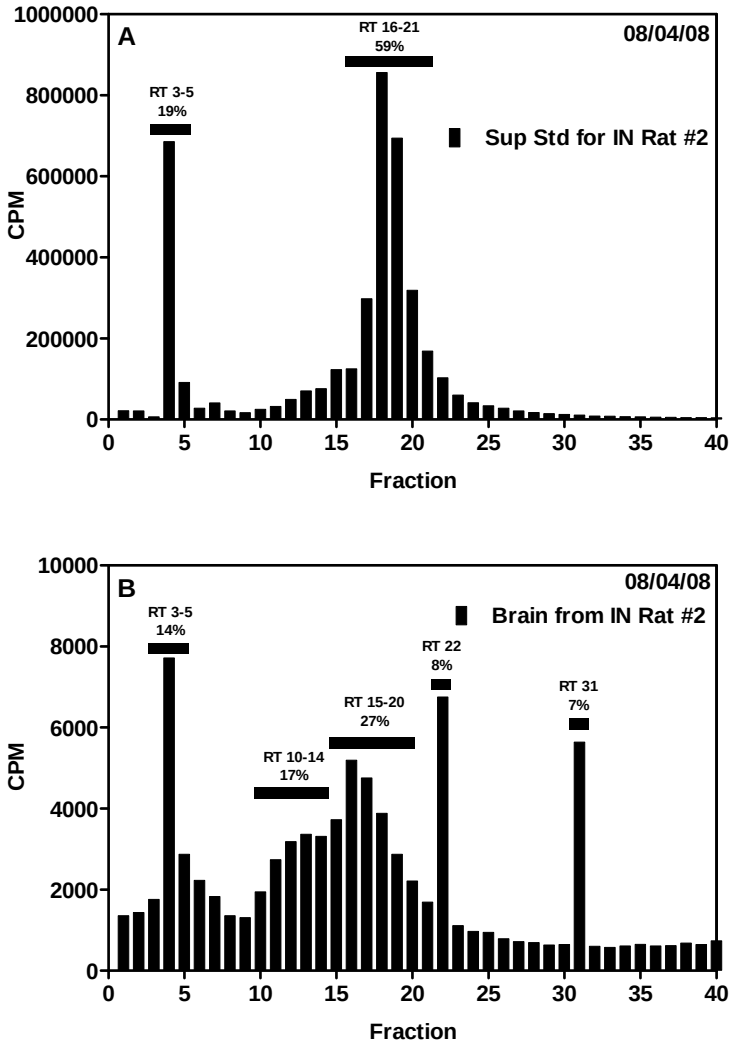

Supplementary Material (2.7.1) Figure 8: <u>Brain</u> Supernatant Following <u>Intranasal</u> Administration to Rat #3

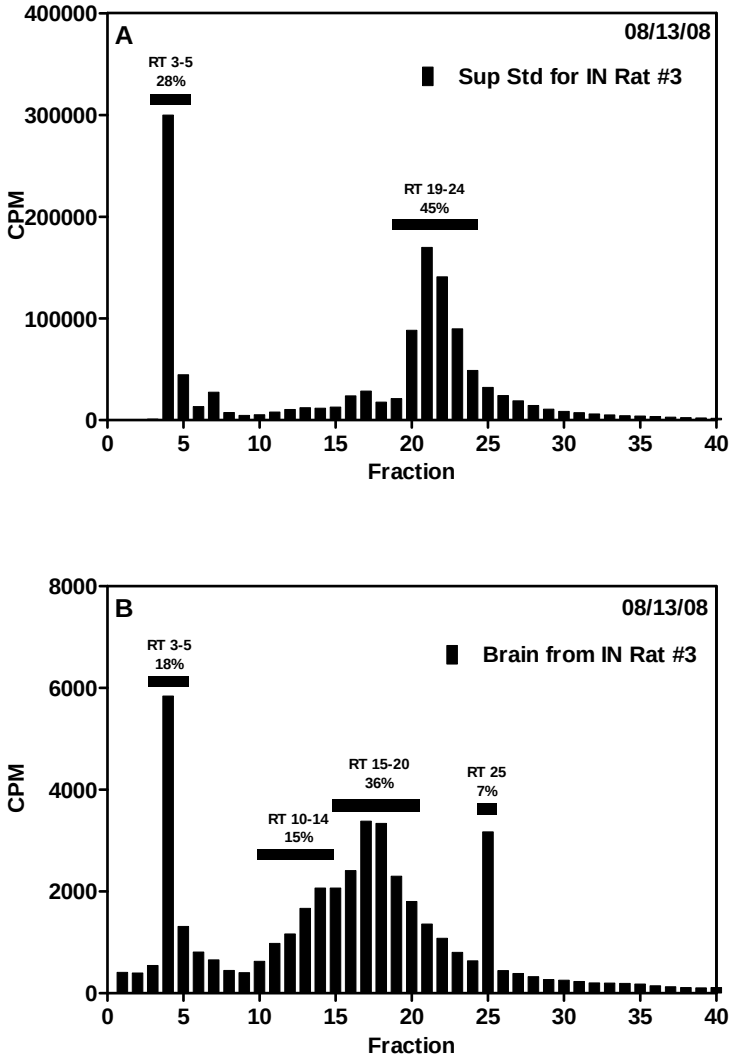

Supplementary Material (2.7.1) Figure 9: Brain Supernatant Following Intranasal Administration to Rat #4

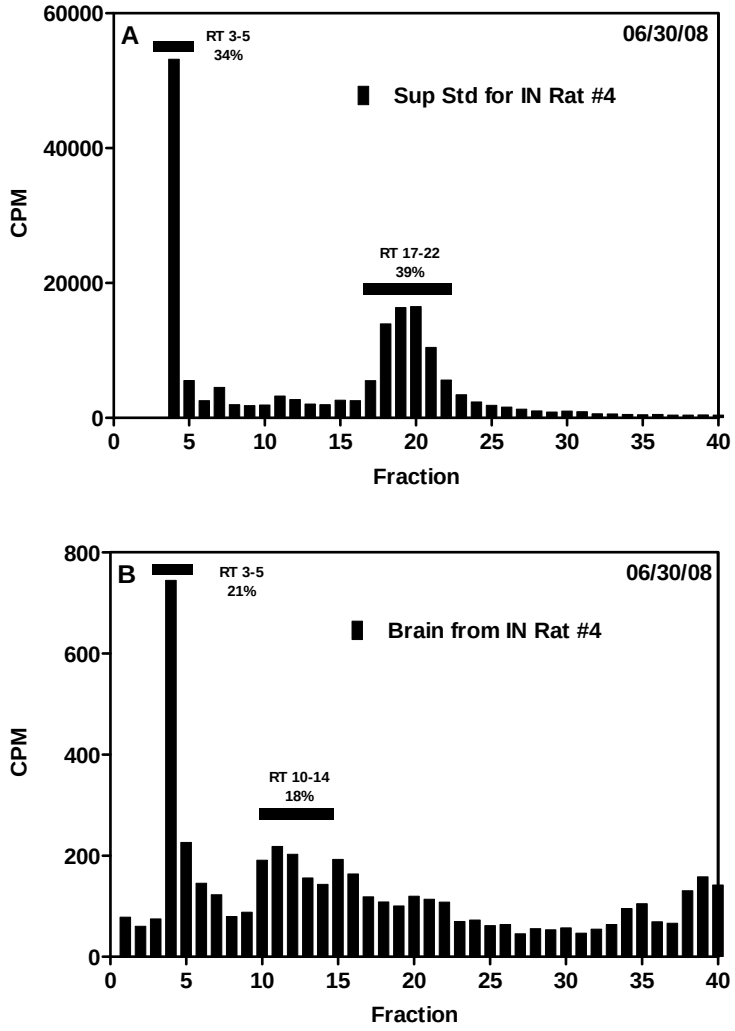

Supplementary Material (2.7.1) Figure 10: <u>Brain</u> Supernatant Following <u>Intravenous</u> Administration to Rat #2

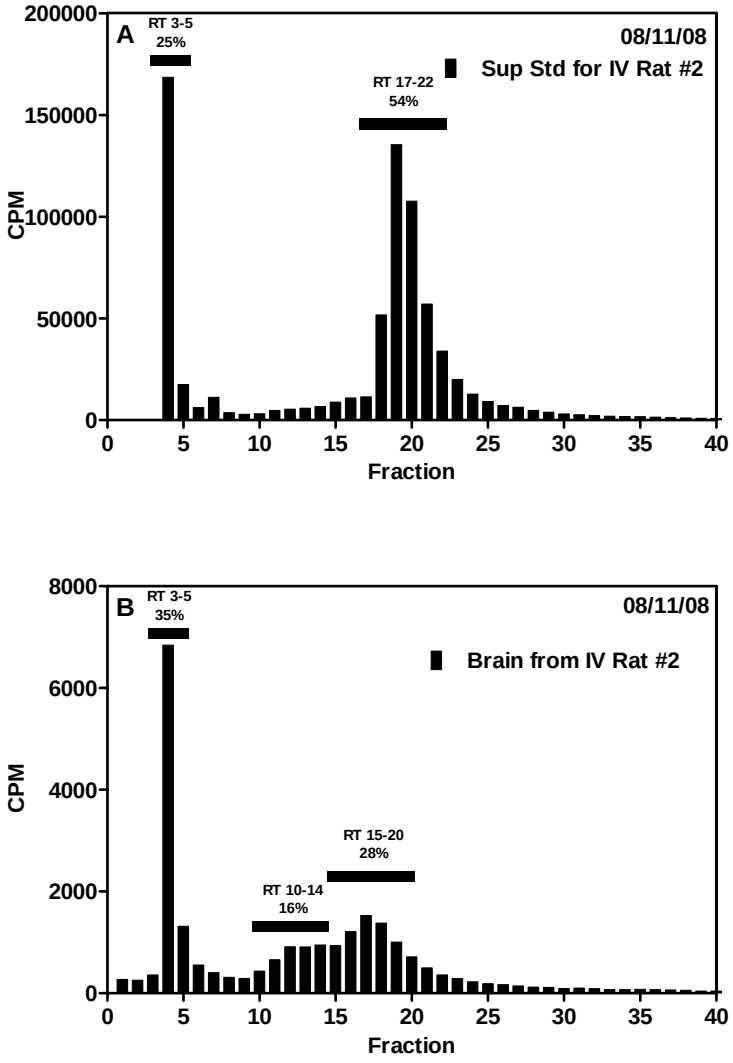

Supplementary Material (2.7.1) Figure 11: <u>Brain</u> Supernatant Following <u>Intravenous</u> Administration to Rat #3

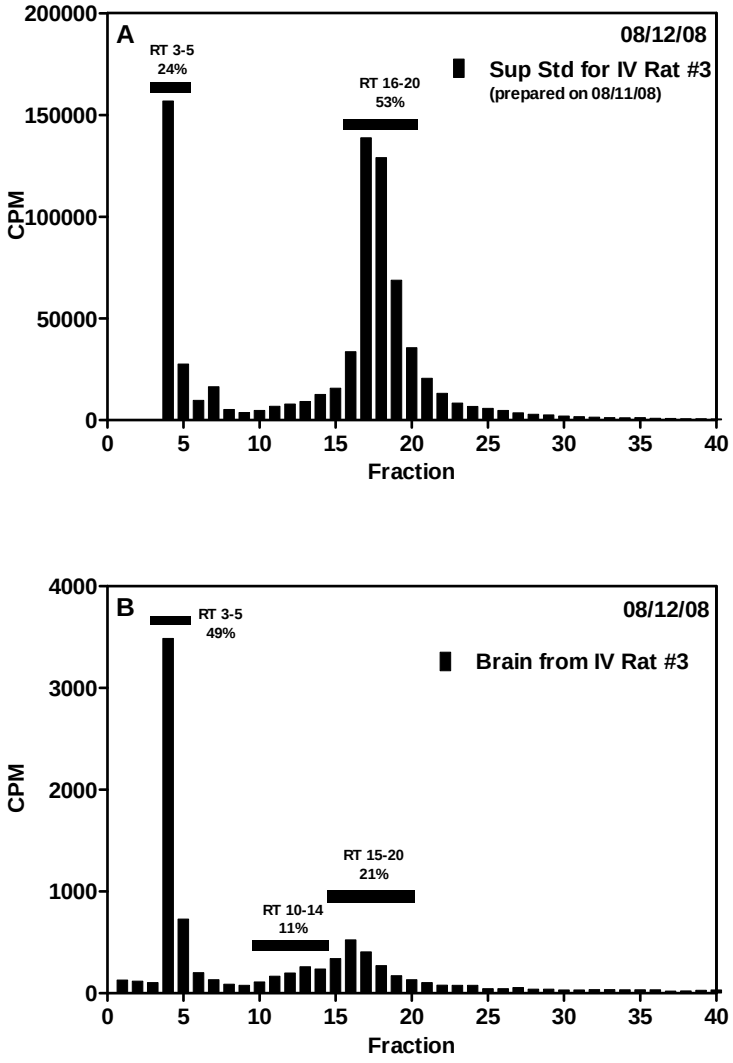

Supplementary Material (2.7.1) Figure 12: <u>Blood</u> Following <u>Intranasal</u> Administration to Rat #2 and Rat #3

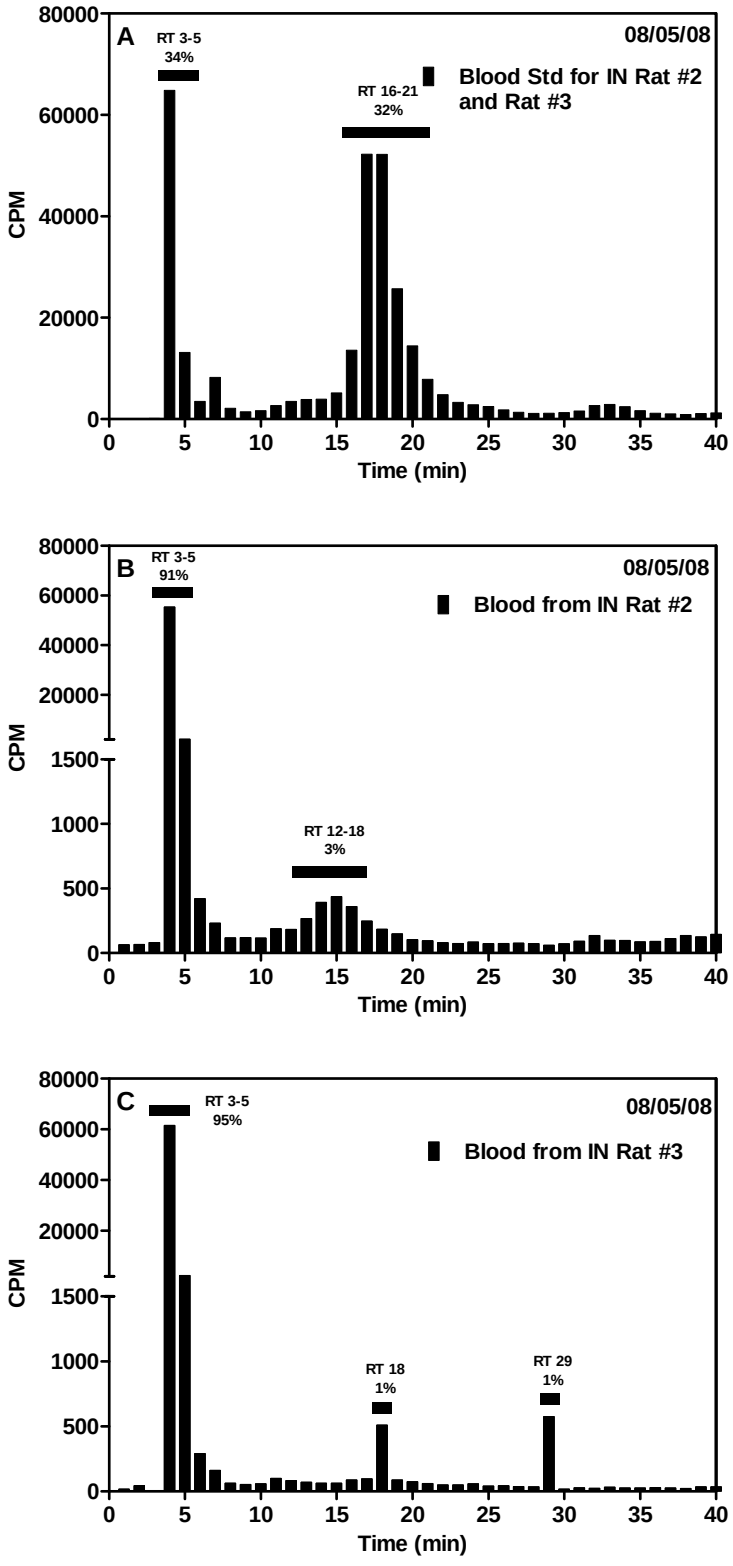

Supplementary Material (2.7.1) Figure 13: <u>Blood</u> Following <u>Intranasal</u> Administration to Rat #4

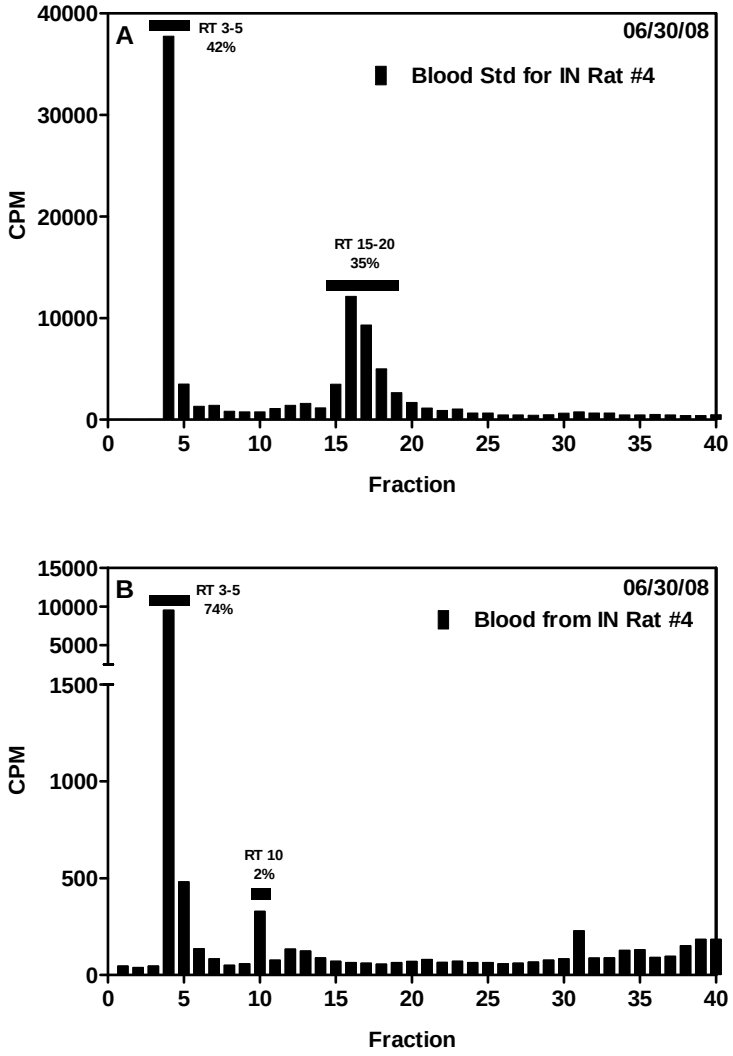

Supplementary Material (2.7.1) Figure 14: Blood Following Intravenous Administration to Rat #2 and Rat #3

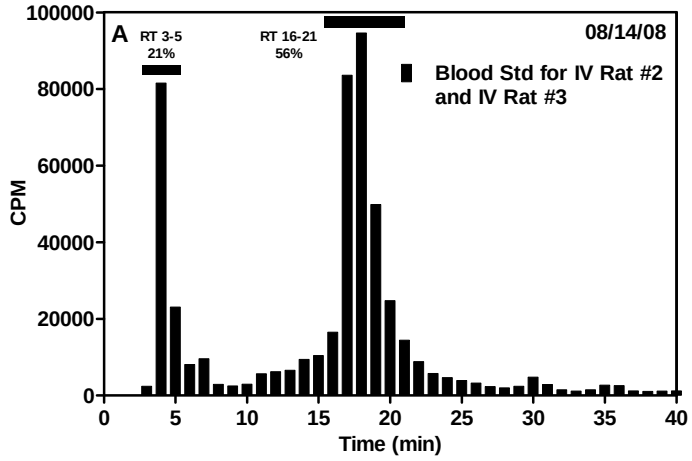

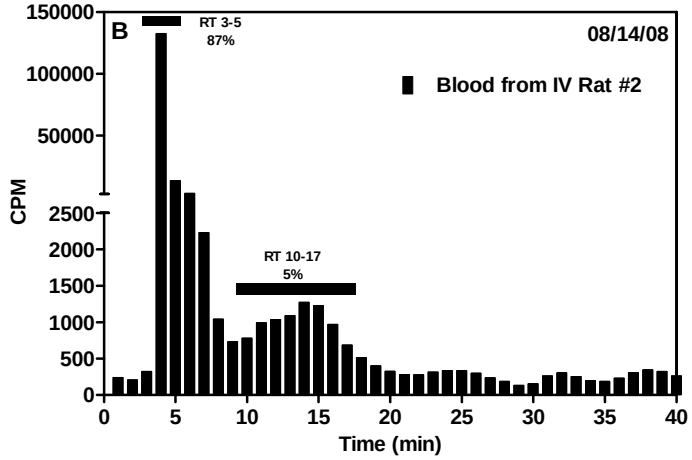

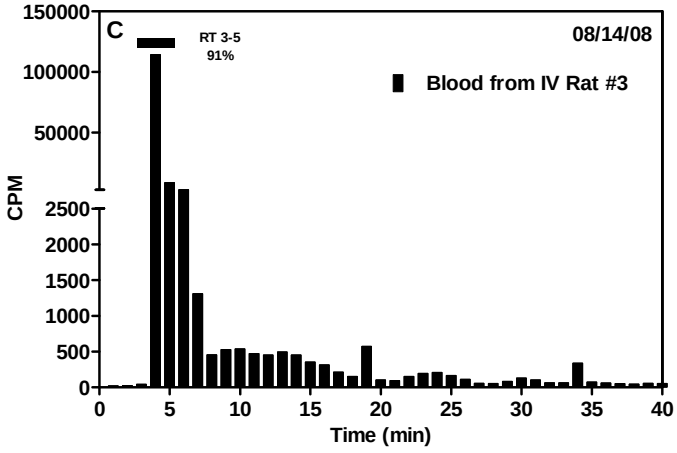

CHAPTER 3

BEHAVIORAL ASSESSMENTS AFTER INTRANASAL ADMINISTRATION OF HYPOCRETIN-1 (OREXIN-A) IN RATS: EFFECTS ON APPETITE AND LOCOMOTOR ACTIVITY

3.1 Introduction

Hypocretin-1 (HC, orexin-A) and hypocretin-2 (HC-2, orexin-B) are neuropeptides synthesized from the precursor protein, preprohypocretin, exclusively in neurons located in the lateral hypothalamus (Sakurai et al., 1998). HC contains 33 amino acids (MW 3562) and two disulfide bridges, while HC-2 is a linear peptide comprised of 28 amino acids (MW 2937), making it relatively less stable. Hypocretin neurons send extensive projections throughout the central nervous system (CNS), including the olfactory bulbs, cerebral cortex, diencephalon, and brainstem, to exert effects on numerous physiological functions (Peyron et al., 1998; Date et al., 1999; Nambu et al., 1999). CNS effects of hypocretin peptides are mediated by the G-protein-coupled receptors, hypocretin receptor 1 (HC-R1) and hypocretin receptor 2 (HC-R2), which are differentially distributed throughout the CNS (Trivedi et al., 1998; Marcus et al., 2001). HC binds to HC-R1 with greater affinity than HC-2 (EC_{50} = 30 nM and 2500 nM), whereas HC and HC-2 demonstrate similar affinity for HC-R2 (EC_{50} = 34 nM and 60 nM, respectively) (Sakurai et al., 1998). Receptor stimulation with HC in cell culture has been shown to activate downstream targets of the mitogen-activated protein kinase (MAPK) signaling pathway (extracellular signal-regulated kinases, ERK) and the

phosphatidyl-inositol 3-kinase (PI3K) signaling pathway (phosphoinositide-dependent kinase-1, PDK-1), though the mechanism by which G-protein-coupled receptors are involved in these pathways are not clear (Ammoun et al., 2006b; Ammoun et al., 2006a; Goncz et al., 2008).

Hypocretin neuropeptides are involved in activities related to the awake state of animals. Intracerebroventricular administration or direct injection of HC into hypothalamic nuclei increases food consumption (Sakurai et al., 1998; Sweet et al., 1999), wakefulness (Mieda et al., 2004), water intake (Kunii et al., 1999), locomotion (Nakamura et al., 2000; Kotz et al., 2006), and memory (Jaeger et al., 2002; Aou et al., 2003). HC deficiency is observed in neurological and psyhiatric diseases, including Alzheimer's disease, Parkinson's disease (Thannickal et al., 2007, 2008), narcolepsy (Chemelli et al., 1999; Nishino et al., 2000; Thannickal et al., 2000; Hara et al., 2001; Ripley et al., 2001), depression (Salomon et al., 2003; Allard et al., 2004; Brundin et al., 2007; Feng et al., 2008), and traumatic brain injury (Baumann et al., 2005). Targeting of HC to the CNS has potential for treating these diseases and for modulating numerous CNS functions.

A significant challenge to CNS drug delivery is the presence of the blood-brain barrier (BBB), which limits the bioavailability of therapeutics to the CNS following systemic administration. Intranasal administration is a convenient method to bypass the BBB, minimize systemic exposure, and rapidly target therapeutics to the CNS along olfactory and trigeminal nerves, which lead directly from the nasal cavity to the CNS (Thorne et al., 2004; Dhanda et al., 2005).

It was previously demonstrated that intranasal administration of HC (10 nmol) resulted in rapid delivery to multiple brain areas, including the target site of the hypothalamus, in both mice (Hanson et al., 2004) and in rats (Dhuria et al., 2008). Recent studies indicate that intranasal administration of HC improves cognitive ability following sleep deprivation in nonhuman primates (Deadwyler et al., 2007) and restores olfactory function in humans with narcolepsy (Baier et al., 2008). As a preliminary step for evaluating the therapeutic utility of intranasal HC, the purpose of this study was to assess behavioral effects following intranasal administration of HC in a rat model and to understand the cellular mechanisms underlying the HC-mediated CNS effects. To ensure an adequate response, rats were intranasally treated with 100 nmol of HC and subsequently monitored for food consumption, water intake, and wheel running activity. In addition, radiotracer methods were used to assess the biodistribution in the CNS and Western blot was used to measure activation of downstream cell signaling proteins (ERK and PDK-1) following intranasal administration of HC.

3.2 Material and Methods

3.2.1 Animals and Housing

Male, Sprague-Dawley rats (200-300g) were obtained from Charles River Laboratories (Wilmington, MA) for the behavioral study conducted at the San Francisco VA Medical Center or from Harlan (Indianapolis, IN) for the cell signaling and biodistribution studies conducted at the Alzheimer's Research Center. Animals were maintained on a 12 h light/dark cycle with food and water provided *ad libitum.*

Animals were cared for in accordance with institutional guidelines and all experiments were approved by the San Francisco VA Medical Center Animal Care and Use Committee and by Regions Hospital, HealthPartners Research Foundation Animal Care and Use Committee.

3.2.2 Drugs and Reagents

Hypocretin-1 (HC, Cat # 46-2-70B) was purchased from American Peptide Company (Sunnyvale, CA). For the biodistribution study, HC was custom ^{125}I-labeled by Perkin Elmer (Boston, MA) using a lactoperoxidase method resulting in radiolabeled product containing less than 5% unbound ^{125}I as assessed by thin layer chromatography and less than 15% acetonitrile. The radiolabeled peptide was used within 2 weeks of synthesis. Phosphate buffered saline (PBS, 10x concentrate) was purchased from Sigma-Aldrich (St. Louis, MO).

3.2.3 Dose Solutions

Intranasal dose solutions contained unlabeled HC dissolved in PBS (10 mM sodium phosphate, 154 mM sodium chloride, pH 7.4) to a final concentration of 1.7 nmol/μL. For the biodistribution study, intranasal dose solutions also contained trace amounts of ^{125}I-HC for a final radioactivity concentration of 0.9 μCi/μL. Animals received 60 μL of the intranasal dose solution for a total dose of 100 nmol. In addition, a lower dose of HC (10 nmol) was evaluated using a more dilute concentration of HC to maintain the dosing volume of 60 μL. For the behavioral and cell signaling studies,

control animals received an equivalent volume of vehicle (PBS). Dose solution aliquots for each experiment were stored at -20 °C until the day of the experiment.

3.2.4 Intranasal Administration

Intranasal administration was performed with animals under anesthesia and lying on their backs on a heating pad maintained at 37°C. For the behavioral studies, animals were anesthetized with a mixture of 70% N_2 and 30% O_2 containing isoflurane (5% induction; 2-3% maintenance) administered through a nose cone. For the terminal biodistribution and cell signaling studies, animals were anesthetized with sodium pentobarbital (Nembutal, 50 mg/kg intraperitoneal, Abbott Laboratories, North Chicago, IL) and a piece of gauze was rolled (1¼ cm diameter) and placed under the neck to maintain a horizontal rat head position. Intranasal administration was accomplished by using a pipettor to administer 6 μL nose drops noninvasively to alternating nostrils every two minutes while occluding the opposite nostril. The drop was placed at the opening of the nostril allowing the animal to snort the drop into the nasal cavity. A total volume of 60 μL of solution (HC or PBS) was administered over 18 minutes. For animals under isoflurane anesthesia for the behavioral study, dosing was accomplished by briefly sliding the nose out of the nose cone to administer the drop. After the final nose drop, the animals were left under isoflurane anesthesia for an additional ten minutes to ensure complete absorption. The use of this head position, drop size, time interval between drops, and occlusion of the opposite nostril facilitates delivery to both the olfactory epithelium and respiratory epithelium of the nasal cavity and prevents drainage of the dose solution into the trachea and esophagus.

3.2.5 Behavioral Study

Behavioral experiments were conducted with a crossover design in two phases with a sample size of n = 6 animals in each phase. Animals were dosed intranasally with HC or PBS at approximately 4 hours into the light cycle under isoflurane anesthesia as described above. At 30 minutes after the onset of intranasal administration, animals were placed in Mini Mitter biotelemetry cages (Bend, OR) containing running wheels and behavior was monitored for a period of 24 hours. The number of wheel revolutions over a 5 minute period was recorded using Vitalview software. Food and water measurements were obtained at 4, 8, and 24 hours after being placed in the cages. At the end of the study period, the animals were returned to their home cages. After a 2 day washout period, the crossover treatment was initiated and behaviors were monitored as described above.

3.2.6 Biodistribution Study

Biodistribution experiments were conducted in a separate group of animals (n = 5 for the high dose; n = 4 for the low dose). For blood sampling and perfusion, the descending aorta was cannulated under anesthesia prior to intranasal administration using a 20G, 1¼ inch catheter (Jelco, Johnson and Johnson Medical Inc., Arlington, TX) connected to a 3-way stopcock (B. Braun Medical Inc., Bethlehem, PA). Blood samples (0.1 mL) were obtained via the descending aorta cannula at 5, 10, 15, 20, and 30 minutes after the onset of intranasal administration, maintaining blood volume during the course of the experiment by replacing with 0.9% sodium chloride (0.35 mL) after every other blood draw.

Peripheral and CNS tissues were obtained approximately 30 minutes after the onset of drug delivery following perfusion and fixation of animals with 60 mL of 0.9% sodium chloride and 360 mL of 4% paraformaldehyde in 0.1 M Sorenson's phosphate buffer, pH 7.4, using an infusion pump (15 mL/min; Harvard Apparatus, Inc., Holliston, MA). A gross dissection of major peripheral organs (muscle, liver, kidney, spleen, and heart) was performed, as well as dissection of the superficial and deep cervical lymph nodes and axillary lymph nodes. The brain was removed and olfactory bulbs were dissected. Serial (2 mm) coronal sections of the brain were made using a rat brain matrix (Braintree Scientific, Braintree, MA). Microdissection of specific brain regions was performed on coronal sections with reference to a rat brain atlas (Paxinos and Watson, 1997). A portion of the trigeminal nerve containing the trigeminal ganglion and sections of the ophthalmic (V1) and maxillary (V2) divisions of the trigeminal nerve was dissected from the base of the cranial cavity from the anterior lacerated foramen to the point at which the nerve enters the pons. Following removal and sampling of the dura from the spinal cord, the spinal cord was dissected into cervical, thoracic, and lumbar sections.

In a separate group of animals (n = 4), CSF was sampled via cisternal puncture approximately 30 minutes after the onset of intranasal administration. CSF sampling was performed in a separate group of animals since it was shown in the Supplementary Material for Chapter 4 that cisternal puncture significantly affects brain concentrations of intranasally applied peptides. A towel was rolled to position the head at an approximate 45 degree angle with the nose pointing downward. A 20G needle attached to 30 cm long polyethylene tubing (PE90) was inserted into the cisterna magna. CSF

was collected (~50 μL) into the tubing until flow stopped or until blood was observed. In some cases, gentle suction was applied using an empty syringe to facilitate CSF flow. The tubing was immediately clamped if blood was observed to avoid contamination due to blood-derived radioactivity. Only CSF samples containing clear fluid were included in the analysis.

Each tissue or fluid sample was placed into a pre-weighed 5 mL tube, and the wet weight was determined using a microbalance (Sartorius MC210S, Goettingen, Germany). Radioactivity in each sample was determined by gamma counting for 5 minutes in a Packard Cobra II Auto Gamma counter (Packard Instrument Company, Meriden, CT). Concentrations (nmol/L) were calculated, assuming minimal degradation of the ^{125}I-HC, based on the specific activity of standards sampled from the dose solution (fmol/CPM), counts per minute measured in the tissue (CPM), tissue weight (g), and a density of 1 g/mL.

3.2.7 Cell Signaling Study

Cell signaling experiments were conducted in a separate group of animals (n = 3) that were intranasally dosed (HC or PBS) at approximately 4 hours into the light cycle under sodium pentobarbital anesthesia. At 30 minutes after the onset of intranasal administration, animals were transcardially perfused with 100 mL of 0.9% sodium chloride containing Complete protease inhibitor cocktail (Roche Diagnostics, Indianapolis, IN) using an infusion pump (15 mL/min; Harvard Apparatus, Inc., Holliston, MA). The brain was dissected on ice into the right and left olfactory bulbs, diencephalon, and brainstem.

Tissues were homogenized in 10 volumes of ice cold radioimmunoprecipitation (RIPA) buffer containing 50 mM Tris-HCl, pH 7.4, 150 mM NaCl, 2 mM ethylenediaminetetraacetic acid (EDTA), 1% sodium deoxycholate, 1% NP-40, 0.1% sodium dodecyl sulfate (SDS), Complete protease inhibitor cocktail, and phosphatase inhibitor cocktail (P5726, Sigma, St. Louis, MO). Samples were sonicated with ten pulses and then centrifuged for 30 minutes at 10,000g at 4°C. Protein concentration of the supernatant was determined using the bicinchoninic acid (BCA) method.

Volumes corresponding to 25 μg of protein were diluted in Laemmli buffer, heated for 5 minutes at 96 °C, and loaded onto 10% SDS polyacrylamide gels. Following gel electrophoresis, proteins were transferred to PVDF membranes and blocked with 5% milk in Tris buffered saline with Tween (TBST) (50 mM Tris-HCl, pH 7.4, 150 mM NaCl, and 0.05% Tween-20) for 1 hour. Membranes were incubated with primary antibodies for phospho-p44/42 MAPK (Thr202/Tyr204) (D13.14.4E) (rabbit monoclonal, 1:1000, Cell Signaling Technology, Beverly, MA) or PDK-1 (rabbit polyclonal, 1:1000, Cell Signaling Technology, Beverly, MA) in TBST-5% BSA at 4 °C overnight. After three-5 minute washes with TBST, membranes were incubated with a horseradish peroxidase-conjugated secondary antibody (anti-rabbit, 1:25,000, Cell Signaling Technology, Beverly, MA) at room temperature for 1 hour. Blots were developed using an Enhanced Chemiluminescence Plus detection kit (GE Healthcare, Buckinghamshire, UK). The signal of each band was scanned and quantified using Image J (available through the National Institutes of Health from http://rsb.info.nih.gov/ij/download.html). Membranes were stripped with 5% SDS for 30 minutes at 60 °C and reprobed for total MAPK and beta actin using primary

antibodies for MAPK (ERK1/ERK2) (rabbit polyclonal, 1:1000, Calbiochem, San Diego, CA) and beta actin (rabbit polyclonal, 1:20,000, Santa Cruz Biotechnology, Santa Cruz, CA), respectively. Blots were incubated with secondary antibody, developed, and quantified, as described above. Optical density values were normalized to values for total MAPK and beta actin to account for differences in sample loading.

3.2.8 Data and Statistical Analysis

For the behavioral study, food and water consumption at each time point (4, 8, and 24 h) were measured, while wheel running activity was assessed by determining the area under the wheel turn-time curve (AUC) in 1 hour segments from 0-8 h after intranasal dosing. A nonparametric two-sample paired t-test (Wilcoxon signed rank test) was used to compare HC and PBS groups. For the biodistribution study, concentrations were calculated in CNS tissues, peripheral tissues, and blood based on measurements of ^{125}I. In addition, the ratio of the tissue concentration at the high dose (100 nmol) to the tissue concentration at the low dose (10 nmol) was determined. The resulting high/low ratio provided an assessment of intranasal delivery efficiency at different doses of HC. For the cell signaling study, the signal of each band was quantified. Phosphorylated MAPK (pMAPK) was normalized to total MAPK and PDK-1 was normalized to actin to account for differences in sample loading. A two-sample unpaired t-test was used to compare HC and PBS groups. For all studies, data are expressed as mean ± standard error (SE). Statistical analysis was performed using GraphPad Prism software (version 5.01, GraphPad Software Inc., San Diego, CA). Differences were considered marginally significant if $p < 0.10$ or significant if $p < 0.05$.

3.3 Results

3.3.1 Behavioral Effects of Intranasal HC (100 nmol)

Intranasal administration of HC (100 nmol) significantly increased food consumption in rats by 71% during the first 4 hours after dosing compared to PBS controls, consistent with the rapid entry of HC into the CNS (Figure 1). After 4 hours, food consumption was significantly reduced by 55% in the HC-treated group compared to PBS controls, and no significant differences in food consumption were observed between groups from 8-24 hours. Water intake was not significantly affected by treatment with intranasal HC (100 nmol) compared to PBS controls over the entire 24 hour study period (Figure 2). Wheel running behavior was increased by treatment with intranasal HC (100 nmol) over the first 4 hours compared to treatment with intranasal PBS (Table 1 and Figure 3). This increase in activity with intranasal HC was found to be marginally significant when comparing the wheel running AUC over the 0-4 hour time period ($p = 0.08$). The greatest effect of HC on wheel running activity was observed between the 1-2 hour time period following intranasal dosing, with a significant 2.2-fold increase in locomotor activity (Table 1 and Figure 3). The effect of intranasal HC diminished by 4 hours after dosing (Table 1), consistent with the time course of the food intake component of this study.

3.3.2 Biodistribution following Intranasal HC (100 nmol and 10 nmol)

Intranasal HC (100 nmol) resulted in delivery throughout the brain and spinal cord within 30 minutes of drug administration, with concentrations ranging from 4.0

nM to 14 nM in the brain, and from 1.9 nM to 8.9 nM in the spinal cord (Table 2). The highest brain concentrations were observed in the olfactory bulbs (14 nM) and hypothalamus (13 nM), while the lowest concentrations were found in the caudate nucleus (4.0 nM) and frontal cortex (4.2 nM). In the spinal cord, a decreasing concentration gradient was observed from the rostral to caudal direction. Intranasal HC also resulted in delivery to CNS-related tissues, including the trigeminal nerve, CSF, and meningeal membranes surrounding the brain and spinal cord (Table 2). Concentrations in the trigeminal nerve were significantly greater compared to concentrations in other brain areas. In addition, intranasal administration of HC (100 nmol) resulted in exposure to peripheral compartments within 30 minutes of delivery (Table 3). The highest concentration outside of the CNS was found in the deep cervical lymph nodes (222 nM), consistent with drainage pathways from the nasal cavity to the lymphatic system (Bradbury and Westrop, 1983; Kida et al., 1993; Nagra et al., 2006; Walter et al., 2006a). Blood concentrations gradually increased from 6.8 nM at 5 minutes to 45 nM at 30 minutes, and high concentrations were noted in the kidney, liver, and spleen.

HC concentrations were dose dependent, with a 10-fold lower dose of HC resulting in 10-fold lower concentrations in the olfactory bulbs, trigeminal nerve, blood, liver, and kidney (Table 2 and Table 3). A 10 nmol dose of HC resulted in concentrations that were 5- to 13-fold lower in other CNS tissues (Table 2) and 5- to 9-fold lower in other peripheral tissues (Table 3) compared to the 100 nmol dose of HC.

3.3.3 Cell Signaling Effects of Intranasal HC (100 nmol)

Intranasal administration of 100 nmol of HC resulted in a marginally significant reduction in levels of phosphorylated MAPK (pMAPK) in the olfactory bulbs (66% reduction), with no effect in the diencephalon or brainstem, compared to PBS controls at 30 minutes (Figure 4). While intranasal HC resulted in a marginally significant reduction on PDK-1 levels in the olfactory bulbs (21% decrease), significant increases in PDK-1 levels were observed in the diencephalon (26% increase) and brainstem (21% increase) at 30 minutes after intranasal dosing (Figure 5). Basal levels of pMAPK differed across brain areas, with the greatest phosphorylated protein levels in the olfactory bulbs (Figure 4). Levels of PDK-1, however, were consistent throughout the brain (Figure 5).

3.4 Discussion

In the present behavioral study, intranasal administration of HC (100 nmol) significantly increased food consumption and wheel running activity in rats within 4 hours of dosing. Interestingly, these behavioral effects were observed during the light-phase of the light-dark cycle when animals are normally in the resting state, indicating that the HC reaching the brain was sufficient to overcome signals of satiety and inactivity. These findings are consistent with results showing that intracerebroventricular (ICV) administration of HC during early light phase dose-dependently increased food consumption (Sakurai et al., 1998) and locomotor activity (Nakamura et al., 2000) in rats. Results from this study confirm the presence of biologically active HC in the CNS following intranasal administration in rats.

Despite the small sample size of the study (n = 12) and the considerable variability of the wheel running activity in animals (standard error bars excluded for clarity), the findings of increased feeding and increased locomotor activity are encouraging since the results are likely an underestimation of the effects of intranasal HC on rodent behavior. Unlike in the reported ICV studies, anesthesia was required for intranasal delivery to rats, which could have adverse side effects in the animals and reduce appetite and activity. Wheel running activity during the first 30 minutes following intranasal dosing was reduced for animals, regardless of the treatment (Figure 3), suggesting that there was a lingering effect of anesthesia. Adverse effects from the anesthesia could partially explain the lack of effect of intranasal HC on water intake. In addition, locomotor activity was measured using a wheel running apparatus that measures the number of wheel turns every five minutes. However, the system does not capture other locomotor behaviors such as grooming, rearing or exploratory movement that could have been occurring in the rats due to the effects of intranasal HC. Microanalysis of video recordings (Jones et al., 2001) or use of cages equipped with beam break detectors (Nakamura et al., 2000; Kotz et al., 2006) could provide greater sensitivity in these measures of locomotor behaviors. It is also not clear whether locomotor activity is affected by animals being in a familiar or unfamiliar environment (Smith and Morrell, 2007; Buddenberg et al., 2008). ICV administration of HC-2 increased locomotor activity in both familiar and novel environments (Jones et al., 2001), while corticotropin-releasing factor increased activity in a familiar environment (Jones et al., 1998), but decreased activity in a novel environment (Dunn and Berridge, 1990). In the present behavioral study, animals were not allowed to acclimate to the

new environment, so it is possible that stress could have also diminished the effects of intranasal HC. Despite these adversities, intranasal HC was shown to increase food consumption and wheel running activity during the inactive period of the day.

To understand the molecular mechanisms underlying the observed behavioral effects, biodistribution and cell signaling pathways were studied using radiotracer methods and Western blot. Intranasal administration of HC (100 nmol) resulted in widespread distribution in the brain, consistent with the distribution of hypocretin receptors in rat brain (Trivedi et al., 1998; Marcus et al., 2001), with concentrations in the range of the affinity of HC for hypocretin receptors (Sakurai et al., 1998). These concentrations were sufficient to activate hypocretin receptors to affect downstream targets of the MAPK cell signaling pathway and the PI3K cell signaling pathway. In cell culture, HC was reported to dose- and time-dependently increase levels of phosphorylated MAPK (pMAPK) and PDK-1 following activation of hypocretin G-protein-coupled receptors (Ammoun et al., 2006b; Ammoun et al., 2006a; Goncz et al., 2008). Phosphorylation of MAPK is rapid, with elevated levels observed within minutes and lasting over an hour before declining to basal levels (Ammoun et al., 2006b). In the present cell signaling study, intranasal HC (100 nmol) reduced levels of pMAPK in the olfactory bulbs compared to PBS controls at 30 minutes, but had no affect on pMAPK in the diencephalon or brainstem. Cell-type specific differences in HC receptor signaling pathways could account for these differences observed between *in vitro* and *in vivo* studies (Ammoun et al., 2006b). It is also possible that evaluating pMAPK levels at a different time point may yield different results. Intranasal HC (100 nmol) resulted in reduced PDK-1 levels in the olfactory bulbs at 30 minutes. However

in the diencephalon and brainstem, which are brain areas involved in the regulation of appetite and arousal, respectively, PDK-1 levels were significantly increased. Signaling studies at additional time points could provide greater insight into the cellular mechanisms underlying the behavioral effects of intranasal HC. These findings provide preliminary evidence that suggests that the increases in food consumption and locomotor activity observed within 4 hours of intranasal administration of HC may be due, in part, to the activation of HC signaling pathways involving PDK-1.

Results from the biodistribution study also revealed that concentrations were dose-dependent in most CNS and peripheral tissues. In Chapter 2 of this dissertation, biodistribution data following a 10 nmol dose of HC were reported. Because there may be batch-to-batch variability in the radiolabeled material, in addition to the 100 nmol dose evaluated in the present biodistribution study, the 10 nmol dose was repeated. In several tissues, the high/low ratio was less than 10, indicating that the high dose of 100 nmol resulted in less efficient delivery compared to the low dose of 10 nmol. These findings raise the possibility that a portion of the delivery of HC into the brain may be carrier-mediated. However, Kastin and Akerstrom (1999) have demonstrated that HC passively diffuses across the BBB via nonsaturable mechanisms (Kastin and Akerstrom, 1999). It is also possible that a portion of intranasally administered therapeutics binds nonspecifically in the nasal mucosa (Ross et al., 2004).

In conclusion, results from these studies indicate that intranasal administration of a 100 nmol dose of HC results in brain concentrations sufficient to affect CNS behaviors mediated by HC over a short time period. The increases in food consumption and wheel running activity may involve activation of PI3K cell signaling pathways.

The rapid nature of the effects on appetite and locomotion provide support for a rapid, extracellular pathway of delivery of intact and biologically active HC to the CNS following intranasal administration. These data add to the emerging evidence demonstrating the potential of using intranasal HC for the treatment of neurological and psychiatric disorders involving the hypocretinergic system.

Table 1: Time Course of Effect of Intranasal HC (100 nmol) on Wheel Running Activity

Time	PBS AUC[a]	HC AUC[a]	Fold-Difference	p-value[b]
0-1 h	41.3 ± 12.9	101.0 ± 44.2	2.4	0.31
1-2 h	96.7 ± 39.6	210.2 ± 56.2	2.2	0.02*
2-3 h	172.9 ± 49.2	245.0 ± 85.3	1.4	0.32
3-4 h	175.4 ± 64.2	214.2 ± 64.7	1.2	0.34
4-5 h	182.3 ± 57.6	155.2 ± 42.0	0.9	0.91
5-6 h	63.8 ± 27.4	66.0 ± 44.3	1.0	1.00
6-7 h	46.9 ± 31.0	65.8 ± 27.7	1.4	0.55
7-8 h	137.7 ± 43.3	89.8 ± 28.5	0.7	0.70

[a]Mean area under the curve (AUC) generated from wheel running-time profile over 1 hour segments; p-value comparing hypocretin-1 (HC) and phosphate-buffered saline (PBS) control AUC over 0-4 hour segment was marginally significant (781.8 ± 200.4 versus 494.2 ± 121.9, p = 0.08)

[b]Compared AUC using paired sample Wilcoxon signed rank test.

Table 2: Biodistribution in CNS and CNS-Related Tissues Following Intranasal Administration

	Intranasal HC[a] (100 nmol, n = 5)	Intranasal HC[a] (10 nmol, n = 4)	High/Low Ratio
CNS Tissues			
Olfactory Bulbs	14.0 ± 3.12	1.46 ± 0.67	10
Ant. Olfactory Nucleus	5.61 ± 1.33	0.75 ± 0.25	7
Frontal Cortex	4.18 ± 0.46	0.72 ± 0.20	6
Caudate/Putamen	3.96 ± 1.02	0.77 ± 0.26	5
Septal Nucleus	5.66 ± 1.66	0.94 ± 0.48	6
Parietal Cortex	4.60 ± 0.78	0.68 ± 0.24	7
Hippocampus	4.77 ± 1.69	0.72 ± 0.30	7
Thalamus	5.73 ± 2.43	0.75 ± 0.32	8
Hypothalamus	12.5 ± 4.35	0.99 ± 0.47	13
Midbrain	5.91 ± 2.59	0.87 ± 0.45	7
Pons	6.17 ± 2.99	0.89 ± 0.44	7
Medulla	7.20 ± 3.84	1.08 ± 0.64	7
Cerebellum	5.05 ± 2.10	0.83 ± 0.41	6
Upper Cervical Spinal Cord	8.91 ± 5.60	1.26 ± 0.81	7
Lower Cervical Spinal Cord	3.63 ± 1.71	0.49 ± 0.11	7
Thoracic Spinal Cord	1.93 ± 0.38	0.37 ± 0.06	5
Lumbar Spinal Cord	2.19 ± 0.41	0.32 ± 0.05	7
CNS-Related Tissues			
Trigeminal Nerve	33.7 ± 9.56	3.52 ± 1.61	10
Cerebrospinal Fluid[b]	5.42 ± 1.38	-	-
Dorsal Meninges	19.3 ± 9.36	3.49 ± 1.10	6
Ventral Meninges	66.0 ± 24.0	29.4 ± 15.8	2
Spinal Meninges	16.6 ± 12.1	1.42 ± 0.14	12

[a] ^{125}I-Hypocretin-1 (HC) concentrations expressed as mean (nM) ± standard error (SE).

[b] Cerebrospinal fluid obtained from a separate group of animals (n = 4) following intranasal dose of 100 nmol only; refer to Chapter 2 for concentrations after a 10 nmol dose.

Table 3: Biodistribution in Blood, Peripheral Tissues, and Lymph Nodes Following Intranasal Administration

	Intranasal HC[a] (100 nmol, n = 5)	Intranasal HC[a] (10 nmol, n = 4)	High/Low Ratio
Blood[b]			
5 min	6.75 ± 0.52	1.03± 0.08	7
10 min	14.9 ± 1.34	2.12 ± 0.04	7
15 min	25.1 ± 2.32	3.65 ± 0.11	7
20 min	38.2 ± 1.87	4.41 ± 0.15	9
30 min	45.4 ± 2.38	4.56 ± 0.15	10
Peripheral Tissues			
Muscle	6.52 ± 1.12	1.53 ± 0.86	4
Liver	9.41 ± 0.81	0.96 ± 0.07	10
Kidney	31.2 ± 9.53	3.23 ± 0.99	10
Spleen	10.6 ± 1.55	1.19 ± 0.17	9
Heart	3.40 ± 0.42	0.59 ± 0.11	6
Lymph Nodes			
Superficial Cervical	18.4 ± 3.46	3.49 ± 1.10	5
Deep Cervical	221 ± 80.5	29.4 ± 15.8	8
Axillary	9.28 ± 2.06	1.42 ± 0.14	7

[a] ^{125}I-Hypocretin-1 (HC) concentrations expressed as mean (nM) ± standard error (SE)

[b] Based on mean concentrations from n = 9 (5 animals + blood from 4 animals during CSF sampling experiments)

Figure 1: Changes in Food Consumption Following Intranasal HC (100 nmol). Intranasal treatment with hypocretin-1 (HC) (100 nmol) during early light-phase significantly increased food consumption over the first 4 hours after dosing by 71% compared to intranasal treatment with phosphate-buffered saline (PBS) ($p < 0.05$, paired sample Wilcoxon signed-ranked test). During the 4-8 hour time period after dosing, food consumption was significantly decreased by 55% with intranasal HC ($p < 0.05$, paired sample Wilcoxon signed-ranked test). No differences in food consumption were observed for the remainder of the study.

Figure 1:

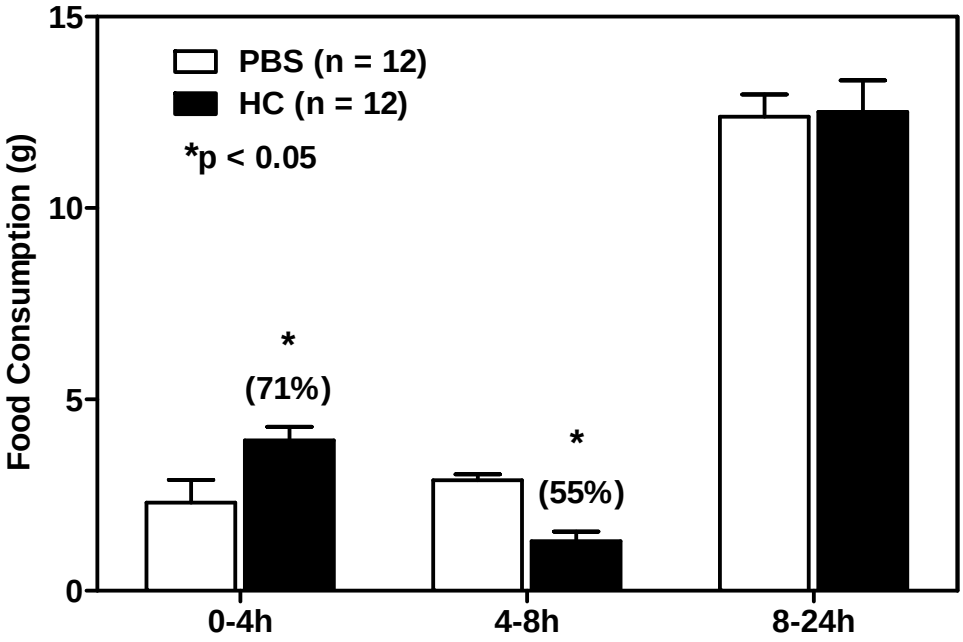
15
10
5
0
Food Consumption (g)
PBS (n = 12)
HC (n = 12)
*p < 0.05
*
(71%)
*
(55%)
0-4h
4-8h
8-24h

Figure 2: Effect on Water Intake Following Intranasal HC (100 nmol). Intranasal treatment with hypocretin-1 (HC) (100 nmol) during early light-phase had no significant effect on water intake over the entire 24 hour study ($p > 0.05$, paired sample Wilcoxon signed-ranked test).

Figure 2:

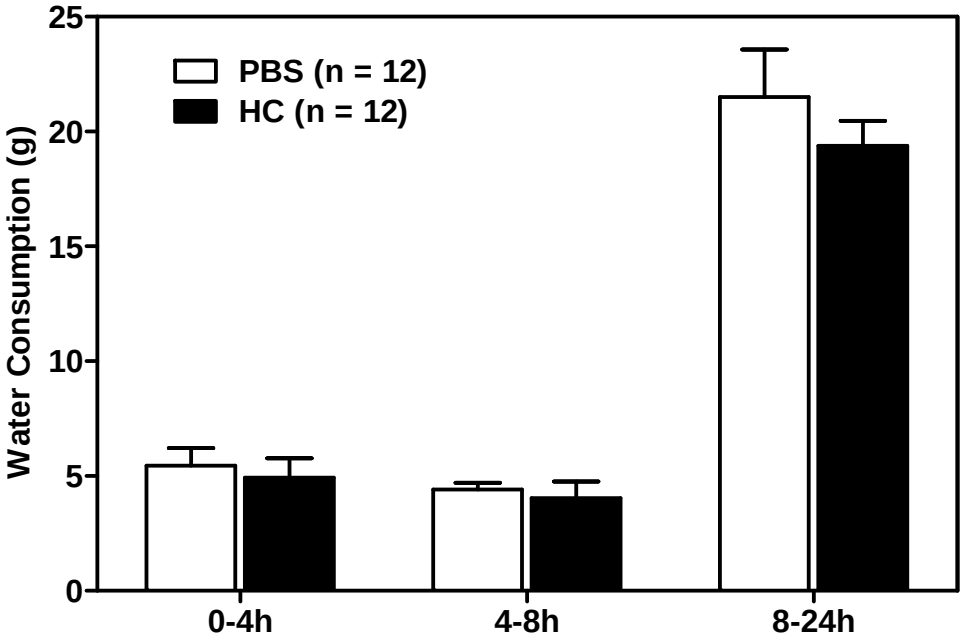

Figure 3: Wheel Running Activity Following Intranasal HC (100 nmol). Intranasal treatment with hypocretin-1 (HC) (100 nmol) during early light-phase resulted in a marginally significant increase in wheel running activity over the first 4 hours after dosing compared to intranasal treatment with phosphate-buffered saline (PBS) ($p < 0.10$, paired sample Wilcoxon signed-rank test comparing area under the curve from 0-4 hours). The greatest difference in activity between HC and PBS animals was observed during the 1-2 hour time period after dosing ($p < 0.05$, paired sample Wilcoxon signed-ranked test).

Figure 3:

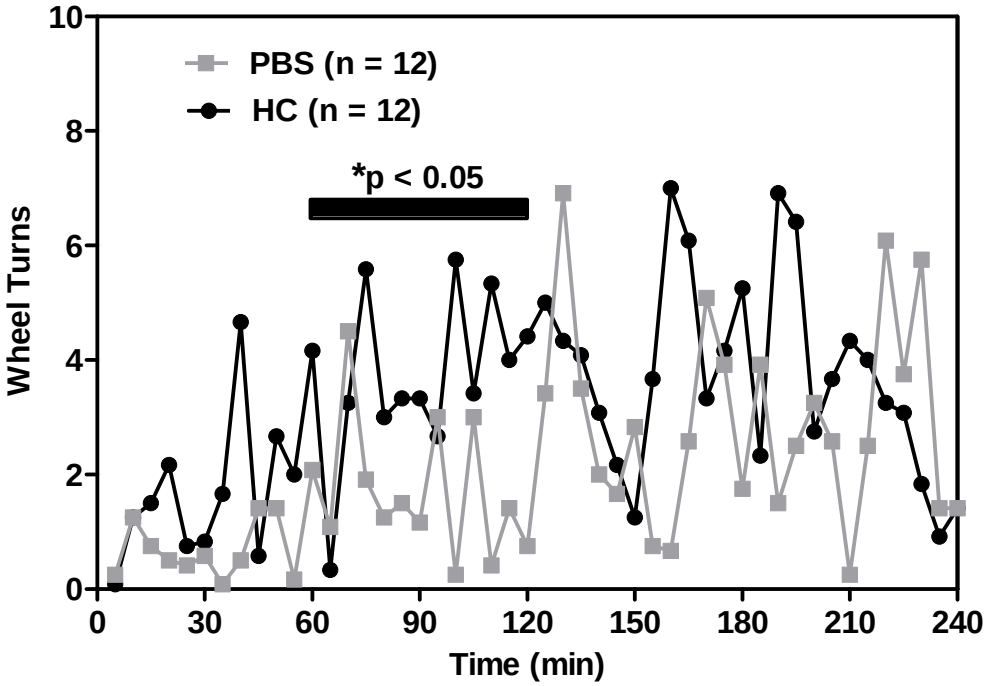
PBS (n = 12)
HC (n = 12)
*p < 0.05
Wheel Turns
Time (min)
0
2
4
6
8
10
0
30
60
90
120
150
180
210
240

Figure 4: Phosphorylated MAPK in Brain at 30 Minutes Following Intranasal HC (100 nmol). Intranasal administration of hypocretin-1 (HC) (100 nmol) during early light phase resulted in a marginally significant reduction in the fraction of phosphorylated mitogen-activated protein kinase (pMAPK) present in the olfactory bulbs compared to phosphate-buffered saline (PBS) controls at 30 minutes (66% reduction, $p < 0.05$, unpaired two-sample t-test). No significant effect of HC on pMAPK was observed in the diencephalon and brainstem.

Figure 4:

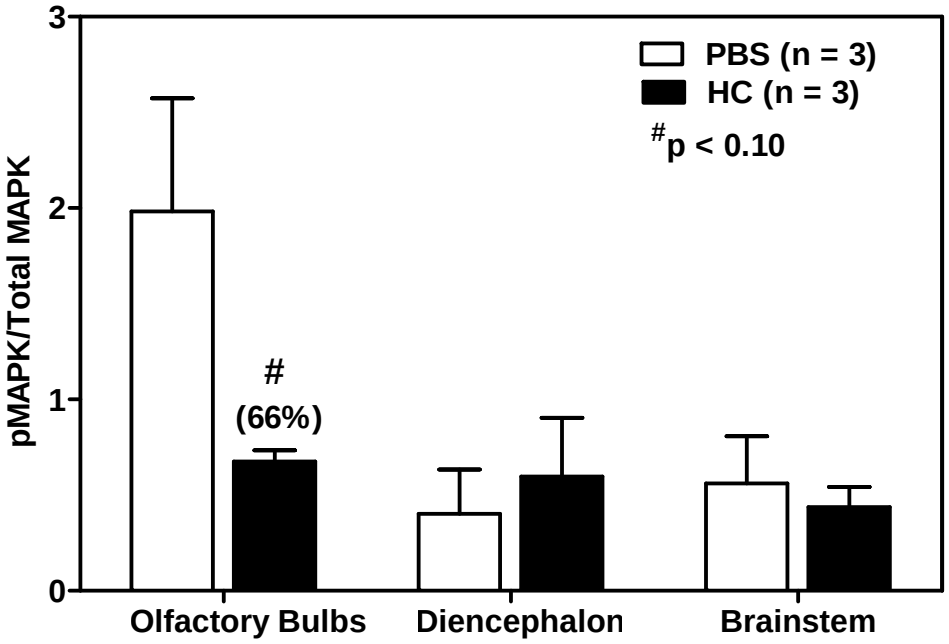
3
2
1
0
pMAPK/Total MAPK
PBS (n = 3)
HC (n = 3)
#p < 0.10
#
(66%)
Olfactory Bulbs
Diencephalon
Brainstem

Figure 5: PDK-1 in Brain at 30 Minutes Following Intranasal HC (100 nmol). Intranasal administration of hypocretin-1 (HC) (100 nmol) during early light phase resulted in a marginally significant decrease phosphoinositide-dependent kinase-1 (PDK-1) levels normalized to actin levels in the olfactory bulbs (21% decrease, $p < 0.10$, unpaired two-sample t-test). Intranasal HC significantly increased PDK-1 levels in the diencephalon (26% increase) and brainstem (21% increase) compared to phosphate-buffered saline (PBS) controls at 30 minutes ($p < 0.05$, unpaired two-sample t-test).

Figure 5:

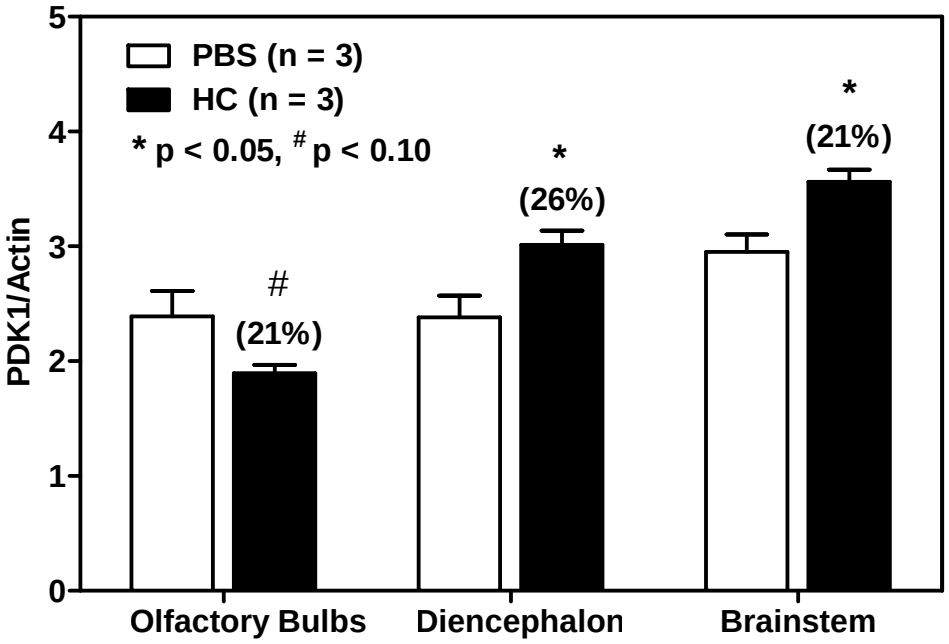
PBS (n = 3)
HC (n = 3)
* p < 0.05, # p < 0.10
PDK1/Actin
0
1
2
3
4
5
#
(21%)
*
(26%)
*
(21%)
Olfactory Bulbs
Diencephalon
Brainstem

CHAPTER 4

NOVEL VASOCONSTRICTOR FORMULATION TO ENHANCE INTRANASAL TARGETING OF NEUROPEPTIDES TO THE CENTRAL NERVOUS SYSTEM[1]

4.1 Introduction

It has been reported that greater than 98% of small molecule and nearly 100% of large molecule central nervous system (CNS) drugs developed by the pharmaceutical industry do not cross the blood-brain barrier (BBB) (Pardridge, 2005). Intracerebroventricular or intraparenchymal drug administration can directly deliver therapeutics to the brain; however, these methods are invasive, inconvenient, and impractical for the numbers of individuals requiring therapeutic interventions for treating CNS disorders. Intranasal drug administration is a non-invasive and convenient means to rapidly target therapeutics of varying physical and chemical properties to the CNS. While the exact mechanisms underlying intranasal delivery to the CNS are not well understood, the olfactory and trigeminal neural pathways connecting the nasal passages to the CNS are clearly involved (Thorne et al., 2004; Dhanda et al., 2005). In addition to these neural pathways, perivascular pathways, and pathways involving the cerebrospinal fluid (CSF) or nasal lymphatics may play a central role in the distribution of therapeutics from the nasal cavity to the CNS (Thorne et al., 2004). Numerous

[1] Reprinted with permission from American Society for Pharmacology and Experimental Therapeutics. Dhuria SV, Hanson LR, Frey WHF II. Novel vasoconstrictor formulation to enhance intranasal targeting of neuropeptides therapeutics to the central nervous system. Journal of Pharmacology and Experimental Therapeutics (2009) 328:312-320.

therapeutics have been delivered to the CNS following intranasal administration and have demonstrated pharmacological effects in animals and in humans (Dhanda et al., 2005), with clinical investigations currently underway for intranasal treatment of Alzheimer's disease (Gozes and Divinski, 2007; Reger et al., 2008b) and obesity (Hallschmid et al., 2008).

The intranasal method of drug delivery holds great promise as an alternative to more invasive routes, however, a number of factors limit the efficiency of intranasal delivery to the CNS. Absorption of intranasally applied drugs into the capillary network in the nasal mucosa can decrease the amount of drug available for direct transport into the CNS. Additional factors within the nasal cavity, including the presence of nasal mucociliary clearance mechanisms, metabolizing enzymes, efflux transporters, and nasal congestion can also reduce the efficiency of delivery into the CNS (Vyas et al., 2006a).

We investigated the effect of including a vasoconstrictor in neuropeptide nasal formulations. We hypothesized that a vasoconstrictor would enhance intranasal drug targeting to the CNS by limiting absorption into the systemic circulation and increasing the amount of neuropeptide available for direct transport into the CNS. Vasoconstrictors are commonly administered to reduce nasal congestion by reducing blood vessel diameter, reducing blood flow, and increasing blood pressure. Vasoconstrictors have frequently been utilized in combination with other drugs in nasal formulations to prevent adverse systemic effects by reducing systemic absorption (Urtti and Kyyronen, 1989; Kyyronen and Urtti, 1990a, b; Luo et al., 1991; Jarvinen and Urtti, 1992), or to prolong the duration of action by reducing clearance from the delivery site

(Adams et al., 1976; Liu et al., 1995). Vasodilators have also been employed to enhance systemic bioavailability of drugs (Olanoff et al., 1987; Urtti and Kyyronen, 1989). We hypothesized that reduced systemic absorption with a vasoconstrictor would increase residence time and increase deposition in the nasal epithelium. Increased deposition in the nasal epithelium could facilitate CNS delivery along several pathways other than the blood, such as along olfactory and trigeminal neural pathways, perivascular pathways, or pathways involving the CSF or nasal lymphatics, providing additional insight into the mechanisms of intranasal drug delivery to the CNS.

The objective of this research was to evaluate the effect of a short-acting vasoconstrictor on intranasal drug targeting to the CNS of two different neuropeptides. The vasoconstrictor selected was phenylephrine hydrochloride (PHE), which is a nasal decongestant with a rapid onset and short duration of action when given topically (O'Donnell, 1995b). The neuropeptides evaluated were: hypocretin-1 (HC, MW 3562), a 33 amino acid peptide involved in appetite and sleep regulation, and the dipeptide, L-Tyr-D-Arg (D-KTP, MW 337), an enzymatically stable structural analog of the endogenous neuropeptide, kyotorphin (L-Tyr-L-Arg, KTP), demonstrating potent morphine-like analgesic activity. We previously demonstrated that intranasal administration of HC reduced systemic exposure and increased targeting to the brain and spinal cord compared to intravenous administration in rats (Dhuria et al., 2008) and in mice (Hanson et al., 2004). HC was selected as a model peptide to evaluate intranasal targeting to the CNS using a vasoconstrictor formulation. Recent reports indicate that intranasal administration of HC significantly improves performance in sleep deprived non-human primates (Deadwyler et al., 2007) and olfactory function in

patients with narcolepsy (Baier et al., 2008). With a molecular weight that is 10-fold less than that of HC, D-KTP is a considerably smaller peptide that would be expected to enter the nasal vasculature and be affected by a vasoconstrictor to a greater extent than HC. To date, the only investigations of nasal formulations of D-KTP have been conducted in *in situ* nasal absorption studies with absorption enhancers (Tengamnuay and Mitra, 1990; Tengamnuay et al., 2000). In addition, there is one report of intranasal administration of KTP demonstrating neuroprotective effects in rats (Nazarenko et al., 1999).

4.2 Methods

4.2.1 Experimental Design

This study was conducted in two parts. The first part of the study investigated the biodistribution of HC following intranasal administration with and without 1% PHE (n = 23 to 28). Intranasal drug targeting of HC to the CNS relative to intravenous administration was previously assessed in our lab (Dhuria et al., 2008); therefore, these experiments were not repeated here. Preliminary experiments indicated that the time interval between intranasal application of 1% PHE and the onset of intranasal delivery of HC with 1% PHE did not significantly affect concentrations of HC in CNS tissues and blood (data not shown), demonstrating that the effect of topically applied PHE is rapid. As a result, all subsequent experiments were conducted without intranasal pretreatment with the vasoconstrictor (i.e. neuropeptide and PHE were administered together). A separate group of animals (n = 6) was used to evaluate the distribution of

HC into cerebrospinal fluid (CSF) following intranasal administration in the presence and absence of 1% PHE.

The second part of the study investigated intranasal drug targeting of D-KTP to the CNS. First, to assess intranasal drug targeting of D-KTP to the CNS relative to intravenous administration, we compared the biodistribution of D-KTP following both routes of administration (n = 6 to 7). Next, to assess if PHE enhances intranasal drug targeting of D-KTP to the CNS, we investigated the biodistribution of D-KTP following intranasal administration with 1% PHE (n = 8). A higher concentration of PHE (5%) was also evaluated (n = 6) to determine if the effect of the vasoconstrictor was dose dependent. Finally, CSF was sampled from a separate group of animals (n = 4 to 6) after intravenous administration and intranasal administration of D-KTP in the presence and absence of 1% PHE.

For all experiments, a mixture of unlabeled and ^{125}I-labeled neuropeptide (10 nmol of HC or D-KTP) was administered to anesthetized rats. CNS tissues, peripheral tissues, and blood were sampled following perfusion and fixation of animals approximately 30 minutes after the onset of drug delivery. Concentrations were determined based on radioactivity measured in tissues and blood by gamma counting. CNS tissue concentrations were normalized to blood concentrations at 30 minutes, providing an assessment of intranasal drug targeting to the CNS relative to the blood. Comparisons of concentrations and tissue-to-blood concentration ratios were made between different groups.

4.2.2 Materials

Hypocretin-1 (HC, Cat # 46-2-70B, American Peptide Company, Sunnyvale, CA) and (D-Arg^2)-kyotorphin (H-Tyr-D-Arg-OH acetate salt, Cat # G-2455, Bachem, Torrance, CA) were custom ^{125}I-labeled with the lactoperoxidase method (GE Healthcare, Woburn, MA). Solutions contained less than 1% unbound ^{125}I as determined by thin layer chromatography and less than 15% acetonitrile. The radiolabeled HC and D-KTP had an average specific activity of 7.4 x 10^4 GBq/mmol at the reference date and were used within 30 days of synthesis. Phosphate buffered saline (PBS, 10x concentrate) and phenylephrine hydrochloride (Cat # 61-76-7) were purchased from Sigma-Aldrich (St. Louis, MO).

4.2.3 Animals

Adult male Sprague-Dawley rats (200-300 g; Harlan, Indianapolis, IN) were housed under a 12-h light/dark cycle with food and water provided *ad libitum*. Animals were cared for in accordance with institutional guidelines and all experiments were approved by Regions Hospital, HealthPartners Research Foundation Animal Care and Use Committee.

4.2.4 Animal Surgeries

Animals were anesthetized with sodium pentobarbital (Nembutal, 50 mg/kg intraperitoneal, Abbott Laboratories, North Chicago, IL). Body temperature was maintained at 37 °C by insertion of a rectal probe connected to a temperature controller and heating pad (Fine Science Tools, Inc., Foster City, CA). For intranasal and

intravenous experiments, the descending aorta was cannulated for blood sampling and perfusion using a 20G, 1¼ inch catheter (Jelco, Johnson and Johnson Medical Inc., Arlington, TX) connected to a 3-way stopcock (B. Braun Medical Inc., Bethlehem, PA). In addition, for intravenous experiments, the femoral vein was cannulated for drug administration using a 25G, ¾ inch catheter (Becton Dickinson, Franklin Lakes, NJ) connected to tubing and a 3-way stopcock (B. Braun Medical Inc., Bethlehem, PA).

4.2.5 Preparation of Formulations

Intranasal and intravenous dose solutions contained a mixture of unlabeled and ^{125}I-labeled neuropeptide (10 nmol, 50-55 μCi) dissolved in PBS (10 mM sodium phosphate, 154 mM sodium chloride, pH 7.4) to a final volume of 48 μL and 500 μL, respectively. For intranasal experiments with vasoconstrictor, 10% PHE (w/v) or 50% PHE (w/v) stock solutions were prepared and added to dose solutions containing neuropeptide to make a final concentration of 1% PHE or 5% PHE, respectively. Dose solution aliquots for each experiment were stored at – 20 °C until the day of the experiment.

4.2.6 Drug Administration

Intranasal administration was performed with animals lying on their backs and rolled gauze (1¼ cm diameter) placed under the neck to maintain rat head position, which prevented drainage of the dose solution into the trachea and esophagus. A pipette (P20) was used to intranasally administer 48 μL of dose solution containing 10 nmol of neuropeptide over 14 minutes. Eight-6 μL nose drops were given to alternating

nares every two minutes while occluding the opposite naris. This method of administration was non-invasive as the pipette tip was not inserted into the naris, but rather, the drop was placed at the opening allowing the animal to snort the drop into the nasal cavity. Intravenous administration through the femoral vein was performed with animals lying on their backs using an infusion pump (Harvard Apparatus, Inc., Holliston, MA) to administer 500 μL of a solution containing an equivalent dose over 14 minutes.

4.2.7 Tissue and Fluid Sampling

Blood samples (0.1 mL) were obtained via the descending aorta cannula at 5, 10, 15, 20, and 30 minutes after the onset of drug delivery. After every other blood draw, 0.9% sodium chloride (0.35 mL) was replaced to maintain blood volume during the experiment.

Peripheral and CNS tissues were obtained at 30 minutes after the onset of drug delivery. Animals were euthanized under anesthesia by perfusion and fixation through the descending aorta cannula with 60 mL of 0.9% sodium chloride and 360 mL of 4% paraformaldehyde in 0.1 M Sorenson's phosphate buffer using an infusion pump (15 mL/min; Harvard Apparatus, Inc., Holliston, MA). A gross dissection of major peripheral organs (muscle, liver, kidney, spleen, and heart) was performed, as well as dissection of the superficial and deep cervical lymph nodes and the axillary lymph nodes. The brain was removed and olfactory bulbs were dissected. Serial (2 mm) coronal sections of the brain were made using a rat brain matrix (Braintree Scientific, Braintree, MA). Microdissection of specific brain regions was performed on coronal

sections using a rat brain atlas as a reference (Paxinos and Watson, 1997). A posterior portion of the trigeminal nerve was dissected from the base of the cranial cavity from the anterior lacerated foramen to the point at which the nerve enters the pons. This tissue sample contained the trigeminal ganglion and portions of the ophthalmic (V1) and maxillary (V2) branches of the trigeminal nerve. Dura from the spinal cord was removed and sampled prior to dissecting the spinal cord into cervical, thoracic, and lumbar sections. The left and right common carotid arteries were dissected from surrounding tissues with the aid of a dissection microscope. Each tissue sample was placed into a pre-weighed 5 mL tube, and the wet tissue weight was determined using a microbalance (Sartorius MC210S, Goettingen, Germany).

CSF was sampled via cisternal puncture at 30 minutes after the onset of drug delivery in a separate group of animals. Animals were placed on their ventral side over a rolled towel to position the head at a 45 degree angle. A 20G needle attached to 30 cm long polyethylene tubing (PE90) was inserted into the cisterna magna. CSF was collected (~ 50 μL) into the tubing until flow stopped or until blood was observed. The tubing was immediately clamped if blood was observed to avoid contamination due to blood-derived radioactivity. Only CSF samples containing clear fluid were included in the analysis.

4.2.8 Sample and Data Analysis

Radioactivity in each tissue sample was determined by gamma counting in a Packard Cobra II Auto Gamma counter (Packard Instrument Company, Meriden, CT). Assuming minimal degradation of the ^{125}I-labeled neuropeptides, concentrations were

calculated using the specific activity of the ^{125}I-labeled neuropeptide determined from standards sampled from the dose solution, counts per minute measured in the tissue following subtraction of background radioactivity, and tissue weight in grams.

Dose-normalized concentrations in blood, CNS tissues, and peripheral tissues from intranasal and intravenous experiments at 30 minutes were calculated and expressed in nmol/L (assuming a density of 1 g/mL) as mean ± SE. Outliers were identified using the Grubbs statistical test for outliers and visually using box plots. The area under the blood concentration-time curve (AUC) from 0 to 30 minutes was calculated using the trapezoidal method without extrapolation to infinity. Since the concentrations observed in CNS after intranasal delivery could be due to absorption from the nasal vasculature and diffusion or receptor-mediated transport across the BBB, CNS tissue concentrations were normalized to blood concentrations at 30 minutes to assess direct transport from the nasal cavity (Chow et al., 1999). If the tissue-to-blood concentration ratios following intranasal delivery with PHE were observed to be greater than those after intravenous or intranasal administration without vasoconstrictor, then this would suggest that the vasoconstrictor enhances delivery along pathways other than vasculature. Intranasal drug targeting to the CNS could be enhanced with the vasoconstrictor if CNS tissue concentrations increased, if blood concentrations decreased or if both effects were observed. Unpaired two-sample t-tests were performed on concentrations and tissue-to-blood concentration ratios at 30 minutes to compare each group to intranasal control animals. Statistical analyses were performed using GraphPad Prism software (version 3.03, GraphPad Software Inc., San Diego, CA) and differences were significant if $p < 0.05$.

4.3 Results

4.3.1 HC Biodistribution With and Without 1% PHE

Intranasal administration of HC with 1% PHE significantly reduced absorption of HC into the blood at all time points measured compared to intranasal HC controls (Figure 1). Intranasal administration of HC over 14 minutes resulted in a gradual increase in blood concentration, ranging from 0.4 nM at 5 minutes to 3.4 nM at 30 minutes, which generated a blood AUC of 56.20 nmol*min/L (Figure 1). 1% PHE significantly reduced the HC blood concentration at 30 minutes to 1.2 nM (65% reduction) and the blood AUC to 16.89 nmol*min/L (70% reduction).

1% PHE significantly increased HC concentrations in the olfactory bulbs, while reducing concentrations to most other CNS tissues (Table 1). Olfactory bulb concentrations significantly doubled from 2.7 nM to 5.6 nM in the presence of 1% PHE (Table 1). Concentrations of HC in the brain (excluding the olfactory bulbs) ranged from 0.6 nM to 1.3 nM for intranasal HC controls. With 1% PHE, no significant differences were observed in HC concentrations in the anterior olfactory nucleus, frontal cortex, caudate/putamen, and septal nucleus, though tissue concentrations were slightly reduced. 1% PHE significantly reduced concentrations by half in remaining brain regions (Table 1). A decreasing concentration gradient was observed in the rostral to caudal direction of the spinal cord after intranasal administration. 1% PHE significantly reduced concentrations in the thoracic and lumbar segments of the spinal cord from 0.4 nM to 0.2 nM (Table 1). CSF distribution of HC was significantly increased from 0.2 nM to 0.3 nM with 1% PHE, and aside from the olfactory bulbs, this

was the only other CNS sample where HC concentrations were increased in the presence of the vasoconstrictor (Table 1). 1% PHE significantly decreased HC concentrations in the dorsal dura from 2.7 nM to 1.5 nM, while concentrations in the ventral dura and spinal dura were unaffected (Table 1).

In the nasal cavity, 1% PHE significantly reduced concentrations of HC in the respiratory epithelium and significantly increased concentrations in the olfactory epithelium. Superficial and deep cervical lymph nodes, which are drainage sites from nasal lymphatic vessels, contained significantly greater concentrations of HC in the presence of 1% PHE (Table 1). In fact, one of the highest concentrations observed outside of the CNS after intranasal delivery was in the cervical lymph nodes (18.3 nM), and with 1% PHE this concentration was doubled. The concentration of HC in the trigeminal nerve, which innervates the nasal cavity and enters the CNS at the level of the brainstem, was significantly reduced by 2.9-fold with 1% PHE from 4.9 nM to 1.7 nM (Table 1). Concentrations of HC in the walls of the carotid artery following perfusion with saline and fixative were increased with 1% PHE from 83 nM to 256 nM, however these differences were not found to be significantly different ($p = 0.31$).

In peripheral tissues, 1% PHE significantly reduced HC concentrations in the spleen and heart, but had no significant effect on concentrations in the muscle, liver, and kidneys (Table 1). The greatest concentration of HC in peripheral tissues was observed in the kidneys both with (2.8 nM) and without 1% PHE (3.0 nM).

4.3.2 HC Drug Targeting to the CNS and Lymphatics With and Without 1% PHE

Intranasal administration of HC with 1% PHE resulted in tissue-to-blood concentration ratios that were significantly greater in all CNS tissues (except the trigeminal nerve) in comparison to intranasal HC control animals (Figure 2). In the brain, significant differences in drug targeting (differences in ratios between control and 1% PHE-treated animals) were observed in the olfactory bulbs (6.8-fold), anterior olfactory nucleus (2.4-fold), frontal cortex (2.3-fold), hippocampus (1.6-fold), hypothalamus (2.0-fold) and cerebellum (1.7-fold). In the spinal cord, drug targeting was significantly increased to the cervical (2.4-fold), thoracic (1.6-fold) and lumbar segments (1.3-fold) (Figure 2). Significantly greater drug targeting to the CSF was observed with 1% PHE (2.7-fold), while no significant differences in ratios were observed in the trigeminal nerve (Figure 2). 1% PHE also significantly increased drug targeting to the superficial and deep cervical lymph nodes (5.7-fold for both) (data not shown). Inclusion of 1% PHE in the nasal formulation also significantly enhanced targeting of HC to the ventral meninges (2.9-fold) and to the dorsal meninges (1.7-fold) (data not shown).

4.3.3 D-KTP Biodistribution Following Intranasal and Intravenous Delivery

Intranasal drug targeting of D-KTP to the CNS was confirmed by comparing intranasal and intravenous drug delivery. Intranasal compared to intravenous administration of D-KTP resulted in significantly lower concentrations in the blood at all time points measured (Figure 3). Intranasal administration of D-KTP over 14 minutes resulted in a gradual increase in blood concentration, with a peak concentration

of 11.7 nM at 30 minutes, while intravenous infusion resulted in a peak concentration of 83 nM at 10 minutes which steadily declined to 55 nM at 30 minutes. The resulting D-KTP blood AUC was significantly less following intranasal administration (145.30 nmol*min/L vs. 1708.83 nmol*min/L).

Intranasal compared to intravenous administration resulted in D-KTP brain and spinal cord concentrations that were significantly lower (~ 3-fold); however the intravenous route was accompanied by 5-fold greater blood concentrations (Table 2). D-KTP brain concentrations after intranasal administration ranged from 1.8 nM to 4.3 nM, with the highest concentration in the olfactory bulbs. Intravenous brain concentrations ranged from 5.0 nM in the pons to 7.5 nM in the caudate/putamen. In the spinal cord, intranasal D-KTP resulted in a decreasing concentration gradient from the rostral to caudal direction, while intravenous delivery resulted in the highest concentration in the lumbar segment of the spinal cord (Table 2). Distribution into the CSF and dorsal dura were significantly greater with intravenous compared to intranasal administration (Table 2).

In the nasal cavity, the respiratory and olfactory epithelia contained very high levels of D-KTP following intranasal compared to intravenous administration (Table 2). Superficial cervical lymph node concentrations were significantly greater with intravenous delivery, while deep cervical lymph node concentrations of D-KTP were significantly greater with intranasal delivery. No statistically significant differences were noted in trigeminal nerve concentrations ($p = 0.41$), although D-KTP levels were slightly elevated in the intranasal group (Table 2). Additionally, no statistically significant differences were observed in concentrations in the carotid artery walls

following perfusion with saline and fixative; however concentrations were higher with intranasal delivery ($p = 0.13$) (Table 2).

In peripheral tissues, intranasal delivery of D-KTP resulted in significantly lower concentrations compared to intravenous administration (Table 2). The kidneys contained the highest peripheral tissue concentration of D-KTP, regardless of route of administration.

4.3.4 D-KTP Biodistribution With and Without PHE

Inclusion of PHE in intranasal formulations reduced absorption of D-KTP into the blood compared to intranasal D-KTP controls (Figure 3). 1% PHE significantly reduced the D-KTP blood concentration at 30 minutes to 5.1 nM (56% reduction) and the blood AUC to 71.48 nmol*min/L (51% reduction). With 5% PHE, D-KTP blood concentration at 30 minutes was further reduced to 4.0 nM (66% reduction) and the D-KTP blood AUC was further reduced to 45.65 nmol*min/L (69% reduction) compared to intranasal D-KTP controls (Figure 3).

PHE dose dependently increased concentrations of D-KTP in the olfactory bulbs to levels higher than those achieved with intravenous delivery, while reducing concentrations in most remaining brain regions (Table 2). 1% PHE did not significantly affect concentrations of D-KTP in the anterior olfactory nucleus, but the presence of the vasoconstrictor significantly reduced concentrations by half to all remaining brain regions, as well as to the spinal cord (Table 2). Similar trends were observed with 5% PHE, except fewer CNS tissues were significantly different from intranasal D-KTP controls (Table 2). 1% PHE reduced D-KTP concentrations in the CSF from 0.5 nM to

0.3 nM, but these differences were not significant ($p = 0.09$) (Table 2). The effect of 5% PHE on CSF distribution of D-KTP was not evaluated. CSF concentrations of D-KTP were relatively low in comparison to concentrations in the brain, regardless of the route of drug administration. No significant effects on D-KTP concentrations in the dura were noted with PHE.

In the nasal cavity, PHE dose dependently increased deposition in the olfactory epithelium (Table 2). D-KTP olfactory epithelium concentrations were found to be predictive of olfactory bulb concentrations, with a positive correlation coefficient of 0.99 (data not shown). 1% PHE significantly increased D-KTP concentrations in the respiratory epithelium, while 5% PHE had no significant effect (Table 2). PHE significantly increased D-KTP concentrations in superficial cervical lymph nodes from 6.5 nM to 21 nM with 1% PHE and to 13 nM with 5% PHE. D-KTP concentrations in the deep cervical lymph nodes were slightly elevated with PHE; however differences were not significant (Table 2). Cervical lymph node concentrations were among the highest observed outside of the CNS following intranasal administration. No statistically significant differences were noted in trigeminal nerve concentrations with PHE; however these values were slightly reduced in the presence of vasoconstrictor (Table 2). Additionally, no significant differences were observed in concentrations of D-KTP in the walls of the carotid artery, though 1% PHE reduced concentrations, while 5% PHE had little effect (Table 2).

PHE significantly reduced exposure of D-KTP to all peripheral tissues sampled (except the heart with 5% PHE) (Table 2). Similar reductions in peripheral tissue

concentrations were observed with 1% PHE and 5% PHE, with the greatest reduction in the kidney and liver.

4.3.5 D-KTP Drug Targeting to the CNS and Lymphatics With and Without PHE

Intranasal compared to intravenous administration of D-KTP resulted in significantly greater brain tissue-to-blood concentration ratios, and 5% PHE, but not 1% PHE, significantly enhanced intranasal drug targeting of D-KTP to the brain and to the trigeminal nerve (Figure 4). The intranasal route of administration targeted D-KTP to the CNS compared to intravenous delivery, with the greatest tissue-to-blood concentration ratios in the trigeminal nerve and the olfactory bulbs, while intravenous administration resulted in relatively uniform ratios throughout the CNS. 1% PHE significantly increased olfactory bulb ratios (5.3-fold increase) compared to intranasal D-KTP controls. No other significant differences in D-KTP drug targeting were observed with 1% PHE (Figure 4). With 5% PHE, intranasal drug targeting of D-KTP was increased to many more CNS tissues (Figure 4). Compared to controls, 5% PHE significantly increased ratios in the olfactory bulbs (16.1-fold), anterior olfactory nucleus (3.2-fold), frontal cortex (2.3-fold), hippocampus (1.5-fold), hypothalamus (3.8-fold), and cerebellum (2.1-fold). In the spinal cord, drug targeting to the cervical spinal cord was increased with 5% PHE, but not significantly ($p = 0.07$). Intranasal drug targeting was also significantly increased to the trigeminal nerve with 5% PHE (2.2-fold) (Figure 4). Inclusion of 1% PHE or 5% PHE in nasal formulations also significantly enhanced targeting to the superficial (5.1-fold and 4.6-fold, respectively) and cervical (3.0-fold and 4.8-fold, respectively) lymph nodes compared to intranasal

D-KTP controls (data not shown). 1% PHE or 5% PHE also significantly enhanced targeting of D-KTP to the meninges, with slightly greater targeting to the ventral portion (3.6-fold and 3.4-fold, respectively) compared to the dorsal portion (2.3-fold and 3.2-fold, respectively).

4.4 Discussion

We hypothesized that inclusion of a vasoconstrictor in nasal formulations would reduce absorption into the blood, increase the residence time of the drug in the nasal epithelium, and facilitate intranasal delivery into the brain along pathways involving the olfactory nerves, trigeminal nerves, CSF or nasal lymphatic channels. Our results indicate that over a 30 minute period, inclusion of a vasoconstrictor in the nasal formulation drastically reduced blood concentrations and enhanced intranasal delivery to the CNS along olfactory neural pathways, while reducing transport along trigeminal pathways. PHE dose dependently increased concentrations of HC and D-KTP in the olfactory epithelium and olfactory bulbs, consistent with delivery along olfactory nerves through the cribriform plate, suggesting that olfactory epithelium deposition is critical for efficient delivery of intranasally applied drugs to rostral brain regions. Unexpectedly, concentrations in the trigeminal nerve and in remaining brain regions were either unchanged or reduced in the presence of PHE. Intranasal drug targeting, assessed by tissue-to-blood concentration ratios, was enhanced with 1% PHE throughout the brain for HC and to the olfactory bulbs for D-KTP, mainly due to the reduction in blood concentrations observed in the presence of the vasoconstrictor. Increasing the vasoconstrictor concentration to 5% PHE increased D-KTP targeting to

additional brain areas. These findings indicate that, at least for two neuropeptides with different molecular weights, inclusion of a vasoconstrictor in nasal formulations can enhance intranasal drug targeting to the brain. Inclusion of PHE in the nasal formulation also enhanced drug targeting of HC and D-KTP to the lymphatic system and to the meningeal membranes surrounding the brain.

The reason for reduced concentrations in the trigeminal nerve following intranasal administration with PHE is not entirely clear. We speculated that trigeminal nerve concentrations were reduced because drug concentration in the respiratory epithelium, which is innervated by this nerve, was also reduced with PHE. However this was only observed for HC and therefore did not completely explain our findings. We also considered the possibility that reduced blood concentrations observed with PHE could have led to reduced transport within or along the trigeminal nerve and to brain tissues innervated by this nerve. There is evidence that blood vessels within the trigeminal nerve are permeable to certain molecules (Malmgren and Olsson, 1980). Because the present findings did not allow us to distinguish between blood-mediated versus non-blood-mediated transport into the CNS, the implications of these results in understanding intranasal drug delivery mechanisms were limited.

We expected the vasoconstrictor effect would be more pronounced for a smaller peptide that would more readily enter the nasal vasculature, however blood AUC over 30 minutes was reduced by 70% for HC and by 51% for D-KTP. This observation may be explained by the presence of the proton-coupled peptide transporter, PEPT2, which is involved in the clearance of di- and tripeptides into the blood (Teuscher et al., 2001; Shu et al., 2002; Bahadduri et al., 2005). PEPT2 transporters in the nasal vasculature

could overcome the ability of the vasoconstrictor to reduce absorption into the blood. When a different peptide similar to D-KTP in molecular weight that has not been reported to interact with transporters was evaluated, an 83% reduction in blood concentration was observed with 1% PHE in the nasal formulation (unpublished observations). The use of a PEPT2 inhibitor in combination with the vasoconstrictor and D-KTP could provide additional insight into mechanisms of intranasal delivery and could be another formulation strategy to enhance intranasal drug targeting to the CNS.

The effect of PHE on the absorption of D-KTP and HC into the blood is in good agreement with previously published data that demonstrated significant reductions in systemic absorption of nasally applied drugs in the presence of vasoconstrictors (Urtti and Kyyronen, 1989; Kyyronen and Urtti, 1990a; Lee et al., 1991; Luo et al., 1991; Jarvinen and Urtti, 1992). However, these findings are not consistent with a recent study by Charlton et al. (2007), which demonstrated that inclusion of 1% ephedrine in a nasal formulation of an angiotensin II-antagonist *increased* blood concentrations (Charlton et al., 2007a). To account for this unexpected finding, they noted that the ephedrine was co-administered with the drug in their study, while vasoconstrictors were applied prior to initiating drug administration in other studies (Kyyronen and Urtti, 1990b; Jarvinen and Urtti, 1992), presumably to allow time for the vasoconstrictor to take effect. However, in our preliminary experiments, no differences were observed between PHE co-administration and pretreatment of the nasal cavity with PHE before beginning intranasal drug administration (data not shown). Further, our findings of increased delivery to the olfactory bulbs in the rostral brain and reduced delivery to most remaining brain areas following intranasal administration with a vasoconstrictor

are not consistent with the Charlton et al. (2007) study, where enhanced delivery to all brain regions was observed with 1% ephedrine. A confounding factor in that study was that animals were not perfused to remove blood from the cerebral vasculature prior to brain dissection, possibly resulting in increased brain concentrations due to the presence of blood-derived drug.

Our findings show that inclusion of a vasoconstrictor in the nasal formulation facilitated transport of HC, but not D-KTP, along pathways involving the CSF and the lymphatic system. Consistent with published findings showing increased CSF distribution after intranasal administration with decreasing molecular weights (Sakane et al., 1995), CSF concentrations were higher for D-KTP than for HC. Concentrations within the CSF were not sufficiently higher than brain concentrations to suggest that brain concentrations were due to entry into the CSF followed by distribution into the brain. Intranasal administration with 1% PHE had opposite effects on HC and D-KTP entry into the CSF. In the lymphatic system, we expected that PHE would increase transport into the cervical lymph nodes due to drainage pathways leading from the nasal cavity to the lymph nodes of the neck (Weller et al., 1992; Kida et al., 1993; Walter et al., 2006a). Increased cervical lymph node concentrations were found for HC, but not for D-KTP, which is consistent with studies evaluating lymphatic uptake of drugs, where absorption into the lymphatic system was higher for larger molecular weight compounds after drug administration (Supersaxo et al., 1990).

High concentrations of HC and D-KTP in the walls of the carotid artery, even after removal of blood with saline perfusion, suggest that intranasally applied neuropeptides have access to perivascular spaces. Concentrations in the walls of the

carotid artery were much higher than blood concentrations following intranasal administration, such that the level of drug present could not be explained by diffusion from blood. Instead, the neuropeptides may have entered the blood vessel walls from the nasal epithelium where high concentrations of drug were present. When PHE was added to the nasal formulation, it is possible that the vasoconstrictor could have entered the brain and reduced cerebral blood flow, which could have affected the distribution of HC and D-KTP within the CNS. Several researchers have demonstrated an important role of arterial pulsations in the distribution of solutes within the CNS, suggesting that reduced blood flow would result in diminished perivascular transport and hence reduced CNS concentrations (Rennels et al., 1985; Hadaczek et al., 2006). Additional experiments evaluating the effect of vasoconstrictors on cerebral blood flow or drug distribution within perivascular spaces could improve our understanding of intranasal drug delivery mechanisms.

The current study was limited by the fact that a single time point after intranasal administration was evaluated, suggesting the need for future studies to characterize the pharmacokinetic profile of vasoconstrictor effects on intranasal drug delivery to the CNS. Additionally, since measurements in this study were based on radioactivity, they may not necessarily reflect intact peptide. In support of this work, we previously demonstrated that intact ^{125}I-HC was detected by HPLC in brain and blood extracts after intranasal and intravenous administration (Dhuria et al., 2008). We also recognize the limitations of translating these findings into clinical applications due to the obvious differences between rodents and humans. Despite species differences, peptides and proteins have been successfully delivered intranasally and are effective in non-human

primates (Deadwyler et al., 2007; Thorne et al., 2008) as well as in humans (Born et al., 2002; Gozes and Divinski, 2007; Baier et al., 2008; Reger et al., 2008b). While it will be important to evaluate the risk of adverse systemic effects and rebound congestion from repeated use of nasal decongestants (O'Donnell, 1995b), a potential advantage of vasoconstrictor formulations is the ability to utilize intranasal treatments in patient populations with nasal congestion due to colds or allergies.

In conclusion, we demonstrated for the first time that inclusion of a short-acting vasoconstrictor in nasal formulations can enhance intranasal drug targeting to the brain, lymphatics, and meninges, while significantly reducing absorption into the blood. This novel strategy for enhancing intranasal targeting to the CNS using vasoconstrictors may be most suitable for potent CNS therapeutics that have adverse effects in the blood or peripheral tissues, are rapidly degraded by enzymes in the blood or gastrointestinal tract, or are extensively bound by tissue or plasma proteins. Vasoconstrictor nasal formulations containing CNS therapeutics could be used to target brain tumors or to treat pain disorders, avoiding undesirable side effects that often accompany traditional routes of drug administration. Inclusion of vasoconstrictors in nasal formulations can result in enhanced drug targeting to multiple brain areas, the lymphatic system, and the meninges, which may hold relevance for the treatment of various neurological disorders, autoimmune disorders, or meningitis.

4.5 Acknowledgments

The authors wish to thank the various staff from the Alzheimer's Research Center at Regions Hospital: Kate Faltesek and Jodi Henthorn for assistance with animal

care and anesthesia; Dr. Paula Martinez and Reshma Rao for training on surgical procedures; Dianne Marti, Tiffany Wang, Jacob Cooner, Aleta Svitak, Rachel Matthews, and Thuhien Nguyen for assistance with tissue dissection and tube weighing; and Yevgenia Friedman for preparation of fixative solutions. The authors thank Dr. Jared Fine (Alzheimer's Research Center at Regions Hospital, HealthPartners Research Foundation, St. Paul, MN) for critical review of the manuscript prior to submission for publication.

Table 1: Concentrations Following Intranasal Administration of HC (10 nmol) with and without 1% PHE

	Intranasal[a]	
	HC Control (n = 28)	HC + 1% PHE (n = 23)
Brain and spinal cord		
Olfactory bulbs	2.68 ± 0.33	5.60 ± 0.49*
Anterior olfactory nucleus	1.11 ± 0.14	0.89 ± 0.07
Frontal cortex	0.93 ± 0.09	0.69 ± 0.08
Caudate/putamen	0.58 ± 0.08	0.40 ± 0.07
Septal nucleus	0.88 ± 0.32	0.54 ± 0.12
Parietal cortex	0.67 ± 0.07	0.39 ± 0.04*
Hippocampus	0.61 ± 0.06	0.32 ± 0.02*
Thalamus	0.60 ± 0.05	0.30 ± 0.02*
Hypothalamus	1.04 ± 0.11	0.68 ± 0.06*
Midbrain	0.65 ± 0.06	0.38 ± 0.03*
Pons	0.93 ± 0.14	0.44 ± 0.04*
Medulla	1.26 ± 0.22	0.76 ± 0.11*
Cerebellum	0.67 ± 0.07	0.38 ± 0.04*
Cervical spinal cord	0.80 ± 0.12	0.96 ± 0.27
Thoracic spinal cord	0.35 ± 0.03	0.19 ± 0.03*
Lumbar spinal cord	0.35 ± 0.02	0.17 ± 0.01*
Cerebrospinal fluid[b]		
Cerebrospinal fluid	0.17 ± 0.02	0.28 ± 0.04*
Meninges		
Dorsal meninges	2.71 ± 0.33	1.51 ± 0.19*
Ventral meninges	7.47 ± 1.19	7.54 ± 1.29
Spinal meninges	2.66 ± 0.59	4.58 ± 1.47
Nasal epithelia		
Respiratory epithelium	19,921 ± 1758	11,457 ± 1348*
Olfactory epithelium	4241 ± 628	13,330 ± 905*
Lymph nodes		
Superficial cervical	3.56 ± 0.25	6.50 ± 0.69*
Deep cervical	18.29 ± 3.94	35.58 ± 3.54*
Trigeminal nerve		
Trigeminal nerve	4.93 ± 0.70	1.71 ± 0.15*
Blood vessels		
Carotid artery	82.70 ± 13.13	256 ± 135
Peripheral tissues		
Blood	3.38 ± 0.16	1.19 ± 0.08*
Muscle	0.53 ± 0.05	0.40 ± 0.10
Liver	0.76 ± 0.05	0.69 ± 0.04
Kidney	3.00 ± 0.30	2.75 ± 0.47
Spleen	0.89 ± 0.06	0.50 ± 0.04*
Heart	0.37 ± 0.06	0.18 ± 0.02*

* $p < 0.05$, unpaired t test comparing to intranasal HC controls.
[a] Data expressed as mean concentration (nanomole/L) ± S.E. at 30 min.
[b] Cerebrospinal fluid obtained from a separate group of animals (n = 6).

Table 2: Concentrations Following Intravenous Administration and Intranasal Administration of D-KTP (10 nmol) with and without PHE

	Intravenous[a]	Intranasal[a]		
	D-KTP ($n = 6$)	D-KTP Control ($n = 7$)	D-KTP + 1% PHE ($n = 8$)	D-KTP + 5% PHE ($n = 6$)
Brain and spinal cord				
Olfactory bulbs	6.88 ± 0.69*	4.33 ± 0.59	12.85 ± 3.28*	24.48 ± 4.64*
Anterior olfactory nucleus	6.18 ± 0.75*	2.42 ± 0.26	2.04 ± 0.41	2.70 ± 0.42
Frontal cortex	6.60 ± 1.93*	2.24 ± 0.23	1.34 ± 0.20*	1.81 ± 0.23
Caudate/putamen	7.54 ± 0.53*	2.13 ± 0.22	0.88 ± 0.13*	1.08 ± 0.29*
Septal nucleus	6.64 ± 0.23*	2.09 ± 0.16	1.24 ± 0.12*	1.27 ± 0.21*
Parietal cortex	7.30 ± 0.82*	2.53 ± 0.12	1.13 ± 0.16*	1.28 ± 0.22*
Hippocampus	6.20 ± 0.67*	1.90 ± 0.20	0.89 ± 0.12*	0.98 ± 0.20*
Thalamus	6.22 ± 0.75*	1.83 ± 0.19	0.86 ± 0.11*	1.49 ± 0.49
Hypothalamus	7.03 ± 0.77*	2.63 ± 0.25	1.66 ± 0.26*	3.64 ± 1.31
Midbrain	5.64 ± 0.62*	1.92 ± 0.18	0.96 ± 0.14*	1.49 ± 0.41
Pons	4.97 ± 0.17*	1.90 ± 0.09	0.86 ± 0.13*	1.97 ± 0.68
Medulla	5.33 ± 0.47*	1.87 ± 0.20	0.89 ± 0.14*	1.87 ± 0.57
Cerebellum	5.98 ± 0.66*	2.10 ± 0.09	0.87 ± 0.12*	1.37 ± 0.29*
Cervical spinal cord	4.99 ± 0.72*	1.62 ± 0.40	0.64 ± 0.17*	1.37 ± 0.40
Thoracic spinal cord	4.34 ± 0.49*	1.27 ± 0.24	0.52 ± 0.10*	0.50 ± 0.07*
Lumbar spinal cord	5.46 ± 0.71*	1.20 ± 0.13	0.46 ± 0.06*	0.45 ± 0.03*
Cerebrospinal fluid[b]				
Cerebrospinal fluid	2.23 ± 0.17*	0.49 ± 0.09	0.27 ± 0.06	
Meninges				
Dorsal meninges	6.26 ± 1.11*	4.34 ± 0.71	3.96 ± 0.84	6.43 ± 1.65
Ventral meninges	10.32 ± 1.23	16.66 ± 3.20	20.45 ± 2.91	20.22 ± 4.50
Spinal meninges	10.12 ± 3.00	5.59 ± 1.94	3.48 ± 0.95	2.88 ± 0.77
Nasal epithelia				
Respiratory epithelium	19.94 ± 7.12*	21,419 ± 2564	36,853 ± 5734*	15,908 ± 1702
Olfactory epithelium	30.67 ± 1.61*	1988 ± 675	5754 ± 1165*	12,492 ± 381*
Lymph nodes				
Superficial cervical	10.50 ± 1.23*	6.45 ± 0.62	20.89 ± 3.39*	13.24 ± 1.32*
Deep cervical	10.24 ± 1.15*	61.58 ± 18.42	71.48 ± 12.27	93.59 ± 12.01
Trigeminal nerve				
Trigeminal nerve	9.44 ± 0.49	12.54 ± 3.33	7.68 ± 1.47	8.63 ± 1.61
Blood vessels				
Carotid artery	18.74 ± 3.37	155.6 ± 77.26	69.20 ± 43.96	165.4 ± 56.57
Peripheral tissues				
Blood	54.88 ± 2.15*	11.68 ± 1.33	5.12 ± 0.47*	3.98 ± 0.30*
Muscle	13.62 ± 6.77*	2.20 ± 0.22	1.42 ± 0.23*	0.68 ± 0.04*
Liver	25.34 ± 4.66*	6.38 ± 1.12	1.70 ± 0.23*	1.58 ± 0.20*
Kidney	143.8 ± 50.9*	49.54 ± 9.46	7.19 ± 1.90*	7.39 ± 0.98*
Spleen	12.51 ± 3.18*	3.58 ± 0.72	1.26 ± 0.14*	1.49 ± 0.16*
Heart	3.72 ± 0.47*	1.46 ± 0.20	0.81 ± 0.08*	1.15 ± 0.25

* $p < 0.05$, unpaired t test comparing to intranasal D-KTP controls.

[a] Data expressed as mean concentration (nanomole/L) ± S.E. at 30 min.

[b] Cerebrospinal fluid obtained from a separate group of animals ($n = 5$ for intravenous and intranasal D-KTP and $n = 4$ for intranasal D-KTP + 1% PHE).

Figure 1: Blood Concentration-Time Profiles of HC Following Intranasal Administration with and without 1% PHE (mean concentration ± SE, n = 23 to 28). Intranasal administration of HC (10 nmol) with 1% PHE resulted in significantly reduced absorption into the blood compared to intranasal HC control animals over the course of 30 minutes (*$p < 0.05$, unpaired t-test comparing to intranasal HC controls).

Figure 1:

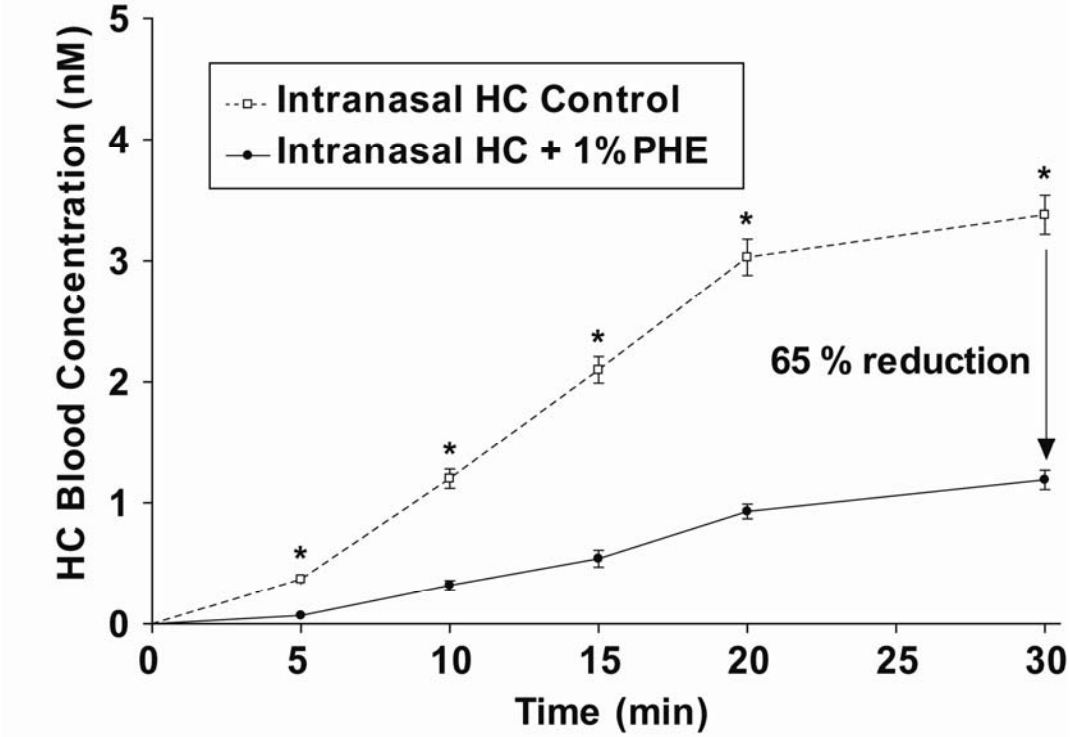
Intranasal HC Control
Intranasal HC + 1% PHE
65 % reduction
HC Blood Concentration (nM)
Time (min)
0
1
2
3
4
5
0
5
10
15
20
25
30
*

Figure 2: CNS Tissue-to-Blood Concentration Ratios of HC at 30 Minutes Following Intranasal Administration with and without 1% PHE (mean concentration ± SE, n = 23 to 28, n = 6 for CSF). Intranasal administration of HC (10 nmol) with 1% PHE resulted in significantly greater drug targeting to all CNS tissues (except the trigeminal nerve) compared to intranasal HC controls (*$p < 0.05$, unpaired t-test comparing to intranasal HC controls). The greatest ratios were observed in the olfactory bulbs, trigeminal nerve, and cervical spinal cord. Tissue abbreviations: olfactory bulbs (OB), anterior olfactory nucleus (AON), frontal cortex (FC), hippocampus (HC), hypothalamus (HT), cerebellum (CB), cervical spinal cord (CSC), thoracic spinal cord (TSC), cerebrospinal fluid (CSF), and trigeminal nerve (TN).

Figure 2:

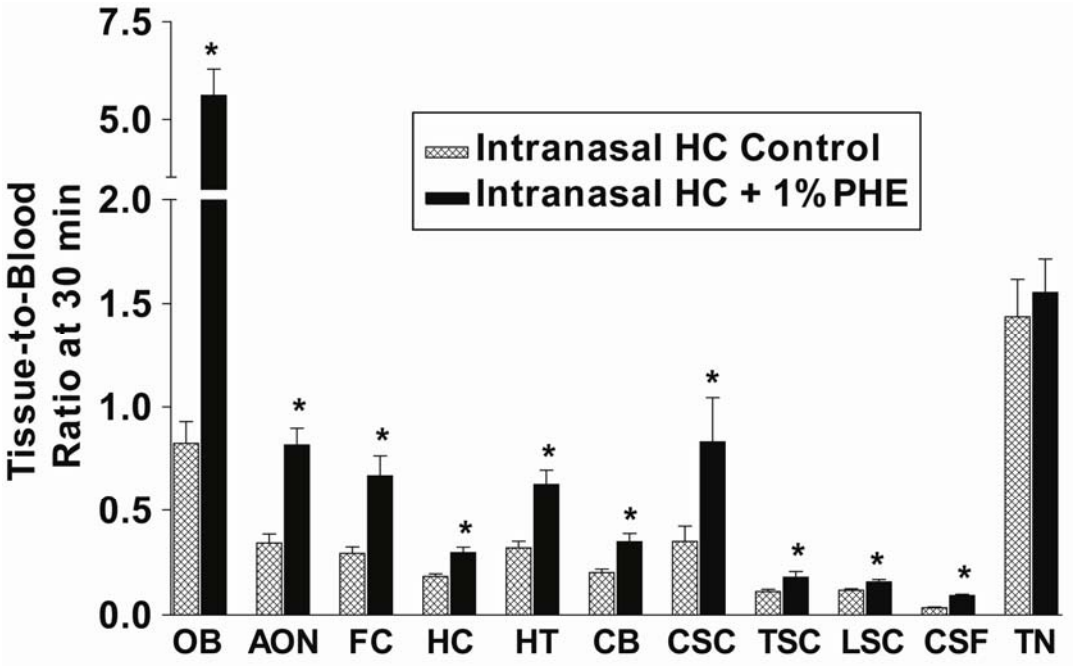
Tissue-to-Blood Ratio at 30 min
7.5
5.0
2.0
1.5
1.0
0.5
0.0
Intranasal HC Control
Intranasal HC + 1% PHE
OB
AON
FC
HC
HT
CB
CSC
TSC
LSC
CSF
TN

Figure 3: Blood Concentration-Time Profiles of D-KTP Following Intravenous Administration, Intranasal Administration without PHE, and Intranasal Administration with 1% PHE or 5% PHE (mean concentration ± SE, n = 6 to 8). Intranasal administration of D-KTP (10 nmol) resulted in significantly less absorption into the blood compared to intravenous administration, and including 1% PHE or 5% PHE in the nasal formulation further reduced blood concentrations compared to intranasal D-KTP controls over the course of 30 minutes (*$p < 0.05$, unpaired t-test comparing to intranasal D-KTP controls).

Figure 3:

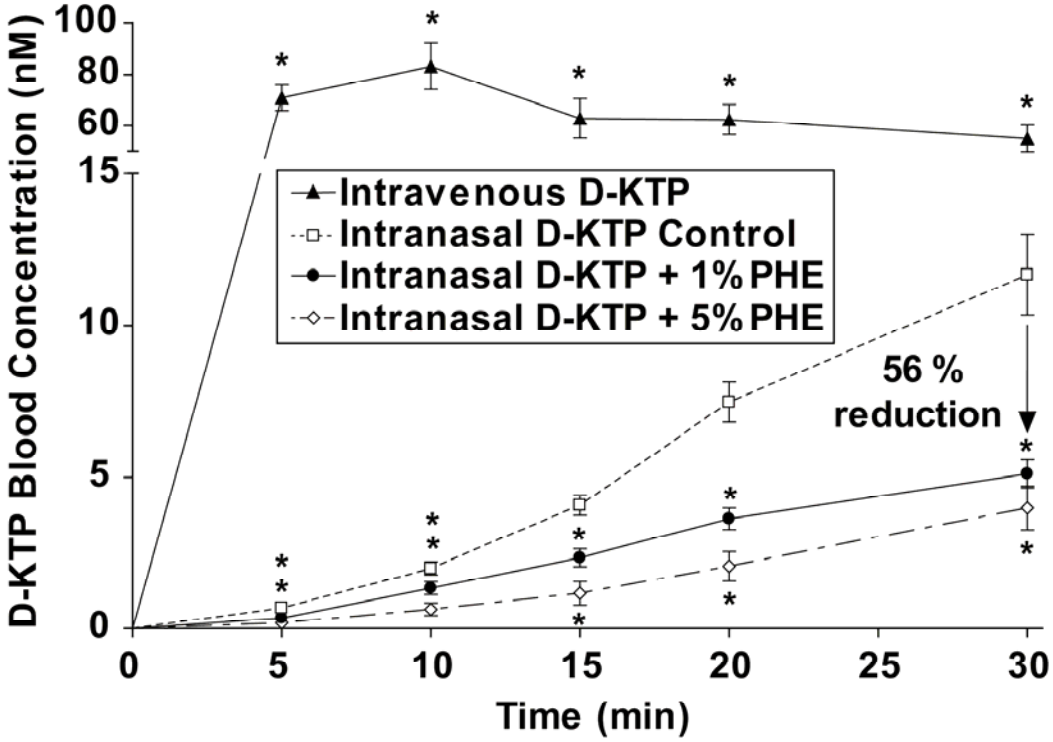
D-KTP Blood Concentration (nM)
100
80
60
15
10
5
0
0
5
10
15
20
25
30
Time (min)
Intravenous D-KTP
Intranasal D-KTP Control
Intranasal D-KTP + 1% PHE
Intranasal D-KTP + 5% PHE
56 %
reduction

Figure 4: CNS Tissue-to-Blood Concentration Ratios of D-KTP at 30 Minutes Following Intravenous Administration, Intranasal Administration without PHE, and Intranasal Administration with 1% PHE or 5% PHE (mean concentration ± SE, n = 6 to 8, n = 4 to 5 for CSF). Intranasal compared to intravenous administration of D-KTP (10 nmol) resulted in significantly greater drug targeting in most CNS tissues (*$p < 0.05$, unpaired t-test comparing to intranasal D-KTP control). Inclusion of 1% PHE or 5% PHE in the nasal formulation significantly increased drug targeting to the olfactory bulbs (*$p < 0.05$, unpaired t-test comparing to intranasal D-KTP control). 5% PHE, but not 1% PHE, significantly enhanced drug targeting of D-KTP to additional CNS tissues. Tissue abbreviations: olfactory bulbs (OB), anterior olfactory nucleus (AON), frontal cortex (FC), hippocampus (HC), hypothalamus (HT), cerebellum (CB), cervical spinal cord (CSC), thoracic spinal cord (TSC), cerebrospinal fluid (CSF), and trigeminal nerve (TN).

Figure 4:

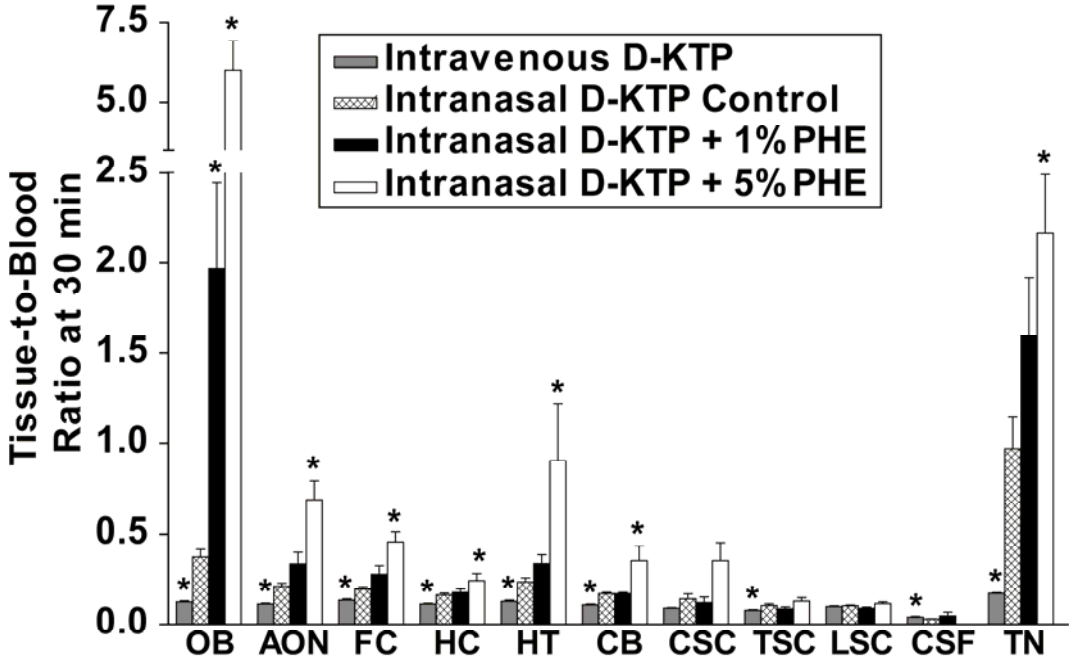
Intravenous D-KTP
Intranasal D-KTP Control
Intranasal D-KTP + 1% PHE
Intranasal D-KTP + 5% PHE
Tissue-to-Blood Ratio at 30 min
7.5
5.0
2.5
2.0
1.5
1.0
0.5
0.0
OB
AON
FC
HC
HT
CB
CSC
TSC
LSC
CSF
TN

4.6 Supplementary Material

4.6.1 Pilot Study to Evaluate Different Vasoactive Agents

Introduction

The purpose of this study was to evaluate different types of vasoconstrictors to identify which one to proceed with for determining the effect of vasoconstrictors on intranasal delivery to the CNS. It was hypothesized that intranasal co-administration or pretreatment with a vasoconstrictor would enhance intranasal drug targeting to the CNS by reducing absorption into the blood, increasing the residence time in the nasal epithelium, and increasing the amount of neuropeptide available for direct transport into the CNS. It was hypothesized that this would facilitate delivery along olfactory and trigeminal neural pathways, perivascular pathways or pathways involving the CSF and lymphatics. In this study, the effect of intranasal application of a vasodilator was also evaluated, which might have opposite effects compared to a vasoconstrictor.

Vasoconstriction results in reduced blood vessel diameter, reduced blood flow, and increased blood pressure. The process involves the activation of alpha-adrenergic receptors, which leads to cell signaling cascades, resulting in increased intracellular calcium. Increased levels of calcium ultimately results in smooth muscle cell contraction and constriction of blood vessels. The relative distribution and contribution of α-adrenergic receptor subtypes (α_1, α_2) to vasoconstriction in the nasal vasculature varies (Johannssen et al., 1997; Kawarai and Koss, 2001; Corboz et al., 2003; Wang and Lung, 2003; Corboz et al., 2005). While there are no reported effects of vasoactive

agents on perivascular spaces, it is also possible that vasoconstriction increases or decreases this space surrounding blood vessels.

Three different vasoconstrictors were chosen for this pilot study (Figure 1): tetrahydrozoline (THZ), phenylephrine hydrochloride (PHE), and endothelin-1 (ET). THZ and PHE have a rapid onset and short duration of action following topical administration with effects observed within 15-30 minutes (O'Donnell, 1995a) and lasting approximately 4-6 hours (Engle, 1992). Other commonly used short-acting vasoconstrictors include ephedrine, naphazoline, levodesoxyephedrine, and propylhexedrine (Engle, 1992). THZ is an imidazoline derivative commonly used in ophthalmic solutions at concentrations ranging from 0.05-0.1% (Engle, 1992). PHE, a derivative of epinephrine differing in chemical structure only by lacking a hydroxyl group on the benzene ring (Eccles, 2007), is used orally or topically to alleviate nasal congestion at concentrations of 0.1-1% (Engle, 1992). PHE has been used in ocular formulations containing timolol to reduce systemic absorption and improve ocular bioavailability (Urtti and Kyyronen, 1989; Kyyronen and Urtti, 1990a; Luo et al., 1991; Jarvinen and Urtti, 1992). PHE selectively binds to α_1-adrenergic receptors, while THZ binds to α_1- and α_2-adrenergic receptor subtypes located on vascular smooth muscle cells. ET is a potent vasoconstrictor that is markedly different from THZ and PHE in that it is an endogenous 21 amino acid peptide involved in the regulation of vascular tone and has been shown to decrease nasal blood flow in dogs and humans (Ichimura et al., 1991). In this pilot study, 0.1% THZ and 1% PHE were used based on literature reports showing effects with these concentrations. A lower concentration was used for ET (0.00025%) due to its greater potency compared to THZ and PHE.

The vasodilator evaluated in this pilot study was histamine (HIS) (Figure 1), which has been shown to enhance systemic absorption and effects of intranasal desmopressin (Olanoff et al., 1987). Histamine is commonly used to induce congestion in studies evaluating vasoconstrictor decongestants (Kesavanathan et al., 1995; Lane et al., 1997; Wustenberg et al., 2006; Wustenberg et al., 2007). Histamine exerts effects on nasal blood flow by activating H1 and H2 receptors in the nasal mucosa (Hiley et al., 1978). In this pilot study, a concentration of 1% HIS was used. Other vasodilators that could have been evaluated include pilocarpine and capsaicin.

The effect of vasoactive compounds on intranasal delivery of hypocretin-1 (HC), to the CNS, peripheral tissues, and blood was evaluated. The following experiments were conducted: (i) intranasal co-administration of HC and a vasoactive compound (THZ or HIS) and (ii) intranasal pretreatment with a vasoconstrictor solution (THZ, ET or PHE) 5 minutes or 15 minutes before intranasal co-administration of HC and the vasoconstrictor. The experiments using a pretreatment of the nasal cavity were conducted to allow time for the vasoconstrictor to take effect. After screening and identifying one vasoconstrictor with which to proceed, it was determined whether nasal cavity pretreatment was a necessary step by comparing drug distribution with different pretreatment time intervals (5 min or 15 min).

Methods

Detailed methods are presented in the *Methods* section of Chapter 4. Briefly, male Sprague-Dawley rats were anesthetized and the descending aorta was cannulated for blood sampling and perfusion. Animals were positioned on their backs with their

necks maintained parallel to the surface to prevent drainage of the dose solution into the esophagus and trachea. Intranasal administration was performed by using a pipetter to deliver 6 μL nose drops to alternating nares every two minutes while occluding the opposite naris over the course of 14 minutes. For some experiments, ^{125}I-HC and a vasoactive compound (THZ or HIS) were co-administered (48 μL). Control experiments were carried out in the same way, except using vehicle (phosphate buffered saline, PBS, pH 7.4) in place of the vasoactive compound to maintain equal volumes. For some experiments, the nasal cavity was pretreated with 24 μL of a vasoconstrictor solution (THZ, ET or PHE) and 5 or 15 minutes after the last pretreatment nose drop, intranasal co-administration of ^{125}I-HC and the vasoconstrictor was initiated (48 μL). The pretreatment time interval (0 min, 5 min or 15 min) was the time period to wait after intranasal pretreatment before initiating intranasal drug delivery, where a 0 minute pretreatment time interval was equivalent to no pretreatment of the nasal cavity. Control experiments were similarly conducted using PBS instead of the vasoconstrictor.

Blood was sampled via the descending aorta cannula at 5, 10, 15, 20, and 30 minutes after the onset of intranasal HC administration. After the last blood draw, animals were perfused with 0.9% saline and fixed with 4% paraformaldehyde. CNS and peripheral tissues were dissected and concentrations were determined by measuring radioactivity in tissue samples with gamma counting.

Unpaired two-sample t-tests were used to compare concentrations in CNS, peripheral tissues, and blood from animals treated with a vasoactive compound and control animals. In order to determine if the pretreatment time interval had an effect on intranasal delivery to the CNS, one-way ANOVAs comparing concentrations in the

three groups (0 min or no pretreatment, 5 min, 15 min) from control animals were performed. One-way ANOVAs comparing tissue concentrations in the three groups from the vasoconstrictor-treated animals were also performed. Differences were considered significant if $p < 0.05$ and marginally significant if $p < 0.10$.

Results

Tetrahydrozoline

Intranasal co-administration of HC and 0.1% THZ did not demonstrate a profound effect on the distribution of HC into the CNS, peripheral tissues, and blood compared to intranasal HC controls (Table 1). The blood concentration at 5 minutes was significantly reduced with THZ, however no other differences in blood concentration were observed over the 30 minute time period and no differences in blood AUC were observed. Concentrations of HC in the olfactory epithelium were significantly increased by 6.6-fold, which resulted in a nonsignificant doubling in olfactory bulb concentration (Table 1). Concentrations in remaining brain regions and in the trigeminal nerve were statistically the same or slightly reduced in the presence of THZ.

Pretreatment with 0.1% THZ five minutes before intranasal administration of HC and 0.1% THZ significantly reduced HC blood concentrations at 5 minutes and marginally reduced concentrations at 10 and 15 minutes, resulting in no significant difference in area under the blood concentration-time curve compared to intranasal HC controls (Table 2). Pretreatment with THZ did not increase deposition of HC in the

olfactory epithelium, which is in contrast to the effect of co-administration of HC and THZ on olfactory epithelium concentration mentioned above. As a result, no significant differences were observed in the olfactory bulbs and in most other brain regions (Table 2). Concentrations in the trigeminal nerve, which enters the brain at the level of the pons, were marginally reduced by 50% with THZ pretreatment. This corresponded to significant reductions in concentrations in caudal brain areas such as the pons (34% reduction), cerebellum (27% reduction), and spinal cord (70% reduction in cervical, 28% reduction in thoracic) (Table 1), suggesting that the vasoconstrictor reduced delivery via trigeminal pathways. In peripheral tissues, HC concentrations were only marginally reduced in the kidneys by 83% following intranasal pretreatment with THZ.

Histamine

Intranasal co-administration of HC and 1% HIS marginally increased blood concentrations at 5, 10, and 30 minutes, consistent with the vasodilating effect of histamine (Table 1). The resulting blood AUC was also marginally increased with HIS. With the exception of reduced concentrations in the hippocampus and thalamus, concentrations in brain tissues and in the trigeminal nerve were not found to be significantly different from intranasal HC controls (Table 1).

Endothelin

Intranasal pretreatment with 0.00025% ET five minutes before initiating intranasal HC and 0.00025% ET administration had no significant effect on HC blood concentrations compared to intranasal HC controls over the 30 minute experiment

(Table 2). In addition, no differences in concentration were noted in the olfactory epithelium, olfactory bulbs, and most brain regions. Concentrations of HC in the hypothalamus, pons, medulla, and trigeminal nerve were reduced following pretreatment with ET (Table 2). In addition, concentrations in the dorsal meninges were significantly reduced by 66% with ET.

Phenylephrine

Intranasal pretreatment with 1% PHE five minutes prior to intranasal HC and 1% PHE had significant effects on the distribution of HC into the CNS, blood, and peripheral tissues. Blood concentrations of HC were significantly reduced at all time points measured over the 30 minute period (Table 2). Blood AUC was significantly reduced by 69% following pretreatment with PHE. Olfactory epithelium concentrations were significantly increased by 3.1-fold, which resulted in a 1.8-fold increase in olfactory bulb concentration (Table 2). Concentrations in remaining brain regions were either unaffected or significantly reduced (~ 35% reduction) with intranasal pretreatment with PHE. Concentrations of HC in the trigeminal nerve were significantly reduced by 60%. Significantly increased concentrations were observed in the superficial and deep cervical lymph nodes. In peripheral tissues, concentrations were decreased in muscle, but the liver and kidneys were unaffected by pretreatment with PHE (Table 2).

Since 1% PHE resulted in the most dramatic reduction in blood exposure, this vasoconstrictor was selected for additional studies to determine if pretreatment of the nasal cavity was a necessary step for the observed effects by evaluating different

pretreatment time intervals (0 min or no pretreatment, 5 min, 15 min). The pretreatment time interval was the time period to wait after pretreating the nasal cavity with a 1% PHE solution before initiating intranasal delivery of HC and 1% PHE. One-way ANOVAs comparing concentrations in the three groups (0 min, 5 min, 15 min) from the control animals and from PHE-treated animals were performed. The pretreatment time interval did not significantly affect absorption into the blood over the time course of the intranasal delivery experiments (Figure 2). These statistical analyses also demonstrated that, with a few minor exceptions, the pretreatment time interval did not significantly affect distribution into CNS and peripheral tissues (Table 3 and Table 4). As a result, data obtained from control animals with different pretreatment time intervals were merged and data obtained from PHE-treated animals with different pretreatment time intervals were merged. The resulting merged data were presented in tables and figures in the *Results* section of Chapter 4.

Discussion

The effect of vasoactive agents on intranasal delivery of HC to the CNS was evaluated in this study. The most significant effects were observed with intranasal pretreatment with 1% PHE, where significant reductions in blood concentrations of HC were found. This resulted in increased deposition in the olfactory epithelium, increased delivery to the olfactory bulbs, and either unchanged or reduced concentrations in remaining brain regions. As a result of these findings, additional studies were pursued to evaluate the effect of different pretreatment time intervals (0 min or no pretreatment, 5 min, 15 min) to determine the optimum time to wait prior to initiating intranasal

administration of HC and 1% PHE. Results indicated that pretreatment was not necessary since no significant differences were observed between different pretreatment time intervals in terms of drug distribution into CNS, peripheral tissues, and blood. These findings formed the basis of the rationale for intranasal co-administration of 1% PHE with therapeutics in future studies to characterize the effect of vasoconstrictors on intranasal targeting to the CNS.

Intranasal co-administration of HC and 0.1% THZ or 1% HIS and intranasal pretreatment with 0.1% THZ or 0.00025% ET had minimal effects on HC distribution within the CNS, blood and peripheral tissues. THZ is used in ocular solutions (Visine) and may have different vasoconstricting properties in the conjunctival mucosa compared to the nasal mucosa. The lack of effect observed in the blood could also be related to the concentrations chosen, which may not have been sufficient to constrict blood vessels in the nasal mucosa. HIS increased blood concentrations at certain times, consistent with its vasodilating effects, however no significant changes were observed in the brain. This could be due to the small sample size used in the study (n = 3). The results were not compelling to warrant further investigation, though a higher dose of HIS or a different vasodilator, such as pilocarpine, could be explored in future studies. ET, despite its potent vasoconstrictor properties, failed to affect the distribution of HC following intranasal administration. Additional studies with ET were not pursued because of the increased difficulty in breathing observed with animals. The potent vasoconstricting effects of ET may affect systemic blood pressure in animals, resulting in problems with respiration and heart rate.

A common concern with using vasoconstrictors in nasal formulations, particularly in patient populations with hypertension, is the possibility of observing adverse effects on systemic blood pressure and heart rate. In preliminary studies, attempts were made to measure physiological effects of an intranasal solution of 1% PHE in anesthetized rats. During drug administration, mean blood pressure in the PHE-treated animals (n = 3) was similar to that in control animals (n = 4) and gradually increased over the drug administration period (data not shown). In comparison, intravenously administered PHE resulted in sharp increase in mean blood pressure at the onset of drug administration. Similar trends were observed when evaluating breath distension with a pulse oximeter. However, due to high variability in the data and problems related to the blood pressure apparatus and pulse oximeter equipment, it was difficult to make reliable conclusions regarding the physiological effects of 1% PHE. Oral administration of vasoconstrictors is generally contraindicated in individuals with hypertension, but studies have indicated that topical PHE does not lead to widespread effects on systemic blood pressure when given by either the ocular (Kumar et al., 1986) or nasal route (Myers and Iazzetta, 1982; Chua and Benrimoj, 1988; Bradley, 1991), in some cases at doses much higher than those used in these studies. Other vasoconstrictors, including phenylpropanolamine and ephedrine, have more profound effects on heart rate and systemic blood pressure (Chua and Benrimoj, 1988; Bradley, 1991), precluding their use in the hypertensive population regardless of the route of administration. Additional experiments are needed to assess the physiological effects of vasoconstrictor nasal formulations.

Results from this study were the first preliminary data to demonstrate that depending on the vasoconstrictor selected, inclusion of a vasoconstrictor in a nasal formulation could reduce absorption into the blood, increase delivery to the olfactory epithelium in the nasal cavity, and increase delivery to the olfactory bulbs. This novel formulation approach may be particularly relevant for therapeutics that demonstrate adverse systemic effects, such as chemotherapeutics for brain tumors, where use of a vasoconstrictor nasal formulation would be beneficial to limit the entry of therapeutics into the blood.

Supplementary Material (4.6.1) Table 1: Intranasal Co-Administration of Hypocretin-1 and Vasoactive Compounds[a]

Experimental Group	Intranasal HC Control	Intranasal HC + 0.1% THZ		Intranasal HC Control	Intranasal HC + 1% HIS	
Dose	**42 uL, 10 nmol, 40 uCi**	**44uL, 11 nmol, 43 uCi**		**47 uL, 10 nmol, 46 uCi**	**47 uL, 9 nmol, 45 uCi**	
Sample Size	**n = 4**	**n = 4**		**n = 3**	**n = 3**	
Concentration (nM)	**Mean ± SE**	**Mean ± SE**		**Mean ± SE**	**Mean ± SE**	
Brain						
Olfactory Bulbs	2.11 ± 0.24	4.82 ± 1.55		3.08 ± 1.57	3.30 ± 0.88	
Anterior Olfactory Nucleus	1.13 ± 0.08	1.50 ± 0.42		1.28 ± 0.22	1.27 ± 0.09	
Frontal Cortex	1.31 ± 0.12	1.46 ± 0.39		0.98 ± 0.17	1.05 ± 0.12	
Caudate/Putamen	0.69 ± 0.10	0.75 ± 0.17		1.16 ± 0.31	1.99 ± 0.25	
Septal Nucleus	0.58 ± 0.06	0.94 ± 0.22		2.68 ± 0.44	1.68 ± 0.39	
Parietal Cortex	0.84 ± 0.08	0.81 ± 0.17		1.13 ± 0.05	0.99 ± 0.10	
Hippocampus	0.71 ± 0.03	0.87 ± 0.31		0.81 ± 0.01	0.76 ± 0.02	#
Thalamus	0.70 ± 0.05	0.66 ± 0.14		0.77 ± 0.01	0.70 ± 0.02	*
Hypothalamus	1.89 ± 0.14	1.97 ± 0.58		1.72 ± 0.12	1.53 ± 0.16	
Midbrain	0.69 ± 0.07	0.81 ± 0.24		0.92 ± 0.05	0.86 ± 0.13	
Pons	0.90 ± 0.05	0.83 ± 0.25		0.80 ± 0.06	0.87 ± 0.27	
Medulla	1.13 ± 0.12	1.33 ± 0.42		0.78 ± 0.09	1.21 ± 0.59	
Cerebellum	0.75 ± 0.05	0.79 ± 0.24		0.76 ± 0.01	0.93 ± 0.27	
Spinal Cord						
Cervical	0.78 ± 0.36	0.60 ± 0.15		1.34 ± 0.58	3.32 ± 1.32	
Thoracic	0.48 ± 0.15	0.33 ± 0.02		0.55 ± 0.08	0.71 ± 0.20	
Lumbar	0.49 ± 0.12	0.37 ± 0.03		0.50 ± 0.06	0.52 ± 0.01	
Meninges						
Dorsal Meninges	3.35 ± 0.48	3.88 ± 1.00		2.04 ± 0.58	4.56 ± 2.39	
Ventral Meninges	6.46 ± 1.95	6.68 ± 1.39		10.86 ± 4.59	13.28 ± 3.99	
Spinal Meninges	1.75 ± 1.01	1.09 ± 0.32		2.11 ± 0.63	6.97 ± 3.37	
Nasal Cavity & Lymphatics						
Olfactory Epithelium	1024 ± 462	6745 ± 2133	*	4987 ± 2101	7587 ± 1232	
Trigeminal Nerve	5.38 ± 1.12	3.43 ± 0.63		6.79 ± 2.96	7.61 ± 2.40	
Superficial Cervical Nodes	14.86 ± 2.82	21.97 ± 4.77		6.24 ± 1.96	2.44 ± 0.41	
Deep Cervical Nodes	24.70 ± 6.83	24.38 ± 6.36		28.72 ± 6.62	30.57 ± 4.43	
Peripheral Tissues						
Muscle	0.65 ± 0.16	0.74 ± 0.22		1.26 ± 0.08	1.39 ± 0.17	
Liver	1.89 ± 0.30	1.85 ± 0.27		1.71 ± 0.63	1.02 ± 0.14	
Kidney	6.56 ± 0.87	5.55 ± 1.28		7.49 ± 3.10	3.19 ± 0.73	
Blood						
5 min Blood	1.05 ± 0.18	0.43 ± 0.06	*	0.76 ± 0.15	1.19 ± 0.09	#
10 min Blood	2.50 ± 0.45	1.79 ± 0.15		1.97 ± 0.45	3.11 ± 0.23	#
15 min Blood	3.97 ± 0.52	3.43 ± 0.47		3.50 ± 0.88	4.58 ± 0.22	
20 min Blood	5.38 ± 0.63	5.12 ± 0.72		4.40 ± 1.00	6.11 ± 0.31	
30 min Blood	5.61 ± 0.86	5.82 ± 0.52		4.87 ± 0.68	6.60 ± 0.10	#
$AUC_{0\text{-}30min}$	92.69 ± 10.63	99.82 ± 11.84		86.81 ± 17.94	121.07 ± 4.38	#

[a] Tissue concentrations at 30 minutes after the onset of drug administration; data for intranasal HC controls were obtained from two separate batches of ^{125}I-labeled HC; HC = hypocretin-1, THZ = tetrahydrozoline, HIS = histamine; intranasal co-administration of HC and THZ or HIS (48 μL) was given as 6 μL nose drops every 2 minutes

*$p < 0.05$ or $^{\#}p < 0.10$, unpaired t-test comparing treated group to intranasal HC controls

Supplementary Material (4.6.1) Table 2: Intranasal Pretreatment with Vasoconstrictors, Followed by Intranasal Co-Administration of Hypocretin-1 and Vasoconstrictor Compounds[a]

Experimental Group	Intranasal HC Control	Intranasal HC + 0.1% THZ	Intranasal HC + 0.00025% ET	Intranasal HC + 1% PHE
Dose	**48 uL, 10 nmol, 39 uCi**	**48 uL, 10 nmol, 40 uCi**	**48 uL, 10 nmol, 40 uCi**	**48 uL, 10 nmol, 40 uCi**
Sample Size	**n = 11-12**	**n = 8**	**n = 3**	**n = 12-13**
Concentration (nM)	**Mean ± SE**	**Mean ± SE**	**Mean ± SE**	**Mean ± SE**
Brain				
Olfactory Bulbs	3.00 ± 0.64	3.55 ± 1.54	3.18 ± 2.41	5.25 ± 0.73 *
Anterior Olfactory Nucleus	1.09 ± 0.18	0.79 ± 0.16	0.59 ± 0.15	0.86 ± 0.10
Frontal Cortex	1.03 ± 0.13	0.84 ± 0.21	0.56 ± 0.08	0.81 ± 0.11
Caudate/Putamen	0.39 ± 0.05	0.46 ± 0.06	0.34 ± 0.07	0.43 ± 0.09
Septal Nucleus	0.38 ± 0.09	0.46 ± 0.09	0.13 ± 0.05	0.63 ± 0.18
Parietal Cortex	0.60 ± 0.06	0.46 ± 0.07	0.45 ± 0.05	0.45 ± 0.05 #
Hippocampus	0.56 ± 0.05	0.45 ± 0.06	0.40 ± 0.08	0.34 ± 0.03 *
Thalamus	0.54 ± 0.05	0.45 ± 0.06	0.40 ± 0.08	0.32 ± 0.03 *
Hypothalamus	1.20 ± 0.13	0.81 ± 0.20	0.52 ± 0.10 *	0.71 ± 0.08 *
Midbrain	0.61 ± 0.06	0.46 ± 0.07 #	0.42 ± 0.09	0.41 ± 0.04 *
Pons	0.74 ± 0.07	0.49 ± 0.09 *	0.47 ± 0.10 #	0.48 ± 0.06 *
Medulla	1.10 ± 0.14	1.17 ± 0.24	0.43 ± 0.08 *	1.05 ± 0.15
Cerebellum	0.60 ± 0.05	0.44 ± 0.06 *	0.45 ± 0.08	0.44 ± 0.05 *
Spinal Cord				
Cervical	0.80 ± 0.18	0.24 ± 0.03 *	0.56 ± 0.14	0.53 ± 0.14
Thoracic	0.29 ± 0.02	0.21 ± 0.03 *	0.28 ± 0.04	0.18 ± 0.02 *
Lumbar	0.33 ± 0.02	0.27 ± 0.04 #	0.31 ± 0.05	0.18 ± 0.01 *
Meninges				
Dorsal Meninges	2.43 ± 0.38	1.97 ± 0.75	0.50 ± 0.17 *	1.66 ± 0.29
Ventral Meninges	4.45 ± 0.71	4.75 ± 1.93	1.99 ± 0.66	3.72 ± 0.64
Spinal Meninges	1.90 ± 0.48	0.49 ± 0.11 *	0.77 ± 0.28	2.84 ± 1.19
Nasal Cavity & Lymphatics				
Olfactory Epithelium	4224 ± 1064	3835 ± 1866	5034 ± 3206	13125 ± 1516 *
Trigeminal Nerve	3.99 ± 0.70	2.02 ± 0.64 #	0.89 ± 0.19 #	1.60 ± 0.15 *
Superficial Cervical Nodes	3.61 ± 0.42	9.03 ± 2.53 *	4.43 ± 1.87	7.66 ± 1.11 *
Deep Cervical Nodes	13.72 ± 2.29	12.68 ± 5.50	8.00 ± 0.93	24.29 ± 2.29 *
Peripheral Tissues				
Muscle	0.47 ± 0.06	0.33 ± 0.07	0.59 ± 0.07	0.31 ± 0.07 #
Liver	0.75 ± 0.08	0.72 ± 0.11	1.07 ± 0.15 *	0.70 ± 0.06
Kidney	3.16 ± 0.56	1.73 ± 0.26 #	4.50 ± 1.19	3.17 ± 0.63
Blood				
5 min Blood	0.26 ± 0.05	0.13 ± 0.02 *	0.37 ± 0.17	0.05 ± 0.02 *
10 min Blood	0.97 ± 0.09	0.68 ± 0.13 #	1.45 ± 0.36	0.27 ± 0.04 *
15 min Blood	1.89 ± 0.16	1.37 ± 0.23 #	2.47 ± 0.71	0.42 ± 0.10 *
20 min Blood	2.83 ± 0.14	2.54 ± 0.53	3.02 ± 0.64	0.91 ± 0.08 *
30 min Blood	3.19 ± 0.20	3.23 ± 0.81	3.58 ± 0.86	1.07 ± 0.11 *
$AUC_{0\text{-}30min}$	48.99 ± 2.64	45.10 ± 9.42	60.17 ± 14.78	15.07 ± 1.65 *

[a] Tissue concentrations at 30 minutes after the onset of drug administration; HC = hypocretin-1, THZ = tetrahydrozoline, ET = endothelin, PHE = phenylephrine; intranasal pretreatment with vasoconstrictor (24 μL) was given as 6 μL nose drops every 2 minutes and following a period of 5 minutes after the last pretreatment nose drop, intranasal co-administration of HC and the vasoconstrictor was initiated (48 μL) *$p < 0.05$ or #$p < 0.10$, unpaired t-test comparing each group to intranasal HC control

Supplementary Material (4.6.1) Table 3: Hypocretin-1 Concentrations in CNS and Peripheral Tissues at 30 Minutes with Different Pretreatment Time Intervals in the Absence of Phenylephrine[a]

Experimental Group	HC + PBS Control		
Time Interval	**0 min**	**5 min**	**15 min**
Dose	**48 uL, 10 nmol, 50 uCi**	**48 uL, 10 nmol, 41 uCi**	**48 uL, 10 nmol, 50 uCi**
Sample Size	**n = 9**	**n = 15**	**n = 4**
Concentration (nM)	**Mean ± SE**	**Mean ± SE**	**Mean ± SE**
Brain			
Olfactory Bulbs	2.40 ± 0.52	3.05 ± 0.51	2.17 ± 0.71
Anterior Olfactory Nucleus	1.37 ± 0.32	1.02 ± 0.15	1.09 ± 0.36
Frontal Cortex	0.99 ± 0.20	0.96 ± 0.11	0.56 ± 0.17
Caudate/Putamen	0.81 ± 0.18	0.45 ± 0.07	0.49 ± 0.13
Septal Nucleus	0.86 ± 0.09	0.39 ± 0.08	2.44 ± 1.98
Parietal Cortex	0.81 ± 0.18	0.59 ± 0.07	0.71 ± 0.16
Hippocampus	0.71 ± 0.16	0.56 ± 0.05	0.68 ± 0.17
Thalamus	0.67 ± 0.12	0.56 ± 0.04	0.65 ± 0.16
Hypothalamus	1.03 ± 0.29	1.08 ± 0.12	1.04 ± 0.26
Midbrain	0.79 ± 0.16	0.59 ± 0.05	0.77 ± 0.21
Pons	1.36 ± 0.38	0.70 ± 0.06	0.84 ± 0.23
Medulla	0.97 ± 0.23	0.99 ± 0.13	1.03 ± 0.34
Cerebellum	1.15 ± 0.27	0.60 ± 0.05	0.81 ± 0.22
Spinal Cord			
Cervical	0.75 ± 0.16	0.76 ± 0.16	0.91 ± 0.54
Thoracic	0.35 ± 0.04	0.35 ± 0.04	0.30 ± 0.06
Lumbar	0.34 ± 0.04	0.36 ± 0.03	0.32 ± 0.04
Meninges			
Dorsal Meninges	3.80 ± 0.76	2.24 ± 0.33	2.35 ± 0.73
Ventral Meninges	9.69 ± 2.04	5.20 ± 0.83	11.41 ± 7.43
Spinal Meninges	2.84 ± 1.09	2.72 ± 0.88	1.47 ± 0.93
Nasal Cavity & Lymphatics			
Olfactory Epithelium	3012 ± 639	4950 ± 988	5170 ± 1807
Trigeminal Nerve	6.01 ± 1.18	3.85 ± 0.60 *	8.86 ± 3.06
Superficial Cervical Nodes	3.05 ± 0.37	3.74 ± 0.34	4.39 ± 0.75
Deep Cervical Nodes	12.02 ± 2.08 *	16.51 ± 2.67 *	53.61 ± 19.69
Peripheral Tissues			
Muscle	0.66 ± 0.10	0.47 ± 0.06	0.38 ± 0.16
Liver	0.79 ± 0.07	0.78 ± 0.08	0.55 ± 0.08
Kidney	2.75 ± 0.55	3.22 ± 0.46	2.39 ± 0.25

[a] 0 min time interval is equivalent to no pretreatment; HC = hypocretin-1, PBS = phosphate buffered saline; intranasal pretreatment with PBS (24 μL) was given as 6 μL nose drops every 2 minutes and following a period of 5 minutes after the last pretreatment nose drop, intranasal co-administration of HC and PBS was initiated (48 μL)

*Different from 15 min, $p < 0.05$, ANOVA followed by Bonferroni post-test

Supplementary Material (4.6.1) Table 4: Hypocretin-1 Concentrations in CNS and Peripheral Tissues at 30 Minutes with Different Pretreatment Time Intervals in the Presence of 1% Phenylephrine[a]

Experimental Group	HC + 1% PHE		
Time Interval	**0 min**	**5 min**	**15 min**
Dose	**47 uL, 10 nmol, 49 uCi**	**47 uL, 10 nmol, 41 uCi**	**48 uL, 10 nmol, 50 uCi**
Sample Size	**n = 4**	**n = 15**	**n = 4**
Concentration (nM)	**Mean ± SE**	**Mean ± SE**	**Mean ± SE**
Brain			
Olfactory Bulbs	4.80 ± 0.79	6.00 ± 0.55	5.00 ± 1.88
Anterior Olfactory Nucleus	1.13 ± 0.19	0.91 ± 0.08	0.50 ± 0.12
Frontal Cortex	0.53 ± 0.07	0.78 ± 0.10	0.55 ± 0.26
Caudate/Putamen	0.29 ± 0.05	0.40 ± 0.08	0.50 ± 0.29
Septal Nucleus	0.42 ± 0.09	0.64 ± 0.18	0.28 ± 0.14
Parietal Cortex	0.39 ± 0.05	0.42 ± 0.05	0.27 ± 0.06
Hippocampus	0.33 ± 0.04	0.34 ± 0.03	0.25 ± 0.05
Thalamus	0.30 ± 0.04	0.32 ± 0.03	0.23 ± 0.07
Hypothalamus	0.61 ± 0.11	0.74 ± 0.08	0.53 ± 0.17
Midbrain	0.38 ± 0.08	0.40 ± 0.04	0.30 ± 0.09
Pons	0.46 ± 0.11	0.46 ± 0.05	0.33 ± 0.09
Medulla	0.46 ± 0.17	0.95 ± 0.14	0.32 ± 0.05
Cerebellum	0.34 ± 0.08	0.42 ± 0.05	0.26 ± 0.06
Spinal Cord			
Cervical	0.57 ± 0.32	0.82 ± 0.25	1.90 ± 1.25
Thoracic	0.18 ± 0.03	0.21 ± 0.04	0.12 ± 0.08
Lumbar	0.17 ± 0.01	0.18 ± 0.01 *	0.09 ± 0.01
Meninges			
Dorsal Meninges	1.30 ± 0.27	1.59 ± 0.26	1.45 ± 0.45
Ventral Meninges	8.87 ± 2.55	6.99 ± 1.74	8.63 ± 2.61
Spinal Meninges	2.63 ± 1.40	3.78 ± 1.39	9.54 ± 6.70
Nasal Cavity & Lymphatics			
Olfactory Epithelium	12030 ± 1410	14237 ± 1061	11228 ± 3129
Trigeminal Nerve	1.21 ± 0.30	1.76 ± 0.18	1.91 ± 0.44
Superficial Cervical Nodes	3.81 ± 0.14	7.75 ± 0.90	4.46 ± 0.60
Deep Cervical Nodes	54.47 ± 11.35 +	30.99 ± 3.71	33.91 ± 3.63
Peripheral Tissues			
Muscle	0.19 ± 0.01	0.37 ± 0.10	0.74 ± 0.42
Liver	0.67 ± 0.06	0.70 ± 0.05	0.62 ± 0.09
Kidney	1.33 ± 0.24	3.10 ± 0.64	2.85 ± 1.17

[a]0 min time interval is equivalent to no pretreatment; HC = hypocretin-1, PHE = phenylephrine; intranasal pretreatment with 1% PHE (24 μL) was given as 6 μL nose drops every 2 minutes and following a period of 5 minutes after the last pretreatment nose drop, intranasal co-administration of HC and 1% PHE was initiated (48 μL)
*Different from 15 min, $p < 0.05$, ANOVA followed by Bonferroni post-test
+Different from 5 min, $p < 0.05$, ANOVA followed by Bonferroni post-test

Supplementary Material (4.6.1) Figure 1: Structures of Vasoactive Agents. Tetrahydrozoline is an imidazoline derivative, while phenylephrine is a derivative of epinephrine, differing only in the hydroxyl group on the benzene ring. Endothelin-1 is an endogenous 21 amino acid peptide vasoconstrictor. Histamine is a vasodilator that stems from the decarboxylation of the amino acid histidine.

Supplementary Material (4.6.1) Figure 1:

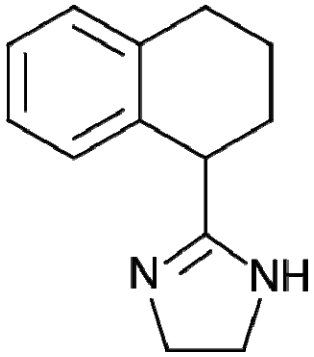

Tetrahydrozoline

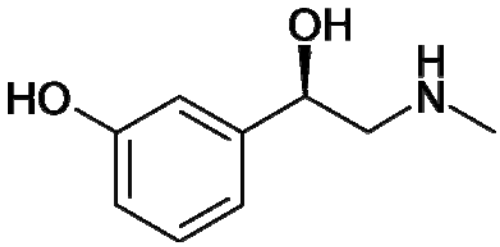

Phenylephrine

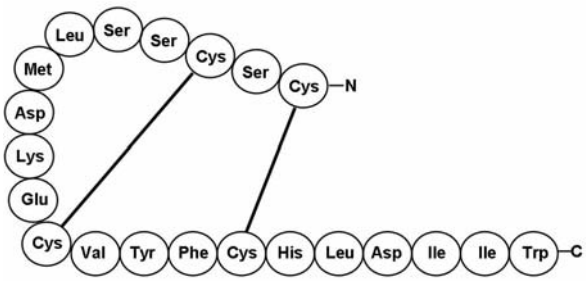

Endothelin-1

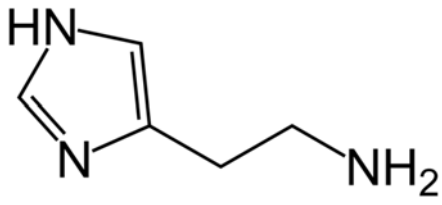

Histamine

Supplementary Material (4.6.1) Figure 2: Effect of Pretreatment Time Interval on Blood Absorption of Hypocretin-1 Following Intranasal Administration in the Presence and Absence of 1% Phenylephrine. No significant differences in blood concentration-time profiles were observed between different pretreatment time intervals for controls (dashed lines). Similarly, no significant differences in blood absorption were observed for 1% phenylephrine (PHE)-treated animals (solid lines).

Supplementary Material (4.6.1) Figure 2:

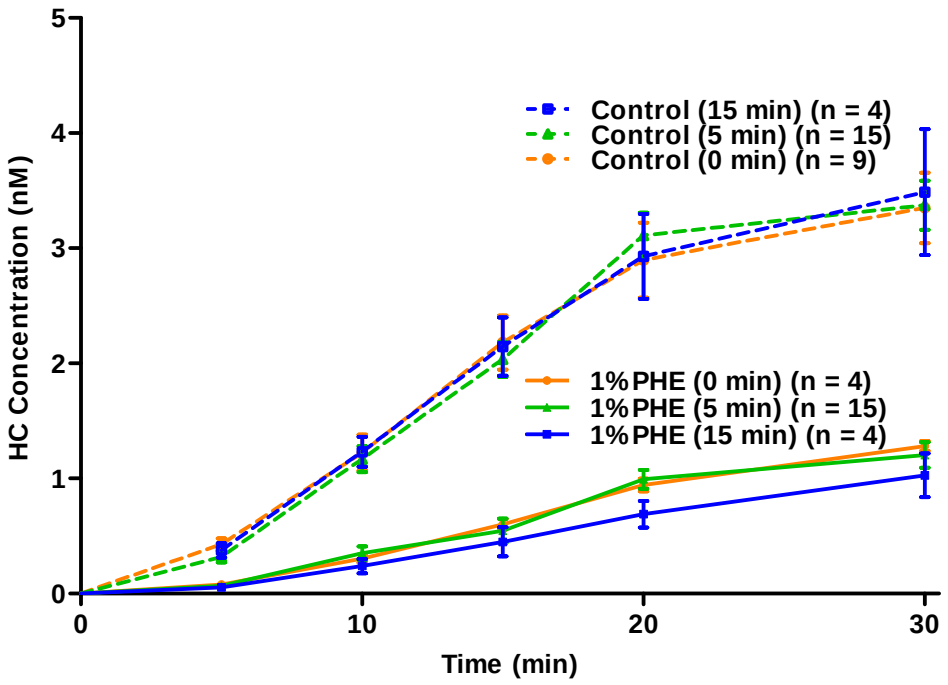

4.6.2 Effect of Cerebrospinal Fluid Sampling on Drug Distribution after Intranasal and Intravenous Delivery of Neuropeptides

Introduction

The purpose of this study was to determine the effect of cerebrospinal fluid (CSF) sampling on drug distribution in the central nervous system (CNS) and nasal cavity following intranasal and intravenous administration of neuropeptides to anesthetized rats. Drugs can gain direct access to the CNS following intranasal administration via olfactory and trigeminal neural pathways connecting the nasal passages to the brain and spinal cord. In addition, drugs can directly access the CSF contained in the subarachnoid space surrounding the brain and spinal cord following intranasal administration due to the anatomical connections between olfactory nerves in the nasal cavity and the CSF. Olfactory pathways arise from olfactory receptor neurons in the olfactory epithelium which send axons through perforations in the cribriform plate to reach the olfactory bulbs. Before reaching the olfactory bulbs, the axons pass through the subarachnoid space containing CSF. Studies show that tracers injected into the lateral ventricles or into the subarachnoid space containing CSF distribute to the underside of the olfactory bulbs to enter channels associated with axons of the olfactory nerves as they pass through the cribriform plate. From there, tracers enter the nasal associated lymphatic tissues (NALT) before reaching the cervical lymph nodes of the neck (Bradbury and Westrop, 1983; Kida et al., 1993; Johnston et al., 2004; Walter et al., 2006b; Walter et al., 2006a). Drugs administered by the intranasal route can be

transported from the olfactory epithelium within channels associated with the olfactory nerves to reach the CSF and other brain areas.

Numerous studies have demonstrated that intranasal administration results in rapid delivery of therapeutic agents to the CSF (Sakane et al., 1991; Born et al., 2002; Banks et al., 2004; van den Berg et al., 2004a; Zhang et al., 2004b; Wang et al., 2007; Nonaka et al., 2008), and the extent of CSF distribution is dependent on both size and degree of ionization, where small, uncharged molecules distribute into the CSF more than larger, charged molecules (Sakane et al., 1994; Sakane et al., 1995). After reaching the CSF contained in the subarachnoid space, drugs reach brain areas distant from the site of drug administration. Studies show distribution patterns consistent with this pathway of drug entry into the CNS, with drug concentrations in the hippocampus, an area that does not come into direct contact with CSF circulating in the subarachnoid space, much less than concentrations in the brainstem (Banks et al., 2004).

In order to reduce the number of animals required for intranasal experiments, some studies are designed so that samples of blood, CSF, and brain tissue can be obtained from the same animal after intranasal administration (Zhang et al., 2004b; Fliedner et al., 2006; Nonaka et al., 2008). However, CSF sampling could affect the integrity of the blood-brain barrier (BBB) and the brain distribution of intranasally applied therapeutics. In this study, the distribution of ^{125}I-labeled neuropeptides in the CNS and in the nasal cavity were compared with and without CSF sampling via cisternal puncture in anesthetized rats.

Methods

Detailed methods are presented in the *Methods* section of Chapter 4. Briefly, male Sprague-Dawley rats were anesthetized and the descending aorta was cannulated for blood sampling and perfusion. For intravenous experiments, the femoral vein was cannulated as well for drug administration. Animals were positioned on their backs with their necks maintained parallel to the surface to prevent drainage of the dose solution into the esophagus and trachea. Intranasal administration was performed by using a pipettor to deliver 6 μL nose drops to alternating nares every two minutes while occluding the opposite nostril. The drop was placed at the opening of the nostril allowing the animal to snort the drop into the nasal cavity. A total volume of 48 μL of solution was administered over 14 minutes for a total dose of 10 nmol (hypocretin-1, HC or L-Tyr-D-Arg, D-KTP; mixture of unlabeled and ^{125}I-labeled neuropeptides). For intranasal experiments with a vasoconstrictor, a 10% PHE stock solution was added to the dose solution containing neuropeptide to a final concentration of 1% PHE. Intravenous administration was accomplished by using an infusion pump to deliver a total volume of 500 μL of solution containing an equivalent dose via the femoral vein over 14 minutes.

Blood samples (0.1 mL) were obtained via the descending aorta cannula at 5, 10, 15, and 20 minutes after the onset of drug administration, maintaining blood volume during the course of the experiment by replacing with 0.9% sodium chloride (0.35 mL) after every other blood draw. CSF was sampled between 25 and 30 minutes after the onset of drug administration by placing the anesthetized rat ventral side down on a rolled towel, angling the head downwards at a 45 degrees angle, and inserting a needle

attached to PE90 tubing into the cisterna magna. CSF was allowed to flow into the tubing, without applying pressure, and the tubing was immediately clamped if blood entered to prevent contamination of CSF from blood-derived drug. A final blood sample was obtained via the descending aorta prior to sacrificing the animals by perfusion with 0.9% sodium chloride (60 mL) and fixation with 4% paraformaldehyde (360 mL). CNS tissues were dissected and concentrations in blood, CSF, and CNS tissues were determined by measuring radioactivity in tissue samples with gamma counting.

Unpaired two-sample t-tests were used to compare concentrations from animals with and without CSF sampling. Blood values up to the 20 minute measurement, which should not be affected by CSF sampling, were used as a control to ensure that there was no batch to batch variability between the radiolabeled neuropeptide used in the CSF sampling experiments and experiments that were completed previously. Differences were considered significant if $p < 0.05$.

Results

HC Blood Concentrations with and without CSF Sampling

HC blood concentrations were significantly greater with CSF sampling than without CSF sampling at all time points (except at 15 minutes for the intravenous CSF group), regardless of the route of drug administration (Figure 1). The observation of dissimilar blood concentrations with and without CSF sampling indicated significant batch to batch variability of ^{125}I-HC. It is also possible that the preparation of the dose

solution was different between the groups. It is more likely that the supplier (GE Healthcare) introduced a change in the iodination process of HC such that the ^{125}I-HC used in the CSF sampling experiments was not comparable to the material used in earlier experiments. Therefore, the effect of CSF sampling on brain concentrations of HC could not be evaluated.

D-KTP Blood Concentration with and without CSF Sampling

D-KTP blood concentrations with CSF sampling were consistent with those without CSF sampling, irrespective of the route drug administration (Figure 2), indicating minimal batch to batch variability of ^{125}I-D-KTP. The data obtained for D-KTP originated from two batches of ^{125}I-D-KTP that were synthesized within a month of each other by GE Healthcare. Intravenous administration resulted in the greatest D-KTP blood concentrations, followed by intranasal administration, followed by intranasal administration with 1% PHE.

D-KTP Concentrations with and without CSF Sampling

CSF sampling had minimal effect on drug distribution following intravenous administration of D-KTP (Figure 3). The only significant increases in concentrations were observed in the olfactory bulbs (1.4-fold, Figure 3) and dorsal meninges (1.4-fold, Figure 4) with CSF sampling.

Drug distribution following intranasal administration was more profoundly affected with CSF sampling. D-KTP brain concentrations were significantly ($p < 0.05$) or marginally ($p < 0.10$) increased by 1.4-fold to 4.4-fold after CSF sampling (with the

exception of the cerebellum) (Figure 5). The brain areas most affected by CSF sampling in the intranasal group included the olfactory bulbs (4.4-fold), hypothalamus (3.6-fold), and anterior olfactory nucleus (2.6-fold). Additionally, significant increases in concentrations were found in the olfactory epithelium (2.6-fold) and dorsal meninges (2.6-fold) with CSF sampling (Figure 6). Trigeminal nerve concentrations were increased with CSF sampling from 12.5 nM to 30.3 nM, however these differences did not reach statistical significance (Figure 6).

In the presence of 1% PHE, CSF sampling affected intranasal drug distribution to a greater extent than in the absence of the vasoconstrictor. D-KTP brain concentrations significantly increased by 3.1-fold to 10-fold (Figure 7) with CSF sampling, greatly affecting all brain areas including the anterior olfactory nucleus (10-fold), olfactory bulbs (8.0-fold), and frontal cortex (6.4-fold), thalamus (6.2-fold), and hypothalamus (5.5-fold). Within the nasal cavity, concentrations in the respiratory epithelium were marginally decreased by 1.9-fold, while olfactory epithelium concentrations were significantly increased to a similar extent (Figure 8). Concentrations in the dorsal and ventral meninges were significantly increased with CSF sampling by 8.4-fold and 4.2-fold, respectively (Figure 8). Trigeminal nerve concentrations were also significantly increased by 2.7-fold (Figure 8).

Discussion

Results from these studies clearly indicate that CSF sampling via cisternal puncture in anesthetized rats following intranasal administration, but not intravenous administration, significantly alters drug distribution within the CNS. While minimal

changes in D-KTP distribution were observed with CSF sampling following intravenous administration, brain concentrations were increased in nearly all brain areas, as well as in the olfactory epithelium, meninges, and the trigeminal nerve after CSF sampling with intranasal administration.

The reason for the increase in drug distribution with CSF sampling following intranasal administration could be attributed to changes in intracranial pressure leading to enhanced transport to the CNS. Under normal conditions, intracranial pressure is determined by the volume of the brain, blood, and CSF. Tracer studies with India ink demonstrate that when intracranial pressure is increased by infusion into the cisterna magna of rats, the tracer flows towards the olfactory bulbs, through the cribriform plate, and into the nasal cavity (Brinker et al., 1997). In the present study, intracranial pressure was reduced because of CSF outflow during cisternal puncture. The resulting hydrostatic pressure gradient could have resulted in fluid flow from the nasal epithelium, through channels associated with the olfactory nerve, and into the CSF contained in the subarachnoid space underlying the olfactory bulbs. Drug present in the nasal epithelium could have entered the CNS during CSF sampling via bulk flow mechanisms. Following intranasal administration, the nasal epithelium contained a large depot of drug and with 1% PHE, the concentration in the nasal epithelium was further increased due to reduced absorption into the blood with the vasoconstrictor. As a result, CSF sampling had a more profound effect on brain concentrations with 1% PHE. It is also possible that after intranasal administration, the vasoconstrictor itself could have entered the CNS, having the effect of constricting blood vessels, increasing blood pressure, and lowering the cerebral blood volume. This would further lower

intracranial pressure and could explain why CSF sampling had a more profound effect in the presence of 1% PHE. Few differences were observed in the intravenous group because the level of drug present in the nasal epithelium was considerably lower than in the intranasal groups.

The technique of CSF sampling via the cisterna magna is limited because of the possibility of altering the BBB or introducing injuries to nearby brain tissues, meningeal membranes, and blood vessels (Westergren and Johansson, 1991; Huang et al., 1996). Damage to blood vessels could lead to contamination of CSF and brain tissues due to the presence of blood-derived drug, which may result in artificially elevated CNS concentrations. In the present study, care was taken to reduce contamination of CSF samples from blood by immediately clamping the tubing containing CSF if blood was observed and by only analyzing clear CSF samples. When brains were visually inspected after perfusion and removed from the skull, blood clots were occasionally observed in the area at the base of the cerebellum where the needle had been inserted. A cotton swab immersed in PBS was used to wash away any blood clots prior to analysis of tissues by gamma counting.

The findings from these experiments suggest that reported brain concentrations from published intranasal studies (Zhang et al., 2004b; Fliedner et al., 2006; Nonaka et al., 2008) may be artificially inflated due to changes in CNS physiology that occurs from CSF sampling. For intranasal experiments where drug distribution in the brain and CSF will be evaluated, a separate group of animals should be used for CSF sampling. An alternative method could also be used where concentrations can be measured in-line without removing CSF and without significantly affecting CNS

physiology. Microdialysis techniques used in conjunction with intranasal delivery could achieve this goal (Wang et al., 2006b).

Supplementary Material (4.6.2) Figure 1: Hypocretin-1 Blood Concentrations with and without Cerebrospinal Fluid Sampling. Concentrations of hypocretin-1 (HC) in the blood following intravenous administration, intranasal administration, and intranasal administration with 1% phenylephrine (PHE) with and without cerebrospinal fluid (CSF) sampling via the cisternal magna were significantly different ($p < 0.05$, unpaired t-test, except at 15 minutes for the intravenous group), suggesting that there was batch to batch variability of ^{125}I-HC across experiments. The blood should not have been affected by CSF sampling, particularly up to the 20 minute measurement. As a result, the effect of CSF sampling could not be evaluated for HC.

Supplementary Material (4.6.2) Figure 1:

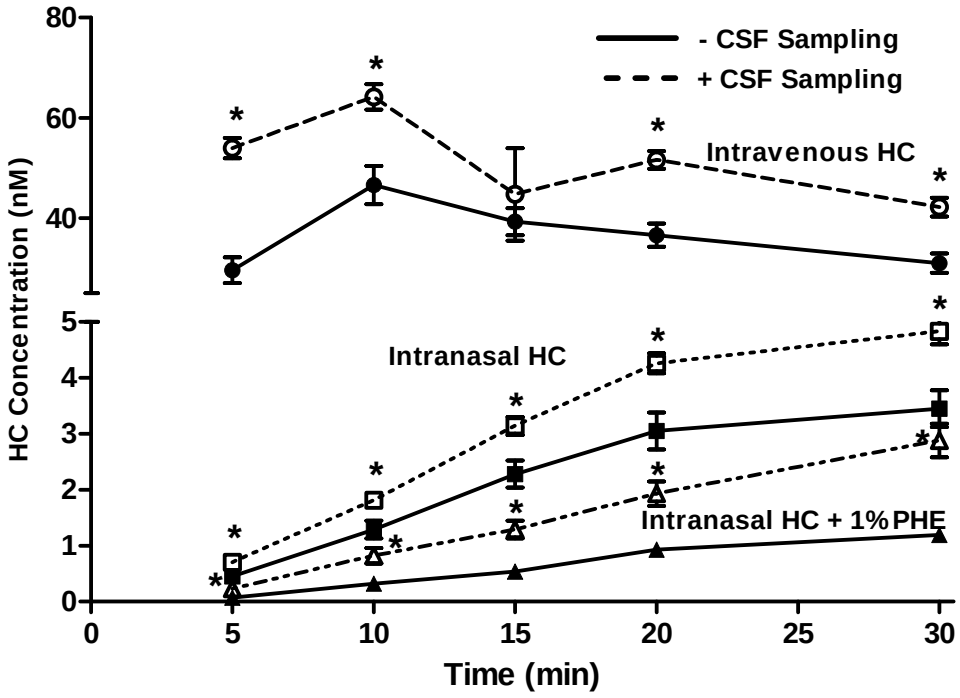

Supplementary Material (4.6.2) Figure 2: L-Tyr-D-Arg Blood Concentrations with and without Cerebrospinal Fluid Sampling. Concentrations of L-Tyr-D-Arg (D-KTP) in the blood following intravenous administration, intranasal administration, and intranasal administration with 1% phenylephrine (PHE) with and without cerebrospinal fluid (CSF) sampling via the cisternal magna were not significantly different ($p > 0.05$, unpaired t-test), which was expected since the blood should not have been affected by CSF sampling.

Supplementary Material (4.6.2) Figure 2:

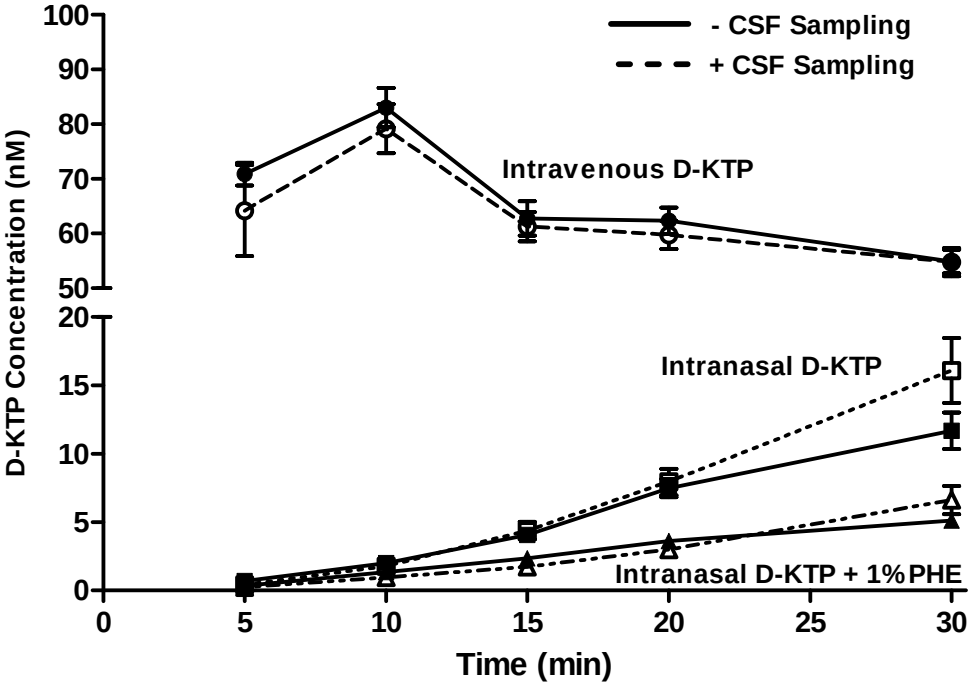

Supplementary Material (4.6.2) Figure 3: Effect of Cerebrospinal Fluid Sampling on L-Tyr-D-Arg Concentrations in the Brain after Intravenous Administration. With the exception of increased concentrations in the olfactory bulbs, cerebrospinal fluid (CSF) sampling had minimal effect on the distribution of L-Tyr-D-Arg (D-KTP) in the brain after intravenous administration ($p > 0.05$, unpaired t-test).

Supplementary Material (4.6.2) Figure 3:

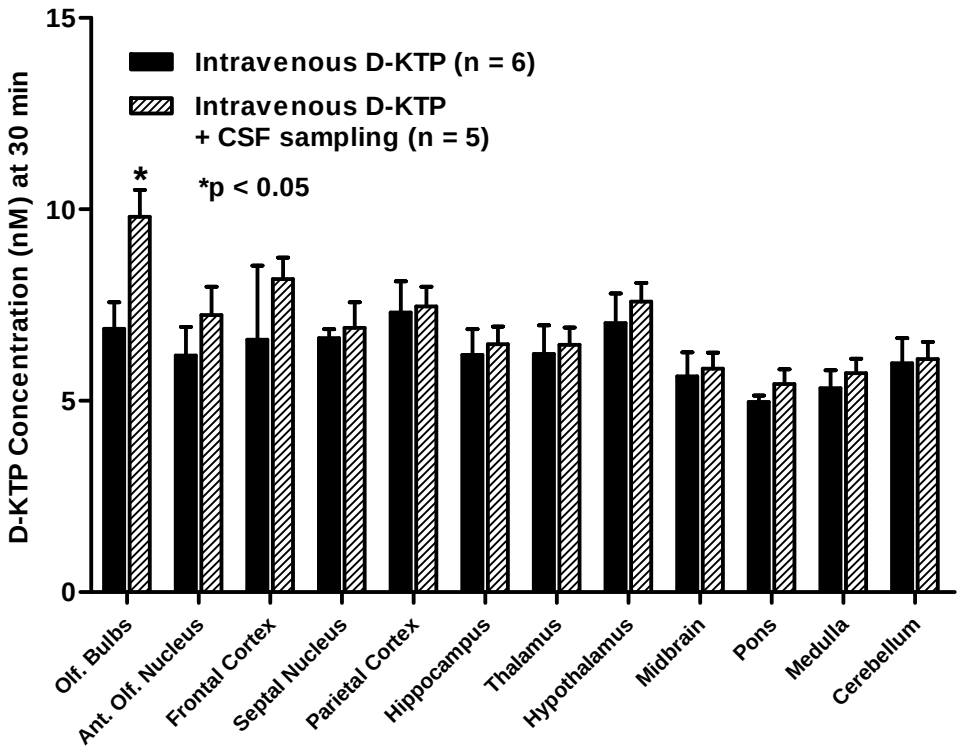

Supplementary Material (4.6.2) Figure 4: Effect of Cerebrospinal Fluid Sampling on L-Tyr-D-Arg Concentrations in Other Tissues after Intravenous Administration. With the exception of increased concentrations in the dorsal meninges, cerebrospinal fluid (CSF) sampling had minimal effect on the distribution of L-Tyr-D-Arg (D-KTP) in the nasal epithelium, ventral meninges, and trigeminal nerve after intravenous administration ($p > 0.05$, unpaired t-test).

Supplementary Material (4.6.2) Figure 4:

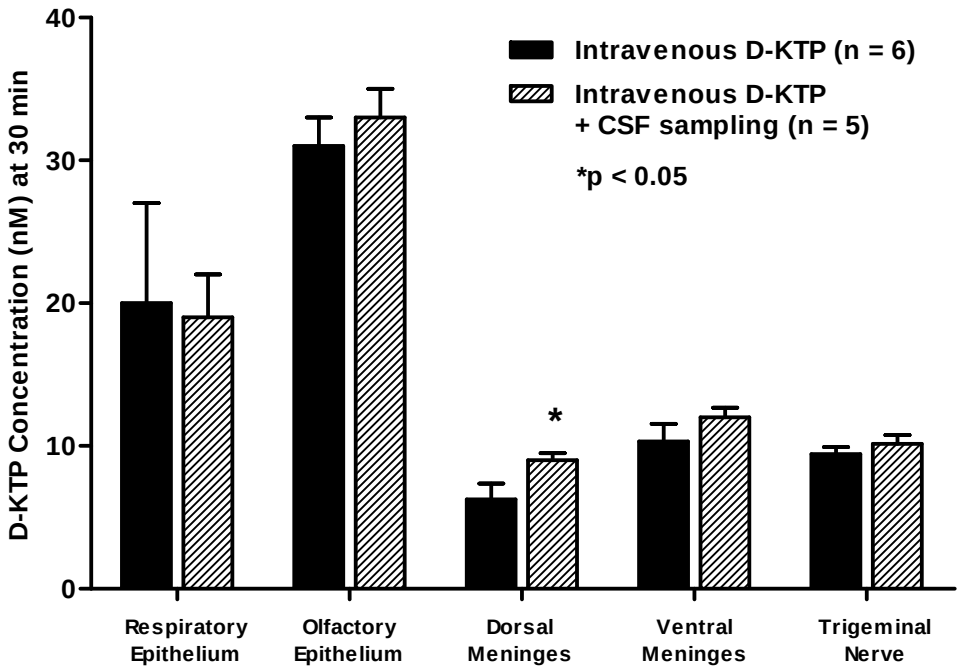

Supplementary Material (4.6.2) Figure 5: Effect of Cerebrospinal Fluid Sampling on L-Tyr-D-Arg Concentrations in the Brain after Intranasal Administration. Cerebrospinal fluid (CSF) sampling marginally ($p < 0.10$, unpaired t-test) or significantly ($p < 0.05$, unpaired t-test) increased the distribution of L-Tyr-D-Arg (D-KTP) in the brain after intranasal administration.

Supplementary Material (4.6.2) Figure 5:

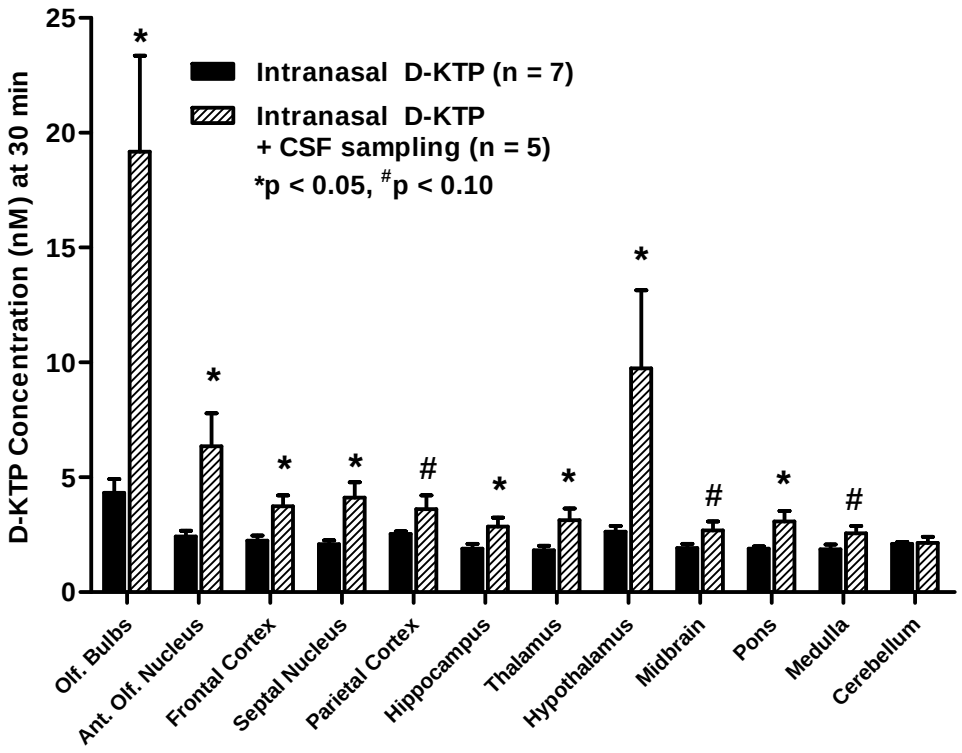

Supplementary Material (4.6.2) Figure 6: Effect of Cerebrospinal Fluid Sampling on L-Tyr-D-Arg Concentrations in Other Tissues after Intranasal Administration. Cerebrospinal fluid (CSF) sampling significantly increased concentrations of L-Tyr-D-Arg (D-KTP) in the olfactory epithelium ($p < 0.05$, unpaired t-test) and marginally increased concentrations of D-KTP in the dorsal meninges ($p < 0.10$, unpaired t-test) after intranasal administration. Concentrations in the respiratory epithelium, ventral meninges, and trigeminal nerve were increased, but not significantly after CSF sampling with intranasal administration.

Supplementary Material (4.6.2) Figure 6:

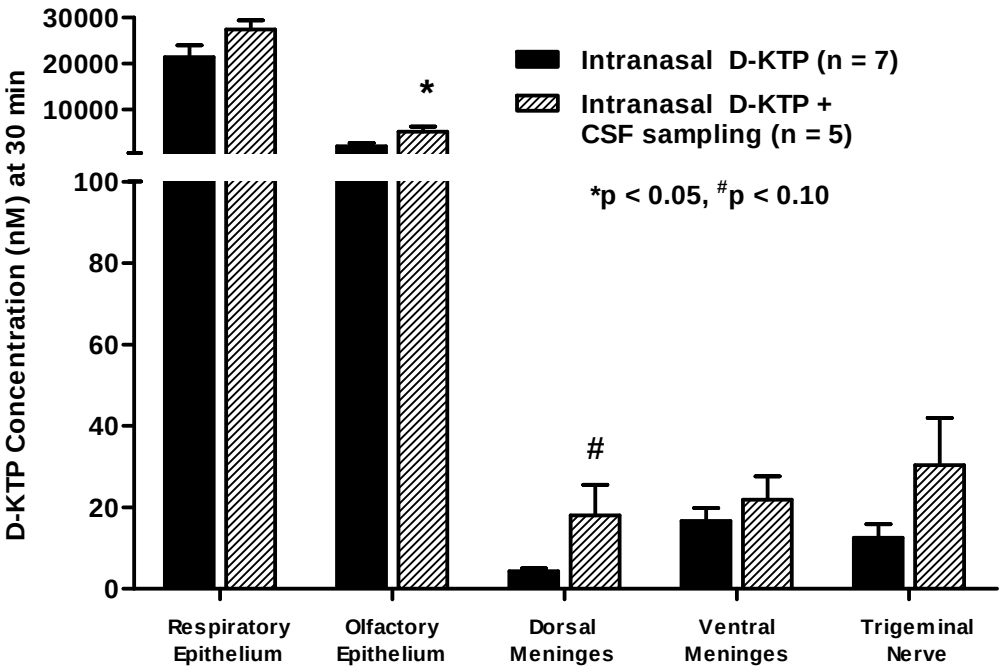

Supplementary Material (4.6.2) Figure 7: Effect of Cerebrospinal Fluid Sampling on L-Tyr-D-Arg Concentrations in the Brain after Intranasal Administration with 1% Phenylephrine. Cerebrospinal fluid (CSF) sampling had pronounced effects on the brain distribution of L-Tyr-D-Arg (D-KTP) after intranasal administration with 1% phenylephrine (PHE), with significant increases in D-KTP concentrations throughout the brain ($p < 0.05$, unpaired t-test).

Supplementary Material (4.6.2) Figure 7:

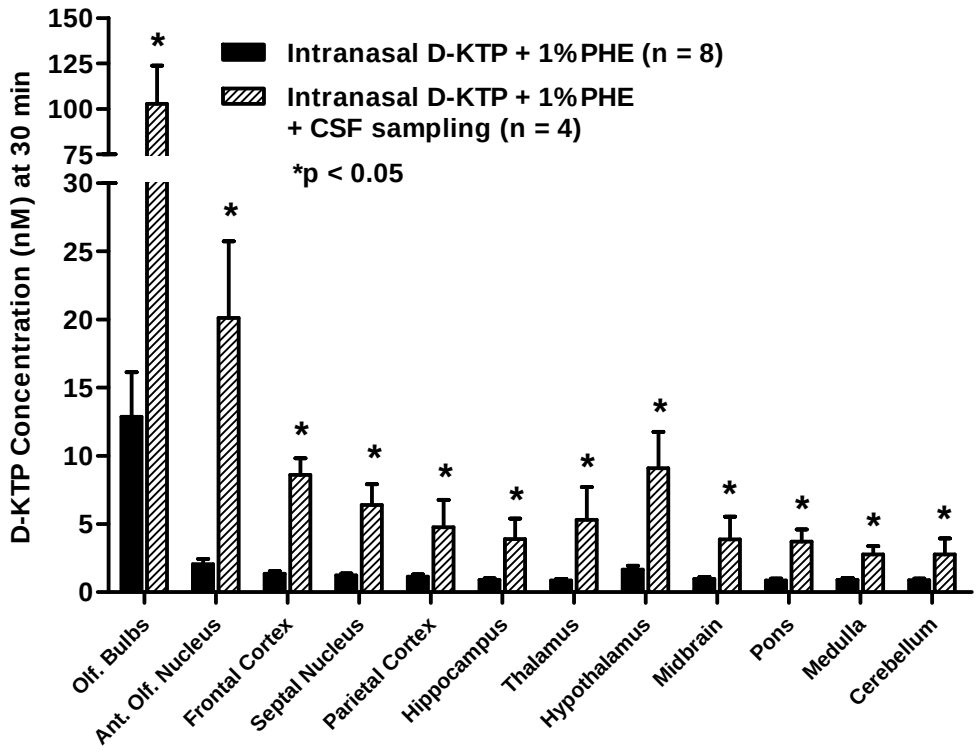

Supplementary Material (4.6.2) Figure 8: Effect of Cerebrospinal Fluid Sampling on L-Tyr-D-Arg Concentrations in Other Tissues after Intranasal Administration with 1% Phenylephrine. With the exception of the respiratory epithelium, cerebrospinal fluid (CSF) sampling significantly increased concentrations of L-Tyr-D-Arg (D-KTP) in the olfactory epithelium, meninges, and trigeminal nerve ($p < 0.05$, unpaired t-test) after intranasal administration with 1% phenylephrine (PHE). Concentrations of D-KTP in the respiratory epithelium were marginally decreased after intranasal administration with 1% PHE and CSF sampling ($p < 0.10$, unpaired t-test).

Supplementary Material (4.6.2) Figure 8:

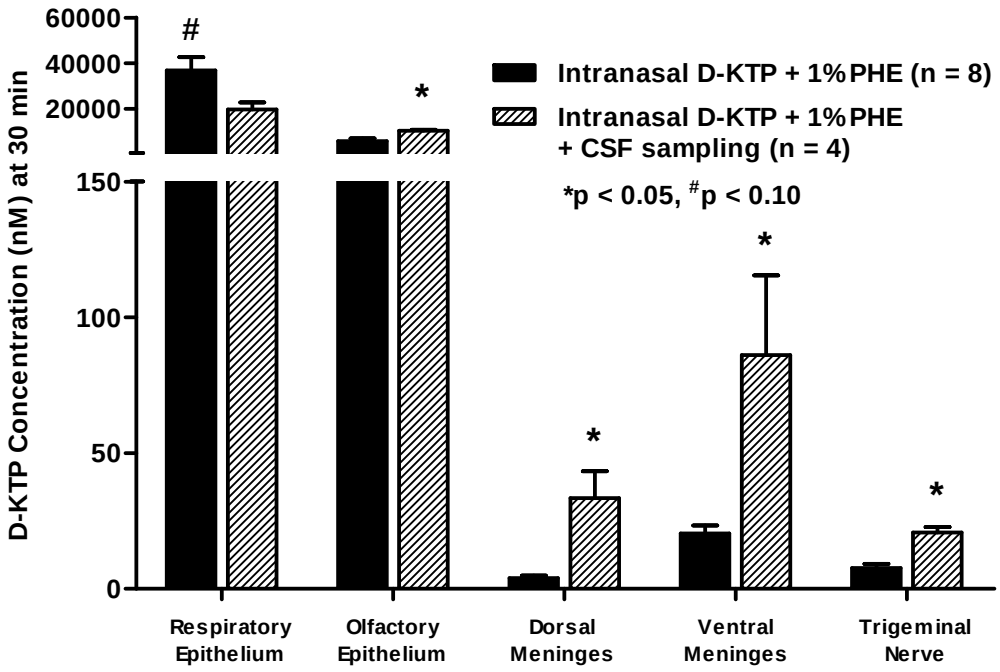

CONCLUSIONS

Objectives

In the research presented in this dissertation, the overall objectives were to assess and enhance intranasal targeting of the neuropeptide, hypocretin-1 (HC, 33 amino acids), to the central nervous system (CNS) and to understand the mechanisms underlying intranasal delivery to the CNS. To determine if intranasal administration targets HC to the CNS, pharmacokinetics and drug targeting were compared over a two hour time period following intranasal and intravenous administration of ^{125}I-HC. To determine if intranasal administration of HC could result in activation of HC signaling pathways and affect HC-mediated behaviors, behavioral effects were monitored following administration. Use of a vasoconstrictor formulation was explored as a strategy to enhance CNS delivery and targeting following intranasal administration. In addition to HC, the dipeptide, L-Tyr-D-Arg (D-KTP, 2 amino acids) was evaluated to determine if the vasoconstrictor effect was different for a smaller sized therapeutic. The strengths of the research included the use of multiple time points to assess overall exposure and targeting to tissues and the use of behavioral studies to supplement the biodistribution studies. Use of a vasoconstrictor formulation was a novel approach to investigate the role of the nasal vasculature in intranasal delivery to the CNS. Further, in this research, the CNS distribution of neuropeptide therapeutics was evaluated in great detail to gain insight into the pathways underlying direct transport from the nasal mucosa to the brain. The research was limited by radiotracer detection methods and the sampling scheme, which did not fully capture the terminal elimination phase of the

therapeutics tested. As a result, only *estimates* of pharmacokinetic parameters and drug targeting were obtained. In addition, the behavioral studies could have provided greater insight by also evaluating effects following intravenous administration or intranasal administration at different doses in the present and absence of a vasoconstrictor.

Key Findings from Chapter 2, "Intranasal Drug Targeting of Hypocretin-1 (Orexin-A) to the Central Nervous System"

Results from this research clearly demonstrated that intranasal administration rapidly targets HC to the CNS along direct pathways when compared to intravenous administration. There was compelling evidence for the involvement of both the trigeminal and olfactory neural pathways in the transport of HC from the nasal mucosa to the CNS, including substantial drug targeting to the trigeminal nerve and to brain areas in close proximity to the site of entry of the trigeminal nerve into the brain, a decreasing concentration gradient within the trigeminal nerve, as well as high delivery to the olfactory bulbs. Concentrations achieved in the brain were similar with intranasal compared to intravenous administration over the two hour time period, despite considerably lower blood concentrations with intranasal delivery, suggesting that pathways other than the vasculature play a role in the transport of HC from the nasal cavity to the CNS. After intranasal administration, only approximately 20% of the observed brain AUC was due to indirect pathways from the blood to the brain, while approximately 80% was due to direct transport pathways from the nasal cavity to the brain.

In addition to increasing CNS targeting from 5- to 8-fold, intranasal administration targeted the lymphatic system and meninges compared to intravenous administration. Drug targeting of HC to the deep cervical lymph nodes, which are drainage sites from the nasal cavity via the nasal associated lymphatic tissues (NALT), was enhanced 20-fold with intranasal compared to intravenous administration. While this could be a potential problem in terms of activating immune responses against peptide and protein therapeutics given intranasally, this finding is promising for the targeting of immunotherapeutics to the lymphatic system for the treatment of multiple sclerosis and malignant tumors. Intranasal compared to intravenous administration also increased drug targeting to the meningeal membranes surrounding the brain. Antibiotics or antiviral therapeutics could be targeted to the meninges with intranasal administration to treat meningitis or encephalitis.

Key Findings from Chapter 3, "Behavioral Assessments after Intranasal Administration of Hypocretin-1 (Orexin-A) to Rats: Effects on Appetite and Locomotor Activity"

Intranasal administration of HC affected CNS-mediated behaviors by significantly increasing food consumption and by increasing wheel running activity in rats. These behavioral effects of intranasal HC were observed within four hours after dosing during the early light phase of the light-dark cycle, during a time of day when animals are normally inactive. These findings indicate that HC reaches the CNS in its active form after intranasal administration at concentrations sufficient to overcome signals of satiety and quiescence. Preliminary cell signaling studies indicated the involvement of the phosphatidyl-inositol 3-kinase (PI3K) signaling pathway. However,

the small sample size from the cell signaling studies conducted suggest the need for additional studies to understand the underlying cellular mechanisms involved in HC-mediated changes in behavior. These preliminary results are encouraging as they are the first reports of CNS effects after intranasal administration of HC in a rodent model and are consistent with the known effects of HC following intracerebroventricular (ICV) injection.

The broader implications of these findings include the development of intranasal treatments for CNS disorders involving the hypocretinergic system. There is a clear role of HC in the pathogenesis of narcolepsy (Chemelli et al., 1999; Lin et al., 1999; Peyron et al., 2000; Thannickal et al., 2000; Ripley et al., 2001) and in the regulation of appetite (Sakurai et al., 1998; Haynes et al., 1999; Yamanaka et al., 2000). There are reports of inhibiting the hypocretinergic system using HC antibodies (Yamada et al., 2000) or HC receptor antagonists (Haynes et al., 2000) for treating obesity. More recently, evidence has emerged linking HC to other CNS diseases and disorders, including Alzheimer's disease (Friedman et al., 2007), Parkinson's disease (Thannickal et al., 2007), and depression (Allard et al., 2004). Targeting therapeutics to the CNS with intranasal administration may be beneficial for treating these diseases and disorders. Intranasal HC was shown to improve cognition in sleep deprived monkeys (Deadwyler et al., 2007), probably due to the enhancing effects of HC on alertness and wakefulness. Currently, intranasal HC is under evaluation for the treatment of narcolepsy in clinical trials.

Key Findings from Chapter 4, "Novel Vasoconstrictor Formulation to Enhance Intranasal Targeting of Neuropeptides to the Central Nervous System"

Results clearly indicated that vasoconstrictor nasal formulations significantly reduce systemic absorption over the course of 30 minutes, at least for two different neuropeptides, HC and D-KTP. Reduced absorption into the blood had the effect of significantly increasing deposition in the olfactory epithelium and increasing delivery along olfactory nerve pathways to the olfactory bulbs in the CNS. Unexpectedly, concentrations in the trigeminal nerve and in most remaining brain tissues were reduced in the presence of the vasoconstrictor formulation. The reduced brain concentrations could have been due to reduced transport within perivascular spaces, within the blood, or within or along the trigeminal nerve. A complete understanding of the effects of the vasoconstrictor on intranasal delivery mechanisms was difficult since it was not possible to separate blood-mediated versus trigeminal-mediated pathways to the CNS. Further, this work was limited by the fact that a single time point was evaluated after intranasal administration with and without a vasoconstrictor. The dramatic reduction in blood concentrations resulted in brain-to-blood concentration ratios that were significantly increased throughout the brain for HC and for D-KTP (at higher vasoconstrictor concentrations), suggesting that targeting to brain tissues relative to the blood can be improved using this novel vasoconstrictor formulation.

The primary benefits of using vasoconstrictor nasal formulations of CNS therapeutics are (1) to reduce systemic exposure and (2) to increase delivery to rostral brain areas. For CNS therapeutics that demonstrate adverse side effects in the blood and/or peripheral tissues or that are extensively degraded or bound to proteins in the

blood, it would be advantageous to minimize systemic exposure by using a vasoconstrictor nasal formulation. For example, chemotherapeutics and analgesics are often accompanied by undesirable side effects and biologics are subject to proteolytic degradation in the blood. Lipophilic drugs are rapidly absorbed into the nasal vasculature following intranasal administration and could be eliminated from the systemic circulation before reaching CNS targets. The use of a vasoconstrictor formulation would be particularly suited for therapeutics having sites of action in rostral brain areas, such as the olfactory bulbs and frontal cortex, since concentrations in these areas were either increased or unaffected with a vasoconstrictor formulation. Delivering therapeutics to the olfactory bulbs could potentially treat anosmia associated with the onset of Alzheimer's disease, narcolepsy, and other neurological disorders. Intranasal delivery of therapeutics to the frontal cortex could treat frontotemporal dementia, personality disorders, cognition disorders, motor dysfunction, and Alzheimer's disease. In addition, immunotherapeutics could be formulated with a vasoconstrictor to treat immune disorders such as multiple sclerosis.

Methodological Challenges and Recommendations for Future Studies

Over the course of conducting this research, an important question arose related to the use of ^{125}I-labeled neuropeptides to assess drug distribution following intranasal and intravenous administration. Concentrations and assessments of drug targeting were based on measurements of radioactivity, which could include a mixture of free ^{125}I, intact ^{125}I-HC, and degraded ^{125}I-HC. As pharmacokinetic parameters can vary for these radiolabeled species, the use of radiolabeled tracers has its limitations. However,

due to the low quantities of peptide reaching the CNS after intranasal administration, the use of radiotracer methods to quantitate drug concentrations was necessary. Further, use of a high-energy gamma emitter such as ^{125}I allowed for direct measurement of radioactivity without the need for processing or extraction, which can affect peptide stability. It is highly recommended for future studies that assessments of stability of radiotracers are included in the experimental design or that alternative detection methods, such as LC-MS, microdialysis or ELISA, should be used to verify results that are obtained based on measurements of radioactivity. For example, comparable brain concentrations were observed from intranasal studies of ^{125}I-nerve growth factor (NGF) measured by gamma counting (Frey et al., 1997) and unlabeled NGF measured by ELISA (Chen et al., 1998). Further, it is recommended that behavior assessments following intranasal administration are used to support biodistribution data.

An important methodological discovery was made relating to the assessment of CNS drug distribution following intranasal administration when brain tissue and cerebrospinal fluid (CSF) are sampled from a single animal. The method commonly used for sampling CSF requires that a tube is inserted into the cisterna magna. It was hypothesized that CSF sampling via cisternal puncture methods could disrupt the integrity of the BBB or alter CNS physiology to significantly affect CNS drug distribution after intranasal administration. Results from this research indicated that drug distribution of D-KTP after intranasal administration, but not intravenous administration, with CSF sampling was significantly elevated throughout the brain compared to animals in which CSF had not been sampled. The process of withdrawing CSF lowers intracranial pressure, likely resulting in fluid flow from the nasal epithelium

through channels associated with the olfactory nerve and into the cranial cavity. This finding is noteworthy because several published studies report brain concentrations after intranasal administration where CSF had been sampled from the same animals and these concentrations may be artificially elevated (Zhang et al., 2004b; Fliedner et al., 2006; Nonaka et al., 2008). From this work, it is recommended that a separate group of animals be used for assessing drug concentrations in the CSF or alternative methods for CSF measurements should be explored in order to report accurate drug concentrations in brain tissues.

Another challenge in this research related to the difficulty in conducting the intranasal delivery experiments in rodents. In general, high inter-subject variability in drug distribution was observed in animals, requiring the use of a large number of animals (10-12 animals per group). The variability was likely due to differences in responses to anesthesia, which were difficult to control from experiment to experiment. Sodium pentobarbital (Nembutal) was selected for anesthesia in the majority of these experiments since this deep anesthetic is commonly used for experiments requiring surgical procedures, such as cannulation of the aorta. Pentobarbital depresses respiration so careful monitoring was necessary to prevent overdose and death. Because of differential responses to anesthesia, respiration and intranasal delivery varied from experiment to experiment. In future studies, use of a different anesthetic with less respiratory depression could reduce the variability observed. Alternatives include the volatile anesthetic, isoflurane or a cocktail of the anesthetic, ketamine, and the muscle relaxant, xylazine. The variability could also have been due to the method of intranasal administration of the formulations. Intranasal administration was

accomplished by using a pipettor to noninvasively administer 6 μL nose drops to alternating nostrils every two minutes while occluding the opposite nostril. The drop was placed at the opening of the nostril allowing the animal to "sniff" the drop to deliver the formulation to respiratory and olfactory epithelium. Differences in drop formation and "sniffing" could affect deposition in the nasal epithelium and delivery to the CNS, accounting for the variability from experiment to experiment. Future animal studies could evaluate the feasibility of alternative delivery techniques, such as insertion of a tube into the nostrils for localized delivery (van den Berg et al., 2002; Van den Berg et al., 2003; Banks et al., 2004; van den Berg et al., 2004b; Vyas et al., 2006b; Charlton et al., 2007b; Gao et al., 2007). However, it will also be critical to evaluate the potentially damaging effects of this method on the nasal epithelium. For intranasal treatments to be successful in humans, it will be important to evaluate intranasal delivery methods using spray devices to maintain control over the deposition of formulations in the nasal passages and CNS exposure of therapeutics.

There is considerable additional research that could be conducted relating to intranasal administration of HC, D-KTP, and vasoconstrictor formulations. Additional studies to assess the CNS effects of HC and D-KTP could help to determine the therapeutic potential of the intranasal route of delivery for these neuropeptides. For HC, it would be constructive to obtain behavioral and cell signaling data from a larger sample size and to add experimental arms using intravenous administration and the vasoconstrictor formulation. For D-KTP, it would be helpful to conduct behavioral assays such as tail flick and hot plate to assess pain responses following intravenous administration and intranasal administration of D-KTP in the presence and absence of a

vasoconstrictor. Additional studies to evaluate the time course of the effect of vasoconstrictors on biodistribution and behavioral responses would be important for obtaining a thorough understanding of the pharmacokinetic and pharmacodynamic effects of vasoconstrictor nasal formulations. Finally, experiments to better understand the effect of vasoconstrictors on the mechanisms involved in intranasal delivery would be beneficial. For example, using a drug that would not be expected to enter the vasculature and evaluating the effect of a vasoconstrictor on CNS distribution might allow for the separation of blood-mediated versus trigeminal-mediated pathways of delivery to the CNS.

REFERENCES

Adams HJ, Blair MR, Jr., Takman BH (1976) The local anesthetic activity of tetrodotoxin alone and in combination with vasoconstrictors and local anesthetics. Anesth Analg 55:568-573.

Alcalay RN, Giladi E, Pick CG, Gozes I (2004) Intranasal administration of NAP, a neuroprotective peptide, decreases anxiety-like behavior in aging mice in the elevated plus maze. Neurosci Lett 361:128-131.

Allard JS, Tizabi Y, Shaffery JP, Trouth CO, Manaye K (2004) Stereological analysis of the hypothalamic hypocretin/orexin neurons in an animal model of depression. Neuropeptides 38:311-315.

Ammoun S, Lindholm D, Wootz H, Akerman KE, Kukkonen JP (2006a) G-protein-coupled OX1 orexin/hcrtr-1 hypocretin receptors induce caspase-dependent and -independent cell death through p38 mitogen-/stress-activated protein kinase. J Biol Chem 281:834-842.

Ammoun S, Johansson L, Ekholm ME, Holmqvist T, Danis AS, Korhonen L, Sergeeva OA, Haas HL, Akerman KE, Kukkonen JP (2006b) OX1 orexin receptors activate extracellular signal-regulated kinase in Chinese hamster ovary cells via multiple mechanisms: the role of Ca2+ influx in OX1 receptor signaling. Mol Endocrinol 20:80-99.

Aou S, Li XL, Li AJ, Oomura Y, Shiraishi T, Sasaki K, Imamura T, Wayner MJ (2003) Orexin-A (hypocretin-1) impairs Morris water maze performance and CA1-Schaffer collateral long-term potentiation in rats. Neuroscience 119:1221-1228.

Bagger M, Bechgaard E (2004a) A microdialysis model to examine nasal drug delivery and olfactory absorption in rats using lidocaine hydrochloride as a model drug. Int J Pharm 269:311-322.

Bagger MA, Bechgaard E (2004b) The potential of nasal application for delivery to the central brain-a microdialysis study of fluorescein in rats. Eur J Pharm Sci 21:235-242.

Bahadduri PM, D'Souza VM, Pinsonneault JK, Sadee W, Bao S, Knoell DL, Swaan PW (2005) Functional characterization of the peptide transporter PEPT2 in primary cultures of human upper airway epithelium. Am J Respir Cell Mol Biol 32:319-325.

Baier PC, Weinhold SL, Huth V, Gottwald B, Ferstl R, Hinze-Selch D (2008) Olfactory dysfunction in patients with narcolepsy with cataplexy is restored by intranasal Orexin A (Hypocretin-1). Brain.

Bailer AJ (1988) Testing for the equality of area under the curves when using destructive measurement techniques. J Pharmacokinet Biopharm 16:303-309.

Balin BJ, Broadwell RD, Salcman M, el-Kalliny M (1986) Avenues for entry of peripherally administered protein to the central nervous system in mouse, rat, and squirrel monkey. J Comp Neurol 251:260-280.

Banks WA (2008) Delivery of peptides to the brain: Emphasis on therapeutic development. Biopolymers 90:589-594.

Banks WA, During MJ, Niehoff ML (2004) Brain uptake of the glucagon-like peptide-1 antagonist exendin(9-39) after intranasal administration. J Pharmacol Exp Ther 309:469-475.

Banks WA, Morley JE, Niehoff ML, Mattern C (2008) Delivery of testosterone to the brain by intranasal administration: Comparison to intravenous testosterone. J Drug Target:1.

Banks WA, Goulet M, Rusche JR, Niehoff ML, Boismenu R (2002) Differential transport of a secretin analog across the blood-brain and blood-cerebrospinal fluid barriers of the mouse. J Pharmacol Exp Ther 302:1062-1069.

Barreiro ML, Pineda R, Gaytan F, Archanco M, Burrell MA, Castellano JM, Hakovirta H, Nurmio M, Pinilla L, Aguilar E, Toppari J, Dieguez C, Tena-Sempere M (2005) Pattern of orexin expression and direct biological actions of orexin-a in rat testis. Endocrinology 146:5164-5175.

Baumann CR, Stocker R, Imhof HG, Trentz O, Hersberger M, Mignot E, Bassetti CL (2005) Hypocretin-1 (orexin A) deficiency in acute traumatic brain injury. Neurology 65:147-149.

Baumann G, Amburn K (1986) The autodecomposition of radiolabeled human growth hormone. J Immunoassay 7:139-149.

Benedict C, Kern W, Schultes B, Born J, Hallschmid M (2008) Differential sensitivity of men and women to anorexigenic and memory improving effects of intranasal insulin. J Clin Endocrinol Metab.

Benedict C, Hallschmid M, Hatke A, Schultes B, Fehm HL, Born J, Kern W (2004) Intranasal insulin improves memory in humans. Psychoneuroendocrinology 29:1326-1334.

Benedict C, Hallschmid M, Schmitz K, Schultes B, Ratter F, Fehm HL, Born J, Kern W (2007) Intranasal insulin improves memory in humans: superiority of insulin aspart. Neuropsychopharmacology 32:239-243.

Bhatnagar BS, Bogner RH, Pikal MJ (2007) Protein stability during freezing: separation of stresses and mechanisms of protein stabilization. Pharm Dev Technol 12:505-523.

Born J, Lange T, Kern W, McGregor GP, Bickel U, Fehm HL (2002) Sniffing neuropeptides: a transnasal approach to the human brain. Nat Neurosci 5:514-516.

Bradbury MW, Westrop RJ (1983) Factors influencing exit of substances from cerebrospinal fluid into deep cervical lymph of the rabbit. J Physiol 339:519-534.

Bradley JG (1991) Nonprescription drugs and hypertension. Which ones affect blood pressure? Postgrad Med 89:195-197, 201-192.

Brinker T, Ludemann W, Berens von Rautenfeld D, Samii M (1997) Dynamic properties of lymphatic pathways for the absorption of cerebrospinal fluid. Acta Neuropathol 94:493-498.

Brundin L, Bjorkqvist M, Petersen A, Traskman-Bendz L (2007) Reduced orexin levels in the cerebrospinal fluid of suicidal patients with major depressive disorder. Eur Neuropsychopharmacol 17:573-579.

Buck LB (2000) The chemical senses. In: Principles of neural science., Fourth Edition (Kandel ER, Schwartz JH, Jessell TM, eds), pp 625-652. New York: McGraw-Hill Companies.

Buddenberg TE, Topic B, Mahlberg ED, de Souza Silva MA, Huston JP, Mattern C (2008) Behavioral actions of intranasal application of dopamine: effects on forced swimming, elevated plus-maze and open field parameters. Neuropsychobiology 57:70-79.

Capsoni S, Giannotta S, Cattaneo A (2002) Nerve growth factor and galantamine ameliorate early signs of neurodegeneration in anti-nerve growth factor mice. Proc Natl Acad Sci U S A 99:12432-12437.

Cauna N (1982) Blood and nerve supply of the nasal lining. In: The nose: upper airway physiology and the atmospheric environment. (Proctor DF, Andersen I, eds), pp 45-69. Amsterdam: Elsevier Biomedical Press.

Charlton ST, Davis SS, Illum L (2007a) Evaluation of effect of ephedrine on the transport of drugs from the nasal cavity to the systemic circulation and the central nervous system. J Drug Target 15:370-377.

Charlton ST, Davis SS, Illum L (2007b) Nasal administration of an angiotensin antagonist in the rat model: effect of bioadhesive formulations on the distribution of drugs to the systemic and central nervous systems. Int J Pharm 338:94-103.

Charlton ST, Whetstone J, Fayinka ST, Read KD, Illum L, Davis SS (2008) Evaluation of direct transport pathways of glycine receptor antagonists and an Angiotensin antagonist from the nasal cavity to the central nervous system in the rat model. Pharm Res 25:1531-1543.

Chemelli RM, Willie JT, Sinton CM, Elmquist JK, Scammell T, Lee C, Richardson JA, Williams SC, Xiong Y, Kisanuki Y, Fitch TE, Nakazato M, Hammer RE, Saper CB, Yanagisawa M (1999) Narcolepsy in orexin knockout mice: molecular genetics of sleep regulation. Cell 98:437-451.

Chen SC, Eiting K, Cui K, Leonard AK, Morris D, Li CY, Farber K, Sileno AP, Houston ME, Jr., Johnson PH, Quay SC, Costantino HR (2006) Therapeutic utility of a novel tight junction modulating peptide for enhancing intranasal drug delivery. J Pharm Sci 95:1364-1371.

Chen XQ, Fawcett JR, Rahman YE, Ala TA, Frey IW (1998) Delivery of Nerve Growth Factor to the Brain via the Olfactory Pathway. J Alzheimers Dis 1:35-44.

Chow HH, Anavy N, Villalobos A (2001) Direct nose-brain transport of benzoylecgonine following intranasal administration in rats. J Pharm Sci 90:1729-1735.

Chow HS, Chen Z, Matsuura GT (1999) Direct transport of cocaine from the nasal cavity to the brain following intranasal cocaine administration in rats. J Pharm Sci 88:754-758.

Chua SS, Benrimoj SI (1988) Non-prescription sympathomimetic agents and hypertension. Med Toxicol Adverse Drug Exp 3:387-417.

Clerico DM, To WC, Lanza DC (2003) Anatomy of the human nasal passages. In: Handbook of olfaction and gustation., Second Edition (Doty RL, ed), pp 1-16. New York: Marcel Dekker, Inc.

Corboz MR, Rivelli MA, Varty L, Mutter J, Cartwright M, Rizzo CA, Eckel SP, Anthes JC, Hey JA (2005) Pharmacological characterization of postjunctional alpha-adrenoceptors in human nasal mucosa. Am J Rhinol 19:495-502.

Corboz MR, Varty LM, Rizzo CA, Mutter JC, Rivelli MA, Wan Y, Umland S, Qiu H, Jakway J, McCormick KD, Berlin M, Hey JA (2003) Pharmacological characterization of alpha 2-adrenoceptor-mediated responses in pig nasal mucosa. Auton Autacoid Pharmacol 23:208-219.

Cserr HF, Harling-Berg CJ, Knopf PM (1992) Drainage of brain extracellular fluid into blood and deep cervical lymph and its immunological significance. Brain Pathol 2:269-276.

Dahlin M, Jansson B, Bjork E (2001) Levels of dopamine in blood and brain following nasal administration to rats. Eur J Pharm Sci 14:75-80.

Danhof M, Stevens J, van der Graff PH, De Lange ECM, Suidgeest E (2008) Development and evaluation of a new, minimal-stress animal model for intranasal administration in freely moving rats. In: American Association of Pharmaceutical Scientists Annual Meeting. Atlanta, GA.

Date Y, Ueta Y, Yamashita H, Yamaguchi H, Matsukura S, Kangawa K, Sakurai T, Yanagisawa M, Nakazato M (1999) Orexins, orexigenic hypothalamic peptides, interact with autonomic, neuroendocrine and neuroregulatory systems. Proc Natl Acad Sci U S A 96:748-753.

Davis SS, Illum L (2003) Absorption enhancers for nasal drug delivery. Clin Pharmacokinet 42:1107-1128.

de Lorenzo AJD (1970) The olfactory neuron and the blood-brain barrier. In: Taste and smell in vertebrates. (Wolstenholme GEW, Knight J, eds), pp 151-175. London: Churchill.

De Rosa R, Garcia AA, Braschi C, Capsoni S, Maffei L, Berardi N, Cattaneo A (2005) Intranasal administration of nerve growth factor (NGF) rescues recognition memory deficits in AD11 anti-NGF transgenic mice. Proc Natl Acad Sci U S A 102:3811-3816.

de Souza Silva MA, Mattern C, Topic B, Buddenberg TE, Huston JP (2009) Dopaminergic and serotonergic activity in neostriatum and nucleus accumbens enhanced by intranasal administration of testosterone. Eur Neuropsychopharmacol 19:53-63.

Deadwyler SA, Porrino L, Siegel JM, Hampson RE (2007) Systemic and nasal delivery of orexin-A (Hypocretin-1) reduces the effects of sleep deprivation on cognitive performance in nonhuman primates. J Neurosci 27:14239-14247.

DeSesso JM (1993) The relevance to humans of animal models for inhalation studies of cancer in the nose and upper airways. Qual Assur 2:213-231.

Dhanda DS, Frey WH, 2nd, D L, UB K (2005) Approaches for drug deposition in the human olfactory epithelium. Drug Del Tech 5:64-72.

Dhuria SV, Hanson LR, Frey WH, 2nd (2008) Intranasal drug targeting of hypocretin-1 (orexin-A) to the central nervous system. J Pharm Sci DOI:10.1002/jps.21604.

Dhuria SV, Hanson LR, Frey WH, 2nd (2009) Novel vasoconstrictor formulation to enhance intranasal targeting of neuropeptide therapeutics to the central nervous system. J Pharmacol Exp Ther 328:312-320.

Djupesland PG, Skretting A, Winderen M, Holand T (2006) Breath actuated device improves delivery to target sites beyond the nasal valve. In: Laryngoscope, pp 466-472.
Domes G, Heinrichs M, Michel A, Berger C, Herpertz SC (2007a) Oxytocin improves "mind-reading" in humans. Biol Psychiatry 61:731-733.
Domes G, Heinrichs M, Glascher J, Buchel C, Braus DF, Herpertz SC (2007b) Oxytocin attenuates amygdala responses to emotional faces regardless of valence. Biol Psychiatry 62:1187-1190.
Dufes C, Olivier JC, Gaillard F, Gaillard A, Couet W, Muller JM (2003) Brain delivery of vasoactive intestinal peptide (VIP) following nasal administration to rats. Int J Pharm 255:87-97.
Dunn AJ, Berridge CW (1990) Is corticotropin-releasing factor a mediator of stress responses? Ann N Y Acad Sci 579:183-191.
Eccles R (2007) Substitution of phenylephrine for pseudoephedrine as a nasal decongeststant. An illogical way to control methamphetamine abuse. Br J Clin Pharmacol 63:10-14.
Ehrstrom M, Gustafsson T, Finn A, Kirchgessner A, Gryback P, Jacobsson H, Hellstrom PM, Naslund E (2005) Inhibitory effect of exogenous orexin a on gastric emptying, plasma leptin, and the distribution of orexin and orexin receptors in the gut and pancreas in man. J Clin Endocrinol Metab 90:2370-2377.
Engle JP (1992) Topical nasal decongestants. Am Pharm NS32:33-37.
Feng P, Vurbic D, Wu Z, Hu Y, Strohl KP (2008) Changes in brain orexin levels in a rat model of depression induced by neonatal administration of clomipramine. J Psychopharmacol.
Fliedner S, Schulz C, Lehnert H (2006) Brain Uptake of Intranasally Applied Radioiodinated Leptin in Wistar Rats. Endocrinology.
Francis GJ, Martinez JA, Liu WQ, Xu K, Ayer A, Fine J, Tuor UI, Glazner G, Hanson LR, Frey WH, 2nd, Toth C (2008) Intranasal insulin prevents cognitive decline, cerebral atrophy and white matter changes in murine type I diabetic encephalopathy. Brain 131:3311-3334.
Frey WH, 2nd (1991) Neurologic agents for nasal administration to the brain. In: (WPTO, ed). US: Chiron Corporation.
Frey WH, 2nd (1997) Method of administering neurologic agents to the brain. In: (USPTO, ed). US: Chiron Corporation
Frey WH, 2nd (2001) Method for administering insulin to the brain. In. US: Chiron Corporation.
Frey WH, 2nd (2002) Bypassing the blood-brain barrier to delivery therapeutic agents to the brain and spinal cord. Drug Del Tech 2:46-49.
Frey WH, 2nd, Liu J, Chen X, Thorne RG, Fawcett JR, Ala TA, Raman Y (1997) Delivery of ^{125}I-NGF to the brain via the olfactory route. Drug Delivery 4:87-92.
Friedman LF, Zeitzer JM, Lin L, Hoff D, Mignot E, Peskind ER, Yesavage JA (2007) In Alzheimer disease, increased wake fragmentation found in those with lower hypocretin-1. Neurology 68:793-794.

Fujiki N, Yoshida Y, Ripley B, Mignot E, Nishino S (2003) Effects of IV and ICV hypocretin-1 (orexin A) in hypocretin receptor-2 gene mutated narcoleptic dogs and IV hypocretin-1 replacement therapy in a hypocretin-ligand-deficient narcoleptic dog. Sleep 26:953-959.

Gao X, Chen J, Tao W, Zhu J, Zhang Q, Chen H, Jiang X (2007) UEA I-bearing nanoparticles for brain delivery following intranasal administration. Int J Pharm 340:207-215.

Goncz E, Strowski MZ, Grotzinger C, Nowak KW, Kaczmarek P, Sassek M, Mergler S, El-Zayat BF, Theodoropoulou M, Stalla GK, Wiedenmann B, Plockinger U (2008) Orexin-A inhibits glucagon secretion and gene expression through a Foxo1-dependent pathway. Endocrinology 149:1618-1626.

Gopinath PG, Gopinath G, Kumar ATC (1978) Target site of intranasally sprayed substances and their transport across the nasal mucosa: a new insight into the intranasal route of drug-delivery. Current Ther Res 23:596-607.

Gozes I, Divinski I (2007) NAP, a neuroprotective drug candidate in clinical trials, stimulates microtubule assembly in the living cell. Curr Alzheimer Res 4:507-509.

Gozes I, Giladi E, Pinhasov A, Bardea A, Brenneman DE (2000) Activity-dependent neurotrophic factor: intranasal administration of femtomolar-acting peptides improve performance in a water maze. J Pharmacol Exp Ther 293:1091-1098.

Graff CL, Pollack GM (2003) P-Glycoprotein attenuates brain uptake of substrates after nasal instillation. Pharm Res 20:1225-1230.

Gray H (1978) Gray's Anatomy. New York: Bounty Books.

Gross EA, Swenberg JA, Fields S, Popp JA (1982) Comparative morphometry of the nasal cavity in rats and mice. J Anat 135:83-88.

Guastella AJ, Mitchell PB, Dadds MR (2008) Oxytocin increases gaze to the eye region of human faces. Biol Psychiatry 63:3-5.

Hadaczek P, Yamashita Y, Mirek H, Tamas L, Bohn MC, Noble C, Park JW, Bankiewicz K (2006) The "perivascular pump" driven by arterial pulsation is a powerful mechanism for the distribution of therapeutic molecules within the brain. Mol Ther 14:69-78.

Hallschmid M, Born J (2008) Revealing the potential of intranasally administered orexin a (hypocretin-1). Mol Interv 8:133-137.

Hallschmid M, Benedict C, Schultes B, Born J, Kern W (2008) Obese men respond to cognitive but not to catabolic brain insulin signaling. Int J Obes (Lond) 32:275-282.

Han IK, Kim MY, Byun HM, Hwang TS, Kim JM, Hwang KW, Park TG, Jung WW, Chun T, Jeong GJ, Oh YK (2007) Enhanced brain targeting efficiency of intranasally administered plasmid DNA: an alternative route for brain gene therapy. J Mol Med 85:75-83.

Hanson LR, Frey II WH, Hoekman JD, Pohl J (2008) Lipid growth factor formulations. In: (EPO, ed): Biopharm and HealthPartners Research Foundation.

Hanson LR, Martinez PM, Taheri S, Kamsheh L, Mignot E, Frey WH, 2nd (2004) Intranasal administration of hypocretin 1 (orexin A) bypasses the blood-brain

barrier & targets the brain: a new strategy for the treatment of narcolepsy. Drug Del Tech 4:66-70.
Hara J, Beuckmann CT, Nambu T, Willie JT, Chemelli RM, Sinton CM, Sugiyama F, Yagami K, Goto K, Yanagisawa M, Sakurai T (2001) Genetic ablation of orexin neurons in mice results in narcolepsy, hypophagia, and obesity. Neuron 30:345-354.
Hashizume R, Ozawa T, Gryaznov SM, Bollen AW, Lamborn KR, Frey Ii WH, Deen DF (2008) New therapeutic approach for brain tumors: Intranasal delivery of telomerase inhibitor GRN163. Neuro Oncol.
Haynes AC, Jackson B, Overend P, Buckingham RE, Wilson S, Tadayyon M, Arch JR (1999) Effects of single and chronic intracerebroventricular administration of the orexins on feeding in the rat. Peptides 20:1099-1105.
Haynes AC, Jackson B, Chapman H, Tadayyon M, Johns A, Porter RA, Arch JR (2000) A selective orexin-1 receptor antagonist reduces food consumption in male and female rats. Regul Pept 96:45-51.
Hiley CR, Wilson H, Yates MS (1978) Identification of beta-adrenoceptors and histamine receptors in the cat nasal vasculature. Acta Otolaryngol 85:444-448.
Horvat S, Feher A, Wolburg H, Sipos P, Veszelka S, Toth A, Kis L, Kurunczi A, Balogh G, Kurti L, Eros I, Szabo-Revesz P, Deli MA (2008) Sodium hyaluronate as a mucoadhesive component in nasal formulation enhances delivery of molecules to brain tissue. Eur J Pharm Biopharm.
Huang YL, Saljo A, Suneson A, Hansson HA (1996) Comparison among different approaches for sampling cerebrospinal fluid in rats. Brain Res Bull 41:273-279.
Hunt CA, MacGregor RD, Siegel RA (1986) Engineering targeting in vivo drug delivery: I. The physiological and physicohemical governing opportunities and limitations. Pharm Res:333-344.
Ichimura K, Okita W, Tanaka T (1991) Vasoactivity of endothelin in nasal blood vessels. Rhinology 29:125-135.
Jaeger LB, Farr SA, Banks WA, Morley JE (2002) Effects of orexin-A on memory processing. Peptides 23:1683-1688.
Jansson B, Bjork E (2002) Visualization of in vivo olfactory uptake and transfer using fluorescein dextran. J Drug Target 10:379-386.
Jarvinen K, Urtti A (1992) Duration and long-term efficacy of phenylephrine-induced reduction in the systemic absorption of ophthalmic timolol in rabbits. J Ocul Pharmacol 8:91-98.
Jogani VV, Shah PJ, Mishra P, Mishra AK, Misra AR (2008) Intranasal mucoadhesive microemulsion of tacrine to improve brain targeting. Alzheimer Dis Assoc Disord 22:116-124.
Johannssen V, Maune S, Werner JA, Rudert H, Ziegler A (1997) Alpha 1-receptors at pre-capillary resistance vessels of the human nasal mucosa. Rhinology 35:161-165.
Johnston M, Zakharov A, Papaiconomou C, Salmasi G, Armstrong D (2004) Evidence of connections between cerebrospinal fluid and nasal lymphatic vessels in humans, non-human primates and other mammalian species. Cerebrospinal Fluid Res 1:2.

Johren O, Neidert SJ, Kummer M, Dendorfer A, Dominiak P (2001) Prepro-orexin and orexin receptor mRNAs are differentially expressed in peripheral tissues of male and female rats. Endocrinology 142:3324-3331.
Jones DN, Kortekaas R, Slade PD, Middlemiss DN, Hagan JJ (1998) The behavioural effects of corticotropin-releasing factor-related peptides in rats. Psychopharmacology (Berl) 138:124-132.
Jones DN, Gartlon J, Parker F, Taylor SG, Routledge C, Hemmati P, Munton RP, Ashmeade TE, Hatcher JP, Johns A, Porter RA, Hagan JJ, Hunter AJ, Upton N (2001) Effects of centrally administered orexin-B and orexin-A: a role for orexin-1 receptors in orexin-B-induced hyperactivity. Psychopharmacology (Berl) 153:210-218.
Kastin AJ, Akerstrom V (1999) Orexin A but not orexin B rapidly enters brain from blood by simple diffusion. J Pharmacol Exp Ther 289:219-223.
Kawarai M, Koss MC (2001) Sympathetic control of nasal blood flow in the rat mediated by alpha(1)-adrenoceptors. Eur J Pharmacol 413:255-262.
Kesavanathan J, Swift DL, Bascom R (1995) Nasal pressure-volume relationships determined with acoustic rhinometry. J Appl Physiol 79:547-553.
Kida S, Pantazis A, Weller RO (1993) CSF drains directly from the subarachnoid space into nasal lymphatics in the rat. Anatomy, histology and immunological significance. Neuropathol Appl Neurobiol 19:480-488.
Kosfeld M, Heinrichs M, Zak PJ, Fischbacher U, Fehr E (2005) Oxytocin increases trust in humans. Nature 435:673-676.
Kotz CM, Wang C, Teske JA, Thorpe AJ, Novak CM, Kiwaki K, Levine JA (2006) Orexin A mediation of time spent moving in rats: neural mechanisms. Neuroscience 142:29-36.
Kumar M, Misra A, Babbar AK, Mishra AK, Mishra P, Pathak K (2008) Intranasal nanoemulsion based brain targeting drug delivery system of risperidone. Int J Pharm.
Kumar V, Schoenwald RD, Barcellos WA, Chien DS, Folk JC, Weingeist TA (1986) Aqueous vs viscous phenylephrine. I. Systemic absorption and cardiovascular effects. Arch Ophthalmol 104:1189-1191.
Kunii K, Yamanaka A, Nambu T, Matsuzaki I, Goto K, Sakurai T (1999) Orexins/hypocretins regulate drinking behaviour. Brain Res 842:256-261.
Kyyronen K, Urtti A (1990a) Improved ocular: systemic absorption ratio of timolol by viscous vehicle and phenylephrine. Invest Ophthalmol Vis Sci 31:1827-1833.
Kyyronen K, Urtti A (1990b) Effects of epinephrine pretreatment and solution pH on ocular and systemic absorption of ocularly applied timolol in rabbits. J Pharm Sci 79:688-691.
Lane AP, Prazma J, Baggett HC, Rose AS, Pillsbury HC (1997) Nitric oxide is a mediator of neurogenic vascular exudation in the nose. Otolaryngol Head Neck Surg 116:294-300.
Lee VH, Luo AM, Li SY, Podder SK, Chang JS, Ohdo S, Grass GM (1991) Pharmacokinetic basis for nonadditivity of intraocular pressure lowering in timolol combinations. Invest Ophthalmol Vis Sci 32:2948-2957.

Lin L, Faraco J, Li R, Kadotani H, Rogers W, Lin X, Qiu X, de Jong PJ, Nishino S, Mignot E (1999) The sleep disorder canine narcolepsy is caused by a mutation in the hypocretin (orexin) receptor 2 gene. Cell 98:365-376.

Liu S, Carpenter RL, Chiu AA, McGill TJ, Mantell SA (1995) Epinephrine prolongs duration of subcutaneous infiltration of local anesthesia in a dose-related manner. Correlation with magnitude of vasoconstriction. Reg Anesth 20:378-384.

Liu XF, Fawcett JR, Hanson LR, Frey WH, 2nd (2004) The window of opportunity for treatment of focal cerebral ischemic damage with noninvasive intranasal insulin-like growth factor-I in rats. J Stroke Cerebrovasc Dis 13:16-23.

Liu XF, Fawcett JR, Thorne RG, DeFor TA, Frey WH, 2nd (2001) Intranasal administration of insulin-like growth factor-I bypasses the blood-brain barrier and protects against focal cerebral ischemic damage. J Neurol Sci 187:91-97.

Loftus LT, Li HF, Gray AJ, Hirata-Fukae C, Stoica BA, Futami J, Yamada H, Aisen PS, Matsuoka Y (2006) In vivo protein transduction to the CNS. Neuroscience 139:1061-1067.

Luo AM, Sasaki H, Lee VH (1991) Ocular drug interactions involving topically applied timolol in the pigmented rabbit. Curr Eye Res 10:231-240.

Mackay-Sim A (2003) Neurogenesis in the adult olfactory neuroepithelium. In: Handbook of olfaction and gustation., Second Edition (Doty RL, ed), pp 93-113. New York: Marcel Dekker, Inc.

Malmgren LT, Olsson Y (1980) Differences between the peripheral and the central nervous system in permeability to sodium fluorescein. J Comp Neurol 191:103-107.

Marcus JN, Aschkenasi CJ, Lee CE, Chemelli RM, Saper CB, Yanagisawa M, Elmquist JK (2001) Differential expression of orexin receptors 1 and 2 in the rat brain. J Comp Neurol 435:6-25.

Martinez JA, Francis GJ, Liu WQ, Pradzinsky N, Fine J, Wilson M, Hanson LR, Frey WH, 2nd, Zochodne D, Gordon T, Toth C (2008) Intranasal delivery of insulin and a nitric oxide synthase inhibitor in an experimental model of amyotrophic lateral sclerosis. Neuroscience 157:908-925.

Matsuoka Y, Gray AJ, Hirata-Fukae C, Minami SS, Waterhouse EG, Mattson MP, LaFerla FM, Gozes I, Aisen PS (2007) Intranasal NAP administration reduces accumulation of amyloid peptide and tau hyperphosphorylation in a transgenic mouse model of Alzheimer's disease at early pathological stage. J Mol Neurosci 31:165-170.

Mieda M, Willie JT, Hara J, Sinton CM, Sakurai T, Yanagisawa M (2004) Orexin peptides prevent cataplexy and improve wakefulness in an orexin neuron-ablated model of narcolepsy in mice. Proc Natl Acad Sci U S A 101:4649-4654.

Miragall F, Krause D, de Vries U, Dermietzel R (1994) Expression of the tight junction protein ZO-1 in the olfactory system: presence of ZO-1 on olfactory sensory neurons and glial cells. J Comp Neurol 341:433-448.

Mitri J, Pittas AG (2009) Inhaled insulin--what went wrong. Nat Clin Pract Endocrinol Metab 5:24-25.

Murao N, Ishigai M, Yasuno H, Shimonaka Y, Aso Y (2007) Simple and sensitive quantification of bioactive peptides in biological matrices using liquid chromatography/selected reaction monitoring mass spectrometry coupled with trichloroacetic acid clean-up. Rapid Commun Mass Spectrom 21:4033-4038.
Myers MG, Iazzetta JJ (1982) Intranasally administered phenylephrine and blood pressure. Can Med Assoc J 127:365-368.
Nagra G, Koh L, Zakharov A, Armstrong D, Johnston M (2006) Quantification of cerebrospinal fluid transport across the cribriform plate into lymphatics in rats. Am J Physiol Regul Integr Comp Physiol 291:R1383-1389.
Nakamura T, Uramura K, Nambu T, Yada T, Goto K, Yanagisawa M, Sakurai T (2000) Orexin-induced hyperlocomotion and stereotypy are mediated by the dopaminergic system. Brain Res 873:181-187.
Nambu T, Sakurai T, Mizukami K, Hosoya Y, Yanagisawa M, Goto K (1999) Distribution of orexin neurons in the adult rat brain. Brain Res 827:243-260.
Nazarenko IV, Zvrushchenko M, Volkov AV, Kamenskii AA, Zaganshin R (1999) [Functional-morphologic evaluation of the effect of the regulatory peptide kyotorphin on the status of the CNS in the post-resuscitation period]. Patol Fiziol Eksp Ter:31-33.
Nishino S, Ripley B, Overeem S, Lammers GJ, Mignot E (2000) Hypocretin (orexin) deficiency in human narcolepsy. Lancet 355:39-40.
Nishino S, Ripley B, Overeem S, Nevsimalova S, Lammers GJ, Vankova J, Okun M, Rogers W, Brooks S, Mignot E (2001) Low cerebrospinal fluid hypocretin (Orexin) and altered energy homeostasis in human narcolepsy. Ann Neurol 50:381-388.
Nonaka N, Farr SA, Kageyama H, Shioda S, Banks WA (2008) Delivery of galanin-like peptide to the brain: targeting with intranasal delivery and cyclodextrins. J Pharmacol Exp Ther 325:513-519.
O'Donnell SR (1995a) Sympathomimetic vasoconstrictors as nasal decongestants. Med J Aust 162:264-267.
O'Donnell SR (1995b) Sympathetic vasoconstrictors as nasal decongestants. Medical Journal of Australia 162:264-267.
Olanoff LS, Titus CR, Shea MS, Gibson RE, Brooks CD (1987) Effect of intranasal histamine on nasal mucosal blood flow and the antidiuretic activity of desmopressin. J Clin Invest 80:890-895.
Owens DR, Zinman B, Bolli G (2003) Alternative routes of insulin delivery. Diabet Med 20:886-898.
Palmerini CA, Fini C, Floridi A, Morelli H, Vedovelli A (1985) High-performance liquid chromatographic analysis of free hydroxyproline and proline in blood plasma and of free and peptide-bound hydroxyproline in urine. J Chromatogr 339:285-292.
Pardridge WM (2005) The blood-brain barrier: bottleneck in brain drug development. NeuroRx 2:3-14.
Paxinos G, Watson C (1997) The rat brain in stereotaxic coordinates., 3rd Edition. San Diego: Academic Press.

Perl DP, Good PF (1987) Uptake of aluminium into central nervous system along nasal-olfactory pathways. Lancet 1:1028.

Peyron C, Tighe DK, van den Pol AN, de Lecea L, Heller HC, Sutcliffe JG, Kilduff TS (1998) Neurons containing hypocretin (orexin) project to multiple neuronal systems. J Neurosci 18:9996-10015.

Peyron C, Faraco J, Rogers W, Ripley B, Overeem S, Charnay Y, Nevsimalova S, Aldrich M, Reynolds D, Albin R, Li R, Hungs M, Pedrazzoli M, Padigaru M, Kucherlapati M, Fan J, Maki R, Lammers GJ, Bouras C, Kucherlapati R, Nishino S, Mignot E (2000) A mutation in a case of early onset narcolepsy and a generalized absence of hypocretin peptides in human narcoleptic brains. Nat Med 6:991-997.

Pollock H, Hutchings M, Weller RO, Zhang ET (1997) Perivascular spaces in the basal ganglia of the human brain: their relationship to lacunes. J Anat 191 (Pt 3):337-346.

Raghavan U, Logan BM (2000) New method for the effective instillation of nasal drops. J Laryngol Otol 114:456-459.

Redman LW, Tustanoff ER (1984) Iodination of [Tyr8]-bradykinin-comparison of chloramine-T and lactoperoxidase techniques. J Immunoassay 5:29-57.

Reger MA, Watson GS, Green PS, Baker LD, Cholerton B, Fishel MA, Plymate SR, Cherrier MM, Schellenberg GD, Frey Ii WH, Craft S (2008a) Intranasal Insulin Administration Dose-Dependently Modulates Verbal Memory and Plasma Amyloid-beta in Memory-Impaired Older Adults. J Alzheimers Dis 13:323-331.

Reger MA, Watson GS, Frey WH, 2nd, Baker LD, Cholerton B, Keeling ML, Belongia DA, Fishel MA, Plymate SR, Schellenberg GD, Cherrier MM, Craft S (2006) Effects of intranasal insulin on cognition in memory-impaired older adults: modulation by APOE genotype. Neurobiol Aging 27:451-458.

Reger MA, Watson GS, Green PS, Wilkinson CW, Baker LD, Cholerton B, Fishel MA, Plymate SR, Breitner JC, DeGroodt W, Mehta P, Craft S (2008b) Intranasal insulin improves cognition and modulates beta-amyloid in early AD. Neurology 70:440-448.

Rennels ML, Gregory TF, Blaumanis OR, Fujimoto K, Grady PA (1985) Evidence for a 'paravascular' fluid circulation in the mammalian central nervous system, provided by the rapid distribution of tracer protein throughout the brain from the subarachnoid space. Brain Res 326:47-63.

Rimmele U, Hediger K, Heinrichs M, Klaver P (2009) Oxytocin makes a face in memory familiar. J Neurosci 29:38-42.

Ripley B, Overeem S, Fujiki N, Nevsimalova S, Uchino M, Yesavage J, Di Monte D, Dohi K, Melberg A, Lammers GJ, Nishida Y, Roelandse FW, Hungs M, Mignot E, Nishino S (2001) CSF hypocretin/orexin levels in narcolepsy and other neurological conditions. Neurology 57:2253-2258.

Ross TM, Zuckermann RN, Reinhard C, Frey WH, 2nd (2008) Intranasal administration delivers peptoids to the rat central nervous system. Neurosci Lett.

Ross TM, Martinez PM, Renner JC, Thorne RG, Hanson LR, Frey WH, 2nd (2004) Intranasal administration of interferon beta bypasses the blood-brain barrier to

target the central nervous system and cervical lymph nodes: a non-invasive treatment strategy for multiple sclerosis. J Neuroimmunol 151:66-77.
Sakane T, Akizuki M, Yamashita S, Sezaki H, Nadai T (1994) Direct drug transport from the rat nasal cavity to the cerebrospinal fluid: the relation to the dissociation of the drug. J Pharm Pharmacol 46:378-379.
Sakane T, Akizuki M, Taki Y, Yamashita S, Sezaki H, Nadai T (1995) Direct drug transport from the rat nasal cavity to the cerebrospinal fluid: the relation to the molecular weight of drugs. J Pharm Pharmacol 47:379-381.
Sakane T, Akizuki M, Yoshida M, Yamashita S, Nadai T, Hashida M, Sezaki H (1991) Transport of cephalexin to the cerebrospinal fluid directly from the nasal cavity. J Pharm Pharmacol 43:449-451.
Sakurai T (2002) Roles of orexins in regulation of feeding and wakefulness. Neuroreport 13:987-995.
Sakurai T, Amemiya A, Ishii M, Matsuzaki I, Chemelli RM, Tanaka H, Williams SC, Richardson JA, Kozlowski GP, Wilson S, Arch JR, Buckingham RE, Haynes AC, Carr SA, Annan RS, McNulty DE, Liu WS, Terrett JA, Elshourbagy NA, Bergsma DJ, Yanagisawa M (1998) Orexins and orexin receptors: a family of hypothalamic neuropeptides and G protein-coupled receptors that regulate feeding behavior. Cell 92:573-585.
Salomon RM, Ripley B, Kennedy JS, Johnson B, Schmidt D, Zeitzer JM, Nishino S, Mignot E (2003) Diurnal variation of cerebrospinal fluid hypocretin-1 (Orexin-A) levels in control and depressed subjects. Biol Psychiatry 54:96-104.
Schaefer ML, Bottger B, Silver WL, Finger TE (2002) Trigeminal collaterals in the nasal epithelium and olfactory bulb: a potential route for direct modulation of olfactory information by trigeminal stimuli. J Comp Neurol 444:221-226.
Scheibe M, Bethge C, Witt M, Hummel T (2008) Intranasal administration of drugs. Arch Otolaryngol Head Neck Surg 134:643-646.
Shimizu H, Oh IS, Okada S, Mori M (2005) Inhibition of appetite by nasal leptin administration in rats. Int J Obes (Lond) 29:858-863.
Shu C, Shen H, Teuscher NS, Lorenzi PJ, Keep RF, Smith DE (2002) Role of PEPT2 in peptide/mimetic trafficking at the blood-cerebrospinal fluid barrier: studies in rat choroid plexus epithelial cells in primary culture. J Pharmacol Exp Ther 301:820-829.
Smith KS, Morrell JI (2007) Comparison of infant and adult rats in exploratory activity, diurnal patterns, and responses to novel and anxiety-provoking environments. Behav Neurosci 121:449-461.
Supersaxo A, Hein WR, Steffen H (1990) Effect of molecular weight on the lymphatic absorption of water-soluble compounds following subcutaneous administration. Pharm Res 7:167-169.
Sweet DC, Levine AS, Billington CJ, Kotz CM (1999) Feeding response to central orexins. Brain Res 821:535-538.
Teuscher NS, Keep RF, Smith DE (2001) PEPT2-mediated uptake of neuropeptides in rat choroid plexus. Pharm Res 18:807-813.
Thannickal TC, Lai YY, Siegel JM (2007) Hypocretin (orexin) cell loss in Parkinson's disease. Brain 130:1586-1595.

Thannickal TC, Lai YY, Siegel JM (2008) Hypocretin (orexin) and melanin concentrating hormone loss and the symptoms of Parkinson's disease. Brain 131:e87.
Thannickal TC, Moore RY, Nienhuis R, Ramanathan L, Gulyani S, Aldrich M, Cornford M, Siegel JM (2000) Reduced number of hypocretin neurons in human narcolepsy. Neuron 27:469-474.
Thorne RG, Emory CR, Ala TA, Frey WH, 2nd (1995) Quantitative analysis of the olfactory pathway for drug delivery to the brain. Brain Res 692:278-282.
Thorne RG, Pronk GJ, Padmanabhan V, Frey WH, 2nd (2004) Delivery of insulin-like growth factor-I to the rat brain and spinal cord along olfactory and trigeminal pathways following intranasal administration. Neuroscience 127:481-496.
Thorne RG, Hanson LR, Ross TM, Tung D, Frey WH, 2nd (2008) Delivery of interferon-b to the monkey nervous system following intranasal administration. Neuroscience.
Trivedi P, Yu H, MacNeil DJ, Van der Ploeg LH, Guan XM (1998) Distribution of orexin receptor mRNA in the rat brain. FEBS Lett 438:71-75.
Urtti A, Kyyronen K (1989) Ophthalmic epinephrine, phenylephrine, and pilocarpine affect the systemic absorption of ocularly applied timolol. J Ocul Pharmacol 5:127-132.
van den Berg MP, Romeijn SG, Verhoef JC, Merkus FW (2002) Serial cerebrospinal fluid sampling in a rat model to study drug uptake from the nasal cavity. J Neurosci Methods 116:99-107.
van den Berg MP, Verhoef JC, Romeijn SG, Merkus FW (2004a) Uptake of estradiol or progesterone into the CSF following intranasal and intravenous delivery in rats. Eur J Pharm Biopharm 58:131-135.
Van den Berg MP, Merkus P, Romeijn SG, Verhoef JC, Merkus FW (2003) Hydroxocobalamin uptake into the cerebrospinal fluid after nasal and intravenous delivery in rats and humans. J Drug Target 11:325-331.
van den Berg MP, Merkus P, Romeijn SG, Verhoef JC, Merkus FW (2004b) Uptake of melatonin into the cerebrospinal fluid after nasal and intravenous delivery: studies in rats and comparison with a human study. Pharm Res 21:799-802.
Vyas TK, Tiwari SB, Amiji MM (2006a) Formulation and physiological factors influencing CNS delivery upon intranasal administration. Crit Rev Ther Drug Carrier Syst 23:319-347.
Vyas TK, Shahiwala A, Marathe S, Misra A (2005a) Intranasal drug delivery for brain targeting. Curr Drug Deliv 2:165-175.
Vyas TK, Babbar AK, Sharma RK, Misra A (2005b) Intranasal mucoadhesive microemulsions of zolmitriptan: preliminary studies on brain-targeting. J Drug Target 13:317-324.
Vyas TK, Babbar AK, Sharma RK, Singh S, Misra A (2006b) Intranasal mucoadhesive microemulsions of clonazepam: Preliminary studies on brain targeting. J Pharm Sci 95:570-580.
Vyas TK, Babbar AK, Sharma RK, Singh S, Misra A (2006c) Preliminary brain-targeting studies on intranasal mucoadhesive microemulsions of sumatriptan. AAPS PharmSciTech 7:E1-E9.

Wajchenberg BL, Pinto H, Torres de Toledo e Souza I, Lerario AC, Ribeiro Pieroni R (1978) Preparation of iodine-125-labeled insulin for radioimmunoassay: comparison of lactoperoxidase and chloramine-T iodination. J Nucl Med 19:900-905.

Walter BA, Valera VA, Takahashi S, Ushiki T (2006a) The olfactory route for cerebrospinal fluid drainage into the peripheral lymphatic system. Neuropathol Appl Neurobiol 32:388-396.

Walter BA, Valera VA, Takahashi S, Matsuno K, Ushiki T (2006b) Evidence of antibody production in the rat cervical lymph nodes after antigen administration into the cerebrospinal fluid. Arch Histol Cytol 69:37-47.

Wang D, Gao Y, Yun L (2006a) Study on brain targeting of raltitrexed following intranasal administration in rats. Cancer Chemother Pharmacol 57:97-104.

Wang M, Lung MA (2003) Adrenergic mechanisms in canine nasal venous systems. Br J Pharmacol 138:145-155.

Wang Q, Chen G, Zeng S (2007) Pharmacokinetics of Gastrodin in rat plasma and CSF after i.n. and i.v. Int J Pharm 341:20-25.

Wang X, Chi N, Tang X (2008) Preparation of estradiol chitosan nanoparticles for improving nasal absorption and brain targeting. Eur J Pharm Biopharm.

Wang X, He H, Leng W, Tang X (2006b) Evaluation of brain-targeting for the nasal delivery of estradiol by the microdialysis method. Int J Pharm 317:40-46.

Weller RO, Kida S, Zhang ET (1992) Pathways of fluid drainage from the brain--morphological aspects and immunological significance in rat and man. Brain Pathol 2:277-284.

Westergren I, Johansson BB (1991) Changes in physiological parameters of rat cerebrospinal fluid during chronic sampling: evaluation of two sampling methods. Brain Res Bull 27:283-286.

Westin U, Piras E, Jansson B, Bergstrom U, Dahlin M, Brittebo E, Bjork E (2005) Transfer of morphine along the olfactory pathway to the central nervous system after nasal administration to rodents. Eur J Pharm Sci 24:565-573.

Wustenberg EG, Scheibe M, Zahnert T, Hummel T (2006) Different swelling mechanisms in nasal septum (Kiesselbach area) and inferior turbinate responses to histamine: an optical rhinometric study. Arch Otolaryngol Head Neck Surg 132:277-281.

Wustenberg EG, Zahnert T, Huttenbrink KB, Hummel T (2007) Comparison of optical rhinometry and active anterior rhinomanometry using nasal provocation testing. Arch Otolaryngol Head Neck Surg 133:344-349.

Yamada H, Okumura T, Motomura W, Kobayashi Y, Kohgo Y (2000) Inhibition of food intake by central injection of anti-orexin antibody in fasted rats. Biochem Biophys Res Commun 267:527-531.

Yamada K, Hasegawa M, Kametani S, Ito S (2007) Nose-to-brain delivery of TS-002, prostaglandin D2 analogue. J Drug Target 15:59-66.

Yamanaka A, Kunii K, Nambu T, Tsujino N, Sakai A, Matsuzaki I, Miwa Y, Goto K, Sakurai T (2000) Orexin-induced food intake involves neuropeptide Y pathway. Brain Res 859:404-409.

Yang Z, Huang Y, Gan G, Sawchuk RJ (2005) Microdialysis evaluation of the brain distribution of stavudine following intranasal and intravenous administration to rats. J Pharm Sci 94:1577-1588.

Zhang Q, Jiang X, Jiang W, Lu W, Su L, Shi Z (2004a) Preparation of nimodipine-loaded microemulsion for intranasal delivery and evaluation on the targeting efficiency to the brain. Int J Pharm 275:85-96.

Zhang QZ, Jiang XG, Wu CH (2004b) Distribution of nimodipine in brain following intranasal administration in rats. Acta Pharmacol Sin 25:522-527.

Zhang QZ, Zha LS, Zhang Y, Jiang WM, Lu W, Shi ZQ, Jiang XG, Fu SK (2006) The brain targeting efficiency following nasally applied MPEG-PLA nanoparticles in rats. J Drug Target 14:281-290.

Zhao HM, Liu XF, Mao XW, Chen CF (2004) Intranasal delivery of nerve growth factor to protect the central nervous system against acute cerebral infarction. Chin Med Sci J 19:257-261.